Members of the Preprotein and Amino Acid Transporter Family Constitute Components of Novel Protein Import Pathways into Chloroplasts

DISSERTATION

zur Erlangung des Grades
- Doktor der Naturwissenschaften -
der Fakultät für Biologie, Chemie und Geowissenschaften
der Universität Bayreuth

vorgelegt von
Claudia Roßig

Bayreuth, im Mai 2011

Vollständiger Abdruck der von der Fakultät für Biologie, Chemie und Geowissenschaften der Universität Bayreuth genehmigten Dissertation zur Erlangung des akademischen Grades Doktor der Naturwissenschaften (Dr. rer. nat.).

Die vorliegende Arbeit wurde unter der Betreuung von Frau PD Dr. Christiane Reinbothe und Herrn Prof. Dr. Steffen Reinbothe in der Zeit vom Dezember 2006 bis November 2009 im Laboratoire Plastes et Différenciation Cellulaire (UJF/CNRS/FRE3017) der Université Joseph Fourier 1 in Grenoble (Frankreich) und vom Januar 2010 bis Mai 2011 am Lehrstuhl für Pflanzenphysiologie der Universität Bayreuth angefertigt.

Das Promotionsgesuch wurde eingereicht am: 04.05.2011

Das Rigorosum fand statt am: 04.10.2011

Der Prüfungsausschuss bestand aus:

PD Dr. Christiane Reinbothe (Erstgutachterin)
Prof. Dr. Angelika Mustroph (Zweitgutachterin)
Prof. Dr. Stephan Clemens (Vorsitz)
Prof. Dr. Konrad Dettner
Prof. Dr. Benedikt Westermann

Folgende Publikationen sind u. a. aus der vorliegenden Arbeit entstanden:

SAMOL I, BUHR F, SPRINGER A, POLLMANN S, LAHROUSSI A, **ROSSIG C**, VON WETTSTEIN D, REINBOTHE C & REINBOTHE S (2011a) Implication of the *oep16-1* mutation in a *flu*-independent, singlet oxygen-regulated cell death pathway in *Arabidopsis thaliana*. *Plant Cell Physiol* **52**, 84-95.

SAMOL I, **ROSSIG C**, BUHR F, SPRINGER A, POLLMANN S, LAHROUSSI A, VON WETTSTEIN D, REINBOTHE C & REINBOTHE S (2011b) The outer choroplast envelope protein OEP16-1 for plastid import of NADPH:protochlorophyllide oxidoreductase A in *Arabidopsis thaliana*. *Plant Cell Physiol* **52**, 96-111.

BARTSCH S, SAKSOU J, YANG M, GRAY J, **ROSSIG C**, REINBOTHE C & REINBOTHE S – A protochlorophyllide (Pchlide) *a* oxygenase involved in plastid import of NADPH:Pchlide oxidoreductase (POR) A is essential for plant viability. Submitted for publication in *Plant Physiology*.

For my parents

CONTENTS

ABBREVIATIONS

5-ALA	5-Aminolevulinic acid (Pchlide precursor)
ABA	Abscisic acid
ACD1	Accelerated cell death 1 protein, homologous to lethal leaf spot 1 protein (LLS1) of maize
αCytb_{559}	α-subunit of Cytochrome b_{559} of photosystem II
AOS	Allene oxide synthase
APS	Ammonium peroxodisulfate
A. thaliana	*Arabidopsis thaliana*
ATPB	F-type ATP synthase subunit B
A. tumefaciens	*Agrobacterium tumefaciens*
BCIP	5-Bromo-4-chloro-3-indolyl phosphate
CAH1	Carbonic anhydrase 1
ceQORH	Chloroplast envelope quinone oxidoreductase homolog
Chlide	Chlorophyllide
D1	Reaction centre protein D1 of photosystem II
DanePy	3-(*N*-diethylaminoethyl)-*N*-dansyl)aminomethyl-2,5-dihydro-2,2,5,5-tetramethyl-1*H*-pyrrole
DEPC	Diethylpyrocarbonate
DIG-dUTP	Digoxigenin-11-2'-deoxy-uridine-5'-triphosphate
DTNB	5,5'-Dithiobis(2-nitro)benzoic acid (Ellman's reagent)
E	Einstein
E. coli	*Escherichia coli*
EDTA	Ethylenediaminetetraacetic acid
ELIP1	Early light-inducible protein 1
FD	Ferredoxin
FLU	Fluorescent protein
FPLC	Fast protein liquid chromatography
GFP	Green fluorescent protein
HEPES	[4(2-Hydroxyethyl)-piperazine]-ethanesulfonic acid
IEP(36)	Chloroplast inner envelope protein (of 36 kDa)
LB	Luria Bertani Broth
LHCII	Light harvesting chlorophyll *a/b* binding protein of PSII
LHPP	Light harvesting POR:Pchlide complex
LOX2	Lipoxygenase 2
LSU	Large subunit of RubisCO
MES	2-(N-morpholino)ethanesulfonic acid
MOPS	3-(N-morpholino)propanesulfonic acid
MeJa	Methyl jasmonate

MS	Murashige and Skoog
NBT	4-Nitroblue-tetrazoliumchloride
Ni-NTA	Nickel-nitrilotriacetic acid
OEC33	Oxygen evolving complex subunit of 33 kDa
OEP(16)	Chloroplast outer envelope protein (of 16 kDa)
Pchlide	Protochlorophyllide
PLB	Prolamellar body
PMSF	Phenylmethylsulfonyl fluoride
POR	NADPH:protochlorophyllide oxidoreductase
PRAT	Preprotein and amino acid transporter
PTC(52)	Pchlide-dependent translocon complex (component of 52 kDa)
QTC/QTC24	ceQORH translocon complex / ceQORH translocon component of 24 kDa
RFP	Red fluorescent protein
RNAi	Ribonucleic acid interference
ROS	Reactive oxygen species
RT-PCR	Reverse transcription-polymerase chain reaction
RubisCO	Ribulose-1,5-bisphosphate-carboxylase/oxygenase
SDS-PAGE	Sodium dodecyl sulfate - polyacrylamide gel electrophoresis
SSC	Sodium citrate
SSU	Small subunit of RubisCO
TAE	Tris-acetate-EDTA
TBS	Tris buffered saline
TCA	Trichloroacetic acid
T-DNA	Transferred DNA
TEMED	N', N', N', N'-Tetramethylethylendiamine
TIC(110)	Translocon (component) of the inner chloroplast membrane (of 110 kDa)
TOC(159)	Translocon (component) of the outer chloroplast membrane (of 159 kDa)
TIM(17)	Translocon (component) of the inner mitochondrial membrane (of 17 kDa)
Tris	Tris (hydroxylmethyl) aminomethane
TTC	2,3,5-Triphenyltetrazolium chloride
wt	Wild-type

Nomenclature information:

GENE	Names of genes are indicated in capital italic letters, the prefix stands for the plant species e.g. *AtTOC159*, gene encoding TOC159 of *A. thaliana*
allele	Names of mutations are indicated in small italic letters
PROTEIN	Proteins are indicated in capital straight letters

SUMMARY

ZUSAMMENFASSUNG

SUMMARY

In order to sustain their structure and metabolism, chloroplasts and other plastid types must import the majority of their proteins from the cytosol across the envelope membranes. Translocons at the outer and inner chloroplast envelope membranes, called TOC and TIC, were identified that mediate the import of proteins. N-terminal transit peptides essential for import of the protein precursors are cleaved after their entry into the stroma. It was thus far believed that all of the different cytosolic precursors would enter the chloroplast through the same, jointly acting TIC/TOC machineries. Recent evidence, however, suggests that multiple, regulated import pathways exist in plastids that involve different import machineries. Different combinations of TIC and TOC proteins were shown to establish different import sites in *Arabidopsis thaliana* with specificity for either photosynthetic proteins (the standard pathway) or non-photosynthetic housekeeping proteins. Moreover, numerous noncanonical import pathways such as the import via the secretory pathway and the substrate-dependent import of the NADPH:protochlorophyllide oxidoreductase A (PORA) mediated by the outer plastid envelope protein OEP16-1 were shown to exist.

Proteomics studies have revealed the presence of a large number of plastid proteins lacking predictable N-terminal transit sequences for import. The import mechanism for the majority of these proteins has not been determined yet. One example of a transit sequence-less precursor is the chloroplast envelope quinone oxidoreductase homologue, ceQORH. This protein is imported into the inner plastid envelope membrane by a non-canonical pathway (TOC159- and TOC75-independent) and without any proteolytic cleavage. In the present study 5 proteins were shown to interact with ceQORH during its import and were designated as ceQORH translocon components (QTC). One of these proteins, QTC24 (also called HP20), is a member of the PRAT family comprising preprotein and amino acid transporters found in chloroplasts, mitochondria and free-living bacteria. In mitochondria, TIM proteins play decisive roles for the translocation and import of proteins into and across the mitochondrial inner membrane. Different expression patterns and localization of PRAT proteins suggest that they are functionally diverse beyond their role in protein translocation. QTC24/HP20 is located in the outer plastid envelope membrane of chloroplasts where it establishes a hydrophilic translocation pore. Thus, chloroplasts contain besides TOC75 and OEP16-1 a third translocation channel component in their outer envelope membrane that

functions in import of transit sequence-less inner envelope proteins. *In vitro* import into chloroplasts of corresponding isolated *A. thaliana* knock-out mutants revealed that the lack of HP20 could not be replaced by its close relative HP22. *Athp20* plants had no phenotype when grown under standard green house conditions. However, minor defects during the very early stage of greening of etiolated seedlings were observed as the expression of mainly plastid-encoded proteins was delayed. These effects could be interpreted in terms of an impaired amino acid import at this stage of development.

A second protein of the PRAT family, HP30, was further subject of this work. However, its role remains unclear at the moment. Isolated homozygous *A. thaliana* knock-out mutants of HP30 did not reveal any phenotype under the growth conditions analysed in this work such as the greening of etiolated seedlings under different light intensities and senescence of mature plants. No differences compared to wild-type plants were detected with regard to the *in vitro* import of precursor proteins and the ability to perform cytosolic and plastidic protein biosynthesis. The preliminary investigation of created stable RNA silencing mutants indicated that the function of HP30 and its close relative HP30-2 is important during the early stages of seedling development. Young leaves of respective mutant plants exhibited a chlorotic phenotype.

A further member of the PRAT family is OEP16-1 that was initially identified as amino acid-selective protein channel. Other studies revealed its role as translocation pore for the PORA precursor. Analysis of the corresponding *A. thaliana* knock-out mutant to dissect these two mutually not exclusive functions has led to the description of different phenotypes. During a re-screen of the original seed stock, four independent OEP16-1-deficient mutant lines were isolated that exhibited different cell death properties. Two mutants contained elevated amounts of free protochlorophyllide (Pchlide) in darkness that was caused by a defect in the Pchlide-dependent import of PORA. Etiolated seedlings of these lines died after light exposure due to the production of singlet oxygen. The two other mutants did not accumulate excessive amounts of free Pchlide and greened normally. Two of the four mutant lines with seemingly no correlation between the lack of PORA and cell death were analysed in more detail in this thesis. Moreover, a complemented *Atoep16-1* mutant that re-expressed functional OEP16-1 protein was shown to restore the wild-type phenotype including PORA import that prevented the accumulation of an excess of free Pchlide and singlet oxygen production upon light exposure of dark-grown seedlings.

ZUSAMMENFASSUNG

Um ihre Struktur und ihren Metabolismus aufrechtzuerhalten, müssen Plastiden den Hauptteil ihrer im Cytosol synthetisierten Proteine importieren, was deren Transfer über die Hüllmembranen erfordert. Importapparate in der äußeren und inneren Hüllmembran, genannt TOC und TIC, wurden identifiziert, die den Import von Proteinen vermitteln. N-terminale Transitpeptide, die für den Import dieser Präproteine/Präkursoren unerlässlich sind, werden nach deren Import im Stroma abgespalten. Bisher wurde angenommen, dass alle verschiedenen im Cytosol gebildeten Präproteine über die gleiche TIC/TOC Maschinerie in den Chloroplasten transportiert werden. Neuere Analysen belegen jedoch die Existenz verschiedener, regulierter Importwege, die unterschiedliche Importapparate involvieren. So konnte in der Modellpflanze *Arabidopsis thaliana* gezeigt werden, dass verschiedene Kombinationen von TIC und TOC Proteinen unterschiedliche Importwege bilden, die vorzugsweise entweder photosynthetisch aktive Proteine (der sogenannte Standardimportapparat) oder nicht-photosynthetisch aktive, sogenannte *housekeeping* Proteine importieren. Weiterhin wurden zahlreiche nicht-klassische Importwege beschrieben, wie zum Beispiel der Import über das endoplasmatische Retikulum und den Golgi-Apparat sowie der substratabhängige OEP16-1-vermittelte Import der NADPH: Protochlorophyllid Oxidoreduktase A (PORA).

Proteomics Analysen ergaben, dass zahlreiche in Plastiden lokalisierte Proteine keine prognostizierbaren N-terminalen Transitpeptide besitzen. Die Art und Weise ihres Imports ist bisher noch relativ unbekannt. Ein Beispiel solcher Proteine ist ein in der plastidären Hüllmembran lokalisiertes Chinon-Oxidoreduktase-Homolog, genannt ceQORH. Dessen Import in die innere Hüllmembran erfolgte unabhängig von TOC159 und TOC75, zwei Komponenten des Standardproteinimportapparates, sowie ohne jede proteolytische Spaltung. In dieser Arbeit wurde gezeigt, dass der Import von ceQORH mindestens 5 Proteine involviert, die nachfolgend als ceQORH *Translocon Component* (QTC) bezeichnet werden. Eines dieser Proteine, QTC24 (auch HP20 genannt), ist ein Mitglied der sogenannten PRAT Familie, die in Chloroplasten, Mitochondrien und freilebenden Bakterien vorkommende Präprotein und Aminosäure Transporter umfasst. TIM Proteine spielen eine entscheidende Rolle im Protein- und Aminosäureimport in die und über die innere mitochondriale Hüllmembran. Die unterschiedliche Lokalisierung und verschiedenen Expressionsmuster der

PRAT Proteine deuten auf eine hohe funktionelle Diversität neben ihrer Rolle in der Proteintranslokation hin. QTC24/HP20 ist in der äußeren plastidären Hüllmembran lokalisiert, wo es eine hydrophile Importpore bildet. Demzufolge besitzen Chloroplasten neben TOC75 und OEP16-1 einen dritten Kanal in ihrer äußeren Hüllmembran, der den Import Transitpeptid-loser Proteine ermöglicht. *In vitro* Import-Experimente unter Verwendung von Chloroplasten, die aus entsprechenden *A. thaliana knock-out* Mutanten (*Athp20*) isoliert wurden, ergaben, dass der Verlust von HP20 nicht durch das ihm hoch verwandte Protein HP22 ausgeglichen werden konnte. Das Wachstum solcher *Athp20* Pflanzen war unter normalen Bedingungen nicht beeinträchtigt. Jedoch wiesen die *Athp20*-Mutanten minimale Defekte in der frühen Phase der Ergrünung etiolierter Keimlinge auf indem hauptsächlich die Expression plastidär codierter Proteine verzögert war. Dieser Effekt könnte möglicherweise durch einen defekten Aminosäureimport in diesem Entwicklungsstadium verursacht werden.
Zudem wurde die Rolle eines zweiten Proteins der PRAT Familie, HP30, in dieser Arbeit untersucht. Jedoch bleibt dessen Funktion bisher unklar. Entsprechende homozygote *A. thaliana knock-out* Mutanten wiesen keine phänotypischen Unterschiede zu Wildtyp-Pflanzen unter den getesteten Bedingungen, wie die Belichtung etiolierter Keimlinge und die Kultivierung grüner Pflanzen in Gegenwart Seneszenz-auslösender Faktoren auf. *In vitro* Import-Experimente und die Analyse der cytosolsischen und plastidären Proteinbiosynthese zeigten keine Unterschiede zu Wildtyp-Pflanzen. Die vorläufige Untersuchung der im Rahmen dieser Arbeit hergestellten RNA *Silencing* Transformanten deutet darauf hin, dass die Funktion von HP30 und seinem verwandten Protein HP30-2 für die frühe Phase der Keimlingsentwicklung von *A. thaliana* bedeutsam ist. Junge Blätter solcher Pflanzenlinien wiesen eine verzögerte Chlorophyllsynthese auf.

Ein weiteres Mitglied der PRAT Familie ist das in der äußeren Hüllmembran lokalisierte OEP16-1, das ursprünglich als Aminosäure-selektives Kanalprotein charakterisiert wurde. Andere Untersuchungen zeigten, dass es eine Rolle im Import des PORA Präkursors spielt. Die Analyse der entsprechenden *A. thaliana knock-out* Mutante zur Aufklärung dieser zwei vorgeschlagenen Funktionen führte zur Beschreibung verschiedener Phänotypen. Während eines *Re-Screens* des Original-SALK-Saatguts konnten vier Mutantenlinien isoliert werden, die unterschiedliche phänotypische Eigenschaften aufwiesen. Während etiolierte Keimlinge zweier dieser Mutanten überschüssiges freies Protochlorophyllid in Folge des gestörten Protochlorophyllid-abhängigen Importes von PORA aufwiesen und nach anschließender

Belichtung durch die Produktion von Singulett-Sauerstoff starben, konnte in den Keimlingen der anderen zwei Linien kein Überschuss an freiem Protochlorophyllid nachgewiesen werden. Zwei Linien, in denen der Zelltod nicht mit der Abwesenheit von PORA korrelierbar war, wurden in dieser Arbeit detailliert untersucht. Weiterhin konnte anhand einer komplementierten OEP16-1 *knock-out* Linie gezeigt werden, dass die Re-Integration funktionellen OEP16-1 Proteins den Protochlorophyllid-abhängigen Import wiederherstellt und damit zu einer Reduktion des Gehaltes an freiem Protochlorophyllid führt. In der Folge wurde die Ausbildung von Singulett-Sauerstoff während der Belichtung etiolierter Keimlinge verhindert, so dass es in der komplementierten Linie, ganz wie im Wildtyp, zur normalen Ergrünung kam.

INTRODUCTION

1.1 The Evolutionary Origin of Chloroplasts

Plastids represent a highly divergent family of organelles. They are ubiquitously found in plant and algal cells and provide essential metabolic and signalling functions within plants (LOPEZ-JUEZ & PYKE, 2005). The hallmark organelles of green plants are chloroplasts which contain the green pigment chlorophyll and perform photosynthesis to ensure the cell-internal energy supply and are therefore indispensable for autotrophic growth. Chloroplasts contain one of the most extensive membrane systems found in nature: interconnecting stroma thylakoids and cylindrical stacked grana thylakoids (Figure 1) form a 3-dimensional network enclosing a single lumen (LOPEZ-JUEZ & PYKE, 2005).

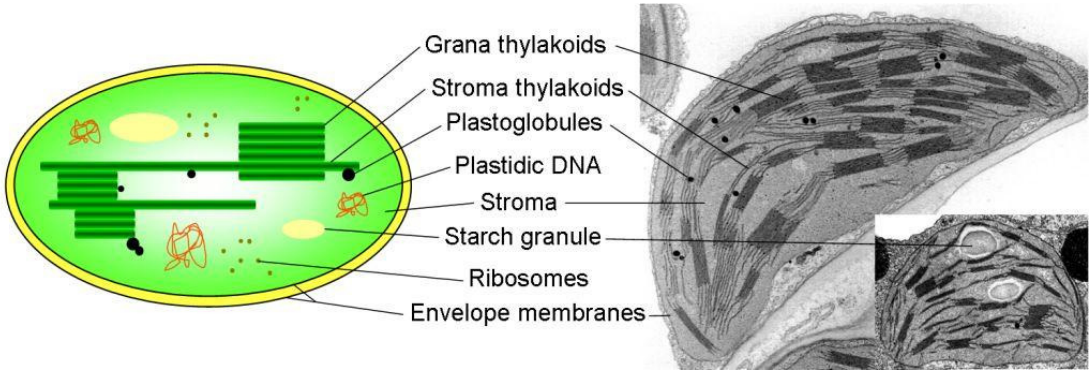

Figure 1. Structure and components of chloroplasts – Schematic presentation and transmission electron micrographs (from botit.botany.wisc.edu). Chloroplasts are surrounded by a double membrane called the envelope and contain beside the stroma a system of photosynthetic membranes (grana and stroma thylakoids), starch granules (depending on the energy status), ribosomes and a small plastid genome (termed plastome). Plastoglobules are lipid protein particles that are associated with thylakoids and are visible in the electron micrographs as black points.

It is the generally accepted view that during evolution, all double membrane-bound plastids evolved monophyletically by a single (primary) endosymbiosis of a cyanobacterium-like progenitor into a nucleated mitochondriate host cell that occurred once about 1-1.5 billion years ago (DOUZERY *et al.*, 2004; YOON *et al.*, 2004; REYES-PRIETO *et al.*, 2007; GOULD *et al.*, 2008). Over evolutionary time, the symbionts acquired many host-derived properties but also lost much of their eubacterial identity. Most importantly, the majority of their genes was either lost or transferred to the host genome and transformed them into semi-autonomous organelles (TIMMIS *et al.*, 2004; KLEINE *et al.*, 2009). Although a relatively high gene transfer rate could be determined experimentally, the real mechanism of the transfer of plastidic DNA into the nucleus is thus far unknown (HUANG *et al.*, 2003; STEGEMANN *et al.*, 2003).

The closest known living relatives of the photosynthetic progenitor belong to the genus *Nostoc* (TIMMIS *et al.*, 2004) with genomes encoding at least 5000 proteins. Instead, contemporary plastids contain ~100 genes, mainly encoding photosynthetic genes and components of the minimal genetic machinery (LOPEZ-JUEZ & PYKE, 2005; KLEINE *et al.*, 2009).

1.2 The Photoprotective Role of PORA during Plant Greening

During plant growth in the presence of light (photomorphogenesis), chloroplasts develop directly from their unpigmented, non-photosynthetic plastid progenitor, the proplastid, and chlorophyll synthesis proceeds concomitantly (WATERS & LANGDALE, 2009). In the absence of light (skotomorphogenesis), e.g., when the seedlings develop underneath the soil or under fallen leaves, chlorophyll synthesis is blocked due to the inactivity of the key enzyme of chlorophyll synthesis, the NADPH:protochlorophyllide oxidoreductase (POR) (ARMSTRONG *et al.*, 1995, HOLTORF *et al.*, 1995). In this case, so-called etioplasts are the prominent plastid type that accumulates large amounts of thylakoid lipids associated with Pchlide and POR as a semicrystalline structure referred to as prolamellar body (PLB; VON WETTSTEIN *et al.*, 1995; SUNDQVIST & DAHLIN, 1997). Upon light exposure of etiolated seedlings the PLB disintegrates and thylakoids are formed. This leads to the transformation of etioplasts into chloroplasts (SUNDQVIST & DAHLIN, 1997).

Chlorophyll and tetrapyrrole biosynthesis is carried out via the C5-pathway (VON WETTSTEIN *et al.*, 1995). This pathway is strictly regulated since free, non-protein-bound tetrapyrrole compounds such as chlorophylls are susceptible to light absorption and can, once excited, interact with oxygen to generate singlet oxygen (OP DEN CAMP *et al.*, 2003; KIM *et al.*, 2008; REINBOTHE *et al.*, 2010). This type of reactive oxygen species (ROS) has harmful effects for plants. It provokes pigment bleaching, lipid peroxidation and protein degradation leading to growth inhibition and cell death. In higher plants, the production and scavenging of ROS is normally counterbalanced by different mechanisms such that perturbations in the tetrapyrrole synthesis usually do not result in the accumulation of free porphyrins and ROS species (REINBOTHE *et al.*, 2010). One strategy to avoid ROS production is that later intermediates of chlorophyll synthesis do not exist in their free forms but are always bound to proteins. Chlorophyll, for example, is complexed together with carotenoids to protein components of the two photosystems. Another strategy is that chlorophyll biosynthesis is strictly regulated by a feedback mechanism that involves the FLUORESCENT (FLU) protein (MESKAUSKIENE

et al., 2001) and Pchlide, the immediate precursor of chlorophyllide (Chlide). When a certain threshold amount of Pchlide has been reached, the activity of the first enzyme of chlorophyll biosynthesis, the glutamyl-tRNA-reductase, is inhibited. Since the conversion of Pchlide into Chlide is a light-dependent step, etiolated seedlings avoid by this negative feedback that too large amounts of Pchlide accumulate before the young sprouts break through the soil after germination and are exposed to light (REINBOTHE *et al.*, 2010). By contrast, mutants defective in the FLU protein such as the *flu* mutant of *A. thaliana* and its orthologous barley line (*tigrina*^{d12}) produce an excess of free Pchlide molecules that trigger photooxidative damage upon light exposure of dark-grown plants (MESKAUSKIENE *et al.*, 2001; LEE *et al.*, 2003a). This effect can be avoided by cultivation of *flu* plants in continuous light when newly synthesized Pchlide is immediately reduced to Chlide.

In barley and *A. thaliana*, two POR isoenzymes, PORA and PORB exist in the PLBs of etioplasts (ARMSTRONG *et al.*, 1995; HOLTORF *et al*., 1995). PORA is only present and active in the very early stages of greening. It is rapidly degraded by a specific light-induced protease, whereas PORB is continuously expressed and maintains chlorophyll biosynthesis in green plants (REINBOTHE *et al.*, 1995b; HOLTORF *et al.*, 1995). Both, PORA and PORB bind Pchlide in etiolated seedlings. Thereby, each isoenzyme interacts with its specific substrate: PORA binds Pchlide *b* and PORB Pchlide *a* (REINBOTHE *et al.*, 1999). Not only two POR isoenzymes but also different spectral forms of Pchlide exist in the PLBs: the so-called photoactive Pchlide (Pchlide-F_{655}) that can be converted into Chlide by a 1 ms white light-flash as well as photoinactive (free) Pchilde (Pchlide-F_{631}) that cannot be converted (Figure 2; REINBOTHE *et al.*, 2010). If excess amounts of free Pchlide are excited upon light exposure, they cause photooxidative damage. Pioneering work performed already in 1962 had shown that a higher molecular weight complex exists in the PLBs of wheat that was termed the Pchlide holochrome (BOARDMAN, 1962). In reconstitution experiments performed for barley, a complex consisting of five ternary PORA-Pchlide*b*-NADPH and one PORB-Pchlide*a*-NADPH complexes was obtained that interacted with the lipids of the PLB (REINBOTHE *et al.*, 1999). A similar complex was shown to exist *in vivo* (REINBOTHE *et al.*, 2003). In this complex, termed light-harvesting POR:Pchlide (LHPP) complex (Figure 2), the light energy is absorbed by the PORA-Pchlide*b*-NADPH complex and transferred to the PORB-Pchlide*a*-NADPH complex that induces the conversion of Pchlide *a* to Chlide *a*. (REINBOTHE *et al.*, 1999; BUHR *et al.*, 2008). Since PORA gained activity for the conversion of Pchlide *b* to Chlide *b* only after the disintegration of the PLB, PORA-bound Pchlide *b*

corresponds to photoinactive Pchlide whereas PORB-bound Pchlide *a* corresponds to photoactive Pchlide. Pchlide-binding in the LHPP complex minimizes possible Pchlide photoreduction and subsequent generation of ROS. Thus, PORA has also a photoprotective role (BUHR *et al.*, 2008). The existence of Pchilde *b* in etioplasts has been questioned since its successful extraction and detection under conditions that were different from those described by REINBOTHE *et al*. (2003) was not successful (KOLOSSOV & REBEIZ, 2003). Also the existence of the LHPP has been debated (ARMSTRONG *et al.*, 2000), although a high-molecular weight POR-Pchlide-NADPH complex was isolated from etiolated wheat seedlings recently (YUAN *et al.*, 2010).

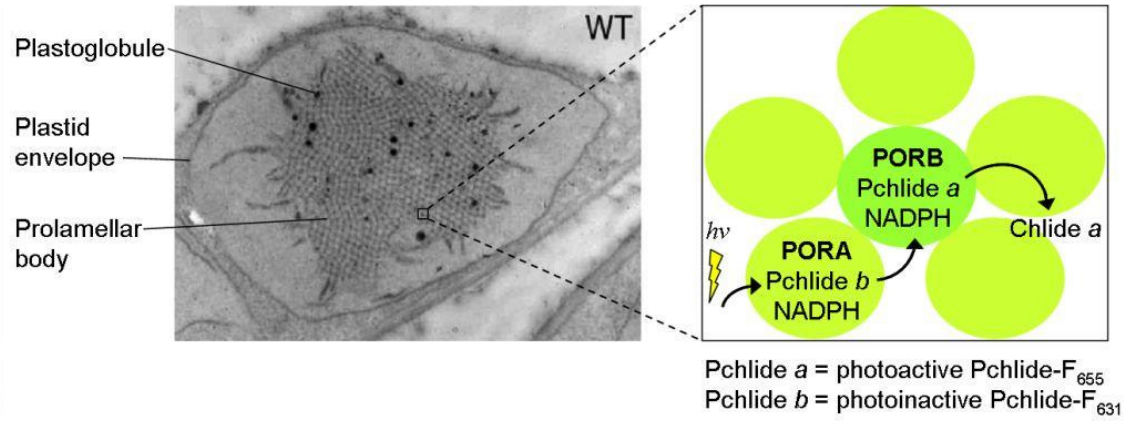

Figure 2. Etioplast ultrastructure and the model of LHPP. Transmission electron micrograph of an *A. thaliana* etioplast (from POLLMANN *et al.*, 2007). The model of LHPP was created according to REINBOTHE *et al.* (1999). The arrows mark the energy transfer upon light exposure.

1.3 The Role of Plastid Envelope Membranes in Protein Import

Due to their endosymbiotic origin plastids depend on the post-translational, energy-dependent protein import across the hydrophobic envelope membranes. Whereas the inner envelope membrane represents the actual permeability barrier, the intermembrane space is assumed to be freely accessible for ions, metabolites and proteins up to a size of 10 kDa (LOPEZ-JUEZ & PYKE, 2005). However, the identification of substrate-specific gated pore-forming proteins (e.g. POHLMEYER *et al.*, 1997) indicates that the existence of a general diffusion pore in the outer membrane is too simple.

The chloroplast envelope membranes represent one of the most complex and dynamic system within plant cells (DOUCE & JOYARD, 1990; BLOCK *et al.*, 2007). Beside their role in protein and metabolite import, chloroplast envelope membranes provide fatty acids for all

plant membranes and are a major site of glycerolipid biosynthesis. Also later steps of chlorophyll biosynthesis take place at the envelope membranes (JOYARD *et al.*, 1990; PINEAU *et al.*, 1993).

Current research indicates that numerous yet uncharacterized proteins are located in the envelope membranes. To enhance the understanding of the complexity of the biochemical machinery of chloroplast envelope membranes and to identify new components of putative transport systems, the envelope purification and the extraction of membrane proteins was optimized in order to allow proteomics analyses to be performed (FERRO *et al.*, 2002; FERRO *et al.*, 2003). About 80 % of the identified proteins had already been known to be components of the envelope membranes and could be classified functionally into proteins implicated in ion, metabolite and protein transport, proteins involved in lipid metabolism and soluble proteins like proteases/chaperones. Remarkably, about one third of the identified proteins still have an unknown and unpredictable function (referred to as HP proteins; FERRO *et al.*, 2003; BLOCK *et al.*, 2007).

1.4 Canonical Protein Import Pathways into Chloroplasts

Estimations of the chloroplast proteome revealed that the number of plastid proteins lies between 2100-4500 (LOPEZ-JUEZ & PYKE, 2005). About 90% of the cytosolic precursor proteins are suggested to use specific translocon complexes at the outer and inner envelope membranes called TOC and TIC machineries (JARVIS, 2008; INABA & SCHNELL, 2008). Indeed, TIC and TOC represent multimeric membrane complexes (translocons) in the inner and outer envelope membrane of chloroplasts that mediate recognition and directed transfer of preproteins into the stroma (Figure 3). Respective subunits of the TIC and TOC machineries have been identified with a number corresponding to their molecular weight (e.g. TOC75) (SCHNELL *et al.*, 1997). Proteins imported by the jointly acting TIC/TOC pathways are usually synthesized with a cleavable N-terminal targeting signal (BRUCE, 2001). Although these so-termed transit peptides are remarkably heterogeneous and structural key features are still unknown, they share a high specificity and are sufficient for the targeting and entry into chloroplasts. They may be functionally divided into a C- and N-terminus for lipid-membrane binding and a central domain for recognition by the respective import machinery (BRUCE, 2001).

1.4.1 The TIC/TOC Pathway – Protein Translocation into the Stroma

Protein import into chloroplasts is generally believed to occur at contact sites where the two membranes are held in close proximity (SCHNELL & BLOBEL, 1993). Depending on the energy requirements, protein translocation into the stroma can be divided into three different stages (SCHNELL & BLOBEL, 1993):

1. Energy-independent binding: The transit peptide interacts reversibly and without energy requirement with receptor components of the TOC complex (PERRY & KEEGSTRA, 1994; KOURANOV & SCHNELL, 1997). This step can be facilitated by cytosolic factors that comprise guidance complexes formed of cytosolic heat shock proteins (HSP) like HSP70, a 14-3-3 protein and the phosphorylated precursor protein or involve HSP90 that guides unphosphorylated precursors to the tetratricopeptide repeat (TPR) domains of TOC64 (MAY & SOLL, 2000; QBADOU *et al.*, 2006).
2. Early import intermediate stage/docking: The precursor protein becomes deeply and irreversibly inserted into the TOC complex and is already in contact with the TIC complex (PERRY & KEEGSTRA, 1994; MA *et al.*, 1996; KOURANOV & SCHNELL, 1997). This step requires low (≤ 100 µM) ATP concentrations as well as GTP in the intermembrane space (KESSLER *et al.*, 1994; YOUNG *et al.*, 1999).
3. Translocation into the stroma: The translocation across the membranes is completed and the transit peptide cleaved by a stromal processing peptidase (SPP, RICHTER & LAMPPA, 1998). High energy concentrations of ≥ 1 mM ATP are required in the stroma (THEG *et al.*, 1989).

The TOC core complex comprises TOC159, TOC75 and TOC34 (Figure 3; SCHLEIFF *et al.*, 2003; INABA & SCHNELL, 2008; JARVIS, 2008; LI & CHIU, 2010). TOC159 and TOC34 are GTPases that control the initial recognition of the precursor protein (KESSLER *et al.*, 1994; SVESHNIKOVA *et al.*, 2000a). Their homologous GTP-binding (G-) domains are largely exposed into the cytosol whereas the C-terminus is integrated into the membrane (M-domain). TOC159 has an additional large N-terminal acidic (A-) domain that may facilitate preprotein binding through electrostatic interactions with transit peptides (BÖLTER *et al.*, 1998). TOC75 represents the aqueous translocation pore in the outer membrane. Its 16-18 transmembrane strands form a β-barrel that is deeply embedded into the membrane (SCHNELL *et al.*, 1994; SVESHNIKOVA *et al.*, 2000b; HINNAH *et al.*, 2002).

The TIC translocation channel is formed by TIC110 and TIC20 (Figure 3; CHEN *et al.*, 2002; HEINS *et al.*, 2002). TIC110 has two short N-terminal transmembrane segments but contradictory results exist about the localization and function of the major hydrophilic rest (LÜBECK *et al.*, 1996; JACKSON *et al.*, 1998; HEINS *et al.*, 2002; INABA *et al.*, 2003). This large C-terminal domain might be exposed into the stroma and be a part of a putative stromal motor complex in which it mediates together with TIC40, a co-chaperone, and HSP93 the recruitment of stromal chaperones like CPN60 (chaperonin of 60 kDa) and HSP70 in order to ensure unidirectional movement of precursor proteins into the stroma (KESSLER & BLOBEL, 1996; JACKSON *et al.*, 1998; JACKSON-CONSTAN *et al.*, 2001; INABA *et al.*, 2003; CHOU *et al.*, 2006).

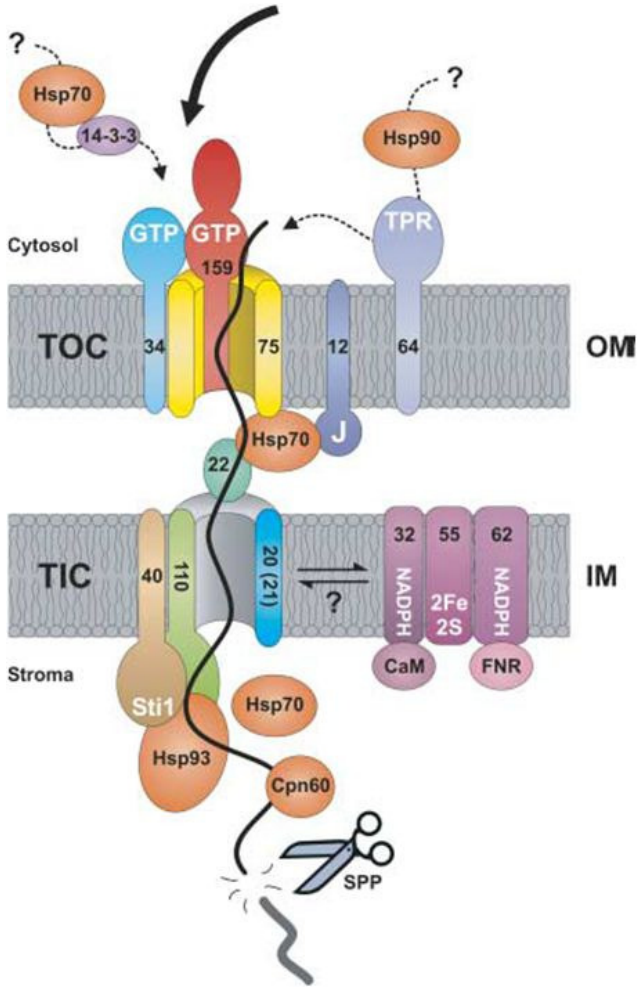

Figure 3. The TIC/TOC protein import apparatus. Schematic overview about the translocation of preproteins with N-terminal transit peptides across the chloroplast envelope membranes and the implicated components (from JARVIS, 2008). TOC components are located in the outer membrane (OM); TIC components in the inner membrane (IM) and are donated as TIC/TOC and a number corresponding to their molecular weight. TOC12, TIC22 and HSP70 facilitate the passage of the preprotein across the intermembrane space whereas the J-domain of TOC12 interacts with HSP70. (KOURANOV *et al.*, 1998; BECKER *et al.*, 2004). The carboxyl-terminal domain of TIC40, Sti1, is implicated in the interaction with HSP90. Explanations of the function of TIC32, TIC55 and TIC62 are given in chapter 1.4.2.

1.4.2 Substrate-Specificity and Regulation of the TIC/TOC Pathway

Plastid protein import is involved in the regulation and response to long- and short-term changes of plant development and the physiological status. For example, DAHLIN & CLINE

(1991) proposed that protein import may be determined by the age and the developmental state of the plant.

Depending on plastid type and import substrates, plastids possess different interconvertible versions of TIC/TOC translocons (INABA & SCHNELL, 2008; JARVIS, 2008; LI & CHIU, 2010). In *A. thaliana*, TOC159 and TOC34 are encoded by small gene families: *AtTOC33* and *AtTOC34* form the TOC34 family (JARVIS *et al.*, 1998; GUTENSOHN *et al.*, 2000) and *AtTOC159*, *AtTOC132*, *AtTOC120* and *AtTOC90* the TOC159 family (BAUER *et al.*, 2000; KUBIS *et al.*, 2004). Based on biochemical data and the characterization of respective *A. thaliana* knock-out mutants, it was proposed that different receptor types are responsible for the recognition/binding of different precursor proteins (BAUER *et al.*, 2000; KUBIS *et al.*, 2003; IVANOVA *et al.*, 2004; KUBIS *et al.*, 2004; SMITH *et al.*, 2004). On the one hand, AtTOC159 associates preferentially with AtTOC33 (and AtTOC75) to form a TOC complex specific for highly abundant photosynthetic proteins. On the other hand, AtTOC132 and/or AtTOC120 form a TOC complex with AtTOC34 (and AtTOC75) that imports preferentially low-abundant non-photosynthetic housekeeping proteins. AtTOC90 may provide a supplementary function in the import of photosynthetic proteins (HILTBRUNNER *et al.*, 2004). The proposed specificity of the TOC complexes correlates with the differential expression of the corresponding TOC receptor components. Whereas AtTOC159 and AtTOC33 are mainly expressed in leaves, AtTOC132, AtTOC120 and AtTOC34 show similar expression levels in roots and leaves (VOJTA *et al.*, 2004). These multiple versions of the TOC machinery enable the adjustment of protein import in time and space and in response to developmental and environmental conditions.

Regulation of protein import occurs also in response to redox signals. Disulfide bonds formed in TOC75 and/or in TOC159, TOC34 and TOC64 inhibit protein import whereas their reduction increases import efficiency (STENGEL *et al.*, 2010). At the inner envelope membrane, redox regulation is mediated by TIC62, TIC55 and TIC32 that have redox-related structural motifs in form of NADPH-binding sites (TIC62, TIC32) or a Rieske-type iron-sulfur centre (2Fe-2S) and a mononuclear iron-binding site in the case of TIC55 (Figure 3; CALIEBE *et al.*, 1997; STENGEL *et al.*, 2010). It is supposed that these three proteins form a redox regulon that associates with the TIC translocon and enables the import of mainly redox-regulated proteins under high $NADP^+$ conditions. By contrast, this redox regulon dissociates from the TIC translocon under high NAPDH conditions and allows redox-independent import of all proteins. Furthermore, TIC32 is able to interact with

calmodulin (CaM), indicating a calcium-mediated redox regulation (CHIGRI *et al.*, 2006). TIC62 possesses an additional binding site for ferredoxin NAD(P) reductase (FNR), suggesting a regulation of protein import in response to the redox status of the photosynthetic electron transport chain (JARVIS, 2008).

1.5 Diversity of Novel Protein Import Pathways

The vast majority of outer envelope proteins do not possess any cleavable transit peptides and their import requires no or few ATP (JARVIS, 2008; INABA & SCHNELL, 2008). Their targeting information might be located in or adjacent to their hydrophobic transmembrane domains (LEE *et al.*, 2001). Their import may involve TOC75 (TU *et al.*, 2004) that is dissociated from the TOC translocon (KOURANOV *et al.*, 1998) since TOC75 protein was detected in a significant higher concentration in the envelope membrane than other TOC components. Additionally, a cytoplasmic ankyrin repeat protein was shown to bind specifically outer chloroplast membrane proteins and to mediate their targeting to the chloroplast surface (BAE *et al.*, 2008). TOC75 is an exceptional outer envelope membrane protein. It is inserted into the membrane by the classic TOC translocon and possesses a unique bipartite targeting signal at its N-terminus composed of a classic transit peptide and an additional cleavable sequence containing a polyglycine stretch that functions as stop-transfer domain for its integration in the outer membrane (TRANEL *et al.*, 1996).

Very few information exist about the import of proteins that reside in either the inner envelope membrane or in the intermembrane space. At least, a stop-transfer pathway (e.g. triose phosphate/ phosphate translocator) or a reinsertion/post-import pathway (e.g. TIC110, TIC40, TIC21; LI & CHIU, 2010) were proposed for the import of inner envelope membrane proteins.

Analysis of the *A. thaliana* chloroplast proteome led to the discovery of large number of plastid proteins (8% of the totally identified) that contain predicted signal peptides for the translocation into the endoplasmatic reticulum (KLEFFMANN *et al.*, 2004). Since there is a close physical proximity and a great biochemical exchange (e.g. fatty acids) between the endoplasmatic reticulum and the outer envelope of chloroplasts (JARVIS, 2008), a protein transport via the endomembrane system would be conceivable. Indeed, a rice α-amylase (CHEN *et al.*, 2004), a rice nucleotide pyrophosphatase/phosphodiesterase (NANJO *et al.*, 2006) and an *A. thaliana* carbonic anhydrase 1 (CAH1) (VILLAREJO *et al.*, 2005) were shown to pass the endoplasmatic reticulum and Golgi apparatus where they are glycosylated.

Moreover, up to ~50 proteins had been experimentally proven to be targeted to both, chloroplasts and mitochondria (CARRIE *et al.*, 2009). Up to now the mechanism of dual-targeting is poorly understood. According to MACKENZIE (2005) dual-targeted proteins are functionally divided in proteins that play a role in DNA and RNA maintenance, proteins synthesis or cellular defence.

1.5.1 Substrate-specific Import of PORA involving the PTC Complex

A unique import pathway was reported for the precursor of PORA (pPORA). While pPORB is imported via the standard TIC/TOC pathway, pPORA was shown to be imported in the presence of its substrate Pchlide *b* by a TIC/TOC-independent pathway (REINBOTHE *et al.*, 1995c; REINBOTHE *et al.*, 2000; SMITH *et al.*, 2004, KIM & APEL, 2004). With the help of cross-linking experiments, 8-10 different components of the Pchlide-dependent translocon complex (PTC) could be co-purified with pPORA in junction complexes between the outer and inner envelope membrane of barley chloroplasts (Figure 4, REINBOTHE *et al.*, 2004a). Four proteins were identified by protein sequencing:

PTC16 forms the translocation channel across the outer envelope membrane and corresponds to OEP16 of barley and pea (POHLMEYER *et al.*, 1997; BALDI *et al.*, 1999). OEP16 from pea was initially characterized as a voltage-gated amino acid-selective channel. The *A. thaliana* genome encodes a small OEP16 gene family (DREA *et al.*, 2006) of which AtOEP16-1 shows the highest degree of sequence relationship to pea OEP16 and barley HvOEP16-1;1. The lack of OEP16-1 protein in the corresponding *A. thaliana* knock-out mutant (SALK_024018) caused a lack of pPORA import, an aberrant etioplast ultrastructure and the accumulation of free, photoexcitable Pchlide leading to a FLU-related cell death phenotype upon light exposure of etiolated seedlings (POLLMANN *et al.*, 2007). However, PHILIPPAR *et al.* (2007) reported a wild-type phenotype for the same mutant and reasoned that OEP16-1 plays no role in a Pchlide-dependent import of pPORA and chloroplast biogenesis (see also chapter 3.2.1). Our own results and an independent analysis of the original Salk seed stock by PUDELSKI *et al.* (2009) showed that it consists of different mutant lines that all carry a T-DNA insertion in the *OEP16-1* gene and at least one or two other second site mutations that might influence their phenotype (see also chapter 3.2.3; PUDELSKI *et al.*, 2009; SAMOL *et al.*, 2011a; SAMOL *et al.*, 2011b).

PTC33 (from barley) is closely related to AtTOC33/AtTOC34 of *A. thaliana* (JARVIS *et al.*, 1998). Cross-linking experiments and *in vitro* protein import studies with chloroplasts from a

TOC33-deficient *A. thaliana* mutant revealed that AtTOC33 is implicated in the import of pPORA (REINBOTHE *et al.*, 2005). Accordingly, reduced levels of PORA and total POR could be obtained after their *in vitro* import into chloroplasts and etioplasts of this mutant (JARVIS *et al.*, 1998). However, the situation seems to be more complex since *in vivo* import studies with mutants lacking TOC33 or TOC34 indicated an involvement of TOC34 rather than TOC33 in the substrate-dependent import of pPORA (KIM *et al.*, 2005).

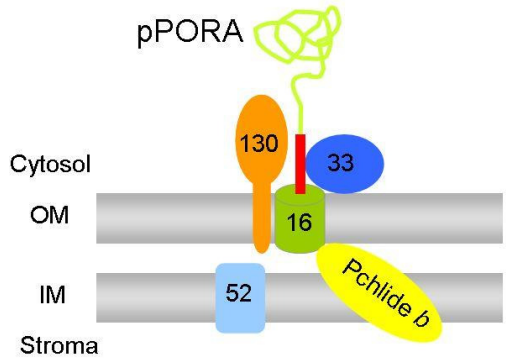

Figure 4. The four most abundant components of the Pchlide-dependent translocon complex (PTC). The PTC subunits are located in the outer (OM) or inner membrane (IM) of chloroplasts and termed PTC with a number corresponding to their molecular weight. According to REINBOTHE *et al.* (2004a) the precursor of PORA interacts at first with PTC130, then PTC33 and PTC16 and at last with PTC52.

PTC47 displayed amino acid sequence similarity to an *A. thaliana* tyrosine amino-transferase that is implicated in the α-tocopherol biosynthesis. In time-course pPORA import experiments coupled with photo-crosslinking, PTC47 could not be crosslinked with pPORA during import but interacted with PTC52 (REINBOTHE *et al.*, 2004a).

PTC52 belongs to a small, 5-member family of ubiquitous non-heme oxygenases that are characterized by two conserved motifs: a Rieske-type iron-sulfur cluster and a mononuclear iron binding site. Other members are TIC55 (chapter 1.4.2), a Chlide *a* oxygenase, a cholin monooxygenase and a pheophorbide *a* oxygenase (PAO) of which PTC52, PAO and TIC55 contain an additional amino acid motif (CxxC) that serves as target for thioredoxins indicating a thioredoxin mediated dark/light regulation of protein import and chlorophyll metabolism (BARTSCH *et al.*, 2008).

However, the PORA import seems to be more complex. *In vivo* and *in vitro* analyses by KIM & APEL (2004) and SCHEMENEWITZ *et al.* (2007) revealed that the substrate-specificity is restricted to etiolated cotyledons that do not contain cytosolic 14-3-3 proteins such that the PTC-mediated import predominates. By contrast, chloroplasts of true leaves possess 14-3-3 proteins and HSP70 that formed guidance complexes with pPORA and targeted the precursor protein to the TIC/TOC machinery and thus imported pPORA in a Pchlide-independent manner. Moreover, the existence of this substrate-dependent import of pPORA

has been questioned in relation to the existence of Pchlide *b* (KOLOSSOV & REBEIZ, 2003) and the observed Pchlide-independent pPORA import into purified chloroplasts and etioplasts (ARONSSON *et al.*, 2000; DAHLIN *et al.*, 2000, PHILIPPAR *et al.*, 2007). Instead, it could be confirmed by *in vitro* import experiments into chloroplasts isolated from barley (YUAN *et al.*, 2010) and the *in planta* studies by KIM & APEL (2004).

1.5.2 Import of Transit Sequence-less Proteins

The proteomics studies by KLEFFMANN *et al.* (2004) further indicated that a large number of plastid proteins lack cleavable transit peptides. Therefore, the existence of alternative targeting signals and import pathways was proposed. Until now, the import of two inner envelope membrane proteins lacking a cleavable transit peptide has been studied: TIC32 (NADA & SOLL, 2004) and a protein homologous to quinone oxidoreductases of bacteria, yeast and animals, a chloroplast-envelope quinone-oxidoreductase homologue (ceQORH, MIRAS *et al.*, 2002).

TIC32, a member of the TIC/TOC translocon complex, was shown to be imported as mature-sized polypeptide in a TOC159-, TOC75- and TOC34-independent way that required low energy amounts (< 20 µM ATP) and therefore excluded also the implication of molecular chaperones in the cytosol (NADA & SOLL, 2004). Import of truncated TIC32 protein versions revealed that the 10 most N-terminal amino acids are essential. A role of OEP16, OEP21 and OEP24 in TIC32 import could also be excluded (NADA & SOLL, 2004). Instead, TIC22 and TIC110 were cross-linked upon import experiments suggesting a tight association of TIC32 with other TIC subunits. Successful TIC32 import was observed in the presence of DEPC which has been shown to abolish TIC/TOC mediated import at the level of the inner envelope favouring a stop-transfer import pathway for TIC32 import.

ceQORH is a peripheral membrane protein that interacts by electrostatic interactions with the stromal site of the inner envelope membrane (MIRAS *et al.*, 2002). Based on the identification of chloroplast envelope-located redox chains and the detection of a NADPH quinone oxidoreductase activity by JÄGER-VOTTERO *et al.* (1997), ceQORH was supposed to be the first proteinaceous components of such a redox chain (MIRAS *et al.*, 2002).

The use of precursors that are imported via the TIC/TOC complex (small subunit (SSU) of the ribulose-1,5-bisphosphate carboxylase/oxygenase (RubisCO) and ferredoxin) in competition studies on the one hand and blocking of the import via the standard import pathway with respective antibodies on the other hand had shown that ceQORH import

occurs independently of TOC159 and TOC75 (MIRAS *et al.*, 2007). But proteinaceous receptor components exposed at the outer plastid surface and high energy concentrations (> 2 mM ATP + 0.1 mM GTP) were indispensable for ceQORH import. Thermolysin treatment that removed these putative protein components revealed that this protein import site seems to be evolutionary conserved in monocotyledonous (barley, wheat) and dicotyledonous (pea, *A. thaliana*) plants. *In vitro* and *in vivo* import of deletion mutants of ceQORH carried out to define import-relevant protein segments revealed that multiple internal regions are necessary for proper import (Figure 5; MIRAS *et al.*, 2007).

Figure 5. Different functional domains of the ceQORH protein are important for its import (according to MIRAS *et al.*, 2007). The overall functional organization matches that of classic transit peptides except of its enormous length and the lack of cleavage during maturation.

Whereas the N-terminus is not required for targeting, the region from amino acids 60-100 is essential for ceQORH import and sufficient to import fused GFP into plastids *in vitro*. This domain was referred to as soluble domain since it was recovered in the soluble fraction after plastid fractionation.

A more interesting observation was that (60-100)-ceQORH-GFP was imported *in vitro* into plastids in a TOC75-dependent manner. Its import was inhibited by TOC75 antibodies and by the precursor of ferredoxin (pFD). Cross-linking experiments revealed TOC159 as interaction partner. By contrast, total ceQORH interacted with a protein of ~30 kDa.

1.6 The Preprotein and Amino Acid Transporter (PRAT) Family

RASSOW *et al.* (1999) described a small family of proteins termed preprotein and amino acid transporter family based on the implication of its main members (TIM17, TIM22, TIM23 and OEP16) in the transport of proteins and/or amino acids into plastids/mitochondria. Accordingly, this family comprises four subgroups (Figure 6).

Based on the topology of the four proteins, the structure of PRAT proteins was defined: four hydrophobic segments that are connected by three hydrophilic loops form the transport

channel (Figure 6 B; RASSOW *et al.*, 1999). The characteristic PRAT motif (Figure 6 C) is found in the central region forming the second and third transmembrane helix. Another protein with similarity in the PRAT motif region is an amino acid permease (LivH) of *Escherichia coli* that is directly involved in the uptake of branched-chain amino acids. Together with its homologs in prokaryotes LivH forms an additional subfamily.

MURCHA *et al.* (2007) have shown that 17 genes encoding PRAT proteins exist in *A. thaliana* of which some may have originated by gene duplications. *In vitro* and *in vivo* localization analysis revealed either a mitochondrial or plastidic localization of all members. Only the gene product of At5g24650, HP30-2, gave rise to a dual localization in mitochondria and chloroplasts, respectively. Despite their transport function, the PRAT members differ in their localization, their gene structures and have different expression profiles (MURCHA *et al.*, 2007).

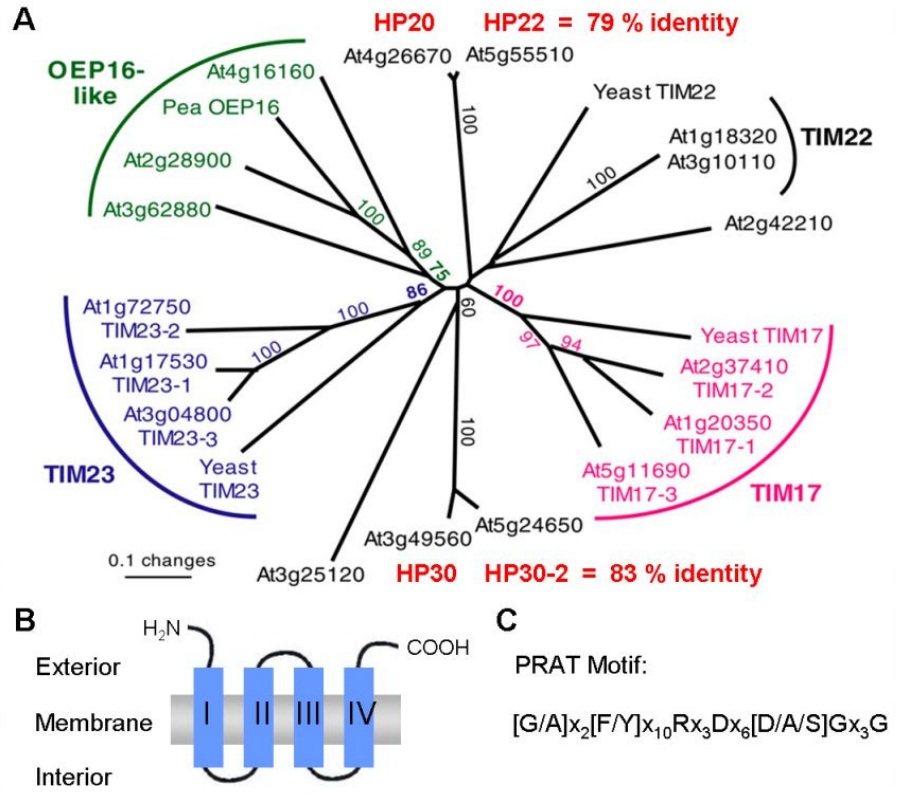

Figure 6. The PRAT family. A, Phylogenetic analysis of the PRAT proteins showing the four PRAT subfamilies in eukaryotes (from MURCHA *et al.,* 2007; modified). At2g28900, At4g16160, At2g42210 and At3g62880 encode AtOEP16-1, AtOEP16-2, AtOEP16-3 and AtOEP16-4. At1g18320 and At3g10110 encode AtTIM22-1 and AtTIM22-2. B, Common structure of PRAT proteins. The N-terminus can also be located in the interior. C, Amino acid sequence of the PRAT motif. x stands for any amino acid.

Remarkably, the PRAT family comprises two protein pairs that share a very high sequence similarity (HP20/HP22 and HP30/HP30-2; Figure 6 A) and are not classified into the four PRAT subgroups. Although all four proteins were found in the chloroplast (envelopes) by proteomics and immunological approaches (FERRO *et al.*, 2002; FERRO *et al.*, 2003; MURCHA *et al.*, 2007) the localization of HP20 and HP30 by *in vitro* import assays yielded unclear results. For example, also a localization of HP30 in the outer membrane of mitochondria was interpreted (MURCHA *et al.*, 2007). The analysis of microarray data indicated a similar expression pattern for At4g26670 (HP20) and At3g49560 (HP30) in chloroplasts which are comparable to that of At2g28900 (OEP16-1). Surprisingly, At5g55510 (HP22) and At5g24650 (HP30-2) have a transcript abundance that is different from a chloroplastic pattern and rather typical for mitochondrial proteins although both proteins were shown to be localized in chloroplasts (MURCHA *et al.*, 2007).

1.7 Aim of this Work

In order to get a deeper insight into the protein repertoire of chloroplast envelope membranes, proteomics analyses were performed which led to the identification of the proteins HP20/HP22 and HP30/HP30-2 (FERRO *et al.*, 2002; FERRO *et al.*, 2003). Because of their relationship to the PRAT family, one could speculate if these four proteins represent members of yet uncharacterized import pathways. The finding that TIC32 and PORA did not compete with ceQORH for import (MIRAS *et al.*, 2007), implies that all three proteins use different import pathways and that at least two additional yet unknown protein import pathways (that of ceQORH and TIC32) exist. On the other hand, these proteins might be active in the transport of amino acids. Therefore, the following experimental approaches were taken to analyse the function of HP20/HP22 and HP30/HP30-2:

1. Identification of proteins implicated in ceQORH import.
2. Bacterial expression of HP20/HP22 and HP30/HP30-2 and production of antibodies.
3. Isolation and characterization of *A. thaliana* knock-out lines for *HP20* and *HP30* and production of stable RNA silencing lines in order to define the role of HP20 and HP30 by a reverse genetic approach.
4. Analysis of the expression pattern of HP20 and HP30 in different plant organs and under different culture conditions.
5. Reassessment of localization studies for HP20 and HP30 by *in vivo* localization analysis of transiently and stably transformed plants.

Moreover, the role of OEP16-1 as translocation channel for pPORA was further analysed in this work. As mentioned before (chapter 1.5.1), completely different phenotypes were described for the *Atoep16-1* knock-out mutant from the Salk collection. POLLMANN *et al.* (2007) described a cell death phenotype after illumination of dark-grown *Atoep16-1* seedlings that was explained by the excess of free non-POR-bound Pchlide. This free Pchlide accumulated due to the lack of PORA import in the absence of OEP16-1 (POLLMANN *et al.*, 2007). However, PHILIPPAR *et al.* (2007) described a wild-type phenotype (and no cell death) during the greening of *Atoep16-1* mutant seedlings. A re-screen of the original Salk seed stock by PUDELSKI *et al.* (2009) revealed two additional T-DNA insertions and at least one point mutation that are present in the original seed stock and can affect the establishment of the cell death phenotype (see also chapter 3.2.3). In context of the work in this PhD thesis, SAMOL *et al.* (2011a) re-screened the original Salk seed stock of the mutant SALK_024018 and isolated and characterized pure *Atoep16-1* mutant lines (without additional T-DNA insertions besides that in the *OEP16-1* gene). Four independent OEP16-1-deficient mutants with different phenotypes during seedling development (greening of etiolated seedlings) were identified and further investigated (chapter 3.2.2.1). Two of these lines should be characterized in more detail in this PhD work. To proof that the phenotype observed by POLLMANN *et al.* (2007) was caused by the lack of OEP16-1, one of the mutant lines was complemented and thus contained the reintroduced *OEP16-1* gene. This complemented line was investigated with regard to pPORA import, the accumulation of an excess of free, photoinactive Pchlide and cell death after light exposure of etiolated seedlings.

RESULTS

2.1 Isolation of Components of the ceQORH-specific Translocon Complex

Protein transfer across the chloroplast envelope usually occurs at contact sites between inner and outer chloroplast envelope membrane which are held together by translocon complexes. To obtain a greater understanding about the translocation mechanism of a certain protein it is necessary to identify and to characterize the implicated components. For their identification SCHNELL *et al.* (1994) produced so-called envelope-bound import intermediates and purified the associated components of the import machinery together with the precursor protein.
In order to identify proteinaceous components that interact with ceQORH during its import the putative translocon complex was co-isolated with ceQORH from the chloroplast envelope membranes at the moment of its passage. Therefore, import intermediates were produced in a first step with the ^{35}S-radiolabelled precursor that contained a $(His)_6$-tag for purification. The second step comprised the purification on Ni-NTA affinity chromatography and the identification of the proteins that interacted with ^{35}S-ceQORH-GFP-$(His)_6$ during its translocation across the chloroplast envelope membranes.

2.1.1 Production of Import Intermediates

Radiolabelled chimeric ceQORH-GFP, fused with a $(His)_6$-tag at its C-terminus, was synthesized as soluble protein in *E. coli* and purified on Ni-NTA agarose. For comparison, a truncated version consisting of amino acids 60-100 of the ceQORH, the soluble domain (MIRAS *et al.*, 2007), was synthesized as a $(His)_6$-tagged GFP fusion. Since this truncated version was shown to enter chloroplasts in a TOC75- and TOC159-dependent manner, its purification from chloroplast envelopes could be analysed by Western blotting using TOC75 antibodies (MIRAS *et al.*, 2007).
The two radiolabelled chimeric proteins were urea-denatured (0.2 M final concentration) and incubated with isolated and energy-depleted *A. thaliana* chloroplasts under conditions that promote their insertion in the outer and inner chloroplast envelope membranes but prevent their complete transfer into the stroma (0.1 mM Mg-ATP and 0.1 mM Mg-GTP). After incubation, the plastids were diluted in ice-cold import buffer lacking ATP and GTP and sedimented by centrifugation. Intact plastids were re-isolated on Percoll and rapidly disrupted under hypotonic conditions. The obtained crude envelope fraction was separated

by flotation through linear sucrose gradients (10-40 %) into a light outer membrane (OM) fraction, an intermediate density fraction (OM-IM) and a slightly denser inner membrane (IM) fraction (SCHNELL *et al.*, 1994). The different fractions were collected and the corresponding proteins precipitated by 5 % (w/v) TCA and analysed by SDS-PAGE and autoradiography and Western blotting using the alkaline phosphatase system with NBT-BCIP, respectively (Figure 7).

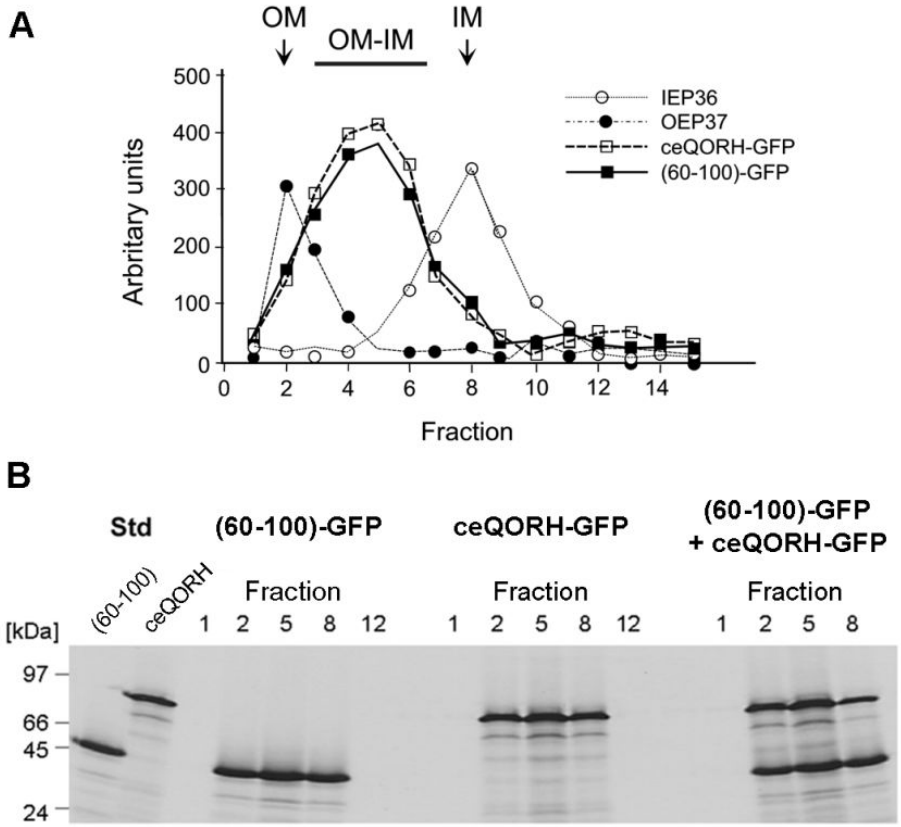

Figure 7. Production of import intermediates during the transport of bacterially expressed, urea-denatured ^{35}S-ceQORH-GFP-$(His)_6$ and ^{35}S-(60-100)-ceQORH-GFP-$(His)_6$ into isolated and energy-depleted *A. thaliana* chloroplasts. A, Distribution of OEP37 and IEP36 as well as ^{35}S-ceQORH-GFP-$(His)_6$ and ^{35}S-(60-100)-ceQORH-GFP-$(His)_6$ in the outer membranes (OM, fractions 1 and 2), OM-IM junction complexes (fractions 3-7) and inner membranes (IM, fractions 8-10), obtained after subfractionation. Arbitrary units correspond to signal intensity on Western blots after detection with NBT-BCIP and to the amount of radioactivity of the ceQORH precursors quantified by a scintillation counter. For Western blotting 20 µg proteins/lane were analysed. B, SDS-PAGE analysis of selected fractions obtained during import experiments with ^{35}S-ceQORH-GFP-$(His)_6$ and ^{35}S-(60-100)-ceQORH-GFP-$(His)_6$ as substrates that had been incubated either separately or together during import. Each lane contained 20 µg proteins. Std defines the amounts of added ^{35}S-ceQORH-GFP-$(His)_6$ and ^{35}S-(60-100)-ceQORH import substrates.

This analysis revealed that ^{35}S-ceQORH-GFP-$(His)_6$ and ^{35}S-(60-100)-ceQORH-GFP-$(His)_6$ were enriched in the mixed envelope fraction (Figure 7 A). By contrast, most of the outer

envelope membrane marker protein OEP37 was present in the light outer membrane fraction whereas most of the inner envelope membrane protein IEP36 was present in the inner membrane fraction (Figure 7 A). When ^{35}S-ceQORH-GFP-(His)$_6$ and ^{35}S-(60-100)-ceQORH-GFP-(His)$_6$ were incubated together with chloroplasts during the insertion reaction, both proteins could be purified together in equal amounts in the mixed envelope fraction (Figure 7 B). This result underscored the observation that both proteins do not use the same import machinery in the outer plastid envelope membrane (MIRAS *et al.*, 2007).

To prove whether the truncated version of ceQORH could be purified along with TOC75 during its import into isolated plastids, Western blotting with TOC75 antibodies was carried out for three fractions of mixed envelope membranes (Figure 8 A). These experiments confirmed the TOC75-dependency of import of ^{35}S-(60-100)-ceQORH-GFP-(His)$_6$ (Figure 8 A, a) and the TOC75-independency of import of ^{35}S-ceQORH-GFP-(His)$_6$ (Figure 8 A, b).

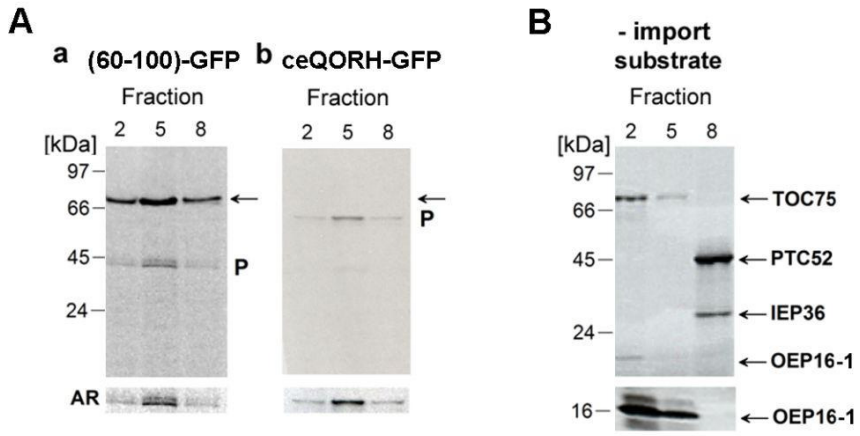

Figure 8. Co-purification of ^{35}S-ceQORH-GFP-(His)$_6$ and ^{35}S-(60-100)-ceQORH-GFP-(His)$_6$ along with TOC75 in mixed envelope fractions during their import into chloroplasts (A) and presence of typical outer and inner membrane proteins (B). Each line contained 10 µg of proteins. A, Western blots to detect TOC75 (arrow) along with (60-100)-ceQORH-GFP-(His)$_6$ (a) and ceQORH-GFP-(His)$_6$ (b) by co-precipitation with antibodies against TOC75 in gradient fractions 2, 5 and 8. The lower panels show representative autoradiograms (AR) to detect ^{35}S-ceQORH-GFP-(His)$_6$ (a) and ^{35}S-(60-100)-ceQORH-GFP-(His)$_6$ (b). P stands for precursor protein. B, Identification of TOC75, PTC52, IEP36 and OEP16-1 in fractions 2, 5 and 8 of chloroplasts incubated in the absence of the import substrates. The upper panel shows a Western blot probed with a mixed antiserum against the indicated proteins. The lower panel shows a replicate filter probed with OEP16-1 antiserum.

When the import reactions were carried out in the absence of the import substrates, OEP16-1 and TOC75, which constitutes the major import site for cytosolic precursors, were likewise present only in the outer envelope fraction (Figure 8 B). Hereby, the lower abundance of the

OEP16-1 *versus* TOC75 may reflect its decreased expression in chloroplasts as compared to etioplasts (REINBOTHE *et al.*, 2004b). The absence of TOC75 in the OM-IM fraction proved that formation of junction complexes between the TOC and TIC machineries requires ^{35}S-(60-100)-ceQORH-GFP-$(His)_6$. On the other hand, the detection of small amounts of the inner envelope marker proteins IEP36 and PTC52 (REINBOTHE *et al.*, 2004a) in the OM-IM fraction (Figure 8 B) suggested the presence of fragments of outer and inner membranes presumably held together by contact sites that had been pre-established in the absence of added import substrate (SCHNELL & BLOBEL, 1993; SCHNELL *et al.*, 1994; REINBOTHE *et al.*, 2004a).

2.1.2 Purification and Identification of Envelope Proteins Involved in ceQORH-Import

For purification of the envelope proteins that interact with ^{35}S-ceQORH-GFP-$(His)_6$ during import, the OM-IM fraction was subjected to mild detergent solubilisation with 2 % Triton-X100 (SCHNELL *et al.*, 1994; REINBOTHE *et al.*, 2004a). The resulting higher molecular weight protein complexes that were composed of the precursor protein and components of its respective translocon were subsequently purified on Ni-NTA agarose and the proteins were analysed by SDS-PAGE, Coomassie staining as well as autoradiography (Figure 9).

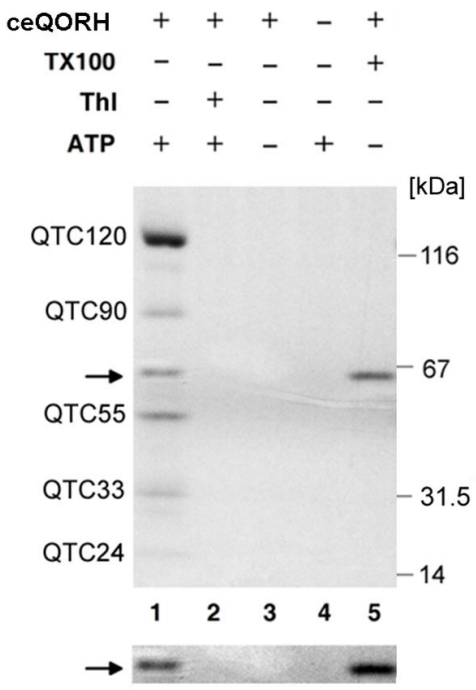

Figure 9. Purification of envelope proteins bound to ^{35}S-ceQORH-GFP-$(His)_6$ during its import into purified, energy-depleted *A. thaliana* chloroplasts. Coomassie staining of envelope proteins that interact with ^{35}S-ceQORH-GFP-$(His)_6$ (arrows) under different conditions (in the presence or absence of either Triton X-100 (TX100), thermolysin (Thl) or ATP; lanes 1-5) as described in the text. QTC stands for ceQORH translocon component and the number for the relative molecular weight. The lower panel shows an autoradiogram of ^{35}S-ceQORH-GFP-$(His)_6$ in the various types of incubation mixtures.

Mainly 5 different polypeptide bands with the size of 120, 90, 55, 33 and 24 kDa as well as the import substrate were identified. As estimated from their staining intensities on the SDS gel, the proteins of 90, 55 and 33 kDa were purified in almost stoichiometric amounts (Figure 9, lane 1). By contrast, the 120 kDa protein was most abundant, while the 24 kDa protein band was underrepresented. The five ceQORH-interacting proteins were designated QTC120, QTC90, QTC55, QTC33 and QTC24 and identified by a number indicating the respective size estimated from the Coomassie stained SDS gel.

In order to verify that the 5 QTC proteins interacted with ^{35}S-ceQORH-GFP-$(His)_6$ specifically in an import-dependent manner, several control experiments were carried out:

First, chloroplasts were pre-treated with thermolysin prior to the import step and re-purified on Percoll. This treatment eliminated proteinaceous components on the outer plastid surface that were shown to be necessary for ceQORH import (MIRAS *et al.*, 2007). As result, these thermolysin-treated plastids were rendered unable for importing ^{35}S-ceQORH-GFP-$(His)_6$ and forming QTCs (Figure 9, lane 2).

Second, omission of Mg-ATP during incubation yielded neither ^{35}S-ceQORH-GFP-$(His)_6$ nor the co-purifying QTCs (Figure 9, lane 3), a result that underscored the requirement of Mg-ATP for ceQORH import (MIRAS *et al.*, 2007).

Third, an import reaction in the absence of import substrate did not yield envelope polypeptides that bound to Ni-NTA agarose (Figure 9, lane 4). This control excluded the non-specific binding of envelope polypeptides present in residual OM-IM junction complexes that may have formed in the absence of precursor.

Fourth, ^{35}S-ceQORH-GFP-$(His)_6$ was added during the solubilisation of the OM-IM fraction in order to demonstrate that it interacted with envelope polypeptides in an import-dependent reaction (Figure 9, lane 5). As result, no QTCs were detectable on the Coomassie stain.

For identification of the five ceQORH-interacting partners, the QTC bands were cut out from replicate gels and subjected to micro sequence analysis according to CHANG (1983). The obtained partial amino acid sequences (Figure 10 A) were aligned with predicted amino acid sequences retrieved from public data banks via protein BLAST analysis. This approach identified QTC24 as being related to a protein annotated as Q9SZ09, also named HP20, which is encoded by the *A. thaliana* gene At4g26670 (chapter 1.6). All three peptide sequences obtained for QTC24 were identified in the predicted amino acid sequence of HP20 (Figure 10 B). Fewer consensus sequence parts were found when the three peptide sequences were compared to the predicted HP22 protein sequence which is related to HP20 (MURCHA *et al.*,

2007). However, the limited sequence information obtained for QTC24 and the quite large extent of identical amino acids in HP20 and HP22 made an unambiguous identification of QTC24 difficult. The presence of all three peptide motifs in the amino acid sequence of HP20 nevertheless favours the conclusion that QTC24 is identical with HP20. Sequencing of the other QTC bands so far did not provide conclusive results and was therefore not persued further.

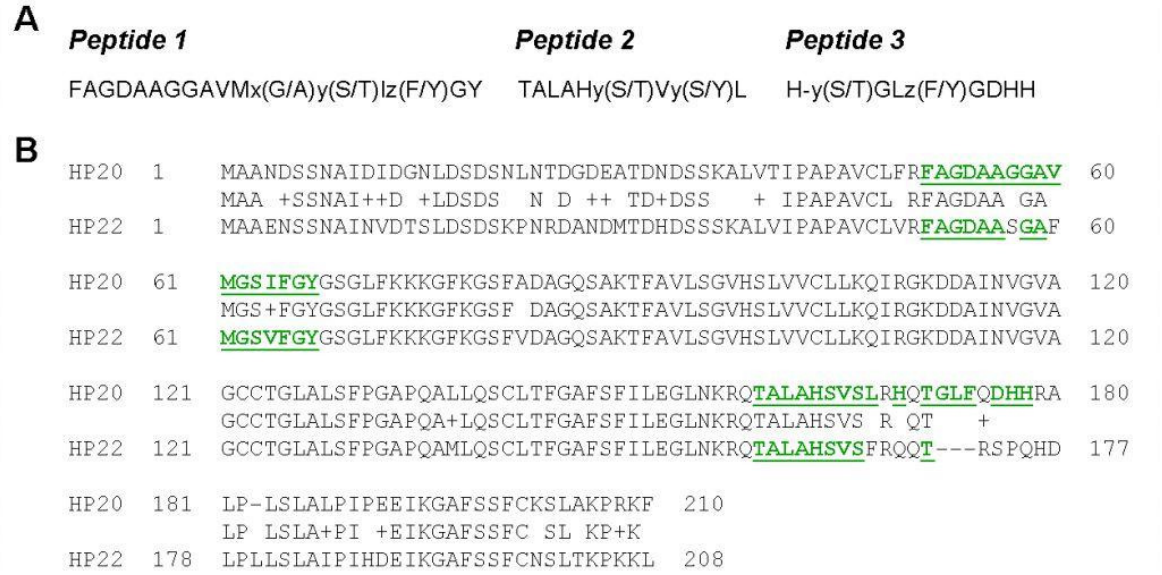

Figure 10. Identification of QTC24. A, Cyanogen bromide-derived and endoproteinase Lys C-derived amino acids sequences of the purified *A. thaliana* QTC24 protein obtained by micro sequence analysis. B, Amino acid alignment of the protein encoded by At4g26670 (HP20) corresponding to QTC24 and its closest relative encoded by At5g55510 (HP22). Peptide sequences identified by micro sequence analysis are highlighted in green colour and underlined.

2.2 Expression and Purification of HP20-$(His)_6$ and HP30-$(His)_6$ – Production and Characterization of Antibodies

2.2.1 Expression and Purification of HP20-$(His)_6$ and HP30-$(His)_6$

For heterologous expression of the corresponding proteins as $(His)_6$-tagged forms allowing their purification via Ni-NTA affinity chromatography the cDNAs of *HP20*, *HP22*, *HP30* and *HP30-2* were cloned into the Gateway destination vector pDEST17. The respective cDNAs were first amplified without their start codon using primers with *attB* sites (Gateway) and integrated into the donor vector pDONR221 by BP reactions. The sequence of the resulting entry-clones was analysed by sequencing using the primers M13-fwd and M13-rev (GATC, Konstanz). Entry-clones with the correct sequence were taken to perform LR reactions with pDEST17 to give rise to expression clones.

Arabinose-induced protein expression was performed in *E. coli* strain BL21-AI. Different clones for each protein were obtained and analysed by pilot expression experiments to find clones with the strongest expression of the recombinant proteins. Therefore, protein expression was induced by the addition of arabinose to 50 ml bacterial cultures. Uninduced control cultures were grown in parallel. Cultivation was performed for a total of 4 h and aliquots were taken after each hour during this time. Protein extracts were prepared from these samples and analysed by SDS-PAGE and Coomassie staining (Figure 11 A, a and D, a). The bacterially expressed plant proteins were identified by Western blotting using an anti-His antibody (Figure 11 A, b and D, b). For both HP20-$(His)_6$ and HP30-$(His)_6$ an *E. coli* clone with strong expression of the plant proteins could be identified.

Next, the bacterial pellets were separated into soluble and insoluble protein fractions in order to decide whether the proteins were present in the soluble fraction or formed insoluble aggregates referred to as inclusion bodies as a result of the strong expression (Figure 11 B and E). This information was necessary to determine the conditions of the purification scheme (native or denaturing conditions). As both proteins were already identified by proteomics analyses in the envelope membranes of chloroplasts (FERRO *et al.*, 2003), one could expect the formation of inclusion bodies due to the insoluble nature of hydrophobic transmembrane domains present in both proteins. Indeed, the two proteins were only found in the insoluble fraction (Figure 11 B and E). The small amount of HP20-$(His)_6$ in the soluble fraction (Figure 11 B) seemed to be rather the consequence of problems to clearly separate both fractions resulting in a contamination from the insoluble fraction. Alteration of the cultivation temperature during the heterologous protein expression did not change the solubility of both proteins.

Based on these findings, both HP20-$(His)_6$ and HP30-$(His)_6$ were purified under denaturing conditions and solubilised with 8 M urea. After Ni-NTA agarose affinity chromatography from the solubilised fractions, the eluated proteins still contained some contaminations, as verified by SDS-PAGE and silver staining (Figure 11 C, a and F, a). For this reason, larger volumes of eluates were separated in preparative gels, the proteins stained with Coomassie and the protein bands corresponding to HP20-$(His)_6$ and HP30-$(His)_6$, respectively, were excised and the gel slices send for antibody production.

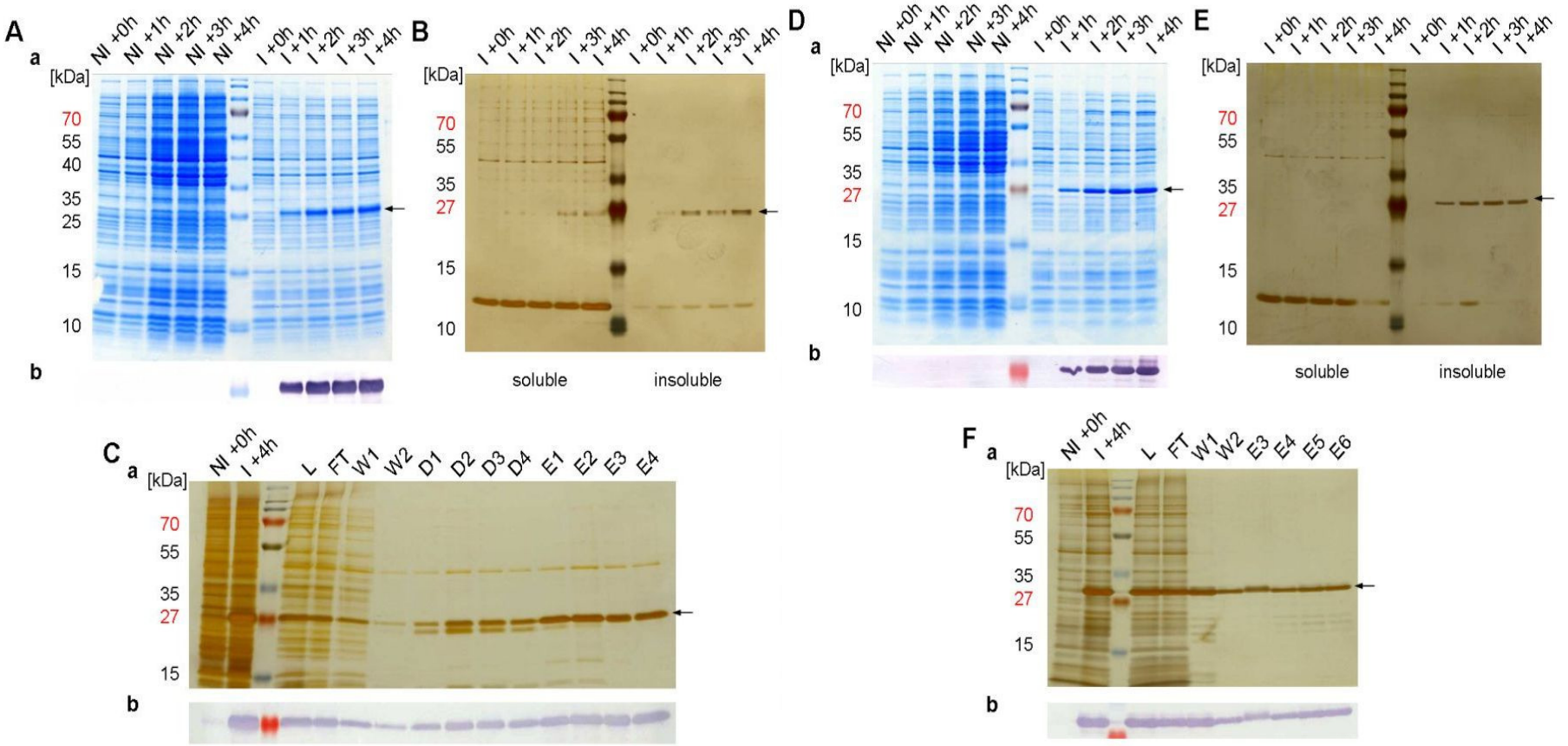

Figure 11. Expression and purification of HP20-$(His)_6$ (A-C) and HP30-$(His)_6$ (D-F). A and D, Expression of HP20-$(His)_6$ (predicted size of 24.3 kDa) and HP30-$(His)_6$ (30.5 kDa) in an induced (I) *versus* uninduced culture (NI) analysed by SDS-PAGE and Coomassie staining (a) or Western blotting with anti-His antibodies (b). 10 µl of each sample were loaded onto the gels. B and E, Separation of induced culture samples into soluble and insoluble fractions and analysis by SDS-PAGE and silver staining. 10 µl of the supernatant samples (soluble fraction) and 5 µl of the pellet samples (insoluble fraction) were loaded onto the gels. C and F, Purification via Ni-NTA affinity chromatography and analysis by SDS-PAGE and silver staining (a) and by Western blotting with anti-His antibodies (b). 2 µg of proteins of each fraction were loaded onto the gel. The arrows mark the bacterially expressed and purified proteins. Abbreviations: L, cleared lysate; FT, flow through; W1 and W2, washings; D1-4 and E1-4 or E3-6, eluates of the purified proteins with the corresponding buffer.

2.2.2 Antibody Characterization

To get a first insight about the functionality and specificity of the raised antibodies against HP20-$(His)_6$ and HP30-$(His)_6$, Western blot analyses were carried out 39 and 67 days after the onset of immunization of two independent rabbits each used per antigen. Dilutions of 1:500 (after 39 days) and 1:1000 (after 67 days) were able to detect the purified proteins whereas the preimmune serum was not reactive (not shown). For the final antisera that were obtained after 82 days after the onset of immunization, initial dilutions of 1:2000 were tested with the purified proteins (Figure 12). Both, the HP20 and HP30 antibodies recognized the corresponding bacterially expressed and purified protein, respectively, but the antibodies against HP30-$(His)_6$ had a much higher sensitivity (Figure 12 B). These antibodies were able to detect 25 ng of the purified protein whereas the antibodies raised against HP20-$(His)_6$ could hardly detect this amount of loaded purified protein (Figure 12 A). Antibody dilutions of 1:1000 were used in the following experiments.

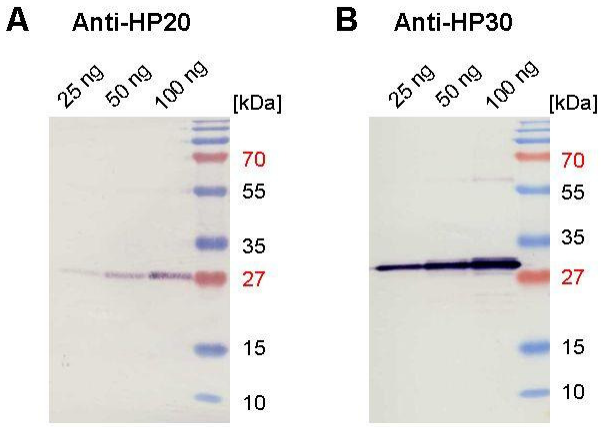

Figure 12. Detection of the purified proteins HP20-$(His)_6$ (A) and HP30-$(His)_6$ (B) by their antibodies (shown for the better working antisera). Quantities of loaded purified HP20-$(His)_6$ and HP30-$(His)_6$ proteins are indicated.

Next, the cross-reactivity of these antibodies to HP20-$(His)_6$ and HP30-$(His)_6$ as well as their close relatives HP22-$(His)_6$ and HP30-2-$(His)_6$, respectively, was investigated. HP20 and HP30 show a very high amino acid identity to their close relatives HP22 (79 %) and HP30-2 (84 %), respectively, as well as an identity of 28 % to each other. In the latter case, most of the identical and similar amino acids were found in the PRAT motif region. Therefore, cross-reactivity of the raised antibodies had to be expected.

To test this hypothesis, the cDNA sequences of HP22 and HP30-2 were cloned without their start-codon into the vector pDEST17 and the arabinose-induced expression was analysed by pilot expression experiments as described for HP20-$(His)_6$ and HP30-$(His)_6$ (chapter 2.2.1).

The identity of the bacterially expressed plant proteins was verified by Western blotting using anti-His antibodies (Figure 13 A). Then, the raised antibodies were directly tested with bacterial protein extracts of clones expressing the plant proteins as well as with the purified proteins (Figure 13 B and C).

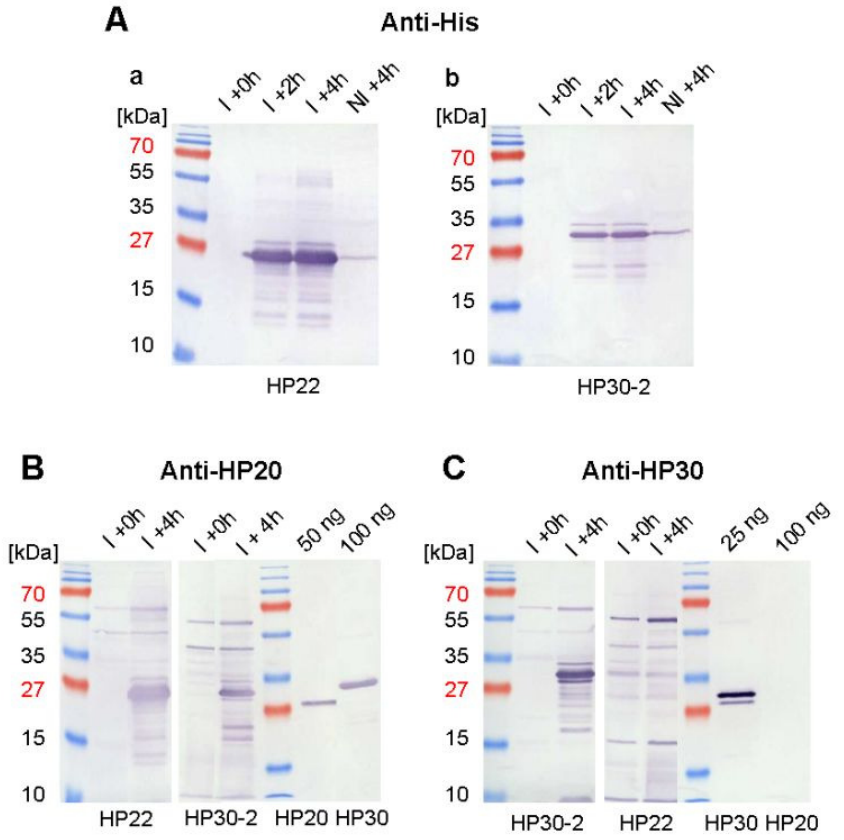

Figure 13. Cross-reactivity of the HP20 and HP30 antisera with HP30-(His)$_6$ and HP20-(His)$_6$ as well as with HP22-(His)$_6$ and HP30-2-(His)$_6$, respectively. A, Expression of HP22-(His)$_6$ (a) and HP30-2-(His)$_6$ (b) after induction with arabinose (I) for 0, 2 and 4 h in comparison with a uninduced control culture (NI) after 4 h of cultivation and detection by anti-His antibodies. The proteins had a calculated size of 25.0 kDa (HP22-(His)$_6$) and 30.4 kDa (HP30-2-(His)$_6$), respectively. 10 µl of each bacterial protein extract were loaded onto the gel. B, Cross-reactivity test of the HP20 antibodies. Comparison of the induced bacterial culture at time point 0 with 4 h of expression of HP22 and HP30-2 (10 µl of each sample loaded). Loaded quantities of purified HP20-(His)$_6$ and HP30-(His)$_6$ proteins are indicated. C, as B, but showing the test for the HP30 antibodies.

The antibodies raised against HP20-(His)$_6$ were able to detect HP22-(His)$_6$, HP30-(His)$_6$ as well as HP30-2-(His)$_6$. By contrast, the antibodies raised against HP30-(His)$_6$ showed a higher specificity and detected only HP30-2-(His)$_6$. A similar observation was also reported by MURCHA *et al*. (2007).

In final studies, the two antibodies were used to detect the corresponding proteins in plant extracts, using different amounts of total leaf proteins prepared from 3 weeks-old *A. thaliana* wild-type plants (Figure 14).

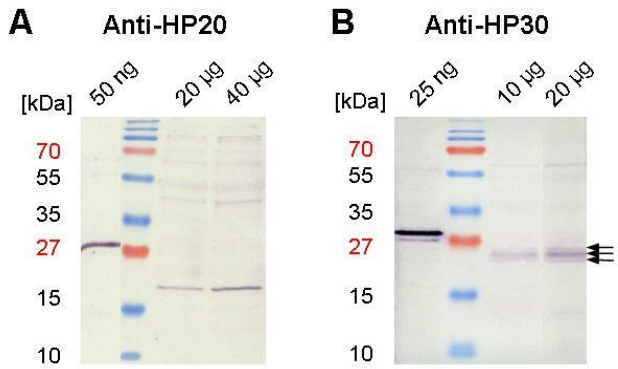

Figure 14. Detection of the purified proteins HP20-$(His)_6$ and HP30-$(His)_6$ (on the left-hand side of the protein marker) and their counterparts in total leaf extracts (on the right-hand side of the protein marker). A, Test of the HP20 antibodies. B, Test of the HP30 antibodies. Loaded protein quantities are indicated. Arrows mark 3 distinct protein bands detected by the HP30 antibodies.

The antibodies raised against HP30 recognized 3 distinct protein bands with molecular masses around 30 kDa matched that could correspond to the *A. thaliana* HP30 protein. On some but not all of the many tested Western blots, only the middle protein was seen (Figure 18 E and K). This intermediate size protein band may correspond to HP30 since it could not be identified in total leaf extracts of the corresponding *A. thaliana* knock-out lines (Figure 18 E and K). The upper band might be HP30-2 based on its migration compared to that of HP30-$(His)_6$ and HP30-2-$(His)_6$. Moreover, on some other blots all three protein bands could not be detected in the corresponding *A. thaliana* mutants (Figure 34), suggesting that all three may represent HP30 isoforms which are the result of post-translational modifications. Similarly, inconclusive results were obtained when protein extracts prepared from chloroplasts were applied for this analysis (data not shown).

The antibodies raised against the bacterially expressed HP20 protein detected a protein of ~22 kDa in total leaf extracts, although high background signals were seen. This size of the ~22 kDa band seems to be in agreement with the predicted size of the *A. thaliana* HP20 protein (21.8 kDa). However, it cannot be excluded that this ~22 kDa protein may be visible due to HP22 since both proteins share a very high degree of identical amino acids and bacterially expressed HP22-$(His)_6$ was recognized by these antibodies.

Surprisingly, no immunoreactive signal was obtained when protein extracts from isolated chloroplasts were analysed (Figure 15 B, Chlpl). Because HP20 and HP22 are integral membrane proteins (see chapter 2.4.3), this could mean that most of their antigenic epitopes may be inaccessible in the envelope membranes. Alternatively, the proteins may be hypersensitive to proteases released from various compartments during plastid isolation and fractionation. Last but not least, the proteins may fold in a way such that they are no longer recognized as antigens when incorporated into the envelope membrane of chloroplasts. In line with this view, *Athp20* mutants expressing a 35S-HP20 construct under the strong 35S cauliflower mosaic virus promotor, in which one might expect high quantities of the corresponding protein in case of multiple insertions of the "foreign" cDNA, did not provide a specific signal on the Western blots (Figure 15 B). That immunoreactive bands were detected in the protein extracts from two independent *HP20* knock-out mutant lines is suggestive of the leakiness of the mutants or of cross-reactivity of the antibodies with HP22 (Figure 15 A).

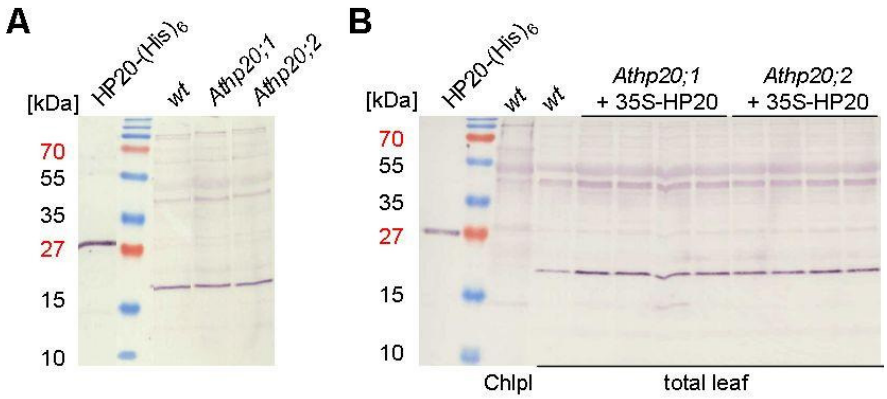

Figure 15. Attempts to identify HP20 in different *A. thaliana* plant types. A, Comparison of wild-type and *Athp20* mutants. Each lane contained 40 µg of total proteins or 50 ng of bacterially expressed and purified HP20-$(His)_6$ protein. B, Comparison of proteins of wild-type chloroplasts (Chlpl) with total leaf extracts of wilt-type and of plants of individual *Athp20+35S-HP20* lines (T_2 generation). Each line contained 20 µg proteins or 50 ng of purified HP20-$(His)_6$ protein, respectively.

Given the difficulty to raise a highly specific antiserum against HP20, a QTC24-specific antiserum was purified from an antiserum against total outer envelope membrane proteins using the ceQORH cross-linked QTC24. Therefore, large scale (50-fold) import experiments were performed with DTNB-activated ceQORH-$(His)_6$ as described for OEP16-1 (REINBOTHE *et al.*, 2004b) and the mass amounts of cross-link product obtained were reduced by 2-mercaptoethanol to yield ceQORH and QTC24. After SDS-PAGE, the QTC24 protein

band was blotted onto a nitrocellulose membrane and used for antiserum clearing as described by HÖHFELD *et al.* (1991). This QTC24 antiserum was able to detect HP20/QTC24 in chloroplasts (for example Figure 22). The specificity of the reaction with HP20 was confirmed by its detection in *A. thaliana* wild-type chloroplasts *versus* chloroplasts of the mutant *Athp20;2,* as the corresponding protein band was absent in the mutant (Figure 25). Nevertheless, since this antiserum was purified against the cross-linked QTC24 that might represent either HP20 or HP22 all subsequent results, especially those in chapter 2.5.1, must be considered with caution.

2.3 Molecular-biological Characterization of *A. thaliana* Knock-out Lines

A. thaliana T-DNA insertion lines were identified in the Salk Institute Genomic Analysis Laboratory collection (ALONSO *et al.*, 2003). Individual plants of the T_3 generation were directly tested by PCR for homozygosity and the position of the T-DNA insertion in the gene of interest was identified by sequencing PCR products obtained with a combination of a forward/reverse gene-specific primer and LBa1 primer specific for the left border of Salk T-DNA (Figure 16; detailed shown in Figure 17 and Figure 18).

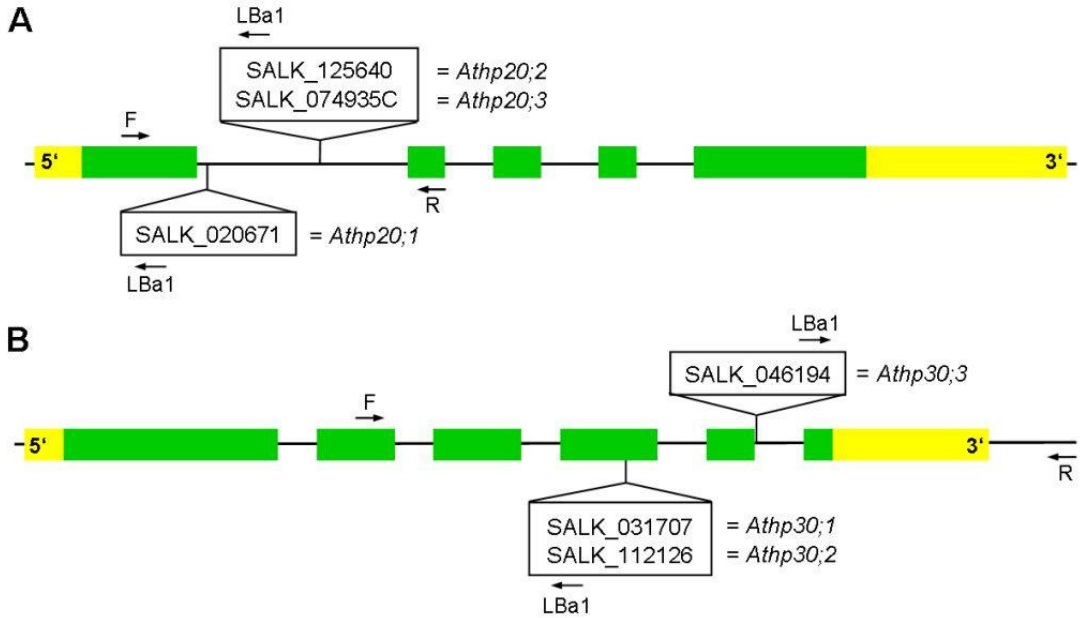

Figure 16. Gene structures of At4g26670 (A) and At3g49560 (B) and locations of the T-DNA insertions in the indicated SALK-lines. 5'- and 3'- untranslated regions are shown in yellow, exons and introns in green and black solid lines, respectively. The ~4.5 kb T-DNA insertions are not drawn to scale. The lines were renamed as indicated. R and F as well as LBa1 mark primers used for PCR analysis (Table 8).

It is important in genetic studies to have at least two or more independent mutant allels for a given gene since the introduction of T-DNA can lead to mutations such as small deletions at the T-DNA insertion site but also to massive rearrangements of host chromosomal DNA (LATHAM *et al.*, 2006). Also the removal of additional undesired T-DNAs (e.g., during back-crosses with the wild-type) can result in secondary effects such as point or footprint mutations eventually provoking phenotypes that are not related to the knock-out of the gene of interest.

Sequence analysis revealed the same position of the T-DNA insertions in lines *Athp20;2* and *Athp20;3* as well as in lines *Athp30;1* and *Athp30;2*, respectively. Therefore, only one of the two mutants was chosen for further work. A second individual mutant line for each gene was provided by the mutants *Athp20;1* and *Athp30;3*.

Moreover, we identified an additional, fourth *Athp20* knock-out line (SALK_125736, *Athp20;4*) that contained ideally one T-DNA insertion as determined by Southern blotting (data not shown). Since the other analysed *Athp20* mutants had multiple T-DNA insertions (Figure 17) and no other knock-out mutants could be identified in the available databases, the focus laid at first on this mutant. Different sets of forward/reverse gene-specific primer and LBa1 (and LBb1, a second primer to characterize Salk knock-out lines hybridizing ~200 bp upstream of LBa1) as well as modified PCR conditions did not give rise to any PCR products. These detailed PCR studies and additional segregation analyses showed that the single T-DNA insertion present in this line is not located in the *HP20* gene.

For the four selected knock-out lines, *Athp20;1* and *Athp20;2* as well as *Athp30;2* and *Athp30;3*, homozygous plants were established and characterized further by Southern, Northern and Western blotting (the latter only for HP30), respectively, as well as growth tests on MS agar medium containing kanamycin (Figure 17 and Figure 18).

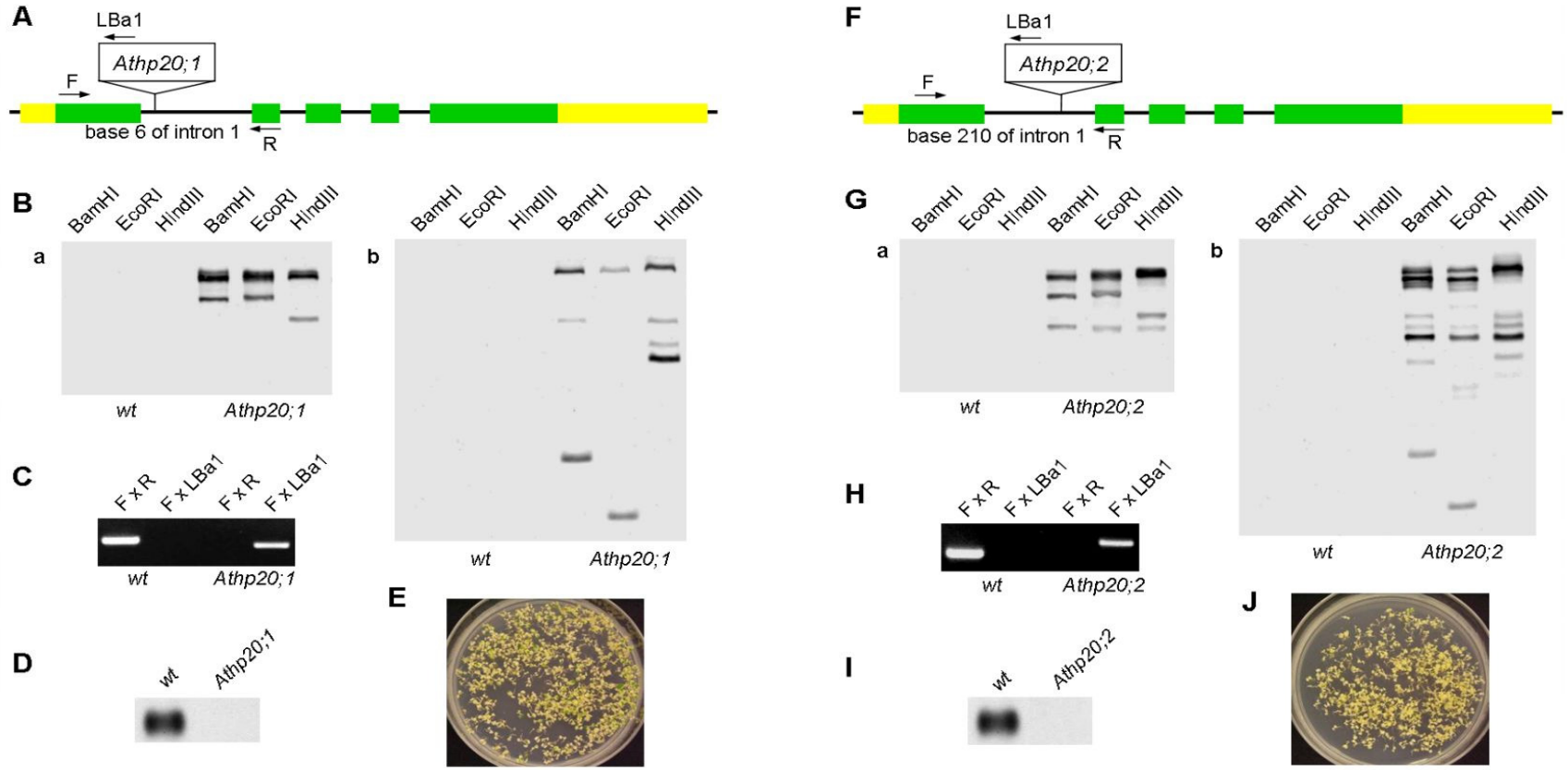

Figure 17. Basic characterization of the T-DNA insertion lines *Athp20;1* (SALK_020671) and *Athp20;2* (SALK_125640; back-crossed once with the wild-type). A and F, Schematic presentation of the *HP20* gene indicating the position of first base of the T-DNA insertions as determined by sequencing PCR products amplified with primers F and LBa1. B and G, Southern blot analysis showing the number of T-DNA insertions by probing against the kanamycin resistance gene of Salk T-DNA (a) and a fragment of the left border (b) after digestion of 10 µg genomic DNA with *Bam*HI, *Eco*RI and *Hind*III. C and H, PCR-genotyping demonstrating the homozygosity of the mutants by absence of the wild-type allele (primers F x R). Primers F and R correspond to HP20PF and HP20PR (Table 8). The sizes of the products are 610 bp (R x F, only obtained with wild-type DNA) and ~ 547 bp and ~ 745 bp (F x LBa1, obtained with mutant DNA). D and I, Northern blot analysis to detect *HP20* transcripts using mRNA isolated from 3 weeks-old plants. E and J, Growth behaviour on selective MS agar containing kanamycin.

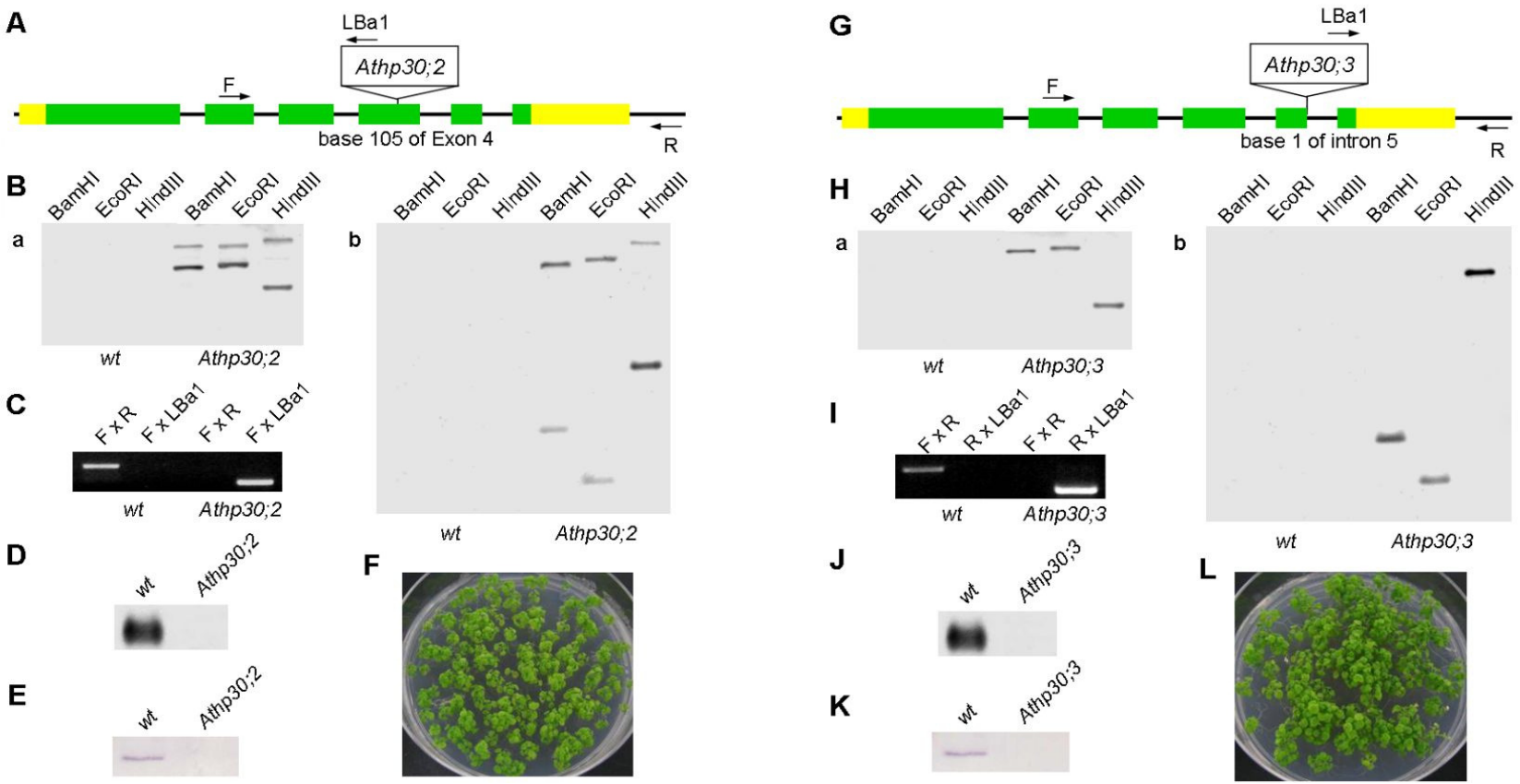

Figure 18. Basic characterization of the T-DNA insertion lines *Athp30;2* (SALK_112126) and *Athp30;3* (SALK_046194). A and G, Schematic presentation of the *HP30* gene indicating the position of the first base of the T-DNAs as determined by sequencing PCR products amplified with primers F/R and LBa1. B and H, Southern blot analysis showing the number of T-DNAs by probing against the kanamycin resistance gene of Salk T-DNA (a) and a fragment of the left border (b) after digestion of 10 µg genomic DNA with *Bam*HI, *Eco*RI and *Hind*III. C and I, PCR-genotyping demonstrating the homozygosity of the mutants by absence of the wild-type allele (primers F x R, corresponding to HP30GT1 and HP30GT2 (Table 8)). The sizes of the products are 1016 bp (R x F, obtained with wild-type DNA) and ~ 742 bp and ~ 750 bp (F x LBa1, obtained with mutant DNA). D and J, Northern blot analysis to detect *HP30* transcripts using mRNA isolated from 3 weeks-old plants. E and K, Western blot analysis of total leaf extracts (40 µg protein/lane) of 3 weeks-old plants and anti-HP30 antibodies. F and L, Growth behaviour on selective MS agar containing kanamycin.

The T-DNA insertions in *Athp20;1* and *Athp20;2* were located in the first intron of the *HP20* gene (Figure 17 A and F). Although there was a risk that insertions located in introns would be spliced out during mRNA-maturation and would have no effect on the gene expression, no transcripts could be detected in the mutants by Northern blot analysis in comparison to wild-type (Figure 17 D and I). This result was confirmed by RT-PCR (not shown). Unfortunately, the absence of the HP20 protein could not be verified (see explanations in chapter 2.2.2), but can be expected because of the transcript absence. Southern blot analyses did not reveal a clear picture on the exact number of T-DNA insertions because the use of different probes for hybridization resulted in different numbers of signals in both mutants (Figure 17 B and G). Augmentation of the temperature during washing did not eliminate putative "false-positive" signals obtained due to unspecific hybridization. Therefore, it can be concluded that line *Athp20;1* has two and line *Athp20;2* at least three T-DNA insertions (Figure 17 B and G). Moreover, the mutant *Athp20;2* had already been crossed once with the wild-type in order to remove extragenic insertions/mutations. Additional back-crosses of both lines with wild-type did not reduce the number of T-DNA insertions. Finally, both mutant lines did not grow on selective MS agar medium containing kanamycin (Figure 17 E and J) although the *nptII* genes were present in the T-DNAs as verified by PCR (not shown).

The *Athp30;2* knock-out line had a T-DNA insertion in exon 4 (Figure 18 A) whereas the insertion in line *Athp30;3* started immediately after the end of exon 5 (Figure 18 G). By contrast to the insertions in the other Salk lines, this insertion was found to be present in an inverse orientation (Figure 18 G and I). The absence of the *HP30* transcript and protein was verified by Northern and Western blotting using the antibodies produced against the bacterially expressed HP30-$(His)_6$ protein (Figure 18 D, E and K, J). Southern blots indicated the presence of two insertions in the case of line *Athp30;2* (Figure 18 B) and a single insertion for *Athp30;3* (Figure 18 H). The hybridization with the probe for the kanamycin resistance gene as well as the probe for a segment of the left border of the T-DNA insertion resulted in exactly the same number of insertions for each line. Finally, both *Athp30* mutants showed resistance for kanamycin (Figure 18 F and L).

2.4 Expression and Localization of HP20 and HP30

2.4.1 Database Analysis and Prediction of the Subcellular Localization of HP20 and HP30

To get an impression about the expression of the *HP20* and *HP30* genes, a data base analysis was performed using the Bio-Array Resource (BAR) of the University of Toronto that is based on microarray data (WINTER *et al.*, 2007).

Both HP20 and HP30 showed a very weak overall expression is all tissues analysed (Figure 49 and Figure 50; appendix I). For comparison, a gene with a strong expression, the light harvesting chlorophyll *a/b*-binding protein of photosystem II (*LHCII*; *At2g05070*) had 10-times higher values. Significant amounts of *HP20* transcripts were found in imbibed seeds, in rosette leaves and in the shoot apex. The largest amounts of *HP30* transcripts were found in dry and imbibed seeds, in rosette leaves and in buds. On the tissue level, an accumulation of HP30 could be found in the shoot apical meristem (peripheral zone).

Other data sets, for example that of hormone and chemical treatments as well as biotic and abiotic stress treatments, did not reveal any kind of increased or regulated expression of both genes. However, a minimal light-dependent regulation of *HP20* and *HP30* expression seems to occur. Thus, 35 days-old plants that were grown on soil under light conditions of 12 h day/night cycles (130 µE white light) showed a slightly higher expression of *HP20* at the end of the light period. Also 7 days-old seedlings grown in day/night cycles (> 90 µE white light) expressed *HP20* in a weak diurnal rhythm. The expression of *HP30* was similar but the accumulation was shifted into the early beginning of the dark phase.

On order to reassess and to get an idea about the subcellular localization of both proteins, diverse prediction programs were applied (Table 1). For comparison, the precursor of ferredoxin (FD) from *Silene pratensis*, a protein with a typical N-terminal transit peptide of 48 amino acid residues that directs the protein towards the chloroplast stroma (SMEEKENS *et al.*, 1985), was used. Additionally, the ceQORH protein which lacks the classic transit peptide (MIRAS *et al.*, 2007) and CAH1, the stroma-localized carbonic anhydrase 1 of *A. thaliana* that was shown to be imported via the secretory pathway (VILLAREJO *et al.*, 2005), were chosen for comparison.

All prediction programs assigned the precursor of ferredoxin unambiguously to the chloroplast. The predicted size of the transit peptide of 46 amino acids was very close to the

described 48 amino acids (SMEEKENS *et al.*, 1985). CAH1 might have a signal peptide of 18-21 amino acids that did not correspond to a plastidic transit peptide and was almost consonantly predicted to use the secretory pathway (Golgi apparatus and ER). These facts, apart from the length of the signal peptide, corresponded to the published data by VILLAREJO *et al.* (2005).

Table 1. Prediction of localization of selected precursor proteins with different programs. ER stands for endoplasmatic reticulum; Golgi for Golgi apparatus and Mito for mitochondria. The numbers indicate the length of the transit peptide.

Program	FD	ceQORH	HP20	HP30	CAH1
ChloroP 1.1	plastid (46)	not plastidic	not plastidic	not plastidic	not plastidic (18)
TargetP 1.1	plastid (46)	– [a]	– [a]	– [a]	secretory (21)
WoLF PSORT	plastid	cytosol	nucleus	cytosol	extracellular
Predotar	plastid	elsewhere[b]	elsewhere[b]	elsewhere[b]	ER
MultiLoc	plastid	cytosol	plastid	cytosol	Golgi/Mito

[a] no prediction of localization and no presence of a chloroplast transit peptide, nor a mitochondrial targeting peptide nor a signal peptide for the use of the secretion pathway

[b] no localization in chloroplasts, mitochondria and the endoplasmatic reticulum

The prediction for ceQORH resulted in contradictory localizations mainly due to the lack of the transit peptide. Its targeting through the secretory pathway was conceptually excluded, based on previous *in vitro* import experiments using cell-free systems (MIRAS *et al.* (2007) and the data shown in chapter 2.1). Contradictory results of prediction were also obtained for HP20 and HP30.

2.4.2 Subcellular Localization of HP20 and HP30

The localization of HP20 and HP30 has previously been analysed *in vitro* by performing import studies into isolated mitochondria and chloroplasts and *in vivo* by ballistic transformation of *A. thaliana* suspension cells with the fluorescence-tagged precursors (MURCHA *et al.*, 2007). However, the results led to some incertitude concerning the localization in multiple organelles. For example, HP20 could not be imported *in vitro* into isolated mitochondria and chloroplasts and the radiolabelled precursor was degraded by protease treatment. *In vivo* localization of C- and N-terminally tagged GFP did also not present a clear result since N-terminally tagged GFP was not detected in any compartment and C-terminally tagged GFP did not result in a pattern that corresponded to their

localization in plastids or mitochondria. Only Western blot analysis revealed a plastidic localization of HP20.

On the one hand, HP30 protein was clearly localized in chloroplasts by *in vitro* import experiments and *in vivo* by fluorescence tagging and Western blotting. On the other hand, *in vitro* import resulted also in localization in mitochondria as the protease-protected precursor could be detected even in the presence of valinomycin, an inhibitor of mitochondrial import that destroys the membrane potential that is needed for mitochondrial import (SCHLEYER *et al.*, 1982). Since HP30 was degraded upon protease treatment of outer membrane-ruptured mitochondria its integration in the outer membranes of mitochondria was concluded (MURCHA *et al.* 2007).

The contradictory results by MURCHA *et al.* (2007) formed the basis to re-asses the localization of HP20 and HP30 by an *in vivo* approach. The corresponding cDNAs were cloned without their stop-codon into the binary Gateway vector pK7FWG2 to generate a C-terminal GFP-fusion. The constructs were transformed via *Agrobacterium*-mediated transformation into *A. thaliana* wild-type plants. Successful transformation was tested by PCR with specific primers. For the subsequent localization analysis, the leaves of 3 weeks-old plants of the T_2 generation of several transgenic lines (for each transformed construct) were analysed by confocal laser scanning microscopy (Figure 20).

In addition to HP20-GFP and HP30-GFP, the precursor of ferredoxin from *Silene pratensis* with C-terminal GFP (FD-GFP) was used as positive control for plastidic localization. As negative control, plants expressing GFP alone, i.e., without a plastid signal sequence attached to it and thus predicted to be cytoplasmatically, was employed (Figure 19).

HP20-GFP and HP30-GFP as well as FD-GFP and GFP were expressed in mesophyll and in guard/epidermis cells (Figure 19 and Figure 20). While FD-GFP showed a clear plastidic localization in mesophyll and guard cells, as seen by the overlap of its green fluorescence with the red chlorophyll autofluorescence, some signs of accumulation of unimported precursor may be decuced from the punctuate distribution of the GFP marker in the cytosol (Figure 19, white arrows). Smaller plastids (FD-GFP, Figure 19 A) were found in the mesophyll and localized to the close proximity of the epidermis. By contrast, GFP alone, without respective targeting signal, was detectable exclusively in the cytosol. Both, the cell nucleus and the cell walls showed green GFP fluorescence, and no overlay with red chloroplast autofluorescence was obtained (Figure 19).

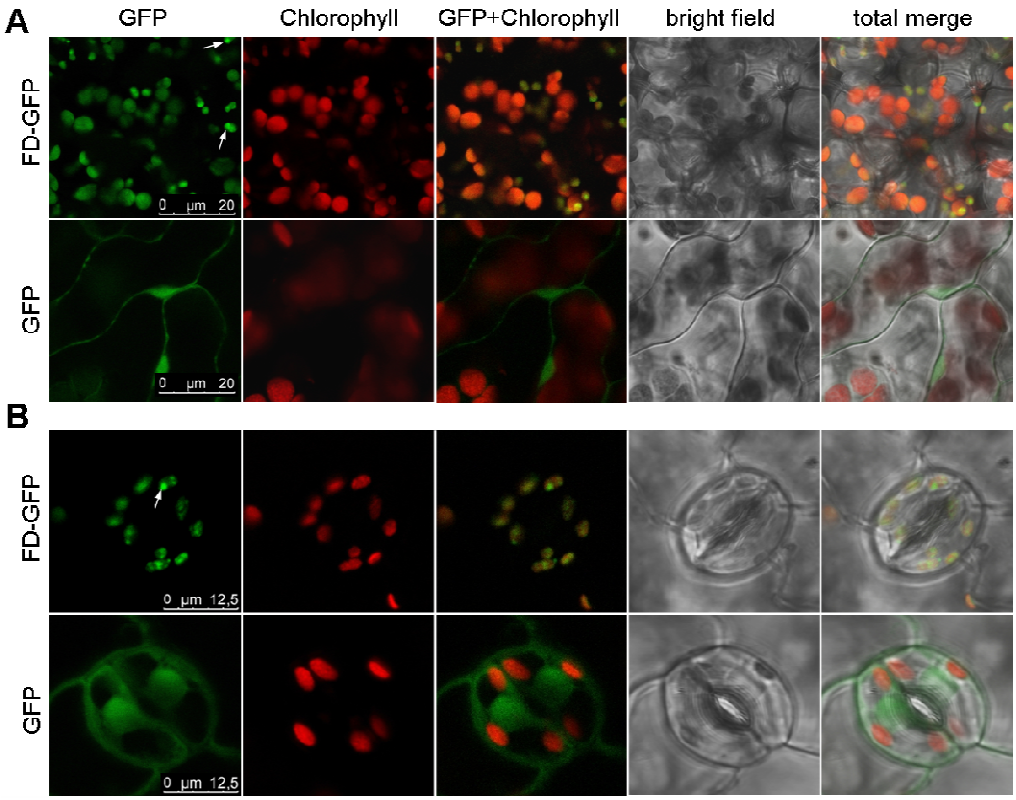

Figure 19. Subcellular localization of FD-GFP and GFP alone in mesophyll cells (A) and guard cells (B) of plants of the T_2 generation of stably transformed *A. thaliana* wild-type plants. Fluorescence signals of GFP (green) and chlorophyll (red) were collected simultaneously by confocal laser scanning microscopy. White arrows mark punctual accumulations of GFP fluorescence.

The expression of HP20-GFP and HP30-GFP was quite strong in most of the generated transgenic lines favouring the formation of large "aggregates" with a bright fluorescence over large areas of the *A. thaliana* leaves that made subsequent analysis impossible. Since HP20 and HP30 are normally expressed in very low amounts in *A. thaliana* (chapter 2.4.1), a too strong expression driven by the 35S cauliflower mosaic virus promotor could cause missorting of the precursor and would promote the formation of such GFP-aggregates in the cytosol. Furthermore, often no expression of either protein was detectable in mesophyll cells. Only in rare cases, some mesophyll cells expressed the transformed constructs. At least two transgenic lines were found for each protein to perform the localization studies (Figure 20).

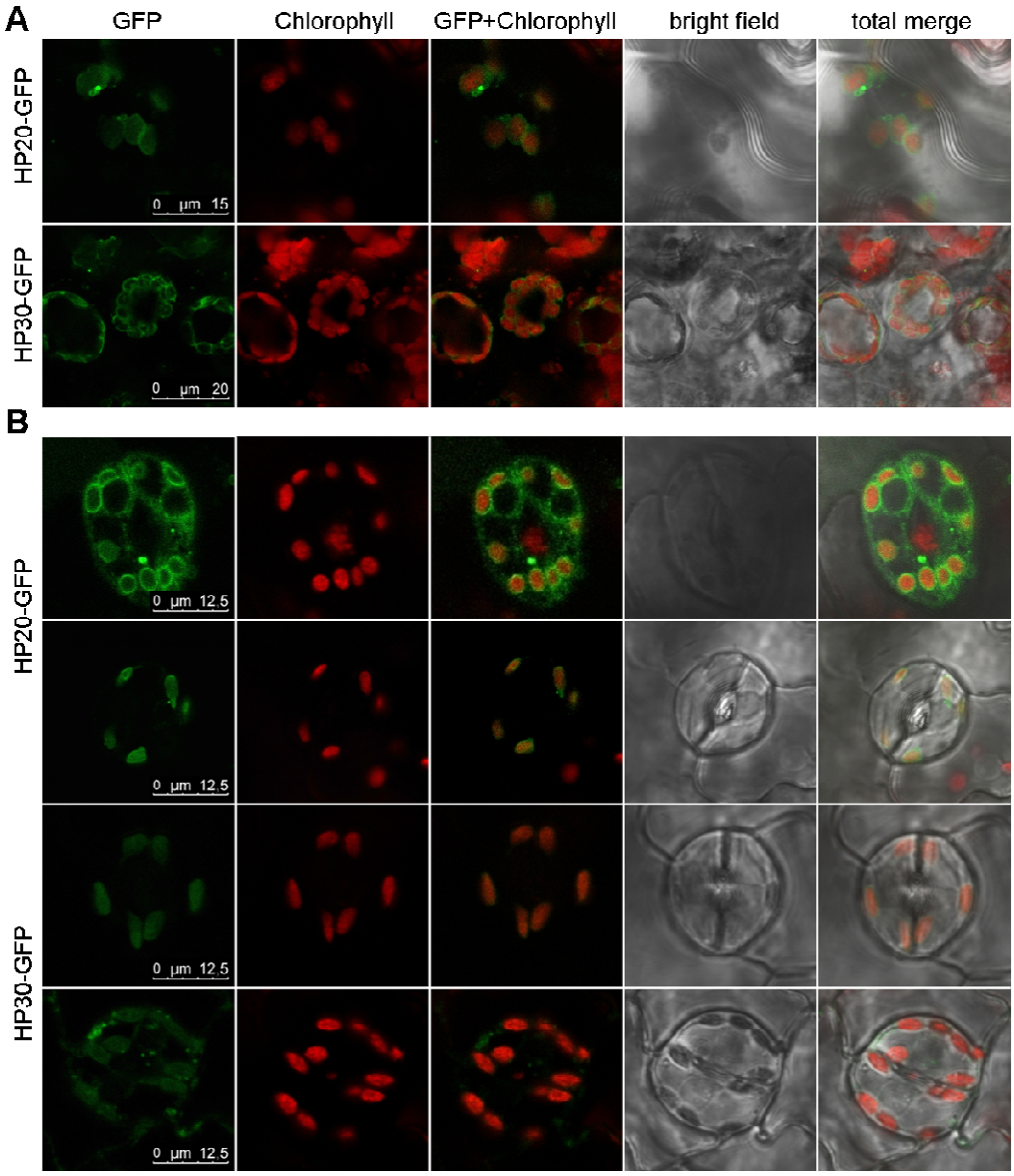

Figure 20. Subcellular localization of HP20-GFP and HP30-GFP in mesophyll cells (A) and guard cells (B) of plants of the T_2 generation of stably transformed *A. thaliana* wild-type plants. Fluorescence signals of GFP (green) and chlorophyll (red) were collected simultaneously by confocal laser scanning microscopy.

Figure 20 highlights that both HP20-GFP and HP30-GFP co-localized with chloroplasts of mesophyll cells (Figure 20 A). In most cases, only mesophyll chloroplasts that were located very close to the epidermis showed imported HP20-GFP and HP30-GFP. The pattern of GFP fluorescence and accumulation at the outer edges of the chloroplast is consistant with that of other envelope membrane proteins (LEE *et al.*, 2001; ASEEVA *et al.*, 2004; DUY *et al.*, 2007). By contrast, the signals obtained in case of FD-GFP showed no comparable GFP-distribution around the plastids; rather, GFP accumulated all over the plastid compartment and seemed to form small aggregates in the stroma that were somehow associated with the plastids. The

unequivocal demonstration of HP20 and HP30 in the plastid envelope membranes would be consistent with the initial identification of both proteins as chloroplast envelope proteins (FERRO *et al.*, 2002; FERRO *et al.*, 2003).

In guard cells, both a plastidic and a cytosolic localization could be inferred for both HP20-GFP and HP30-GFP. In at least two of the generated transgenic HP20-GFP and HP30-GFP lines the GFP signals were confined to the plastids. Thus, HP20 and HP30 can be targeted to the plastids both in mesophyll and guard cells. However, in some of the generated transgenic lines, the distribution of GFP fluorescence was similar to that of FD-GFP and indicative of a rather stromal localization of HP20-GFP and HP30-GFP. In some other lines GFP fluorescence of HP20-GFP was spread allover the cell and most heavily labelled the cell wall without accumulation in the nuclei or the cytosol.

In order to obtain more consistent results concerning the localization of HP20 and HP30 a transient approach was additionally applied. Tobacco (*Nicotiana benthamiana*) leaves were transiently transformed by infiltration with agrobacteria containing respective expression plasmids for HP20-GFP, HP30-GFP, FD-GFP and GFP alone. Two days after transformation, protoplasts were prepared and analysed by confocal laser scanning microscopy. Figure 21 shows FD-GFP images that unveiled only weak expression of the transgene in the transformed tobacco leaves. Nevertheless, the collected GFP signal was clearly plastidic, as evidenced by the superposition of GFP and chlorophyll fluorescences. As found before in the stable tranformants of *A. thaliana*, GFP fluorescence was spread around the chloroplasts with some punctual accumulations. GFP alone was strongly expressed in the isolated tobacco protoplasts and accumulated around the nucleus and in the cytoplasm. Co-localization of GFP with chloroplasts could clearly be excluded since the green fluorescence did not overlap with that of chlorophyll.

As found before for the stable *A. thaliana* transformants, HP20-GFP and HP30-GFP were often expressed in very high amounts leading to large, fluorescent “aggregates”. In protoplasts with least expression, both proteins appeared to be attached to chloroplasts, forming edges with a higher density at the envelope membranes (Figure 21). Part of the expressed fusion proteins were found in close contact to the plasma membrane and marked the cytoplasm strands (the latter is shown for HP30-GFP), but no fluorescence was associated with the nucleus. Together, these results ultimately confirm the plastidic localization of HP20 and HP30, in line with previous observations made by other groups (FERRO *et al.*, 2002; FERRO *et al.*, 2003; MURCHA *et al.,* 2007).

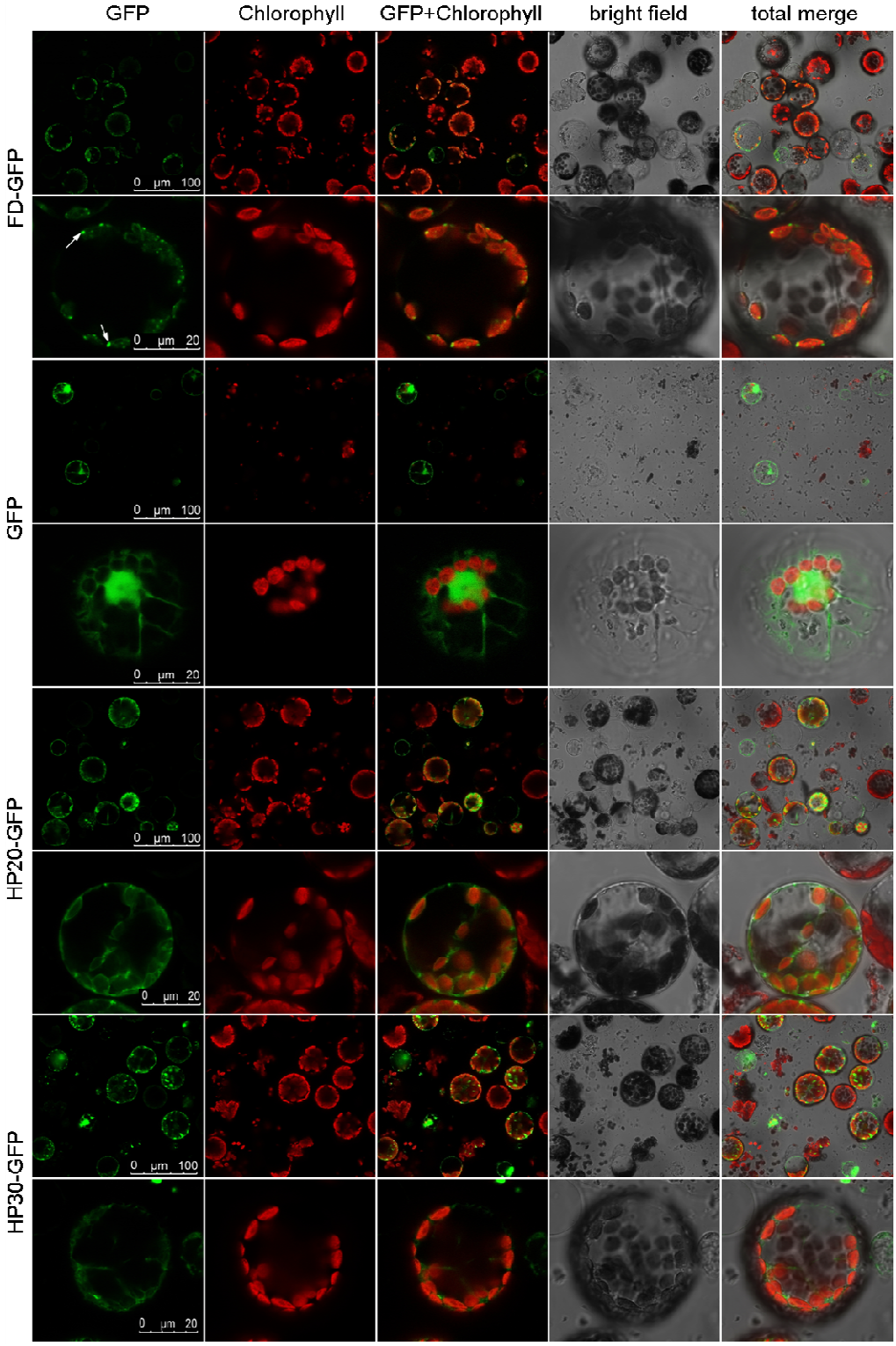

Figure 21. Subcellular localization of HP20-GFP and HP30-GFP in tobacco protoplasts. The tobacco leaves were transiently transformed with plasmids harbouring FD-GFP and GFP alone as controls for plastidic and cytosolic localization, respectively, and HP20 and HP30 also carrying C-terminal GFP as fluorescence tag. The protoplasts were prepared two days after transformation and examined by confocal laser scanning microscopy. White arrows indicate punctual accumulations of GFP signals in the case of FD-GFP.

2.4.3 Biochemical Localization of HP20/QTC24 and its Characterization as Envelope Membrane Protein

During the *in vitro* import of ceQORH a protein of 24 kDa named QTC24 was identified that is related to or identical with HP20/HP22 (chapter 2.1.2). The *in vivo* localization data of HP20 pointed to a plastidic localization. In order to confirm these results and to get more detailed information about the intraplastidic localization of this protein, plastid fractionation experiments were carried out.

To detect HP20/QTC24, the QTC24-specific antiserum, which was purified from the antiserum against total outer membrane proteins for the ceQORH cross-linked QTC24 (chapter 2.2.2), was used. Using this highly specific antiserum, the HP20/QTC24 protein was detectable as single protein band in isolated chloroplasts but not in total leaf extracts (Figure 22 A, a). Highest amounts of HP20/QTC24 were found in OM-IM junction complexes that contained the *in vitro* imported ^{35}S-labelled ceQORH-GFP-$(His)_6$ protein. The seeming absence of HP20/QTC24 in total leaf extracts supports the low expression level seen from the expression data summarized in chapter 2.4.1.

Next, highly purified chloroplasts were treated by two types of proteases with different capabilities to degrade outer and inner plastid envelope membrane proteins. Thermolysin is known to degrade only surface-exposed plastid proteins, whereas trypsin penetrates the outer envelope and breaks down inner plastid envelope proteins up to their membrane parts (CLINE *et al.*, 1984; KESSLER & BLOBEL, 1996). Western blotting revealed that the HP20/QTC24 protein was partially sensitive to added thermolysin but completely degraded by trypsin (Figure 22 A, b). This indicates that HP20/QTC24 is located in the (outer) envelope membrane and that it possesses domains that are integrated in the chloroplast envelope membranes and are protected during thermolysin treatment whereas other domains are surface-exposed that were sensitive to thermolysin.

When ruptured chloroplasts were subfractionated into mixed envelope membranes, inner and outer envelope membranes, thylakoids and stroma, the HP20/QTC24 protein was detected in the mixed and outer envelope membrane fraction (Figure 22 A, c). This result is in agreement with the fact that this protein was identified by proteomics analyses in the chloroplast envelopes (FERRO *et al.*, 2002; FERRO *et al.*, 2003).

Next, isolated outer envelope membranes were extracted with 1 N NaCl or 0.1 M Na_2CO_3, pH 11. Then, the assay mixtures were centrifuged and proteins present in the pellet and the supernatant fractions were subjected to Western blotting. This test was used to gain

information about the topology of HP20/QTC24 as an integral membrane protein or peripheral membrane protein (Figure 22 A, d). Because HP20/QTC24 protein could be detected only in the membrane pellets after either treatment, we concluded that HP20/QTC24 is an integral membrane protein of the outer plastid envelope of chloroplasts.

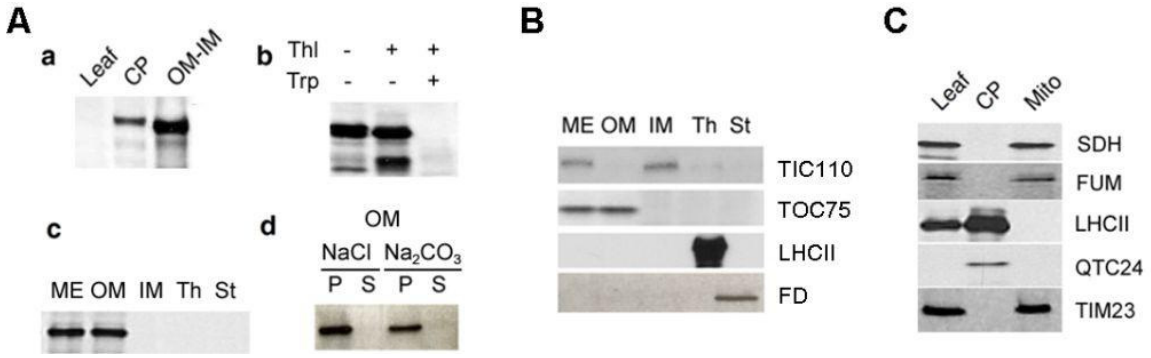

Figure 22. Plastidic and intraplastidic localization of QTC24. A, a, Detection of QTC24 in leaves, purified chloroplasts (CP) and OM-IM junction complexes containing *in vitro*-imported ceQORH (chapter 2.1.1) by Western blotting and the purified QTC24 antiserum. A, b, Protease sensitivity of QTC24 in chloroplasts. Intact plastids were subjected to thermolysin (Thl) and/or trypsin (Trp) treatment and the plastid protein probed with QTC24 antiserum. A, c, Intact chloroplasts were fractionated into mixed envelopes (ME), outer envelopes (OM), inner envelopes (IM), thylakoids (Th) and stroma (st) and QTC24 detected by Western blotting. A, d, Isolated outer envelope membranes were extracted with 1 N NaCl or 0.1 N Na_2CO_3, pH 11, and sedimented. QTC24 presence in the supernatant (S) and membrane pellet (P), respectively, was analysed by Western blotting as before. Each line contained 25 µg of proteins. B, Western blots showing the indicated outer and inner envelope marker proteins in mixed envelopes (ME), outer envelopes (OM), inner envelopes (IM), thylakoids (Th) and stroma (st). Each line contained 10 µg proteins. C, Cross-contamination of the purified chloroplast and mitochondrial fractions. Replicate filters were probed with antisera against the indicated plastid (QTC24, LHCII) and mitochondrial (Succinate Dehydrogenase (SDH), Fumarase (FUM), TIM23 marker proteins. 10 µg of proteins were loaded on each lane.

Finally, the purified chloroplasts and their subfractions were tested for the presence of cross-contaminating proteins (Figure 22 B and C). Whereas TIC110 and TOC75 were detected only in the membrane fractions, the LHCII protein and FD were detectable only in the thylakoids and in the stroma, respectively (Figure 22 B). A contamination with mitochondrial protein could also be excluded since the corresponding marker proteins like succinate dehydrogenase, fumarase and TIM23 were only identified in the mitochondrial fraction, whereas typical chloroplast proteins like LHCII were not present (Figure 22 C). Thus, no contaminating proteins could be identified in each fraction indicating that HP20/QTC24 is located in chloroplasts but not in mitochondria.

2.4.4 Topology of HP20 and HP30 as Integral Membrane Proteins

In order to gain insight on how HP20 may integrate into the outer plastid envelope membrane of chloroplasts, hydrophobicity analysis was carried out and putative hydrophobic transmembrane spans were determined. The results of the analysis using three different programs (chapter 4.1.6) that were obtained from the Plant Membrane Protein Database of the University of Cologne (aramemnon website) are summarized (Figure 23). For comparison, HP30 was used.

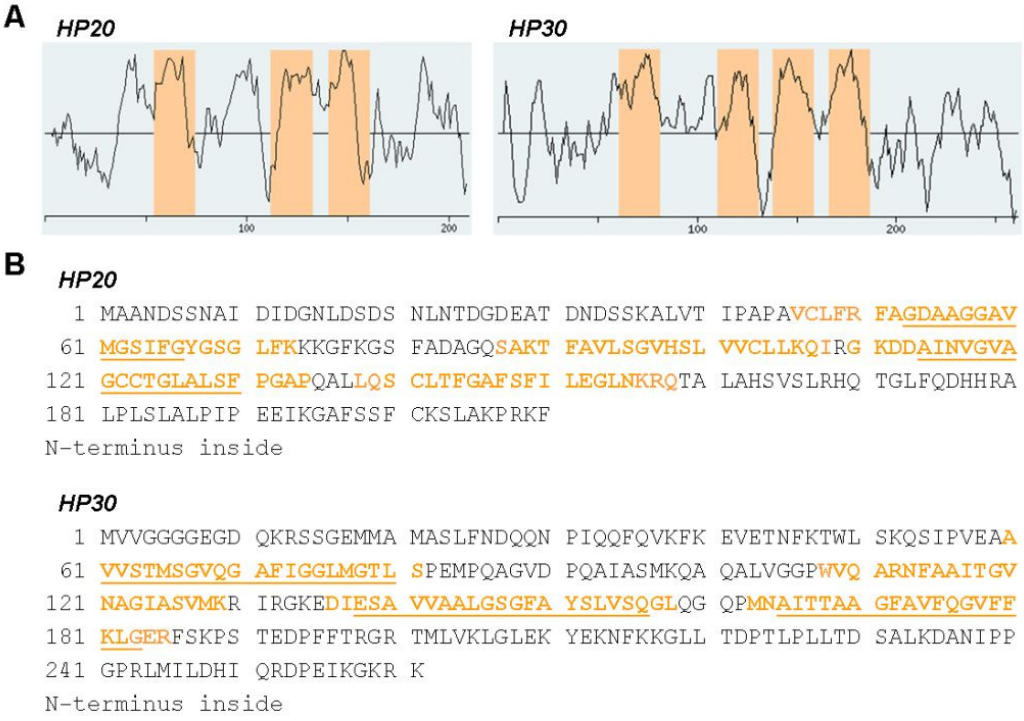

Figure 23. Membrane protein structure prediction and hydrophobicity analysis of HP20 and HP30. A, Hydrophobicity graphs of HP20 and HP30 analysed by HmmTop_v2. Orange sections mark transmembrane alpha helices. Protein parts located over the middle line represent hydrophobic domains. B, Amino acid sequences of HP20 and HP30 showing the position of potential transmembrane spans (orange) and the localization of the N-terminus summarizing the prediction of three different programmes. Underlined sequences mark potential transmembrane helices predicted by all three programs.

At least two of the programs predicted 4 transmembrane spans for HP20 and HP30 with both N-termini exposed to the inner side of the organelle. The first and the third marked transmembrane domain of HP20 are the most probable ones as they were predicted by all three programs. The other transmembrane domains were predicted by only two of the three programs. HP30 most likely contains 4 transmembrane spans whereas the existence of the second one was not predicted by all programs (Figure 23).

2.5 Functional Analysis of HP20 as Component of a Protein Import Pathway

The role of HP20 and HP30 in protein import into chloroplasts was analysed further. The interest was mainly focussed on HP20 because of its co-purification with ceQORH (chapter 2.1). *In vitro* import experiments using a set of radiolabelled precursors and purified chloroplasts of the isolated *A. thaliana* knock-out lines as well as *in vivo* targeting of fluorescence-tagged precursors in stably transformed *A. thaliana* mutants were applied to achieve this goal.

2.5.1 Role of HP20/QTC24 during ceQORH-Import into Plastids

The first set of experiments should answer the question whether HP20/QTC24 would operate as a receptor or as a hydrophilic translocation channel during the import of ceQORH. Taking into account a report by TOKATLIDIS *et al.* (1996), we assumed that precursors during their transit through the outer and inner plastid envelope membranes would be in such close physical proximity to components of the import machinery that would allow the formation of mixed disulfide bonds. If a thiol group of a precursor is activated with DTNB (Ellman's reagent, 5,5'-dithiobis (2-nitro)benzoic acid; HABEEB, 1972), it can react with thiol groups of nearby proteins and establish covalent cross-link products (TOKATLIDIS *et al.*, 1996).

Fab fragments were prepared from the QTC24 antiserum and bound to purified *A. thaliana* wild-type chloroplasts during a pre-incubation step. In parallel, a ^{35}S-labelled version of ceQORH lacking GFP and the $(His)_6$-tag, named ^{35}S-ceQORH, was activated with DTNB. *In vitro* import reactions contained either 0.1 mM Mg-ATP and 0.1 mM Mg-GTP (for plastid binding of the precursor) or 5 mM Mg-ATP and 0.1 mM Mg-GTP (for complete translocation of the precursor into the chloroplasts). After 15 min, the import reactions were stopped on ice and intact plastids re-isolated on Percoll. After protein extraction, cross-link product formation was assessed by co-immunoprecipitation using total HP20/QTC24 antiserum, respective Fab fragments and preimmune serum and non-reducing SDS-PAGE and autoradiography. In parallel samples, the import mixtures were centrifuged and the supernatants and plastid fractions analysed separately. Protein found in the supernatant was precipitated with 5 % (v/v) TCA. Plastids recovered in the pellet after centrifugation were treated with thermolysin in order to degrade unimported ^{35}S-ceQORH and were processed for SDS-PAGE. From the amounts of unimported ^{35}S-ceQORH in the supernatant obtained after

the first centrifugation step and the amounts of imported, thermolysin-resistant ^{35}S-ceQORH in the plastid fraction determined in a scintillation counter, import kinetics could be established (Figure 24 B and D).

The ability of QTC24 antibody and of respective Fab fragments to precipitate HP20/QTC24-bound ^{35}S-ceQORH was confirmed by the detection of the ~54 kDa cross-link band consisting of the disulfide-bridged ^{35}S-ceQORH and QTC24 (Figure 24 A, lanes b, c, e and f). By contrast, preimmune serum was inactive (Figure 24 A, lane d).
When Fab-decorated chloroplasts were used for studying import of ^{35}S-ceQORH, a ca. 20-25 % inhibition of ^{35}S-ceQORH binding was observed at 0.1 mM Mg-ATP in comparison with mock-incubated plastids (Figure 24 B, lane 3 versus lane 1). More importantly, an almost complete block in ceQORH translocation occurred in the presence of bound QTC24 Fab fragments against QTC24 (Figure 24 B, lane 4 versus lane 2). In this case, also no 54 kDa cross-link product was formed (Figure 24 C). The inhibition of plastid import of ^{35}S-ceQORH was specific since no block of either plastid binding or translocation occurred for ^{35}S-pSSU (Figure 24 B, lanes 5-8). This result is in agreement with the known requirement of the TIC/TOC import machineries in import of photosynthetic proteins including pSSU (SCHNELL *et al.*, 1994) and the unique import requirement for QTC24 of ceQORH.

Additional time course import experiments were conducted to back up the differential effects of QTC24 antiserum and respective Fab fragments on the ceQORH and pSSU import findings (Figure 24 D). DTNB-activated ^{35}S-ceQORH was incubated with chloroplasts that contained or lacked the prebound QTC24 Fab fragments in the presence of 5 mM Mg-ATP. After import (for up to 15 min), the amount of imported and unimported ceQORH was determined as described above. In the case of mock-incubated plastids, the amount of bound and imported ^{35}S-ceQORH precursor increased (Figure 24 D, filled triangles), whereas the amount of unimported ^{35}S-ceQORH decreased (Figure 24 D, filled circles). By contrast, the presence of chloroplast-bound QTC24 Fab fragments diminished ^{35}S-ceQORH import (Figure 24 D, open circles and triangles). Because the precursor could not enter a productive import pathway, most of it was recovered in the supernatant.

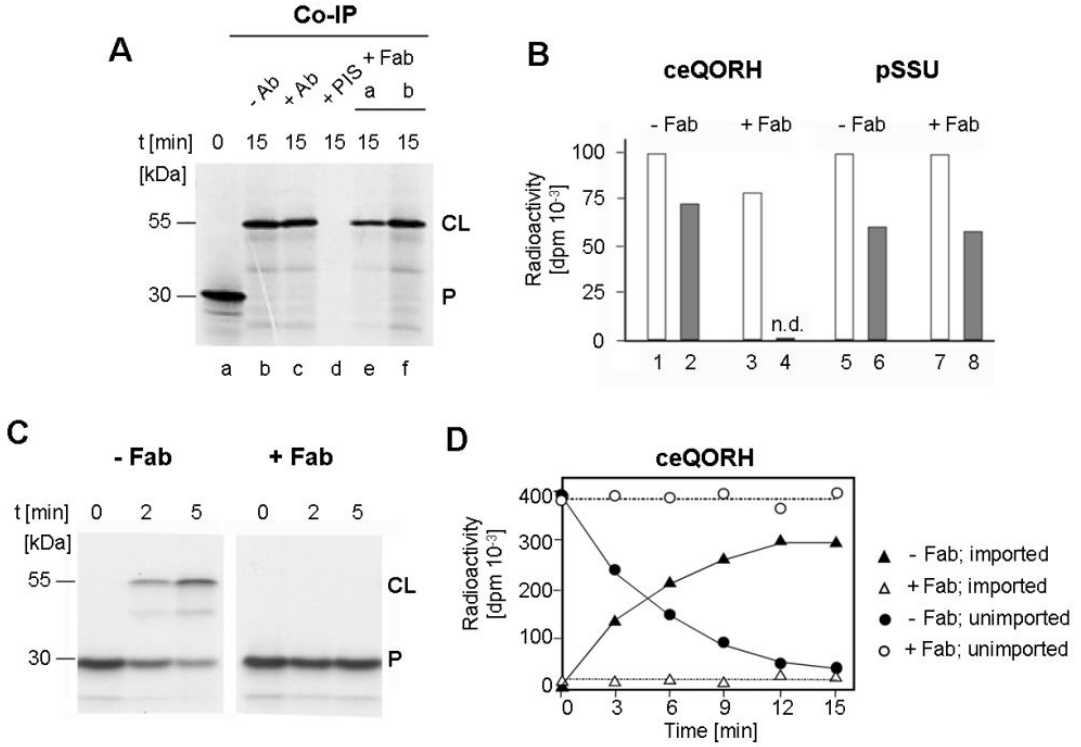

Figure 24. Inhibition of translocation, but not plastid binding of ceQORH by QTC24 Fab fragments. A GFP- and $(His)_6$-free variant of ^{35}S-ceQORH was activated with DNTB and incubated with isolated, energy-depleted chloroplasts that have been decorated with or without Fab fragments against QTC24. Import reactions contained either 0.1 mM Mg-ATP (to study the binding of ^{35}S-ceQORH) or 5 mM Mg-ATP (translocation of ^{35}S-ceQORH). P stands for ^{35}S-ceQORH precursor, CL for cross-link product. A, Co-immunoprecipitations (Co-IP) by 10 µl of QTC24 antibodies (Ab) or 2 µl (a) and 5 µl (b) of respective Fab fragments (Fab) as well as 10 µl of preimmune serum (PIS) of the cross-link product formed between ^{35}S-ceQORH and QTC24 at 0.1 mM Mg-ATP. B, Quantification of ^{35}S-ceQORH binding (white columns) and import (grey columns) determined for Fab-pretreated (+Fab) and mock-incubated (-Fab) *A. thaliana* chloroplasts at 0.1 mM Mg-ATP. C, Inhibition of the cross-link product formation between ^{35}S-ceQORH and QTC24 by QTC24 Fab fragments. Cross-linking was performed with DNTB-activated ^{35}S-ceQORH at 5 mM Mg-ATP for the indicated time periods and directly analysed by non-reducing SDS-PAGE. D, Time course of ^{35}S-ceQORH import into *A. thaliana* chloroplasts containing or lacking anti-QTC24 Fab fragments. DTNB-activated ^{35}S-ceQORH was incubated with chloroplasts containing or lacking prebound anti-QTC24 Fab fragments at 5 mM Mg-ATP and the amounts of unimported ^{35}S-ceQORH and imported ^{35}S-ceQORH were determined. Prior to analysis, the plastids were treated with thermolysin (Thl) in order to degrade surface-bound but unimported ^{35}S-ceQORH molecules.

Next, comparative *in vitro* import experiments were conducted for chloroplasts as well as etioplasts that were isolated from the *A. thaliana* knock-out line *Athp20;2*. *In vitro* import reactions were carried out in the presence of 5 mM Mg-ATP and 0.1 mM Mg-GTP to ensure the complete translocation of ^{35}S-ceQORH precursor into both plastid types.

In pilot experiments, this mutant was analysed with regard to the presence of the protein import translocon components HP20/QTC24, as well as TOC75 and TIC110 that represent translocation pores of the TIC/TOC complex in the outer and inner chloroplast envelope membrane, respectively (Figure 25). Western blotting revealed the complete absence of the HP20/QTC24 protein which confirmed the Northern blotting data (Figure 17). No effect of the *Athp20;2* mutation on the levels of TOC75 and TIC110 was observed, and both proteins were present in the same amounts as those seen in the wild-type. As well, TIC32 and OEP16-1, two examples of inner and outer plastid envelope membrane proteins, respectively, that lack cleavable transit sequences for import (POHLMEYER *et al.*, 1997; NADA & SOLL, 2004), as well as SSU showed wild-type levels in the *Athp20;2* mutant.

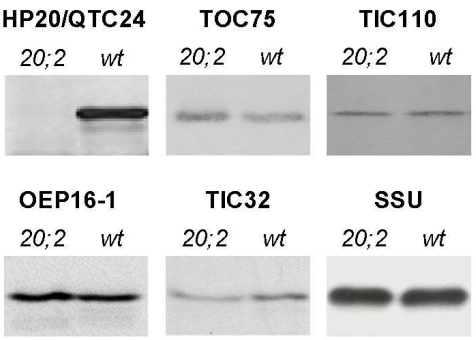

Figure 25. Expression of HP20/QTC24 protein in chloroplasts of the *Athp20;2* mutant (*20;2*) in comparison with wild-type chloroplasts. Replicate blots were probed with the indicated antisera. 25 µg of proteins extracted from chloroplasts were loaded on each line.

The import experiments with etioplasts included ^{35}S-labelled pPORA and pPORB because the former precursor protein uses OEP16-1 that is distantly related to HP20 and a member of the PRAT family. For comparison, import of ^{35}S-pSSU, ^{35}S-pFD and ^{35}S-pLHCII was tested for isolated plastids of wild-type and *Athp20;2* plants. All incubations were performed under safe green light to avoid photooxidative damages and allow the accumulation of imported PORA. As shown previously, imported PORA easily converts Pchlide to Chlide and is at the same time destabilized and proteolytically degraded upon illumination (REINBOTHE *et al.*, 1995b). After 15 min of import, the plastids were centrifuged and the supernatant was subjected to protein precipitation whereas the sedimented plastids were treated with thermolysin in order to distinguish between imported, protease-resistant and unimported, protease-sensitive precursors. Quantification of imported (plastid fraction) and unimported (supernatant fraction) ^{35}S-ceQORH was performed with a scintillation counter (Figure 26 A and C). Additionally, the analysis of the import reactions was carried out by SDS-PAGE and autoradiography (Figure 26 B and D).

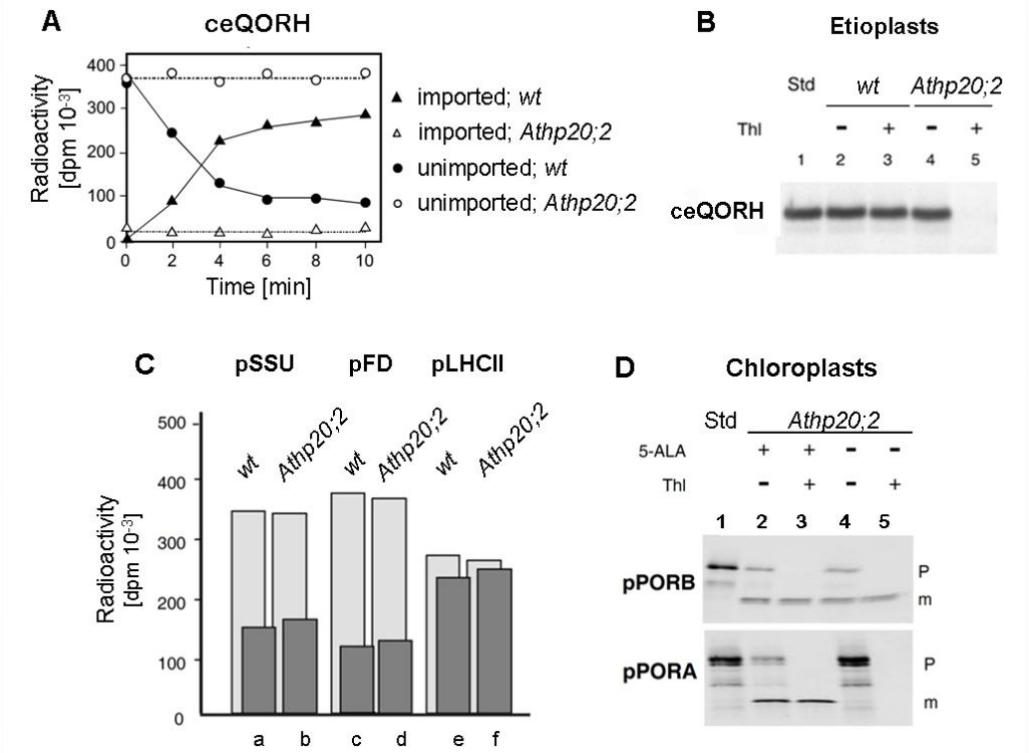

Figure 26. Lack of import of wheat-germ translated ^{35}S-ceQORH into plastids of the *Athp20;2* mutant. Import reactions were performed in the presence of 5 mM Mg-ATP. A, Time course analysis of ^{35}S-ceQORH import into chloroplasts, isolated from wild-type and *Athp20;2* plants followed by treatment with thermolysin (Thl) in order to distinguish unimported (Thl-sensitive) and imported (Thl-resistant) ^{35}S-ceQORH. B, Import of ^{35}S-ceQORH into etioplasts, isolated from wild-type and *Athp20;2* plants, for 15 min followed by thermolysin-treatment. C, Import of ^{35}S-pSSU, ^{35}S-pFD and ^{35}S-pLHCII into chloroplasts of wild-type and *Athp20;2* plants. Light grey and dark grey columns show precursor and mature protein levels after 10 min of import. D, Import of ^{35}S-pPORA and ^{35}S-pPORB into *Athp20;2* chloroplasts. Substrate-dependent import of pPORA was induced by supplementation with 5-aminolevulinic acid (5-ALA) giving rise to Pchlide. Parallel mock incubations contained phosphate buffer. After 15 min, the assays were supplemented with or without thermolysin (Thl) as indicated. Unimported (P) and imported, processed precursors (i.e., mature proteins, m) were detected by SDS-PAGE and autoradiography. Std stands for standard and indicates the quantity of used precursor protein.

The time course analysis of ^{35}S-ceQORH import demonstrated a specific lack for chloroplasts of the *Athp20;2* mutant. This is obvious from the constant amounts of unimported ^{35}S-ceQORH molecules in the supernatant and the lack of protease-resistant ^{35}S-ceQORH molecules in the sedimented plastids (Figure 26 A, open triangles and open circles). By contrast, wild-type chloroplasts imported ^{35}S-ceQORH, leading to its depletion from the supernatant fraction and accumulation in the plastid fraction obtained after centrifugation of the assays (Figure 26 A, filled triangles and circles). Similar results were

obtained for *Athp20;2* etioplasts (Figure 26 B). Notably and unlike typical precursor proteins with N-terminal transit peptides, such as pPORA and pPORB (Figure 26 D), the ceQORH precursor was not subject to proteolytic processing during its import into the outer envelope (Figure 26 B).
Additional uptake experiments carried out for ^{35}S-pSSU, ^{35}S-pLHCII, and ^{35}S-pFD, that are known to be import substrates of the TIC/TOC standard protein import machinery comprising TOC159 and TOC75 (PERRY *et al.*, 1991, SCHNELL *et al.*, 1991; REINBOTHE *et al.*, 1995c), underscored the specific import defect of *Athp20;2* for ceQORH. Indeed, no differences in import of these precursor proteins was detectable between the plastids of wild-type and *Athp20;2* mutant plants (Figure 26 C).

Collectively these results identified HP20/QTC24 to act as a hydrophilic translocation pore in import of ceQORH into the outer envelope membrane of chloroplasts and etioplasts. An additional role in ceQORH binding cannot rigorously be excluded because the binding of ceQORH was reduced by Fab fragments prepared from the QTC24 antiserum. The most compelling argument in favour of a role of HP20/QTC24 was provided by the *in vitro* import studies, showing that *Athp20;2* mutant plastids are unable to import ceQORH. By contrast, the common import pathway mediated by the TIC/TOC machineries as well as the PTC-mediated import pathway of pPORA that involves OEP16-1 were unaffected by the *Athp20;2* mutation.

2.5.2 *In planta* Targeting of ceQORH and TIC32 in *Athp20* Mutants

To confirm the defect in plastid import of ceQORH in *Athp20;2* plants and to exclude TIC32 as import substrate of QTC24 and the QTC translocon, an *in vivo* approach was taken. Transgenic plants were generated stably expressing ceQORH-GFP and TIC32-RFP.
The cDNAs encoding full-length ceQORH and TIC32 were cloned without their stop-codons into the vector pK7FWG2 and pB7RWG2 to obtain fusion constructs consisting of ceQORH with C-terminal GFP and TIC32 with C-terminal RFP, respectively. These binary vectors were transformed by floral dipping into *A. thaliana* wild-type plants and the mutants *Athp20;1* and *Athp20;2*. Transformed plants were selected on MS agar medium containing kanamycin (pK7FWG2) or by spraying soil-grown seedlings with a Basta solution (pB7RWG2). Herbicide-resistant plants then were proven by PCR for the presence of the transformed constructs. Leaves of plants of the T_2 generation that were not older than

3 weeks were taken from several independent transgenic lines for each construct and analysed by confocal laser scanning microscopy (Figure 27 and Figure 28). The cytosolic localization of transgene-encoded GFP, lacking any plastid targeting signal, and the plastidic localization of FD-GFP were assessed for comparison (Figure 19).

In general, ceQORH-GFP plants showed a very strong expression of the fusion protein that was comparable with that of HP20-GFP and HP30-GFP used previously. This high expression (possibly due to multiple insertions of the created constructs into the genome) also resulted in the formation of large fluorescent "aggregates" which emitted so much fluorescence with the consequence that the GFP fluorescence of lower expressed but possibly proper localized ceQORH-GFP in adjacent tissue was not detectable. Since ceQORH is, beside HP20 and HP30, another protein with a normally low expression level in green tissues (leaves; according to the BAR website), these aggregates are likely to represent artefacts generated because of import limitations and/or protein precipitation. In a large number of leaves analysed no GFP signal was detectable in mesophyll cells, but accumulated in epidermal cells. Nevertheless, some mesophyll cells that were very close to the epidermis displayed good GFP fluorescence and highlighted a clear plastidic localization of ceQORH-GFP in the wild-type as well as in both mutant lines (Figure 27 A). This result could be confirmed for a representative number of the ceQORH-GFP expressing *A. thaliana* lines. Because binding of Fab-fragments against QTC24/HP20 only partially blocked the binding of ceQORH to the plastid envelope, the detection of a ceQORH-GFP signal that is associated with chloroplasts is not surprising. Even plastids of the transformed *Athp20*-lines that lack HP20/QTC24 should be able to sequester the ceQORH-GFP protein in a plastid-bound form, but without importing it into the outer envelope membrane. In contrast to the *in vitro* import studies, the *in planta* assays do not allow to distinguish between plastid-bound but not imported precursor and imported ceQORH protein. This makes it difficult to draw definitive conclusions on the role of HP20 in import of ceQORH into mesophyll chloroplasts from the *in planta* studies.

In guard cells, ceQORH-GFP was rather localised in the cytosol. However, an overlap of GFP fluorescence and chlorophyll fluorescence was sometimes observed, making it as well difficult to assign ceQORH to either the cytosol or the plastids in guard cells of wild-type and *Athp20* plants (Figure 27 B).

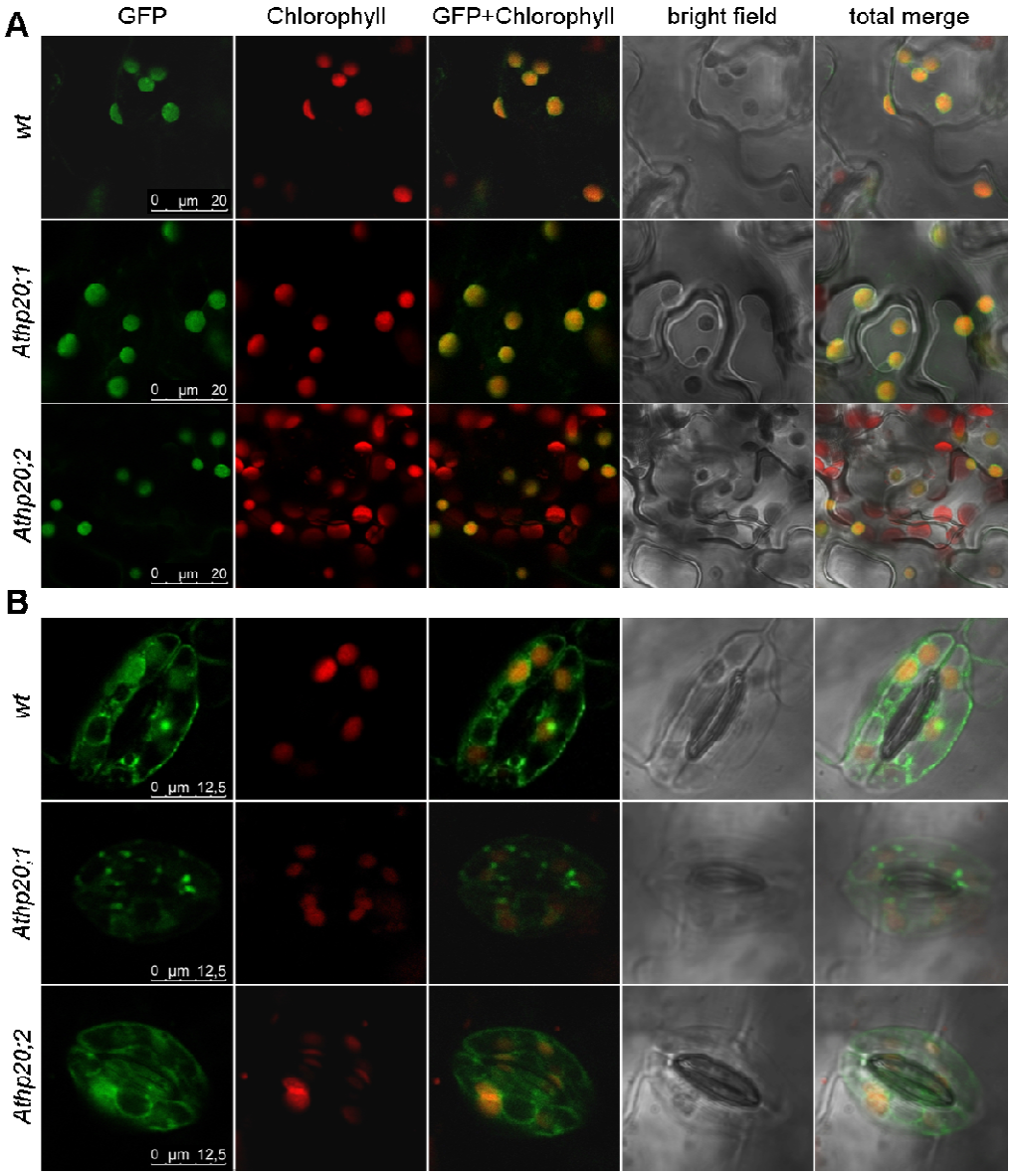

Figure 27. *In planta* import of ceQORH-GFP in mesophyll cells (A) and guard cells (B) of plants of the T_2 generation of stably transformed *A. thaliana* wild-type and the mutants *Athp20;1* and *Athp20;2*. Fluorescence signals of GFP (green) and chlorophyll (red) were collected simultaneously by confocal laser scanning microscopy.

For TIC32-RFP only very few transformed *Athp20;2* plants were obtained. The preliminary results suggested TIC32-RFP to be cytosolic in mesophyll cells of wild-type plants but plastidic in the mutant *Athp20;1* (Figure 28). Guard cells displayed a cytosolic pattern of localization both in wild-type and *Athp20* mutants plants (in multiple generated transformed lines).

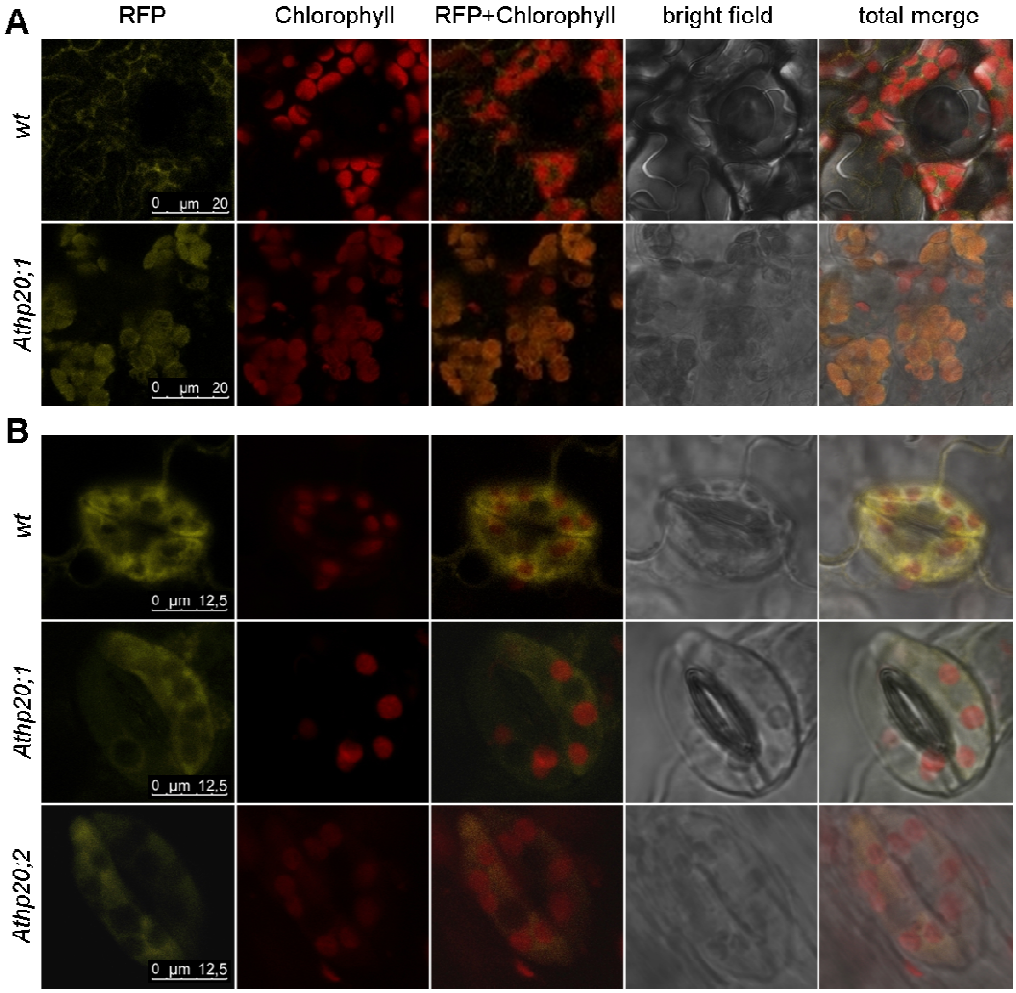

Figure 28. *In planta* import of TIC32-RFP in mesophyll cells (A) and guard cells (B) of plants of the T_2 generation of stably transformed *A. thaliana* wild-type and the mutants *Athp20;1* and *Athp20;2*. Fluorescence signals of RFP (yellow) and chlorophyll (red) were collected simultaneously by confocal laser scanning microscopy.

2.6 Phenotypic Characterization of the *Athp20* and *Athp30* Mutants

Due to the fact that HP20/22 and HP30/HP30-2 are members of the PRAT family a function in amino acid or precursor protein import seemed conceivable (chapter 1.6). For HP20, a role in the import of ceQORH was clearly demonstrated by these studies (chapters 2.1.2 and 2.5.1). In order to get an idea whether HP20/22 and HP30/HP30-2 may accomplish unique or redundant roles, the corresponding knock-out mutants were investigated after cultivation under different growth conditions. If HP20/HP22 and HP30/HP30-2 would be essential for the uptake of amino acids into chloroplasts their lack should have similar, pleiotropic effects on plants growth because plastid protein synthesis required to establish the photosynthetic

apparatus depends on amino acids provided from the cytosol. Any diminishment in the supply of amino acids should be especially pronounced when etiolated seedlings are illuminated and etioplasts develop into chloroplasts and need to synthesize the plastid-encoded components of the photosynthetic apparatus. On the other hand, HP20/HP22 and HP30/HP30-2 could function also in retrograde mechanisms of amino acid export from senescent plants. Thus, any phenotype may be revealed under conditions that induce plant and leaf senescence. The intraplastidic degradation of proteins is accompanied by a massive export of amino acids from the chloroplast to the cytosol (LIM *et al.*, 2007). Therefore, any lack of key amino acid transporters should have severe consequences on the greening process and senescence program. On the basis of these considerations, the *Athp20* and *Athp30* mutants were cultivated under different growth conditions, especially light regimes, and analysed by physiological and biochemical methods.

2.6.1 Plant Growth under Standard Light Conditions

When the different *A. thaliana* lines were cultivated under standard growth conditions on soil with a 16h/8h day/night-regime (70 µE m^{-2} s^{-1}) no visible phenotype could be seen (Figure 29). The mutants had the same number and size of rosette leaves and no difference in leaf colour indicative of the chlorophyll content was visible.

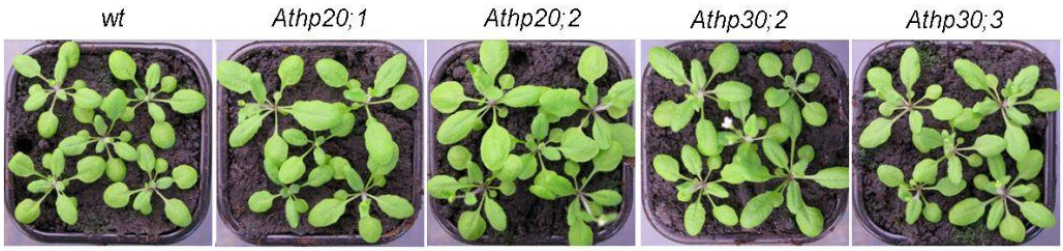

Figure 29. Comparison of *A. thaliana* wild-type and *Athp20* and *Athp30* mutant plants grown for 5 weeks under standard conditions.

Preliminary results of electron microscopy analysis of 7 days-old light-grown seedlings of the *Athp20* mutants and the wild-type underscored this result and showed identical plastid ultrastructures (data not shown). Because the mutants did not display any aberrances in chloroplast ultrastructure drastic changes in photosynthesis caused by lowered rates of plastid protein synthesis can at least be excluded for the *Athp20* mutants.

In order to confirm this conclusion, the synthesis and accumulation patterns of total leaf proteins were analysed. Leaves of 3 weeks-old plants were cut into small pieces, infiltrated

briefly with a solution containing ^{35}S-methionine (chapter 4.10.1) and further incubated under gentle agitation in the light for 2 h. During this incubation, newly synthesized proteins were radioactively labelled. Afterwards, total protein extracts were prepared and analysed by SDS-PAGE and silver staining as well as autoradiography (Figure 30 A).

In a second step, *in organello* labelling was carried out to more specifically investigate intraplastidic protein biosynthesis. Purified chloroplasts of 2.5 weeks-old plants were incubated for 2.5 h in the presence of ^{35}S-methionine in a labelling mix containing or lacking sucrose and thus under conditions in which *in organello* protein synthesis occurred inside intact plastids or in extracts containing or broken plastids. Protein analyses were performed as described before (Figure 30 B).

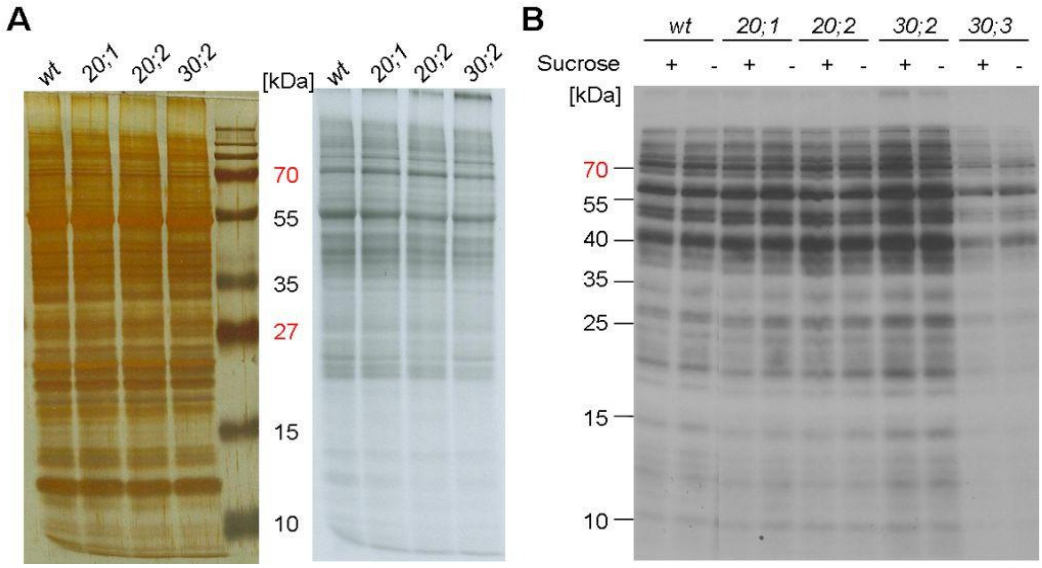

Figure 30. Analysis of protein biosynthesis in *A. thaliana* wild-type and *Athp20* (*20;1* and *20;2*) and *Athp30* (*30;2* and *30;3*) mutant plants. A, *In vivo* labelling of proteins in leaves of 3 weeks-old plants. Labelling was carried out by infiltration of the leaves with a ^{35}S-labelling solution and subsequent incubation for 2 h. Total protein extracts were analysed by SDS-PAGE, silver staining (left) and autoradiography (right). B, *In organello* protein synthesis in isolated chloroplasts of 2.5 weeks-old plants grown under standard conditions. The purified chloroplasts were incubated for 2.5 h with an *in organello* labelling mix and the synthesized proteins investigated by SDS-PAGE and autoradiography. Plastidic protein synthesis was performed either in the presence (+) or absence (-) of sucrose.

The results presented in Figure 30 revealed no gross differences in the pattern of plastidic and cytoplasmic protein synthesis between wild-type, *Athp20* and *Athp30* plants. This result confirms the observations that no visible mutant phenotype was obtained under standard conditions (Figure 29). Obviously, HP20 and HP30 do not play an essential role in the

uptake of amino acids, since neither protein synthesis nor chlorophyll accumulation was impaired in the mutants. The first committed step of tetrapyrrole synthesis leading to chlorophyll requires glutamate (VON WETTSTEIN *et al.*, 1995) and any shortage of its supply thus should have led to a reduced chlorophyll content and photosynthetic performance and growth which was not the case. Also retrograde signalling pathways that are known to control the expression of nucleus-encoded photosynthetic proteins (WATERS & LANGDALE, 2009; INABA, 2010) seemed to be unaffected in *Athp20* and *Athp30* plants. However, it is possible that HP22 and HP30-2 have similar and redundant functions that could not be revealed from the analysis of single mutants for either gene. Last but not least, since HP20 and HP30 are expressed at relatively low levels under standard growth conditions it is tempting to speculate that they may not play a major physiological role in leaf tissues and may do so only during specific developmental periods or under specific growth conditions.

2.6.2 Greening of Etiolated Seedlings under Low Light Conditions

DAHLIN & CLINE (1991) have shown that protein import is developmentally regulated. While the protein import rate was very high in proplastids it declined during the development of chloroplasts and etioplasts, respectively. Moreover, protein import was restored during the differentiation of etioplasts to chloroplasts. In angiosperms, this period also leads to massive synthesis of chlorophyll and requires both amino acids for plastid protein synthesis of plastid-encoded proteins of the photosynthetic apparatus and the uptake of nucleus-encoded, cytoplasmically synthesized precursor proteins. We hypothesized that if HP20 and HP30 were involved in these processes, their lack should have especially pronounced effects on the whole differentiation program of etioplasts to chloroplasts. To test this hypothesis, wild-type, *Athp20* and *Athp30* seedlings were grown on MS agar medium containing 10 g/l sucrose for 4.5 days in the dark and then exposed to continuous white light of 30-40 µE m^{-2} s^{-1} (Figure 31, Figure 32 and Figure 33).

Neither in the dark nor after the dark-to-light transition did the seedlings show differences in their hypocotyl lengths and cotyledon sizes (Figure 31 A). The greening of etiolated *Athp20* seedlings was slightly delayed as compared to that of wild-type seedlings in the early, 6-8 h of irradiation. Preliminary results of the determination of the chlorophyll content might confirm the only slight differences between *Athp20* and wild-type seedling types (Figure 31 B). Confirming previous phenotypic observations, no differences in the chlorophyll contents were detectable for seedlings that had been grown under continuous illumination.

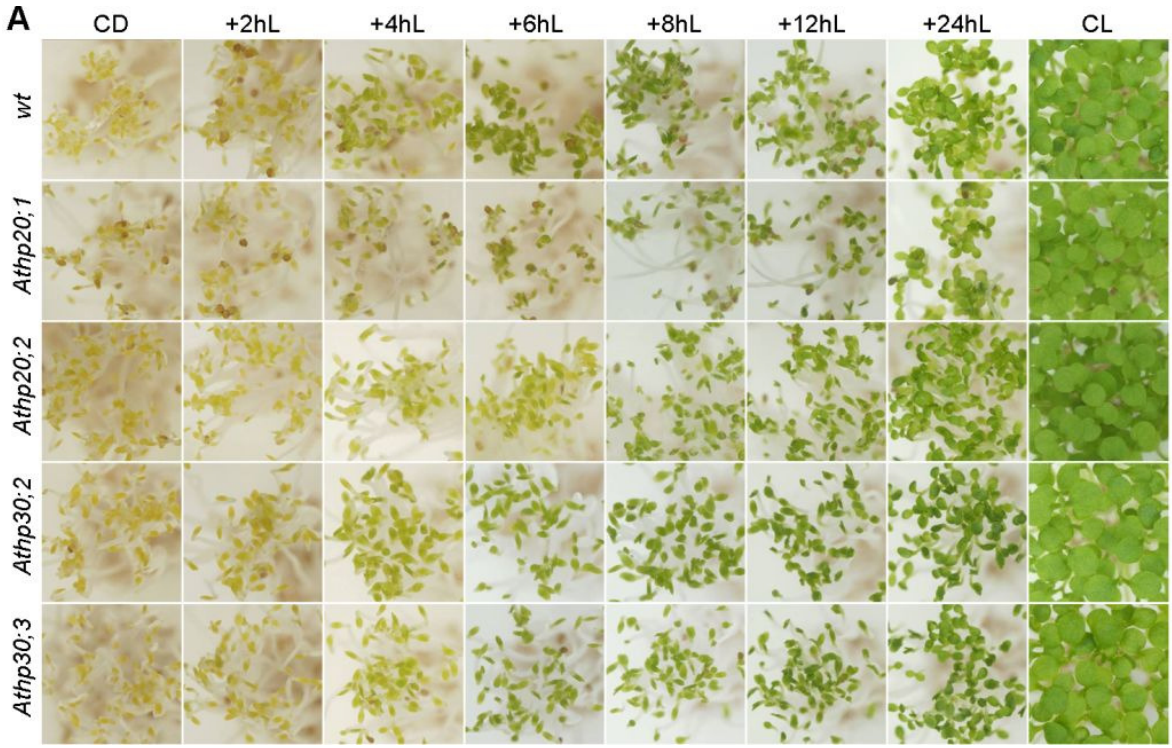

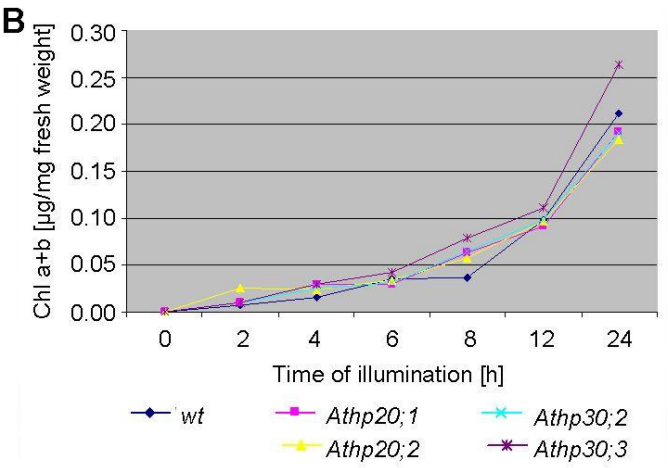

Chlorophyll content of seedlings grown under continuous illumination:

mutant line	chlorophyll a+b content [µg/mg fresh weight]
wt	0.6693 ± 0.0815
Athp20;1	0.7949 ± 0.0746
Athp20;2	0.8958 ± 0.1346
Athp30;2	0.8045 ± 0.2144
Athp30;3	0.7042 ± 0.2475

Figure 31. Greening characteristics of etiolated seedlings of wild-type and *Athp20* and *Athp30* knock-out mutants. 4.5 days-old etiolated seedlings were exposed to low light intensities (40-50 µE m^{-2} s^{-1}) for the indicated time (+xhL). CD and CL stands for growth in continuous dark and light. A, Analysis of the morphology and chlorophyll content. B, Accumulation of chlorophyll during the illumination. The total chlorophyll (Chl) content in the upper third of the seedlings was determined by extraction according to PORRA *et al.* (1989). The average of three independent measurements was correlated to the irradiation time.

To see whether the observed differences in greening in the early hours of the de-etiolation response are due to changes in plastid protein synthesis, Western blot analyses were conducted with antisera against proteins that represent photosystem II subunits, such as the

reaction centre protein D1, the α-subunit of cytochrome *b*-559 and the 33 kDa subunit of the oxygen evolving complex, OEC33 (Figure 32 and Figure 33).
These studies unravelled a delayed accumulation of the D1 protein and αCytb_{559} in the *Athp20* mutants. A delayed expression was also detected for the small and large subunits of RubisCO (SSU, LSU). LSU, αCytb_{559} and D1 protein are synthesized in the chloroplast and their delayed accumulation might be caused by a defect in amino acid import (due to the lack of HP20 as import channel) into the plastids leading to a reduced protein synthesis rate (Figure 32).

Interestingly, the defect in greening and D1, αCytb_{559}, LSU and SSU accumulation seems to be restricted to very young seedlings because no reduction in the protein synthesis rate was detectable by *in organello* labelling studies using chloroplasts of 2.5 weeks-old plants (chapter 2.6.1). More importantly, the measured up-regulation of the early light-inducible protein 1 (ELIP1), is suggestive of photooxidative damage in *Athp20* seedlings. ELIPs are proteins located in thylakoid membranes that are related to light-harvesting chlorophyll *a/b* binding proteins and have a photoprotective role under light-stress conditions (MONTANÉ & KLOPPSTECH, 2000). One might speculate that the extended presence of ELIPs is necessary to compensate for the delayed accumulation of the D1 protein that might exert a certain stress on the developing seedlings.
The proteins PORA and OEP16-1 that are imported into chloroplasts by non-canonical import pathways not requiring the TIC/TOC machineries (REINBOTHE *et al.*, 2004a; JARVIS, 2008) showed no differences in accumulation pattern between wild-type and *Athp20* plastids upon irradiation of etiolated seedlings. Furthermore, PORB, LHCII and the universally existing F-type ATP-synthase (subunit B, ATPB) were not affected by the *HP20* knock-outs and accumulated as in wild-type seedlings. Because the precursors of these latter proteins are imported into plastids through the TIC/TOC machineries, it seems unlikely that the delayed accumulation of SSU reflects a specific import defect but may be due to a reduced stability of the protein when its counterpart, LSU, is lacking in the developing chloroplasts.

In addition to these proteins two other not yet identified proteins showed an expression that was different in the *Athp20* mutants from that of the wild-type seedlings (Figure 32 B, black arrows). In the dark and during the first hours of illumination both proteins were present in higher amounts in the mutant than in wild-type. The apparently light-induced decline of the

smaller protein led to the same amount in both plant types as found in continuously illuminated seedlings.

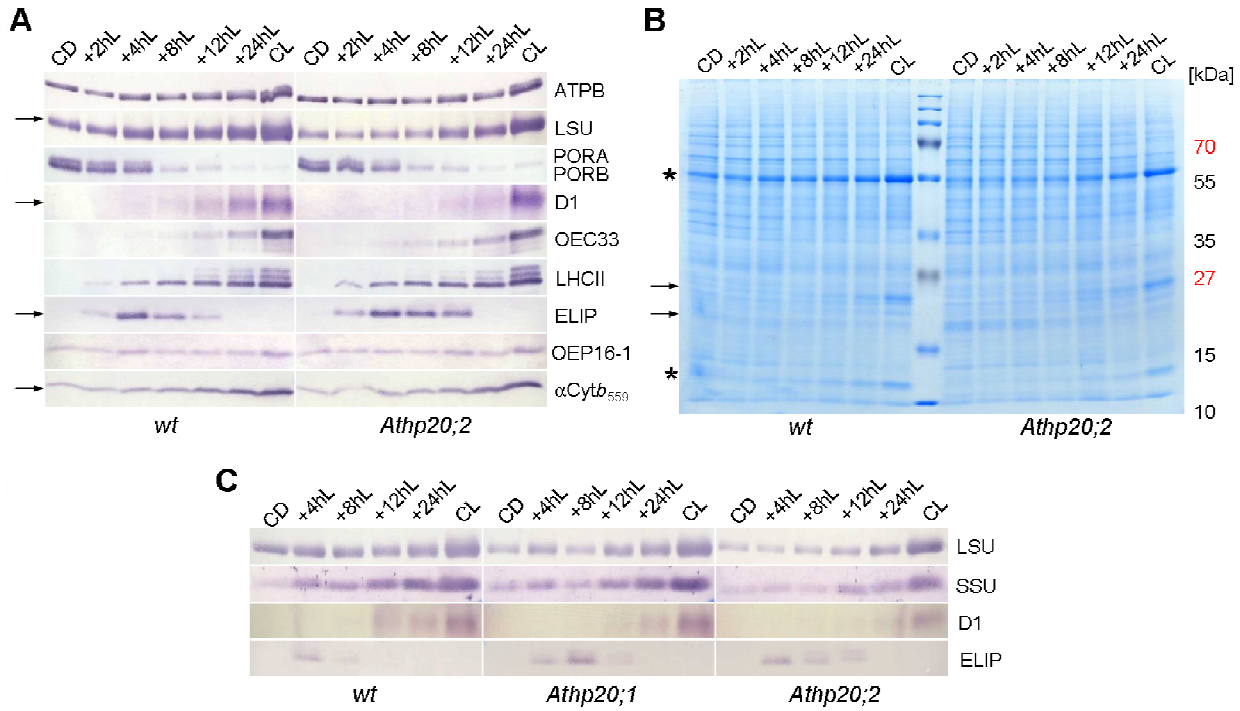

Figure 32. Protein expression during the greening of seedlings of the wild-type and the *Athp20* mutants. Arrows mark proteins with different expression pattern. Asterisks mark LSU (upper protein) and SSU (lower protein) in B. A, Western blot analysis of the expression of the indicated proteins. Depending on the used antisera protein quantities of 10 µg (LSU), 20 µg (OEC33) or 40 µg (ATPB, PORA, PORB, D1, LHCII, ELIP1, OEP16-1, αCytb_{559}) of total protein extracts of the upper third of the treated seedlings (compare with Figure 31) were loaded onto the gels. B, Coomassie staining of a representative separation of the total proteins of greening seedlings. 20 µg of proteins were loaded onto the gel. C, as A, but showing the comparison of the wild-type with both *Athp20* mutants for selected proteins. CD stands for continuous dark, CL for continuous light exposure.

Since it seems very unlikely that the additionally detected T-DNA insertions in both *Athp20* mutants are located in the same genes and prevent their expression (Figure 17), the different accumulation pattern of the tested proteins seems to be related to the loss of HP20 protein in the mutants.

The protein expression pattern of seedlings of both *Athp*30 knock-out lines was similar to that of wild-type seedlings (Figure 33).

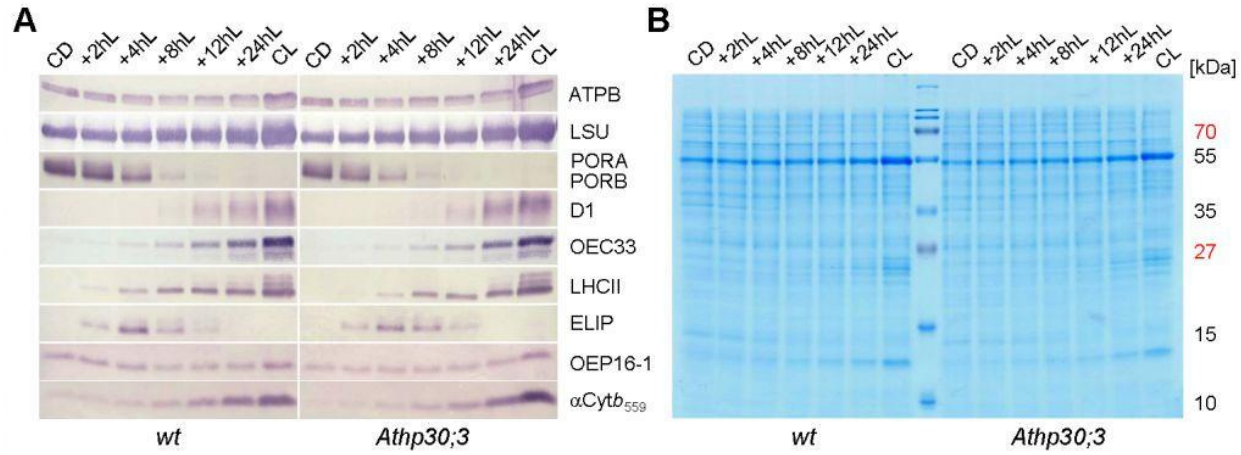

Figure 33. Protein expression during the greening of etiolated wild-type and *Athp30;3* seedlings. A, Western blot analysis to identify and quantify selected plastid proteins. Depending on the used antisera protein quantities of 10 µg (LSU), 20 µg (OEC33) or 40 µg (ATPB, PORA, PORB, D1, LHCII; ELIP1, OEP16-1, αCytb_{559}) of total protein extracts of the upper third of the treated seedlings (compare with Figure 31) were loaded onto the gels. B, Coomassie staining of a representative SDS gel of total proteins of greening seedlings. 20 µg of proteins were loaded onto the gel. CD stands for continuous darkness, CL for continuous light.

Interestingly, when the expression of HP30 was analysed during the greening of etiolated seedlings, three bands were found that differentially changed in the wild-type but were undetectable in the *Athp30* mutants (Figure 34, see also chapter 2.2.2).

Whereas the amount of the smallest protein decreased upon irradiation of wild-type seedlings, the larger proteins (upper bands) were not present in dark-grown seedlings and increased in amount during illumination. The intermediate band was first visible after 4 h of illumination; the upper band appeared after 12 h. After 24 h, the amount of these three proteins had almost reached that of seedlings grown under continuous light exposure.

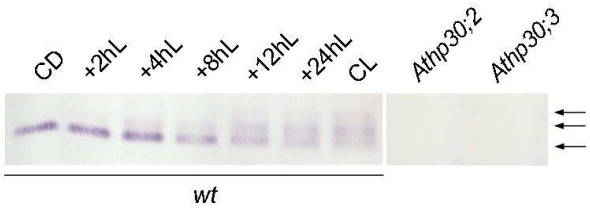

Figure 34. Expression of HP30 in the course of greening of 4.5 days-old etiolated *A. thaliana* seedlings that were irradiated with low white light for the indicated time (+xhL). 40 µg of total protein extracts were loaded. The arrows mark the three protein bands that became visible during illumination. CD stands for continuous dark, CL for continuous light.

We assume that the upper band represents HP30-2 and that the lower band corresponds to HP30 (compare with Figure 14). Analysis of their expression pattern during illumination and dark treatments revealed that HP30 slightly accumulated in the early beginning of the dark period (chapter 2.4.1), whereas HP30-2 expression increased with the time of irradiation of young seedlings and declined in the dark (based on the data of the BAR website).

2.6.3 Greening of Etiolated Seedlings under Light Stress Conditions

HP20 and HP30 belong to the PRAT protein family as OEP16-1. Previous studies had shown that knock-out in the *OEP16-1* gene leads to a lack of import of pPORA, aberrant etioplast ultrastructures and the accumulation of free, photoexcitable Pchlide molecules that triggers cell death via singlet oxygen production upon irradiation of dark-grown seedlings (POLLMANN *et al.*, 2007). This so-called photobleaching phenotype was very similar to that of FLU-deficient *A. thaliana* mutant (MESKAUSKIENE *et al.*, 2001). However, two different cell death programmes could be distinguished in both mutants since the early reprogramming of protein translation, such as the expression of stress-induced proteins, was different (chapter 3.2.4.2).

In order to test whether photobleaching and cell death symptoms similar to those in the *Atoep16-1* or *flu* mutant occur in the *Athp20* and *Athp30* mutants, 4.5 days-old etiolated seedlings that had been grown on MS agar medium without sugar were exposed to strong white light of ~125 µE m^{-2} s^{-1}. As discussed in chapter 3.2.4.1, keeping the seedlings at exactly the same age was especially important since the expression of the photobleaching phenotype depends on the amount of Pchilde accumulated in the cotyledons. As positive control for photobleaching conditions, the mutant *Atoep16-1* was included (POLLMANN *et al.*, 2007). After 30 min, 2 and 4 h of light exposure, the upper third of seedlings was cut and their viability tested by tetrazolium staining. After incubation over-night, the seedlings were photographed and the amount of viable *versus* dead seedlings was determined (Figure 35).
The *Atoep16-1* mutant showed the expected cell death phenotype under the applied conditions (POLLMANN *et al.*, 2007), as dead seedlings were found already after 30 min of illumination. By contrast, the wild-type as well as the *Athp20* and *Athp30* mutants did not show comparable features of photobleaching (Figure 35 A).

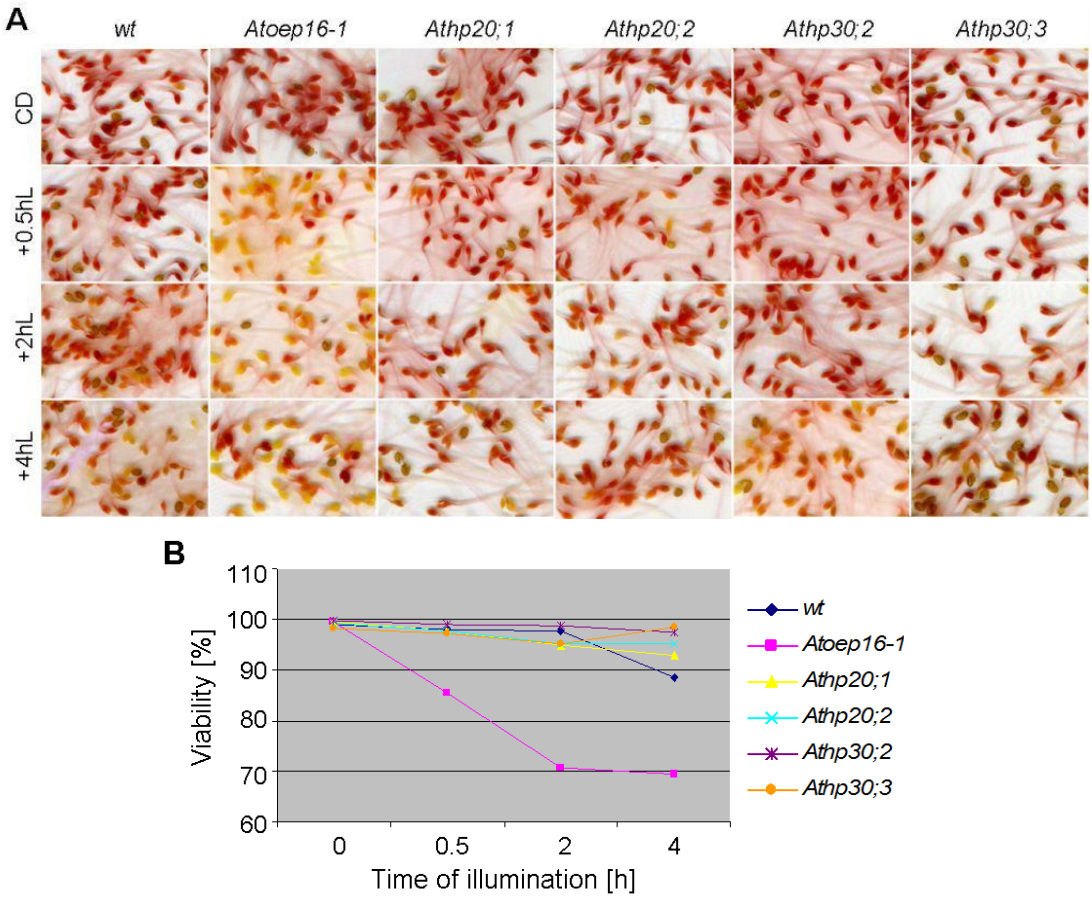

Figure 35. Photobleaching/viability test of *A. thaliana* wild-type and mutant *Atoep16-1* seedlings in comparison with the *Athp20* and *Athp30* mutants. Etiolated 4.5 days-old seedlings (CD) were illuminated with strong white light (125 µE m^{-2} s^{-1}) for the indicated time (+xhL) and the upper third subjected to TTC staining. Red and orange cotyledons represent viable seedlings whereas dead seedlings have a yellow to pale colour. A, Documentation of the seedlings after TTC staining. B, Viability of the seedlings in correlation to the irradiation time.

After quantification of dead seedlings (Figure 35 B), it became evident that 29 % of the tested *Atoep16-1* seedlings showed cell death symptoms after 2 h. This value did not increase significantly during the following 2 h of irradiation (31 % dead seedlings after 4 h). In marked contrast, etiolated wild-type as well as *Athp20* and *Athp30* seedlings did not show any signs of photobleaching and greened normally.

In addition to the staining with tetrazolium, protein synthesis was assessed for the *Athp20* and *Athp30* mutants in order to trace changes indicative of stress responses. Pulse-labelling was carried out with 4.5 days-old etiolated seedlings that had been irradiated for 4 h. The upper third of the seedlings was cut and incubated in a ^{35}S-labelling solution for 2 h prior to harvest. Protein extracts were then prepared and analysed by SDS-PAGE and autoradiography (Figure 36).

The pattern of ^{35}S-methionine-labelled proteins showed no differences between the wild-type and the mutant seedlings in response to strong white light. Obviously, no stress proteins as in *flu* seedlings (Figure 36) were synthesized after 4 h of illumination. No decrease in protein biosynthesis could be observed for wild-type, *Athp20;2* and *Athp30;3* seedlings either. By contrast, *Athp20;1* and *Athp30;2* seedlings reacted – as *Atoep16-1* – to the light-stress with a decrease in protein synthesis after 4 h treatment. This decrease was, however, most likely not part of a cell death response that is traceable by tetrazolium staining (Figure 35 A).

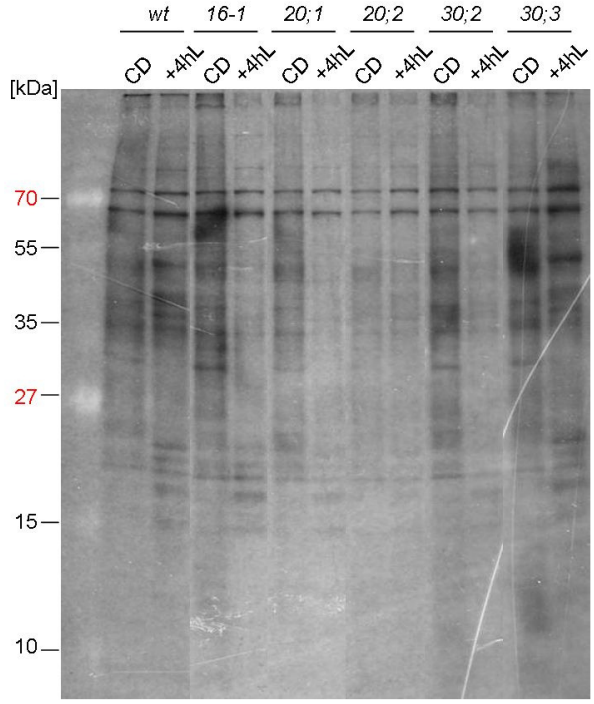

Figure 36. Protein biosynthesis analysed by *in vivo* ^{35}S-labelling of 4.5 days-old (CD) etiolated seedlings during illumination with strong light (125 µE m^{-2} s^{-1}) for 4 h (+4hL) – comparison of *A. thaliana* wild-type (*wt*) with the mutants *Atoep16-1* (*16-1*), *Athp20;1* (*20;1*), *Athp20;2* (*20;2*), *Athp30;2* (*30;2*) and *Athp30;3* (*30;3*). The upper third of the seedlings was incubated during the last 2 h of the irradiation time in a ^{35}S-labelling solution. Total protein extracts were prepared and 20 µg of proteins analysed by SDS-PAGE and autoradiography.

2.6.4 Analysis of Protein Expression during Senescence

The chloroplast is the primary reaction site of leaf senescence (LIM *et al.*, 2007). The earliest and most significant changes comprise the degradation of chlorophyll and macromolecules like proteins, membrane lipids and RNA. Numerous senescence-associated genes (*SAG*s) are induced (LIM *et al.*, 2007). These proteins are responsible for the active degeneration of cellular structures and macromolecules and recycling of nutrients and finally lead to cell death. Since HP20 and HP30 are located in the chloroplast envelope membranes one could assume their implication in recruiting senescence-induced proteins or in the amino acid translocation from the chloroplast into the cytosol. Thus, due to their knock-out the progression of the senescence program might be changed in the *Athp20* and *Athp30* mutants compared to the wild-type.

Hormones that induce senescence comprise ethylene, jasmonic acid, abscisic acid and salicylic acid (GUO & GAN, 2005). HE *et al.* (2002) have demonstrated that senescing *A. thaliana* leaves had 4-fold higher levels of jasmonic acid than non-senescing leaves and that exogenously applied jasmonate caused premature senescence. Abscisic acid (ABA) is a key phytohormone. It mediates many plant responses to environmental stresses and operates in seed germination and plant growth. During stress and senescence endogenous ABA levels were shown to be increased and exogenously applied ABA induced the expression of several *SAGs* (WEAVER *et al.*, 1998). In addition, dark treatment offers the possibility to induce senescence without wounding of the plants that also triggers leaf senescence (LIN & WU, 2004).

Leaves of 3 weeks-old *A. thaliana* plants were cut and immersed in a 0.1 mM ABA solution, a 45 µM methyl jasmonate (MeJa) solution and tap water (as internal control for senescence induced by wounding). Additionally, the plants were subjected to dark treatment.

Figure 37 depicts leaves of *A. thaliana* wild-type and the *Athp20;2* and *Athp30;3* mutant, photographed during the first phase of senescence. These results did not reveal major differences in senescence progression for leaves that had been dissected from the different plants types.

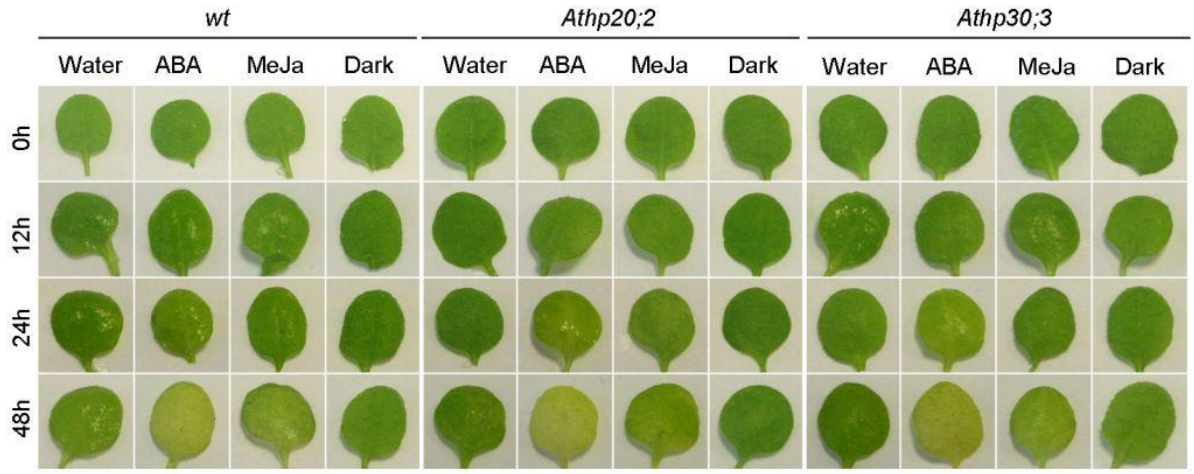

Figure 37. Visual inspection of leaves of 3 weeks-old plants of *A. thaliana* wild-type and mutants *Athp20;2* and *Athp30;3* that were immersed in tap water, a 0.1 mM ABA solution, a 45 µM MeJa solution and subsequent illumination (40 µE m^{-2} s^{-1}) or subjected to dark treatment for the indicated time. A representative leaf is shown for each treatment.

Next, proteins that are known to be degraded (LSU and LHCII) or induced (ACD1, AOS, LOX2) during senescence were analysed.

ACD1 (accelerated cell death 1) is a protein located in the inner chloroplast envelope membrane which catalyses as pheophorbide *a* oxygenase the cleavage of the porphyrin ring of pheophorbide during chlorophyll catabolism (PRUZINSKÁ *et al.*, 2003). Since this protein is induced and only active during senescence it was denoted as the key enzyme of chlorophyll catabolism. The detection of this protein is therefore an indicator of chlorophyll breakdown. Chlorophyll catabolism is accompanied by the degradation of proteins like LHCII, which harbour chlorophylls for light harvesting (PRUZINSKÁ *et al.*, 2003). Another marker protein for plastidial protein degradation is the predominanat RubisCO (GUO & GAN, 2005)
AOS (allene oxide synthase) and LOX2 (lipoxygenase 2) represent two proteins that are involved in jasmonic acid synthesis (SCHALLER *et al.*, 2008) and were shown to be induced during senescence in *A. thaliana* (LAUDERT & WEILER, 1998) and barley (VÖRÖS *et al.*, 1998) and in response to MeJa treatment.

In line with the visual observations, ABA and MeJa promoted leaf senescence and caused a decline in the amounts of LSU and SSU. This is evident from the analysis of the Coomassie stained gels and respective immunoblots (Figure 38 and Figure 39).

On the contrary to SSU and LSU, ACD1 was induced by all tested treatments both in wild-type and *Athp20;2* and *Athp30;3* plants. By contrast, AOS and LOX levels did not change during water treatment or dark incubation, whereas their expression increased in response to MeJa treatment. Comparison of the Coomassie-stained gels did not reveal major differences in the overall protein pattern in wild-type as well as *Athp20;2* and *Athp30;3* plants, except for the induction of an additional protein band of ~60-65 kDa that was detected after 48 h of water, MeJa and to a minor extent after dark treatment in *Athp30;3* plants. This protein could not be detected in wild-type and *Athp20;2* leaves. To identify this protein, a 2-dimensional separation of the protein extracts and subsequent sequencing could be carried out.

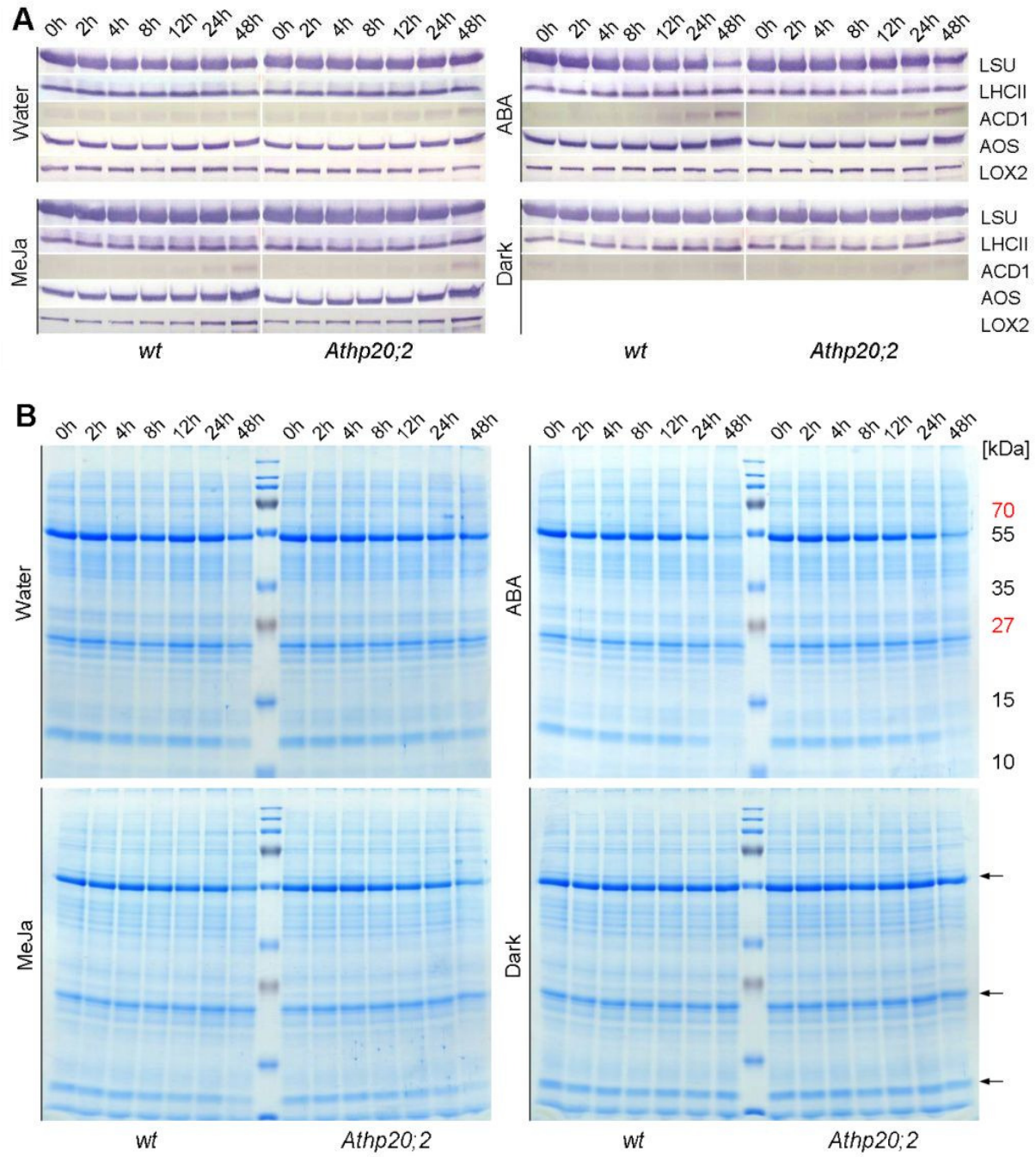

Figure 38. Protein expression in *A. thaliana* wild-type and mutant *Athp20;2* during senescence. The leaves of 3 weeks-old *A. thaliana* plants grown under standard conditions were cut and incubated in 0.1 mM ABA, 45 µM MeJa for senescence induction, in tap water or kept in continuous darkness for the indicated time. A, Analysis of selected proteins by Western blotting. Depending on the specificity of the antisera amounts of 20 µg (LSU, LHCII and LOX2) and 40 µg (ACD1, AOS) of total protein extracts were used for analysis. B, Coomassie staining of a representative separation of total proteins (20 µg/lane). The arrows mark LSU (~55 kDa), LHCII (~27 kDa) and SSU (~12 kDa).

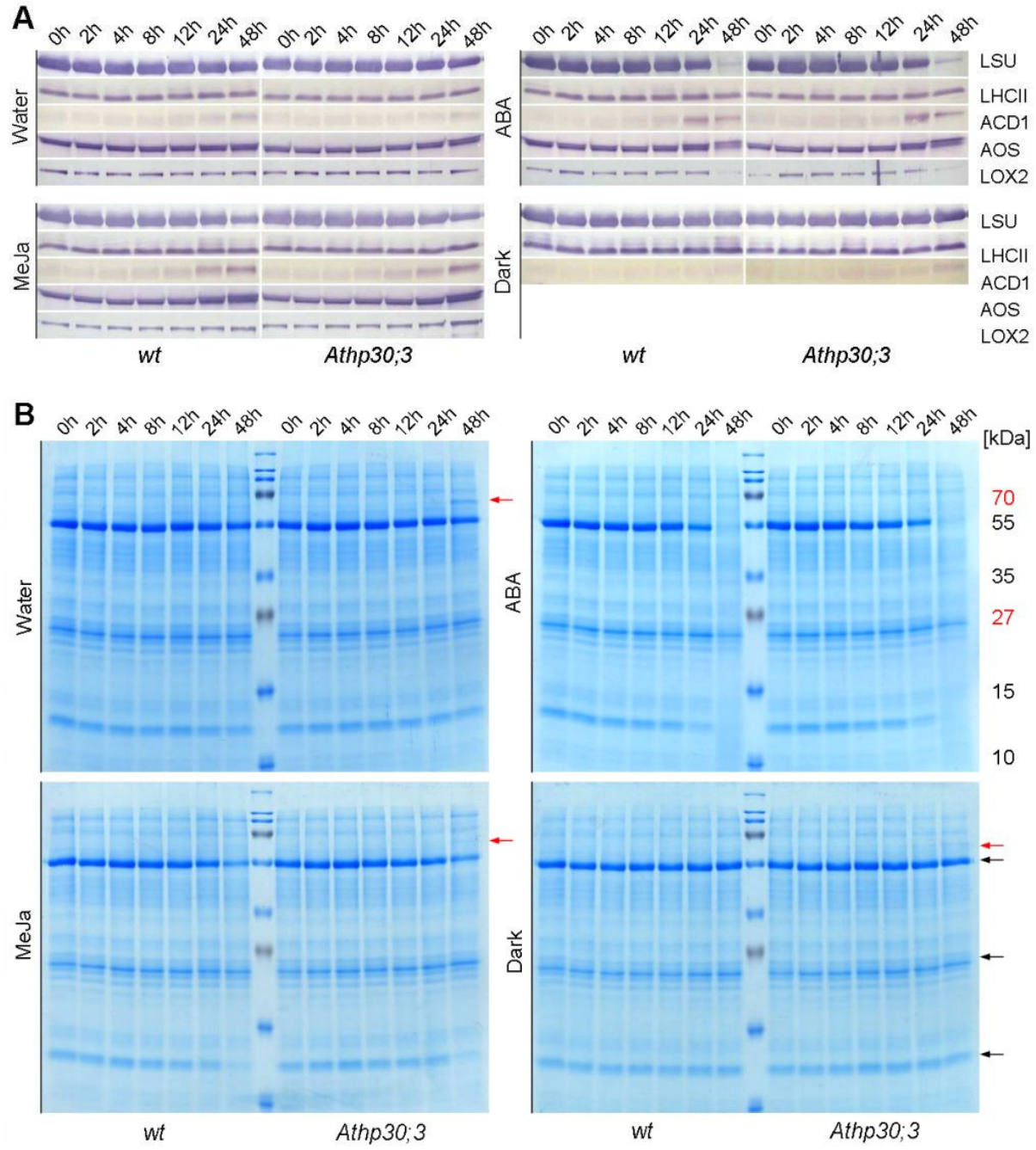

Figure 39. Protein expression in *A. thaliana* wild-type and mutant *Athp30;3* during senescence. The leaves of 3 weeks-old *A. thaliana* plants grown under standard conditions were cut and incubated in 0.1 mM ABA, 45 µM MeJa for senescence induction, in tap water or kept in continuous darkness for the indicated time. A, Analysis of selected proteins by Western blotting. Depending on the specificity of the antisera protein 20 µg (LSU, LHCII and LOX2) and 40 µg (ACD1, AOS) of total protein extracts were used for analysis. B, Coomassie staining of a representative separation of total proteins (20 µg/lane). Black arrows mark LSU at ~55 kDa, LHCII at ~27 kDa and SSU at ~12 kDa. Red arrows indicate an additional protein induced in the mutant after 48 h of treatment.

2.7 Post-transcriptional Silencing of *HP20* and *HP30* in *A. thaliana*

In addition to the reverse genetic approach using *A. thaliana* knock-out plants, a RNA interference approach was used to drop the expression of HP20 and HP30. Post-transcriptional gene silencing or RNA silencing is a generally accepted approach to determine the function of unknown genes. This method circumvents misinterpretations caused by multiple T-DNA insertions in knock-out stocks. It was used to achieve a simultaneously reduced expression of the highly identical proteins pairs HP20/HP22 and HP30/HP30-2 that were hoped to give rise to stronger phenotypes than single mutations.

According to the current model for gene silencing, double-stranded RNA is cut by an enzyme of the RNaseIII-type, called dicer, into short interfering (si)RNA with the size of ~21-25 nucleotides (RUIZ-FERRER & VOINNET, 2009). These siRNAs are incorporated into a RNA-induced silencing complex and serve in their unwound form as template for the directed degradation of mRNA. Double-stranded RNA can arise through aberrant gene expression, virus infection or tandem/inverted repeats due to the insertion of a transposon.

Since the mRNA sequences of both HP20/HP22 and HP30/HP30-2 show high identities, one might achieve co-silencing. By contrast, other members of the PRAT family should not be affected by the generated siRNAs that arise from the *hp20*- and *hp30*-specific inverted repeats. To induce stable RNA silencing in plants, inverted repeat constructs were established in the vector pHannibal and cloned into a binary vector (pArt27) prior to plant transformation by floral dipping.

2.7.1 Created RNA Silencing Constructs

For the creation of inverted repeat constructs, the guidelines listed on the website of the RNAi (RNA interference) WEB were followed in order to achieve a specific silencing of the *HP20/HP22* and *HP30/HP30-2* genes. To avoid co-silencing of other members of the PRAT family, a multiple sequence alignment of the mRNAs of all PRAT members was carried out using the GCG (W^2H) program (chapter 4.1.6) to visualize mRNA sequence parts with a high and low degree of identical nucleobases (appendix II). Figure 40 shows the cDNA sequence parts that were chosen for RNAi as well as the created constructs.

The cDNA segments of both, *HP20* and *HP30* showed the highest consensus in the central region. This region contained large parts of the PRAT motif encoding region. Nucleotide BLAST analyses revealed that the selected cDNA parts of *HP20* and *HP30* were over 80 %

identical to the cDNAs of *HP22* and *HP30-2*, respectively, but not to other members of the PRAT family. Therefore, one might expect a specific silencing of HP20 and HP30 genes.

The constructs were transformed into *A. thaliana* wild-type plants and transgenic plants selected on MS agar medium containing kanamycin and checked by PCR whether they contained the PDK intron.

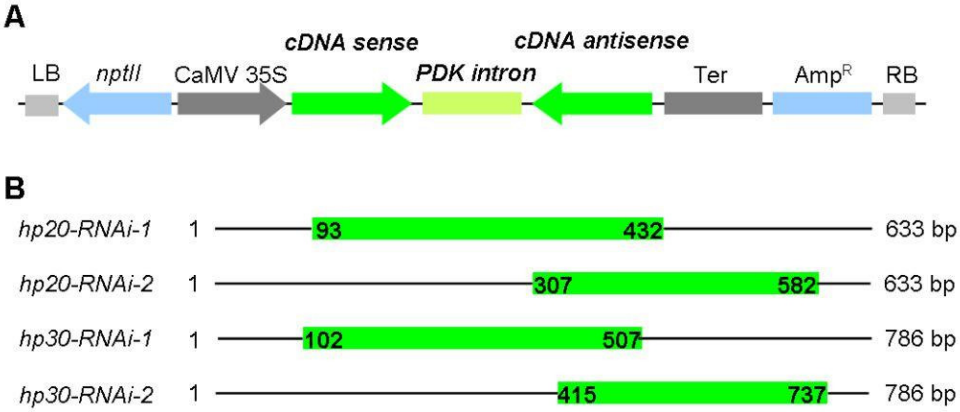

Figure 40. Schematic presentation of the created RNAi constructs for stable RNA silencing in *A. thaliana*. A, RNAi constructs in the binary vector pArt27 for stable plant transformation indicating the RNAi inducing-relevant components between left (LB) and right border (RB). B, Presentation of the mRNA sequences of *HP20* and *HP30* (green parts) that were selected, in sense direction. Abbreviations: *nptII*, kanamycin resistence gene (plant selection marker); CaMV 35S, 35S cauliflower mosaic virus promotor; PDK, pyruvate orthophosphate dikinase; Ter, Terminator; Amp^R, ampicillin resistence gene for bacterial selection.

2.7.2 Preliminary Phenotypic Characterization of RNAi Plants

During standard growth under continuous light conditions young seedlings of *Athp30-RNAi* plants were drastically impaired in greening, as evident by the white colour of many cotyledons. Also the next leaf pair showed this phenotype during its early development. This defect, however, was not observed in older plants (Figure 41 A). After two weeks of cultivation, almost no whitish leaves could be discovered.

Plants containing the construct *Athp30-RNAi-1* had a less strong phenotype. Seedlings belonging to the same transgenic line had different phenotypes including seedlings with strong defects up to seedlings that grew normally. This can be explained by the fact that this seed population represented a mixture of homozygous, heterozygous RNAi as well as wild-type plants (normal growth behaviour). The different extend of the greening defect in the seedlings can be attributed to different silencing levels possibly due to a different number of T-DNA insertions.

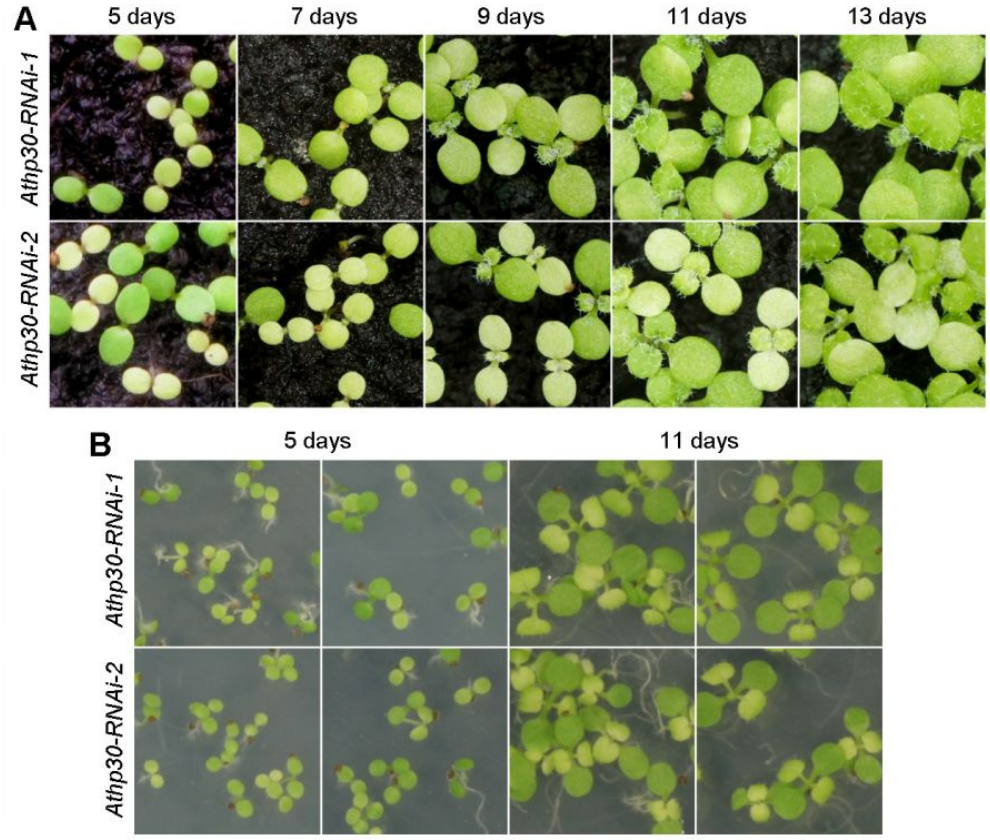

Figure 41. Development of plants of a representative line of the T_2 generation of *Athp30-RNAi* plants. The seedlings were photographed after the indicated time periods. A, Plants were grown on soil in continuous light (70 µE m^{-2} s^{-1}). B, Plants were grown *in vitro* under light-dark-cycles of 16 h light at 60 µE m^{-2} s^{-1} and 8 h dark.

A similar observation was made when the seedlings were grown in light-dark-cycles and under slightly reduced light intensities. In this case, the phenotype was less strong (Figure 41 B). This indicated that this phenotype might depend on the light intensity and light periods. This result further indicates that the protein-pair HP30/HP30-2 might play a role for plastid development during the greening of etiolated seedlings. This hypothesis would be consistent with the expression pattern of HP30 protein during the greening of etiolated seedlings (Figure 34). Moreover, comparison of the single knock-out mutants with the RNAi plants indicates that indeed both HP30 and HP30-2 need to be silenced to obtain a visible phenotype during greening.

In contrast to the *Athp30-RNAi* plants, no phenotype could be observed in *Athp20-RNAi* seedlings under these growth conditions (data not shown).

2.8 Analysis of the Role of OEP16-1

Studies performed with barley and *A. thaliana* on the Pchlide-dependent plastid import of pPORA had shown that a protein in the outer envelope plastid membrane with the molecular weight of 16 kDa (OEP16) functions as translocation channel for this precursor polypeptide (REINBOTHE *et al.*, 2004a; chapter 1.5.1). Consequently, a lack of this protein, e.g. due to a T-DNA insertion in the *OEP16-1* gene, should result in a block of pPORA import and degradation of the unimported precursor protein in the cytosol. As outlined in the introduction, such a knock-out mutant that contained a T-DNA insertion in the *OEP16-1* gene of *A. thaliana* was characterized before (SALK_024018, POLLMANN *et al.*, 2007). In etiolated seedlings of this *Atoep16-1* mutant the lack of OEP16-1 protein correlated with the lack of PORA, elevated levels of free, non-protein-bound Pchlide molecules and a reduced size of the PLB. When etiolated seedlings of this mutant were exposed to light, the free Pchlide molecules are excited and can no longer quench their energy in a meaningful manner and therefore interact with molecular oxygen and produce highly reactive singlet oxygen. This type of ROS caused cellular damage including protein, membrane and pigment destruction and finally leads to cell death. Collectively these effects give rise to a phenomenon termed photobleaching. The observations made for the *Atoep16-1* mutant prove the essential role of PORA for greening. PORA establishes larger light-harvesting POR-Pchlide (LHPP) complexes in the PLBs that function in light trapping and energy dissipation and thereby ensure greening upon light exposure (REINBOTHE *et al.*, 1999).

The *Atoep16-1* mutant has provoked a scientific controversy about the role of the OEP16-1 protein in pPORA import. Apparently the same *Atoep16-1*mutant has been characterized by another group and provided completely different results (PHILIPPAR *et al.*, 2007; PUDELSKI *et al.*, 2009). PHILIPPAR *et al.* (2007) reported wild-type levels of PORA, normally sized PLBs and unimpaired greening, and in fact no signs of photooxidative damage or cell death were found.

In order to explain the contradictory results obtained in our group and that of PHILIPPAR *et al.* (2007) (see also chapter 1.5.1 and 3.2.1), the original Salk seed stock of the *Atoep16-1* mutant (SALK_024018) was re-screened (SAMOL *et al.*, 2011a). Independent homozygous plants were obtained and back-crossed once with the wild-type. Plants were selected from the progeny of this backcross that were homozygous for the T-DNA insertion in the *OEP16-1* gene. These homozygous plants were used for seed propagation and molecular analyses.

Four subclasses of *Atoep16-1* mutants were obtained that displayed different phenotypes with regard to the PORA content, presence of protein-bound and free Pchlide molecules, and cell death (chapter 3.2.2.1). These subclasses were designated *Atoep16-1;5*, *Atoep16-1;6*, *Atoep16-1;7* and *Atoep16-1;8* and are described in detail in SAMOL *et al.* (2011a). Briefly, they remarkably differed in their phenotype. All four mutant types contained a single T-DNA insertion on Southern blots and were consequently devoid of OEP16-1 protein. Mutants *Atoep16-1;5-8* suffered or not from photooxidative damage under high light intensities and contained or lacked PORA. Mutant *Atoep16-1;5* had the strongest phenotype. It lacked PORA and rapidly died upon non-permissive dark-to-light shifts. Mutant *Atoep16-1;6* displayed a weaker phenotype (also Figure 42). Despite the presence of PORA, almost no Pchlide-F_{655} was found. Mutant *Atoep16-1;7* did not show a cell death phenotype as assessed by tetrazolium staining (Figure 42 A). Even without detectable levels of PORA, etiolated seedlings greened normally. Mutant *Atoep16-1;8* contained normal levels of PORA and thus strongly resembles the mutant isolated by PHILIPPAR *et al.* (2007). Mutants *Atoep16-1;6* and *Atoep16-1;7* were characterized further in subsequent experiments to answer the following questions.

Concerning line *Atoep16-1;6:*

- Is functional pPORA synthesized? Point mutations might have led to modifications in the polypeptide structure that result in an inactive protein.
- Is pPORA imported via the TIC/TOC machineries? If Pchlide-dependent import of pPORA requiring OEP16-1 is disturbed, the protein might be imported via the jointly acting TIC/TOC machineries and thereby may not be able to bind Pchlide *b* that in turn would accumulate in a non-protein-bound, free, photodestructive chromophore.
- Is the photobleaching caused by a deregulation of Pchlide biosynthesis, e.g., the lack of feed-back regulation exerted by the FLU protein?

Concerning line *Atoep16-1;7:*

- Is functional pPORA synthesized at wild-type levels? Gene expression might be disturbed at the transcriptional/post-transcriptional level leading to a reduced transcription or the formation and degradation of aberrant transcripts, or at the translational level.
- In the case pPORA would be synthesized at normal levels in the cytosol, is it imported into the plastid compartment? Indeed, unimported pPORA molecules might be

degraded in the cytosol, explaining the lack of mature PORA in etioplasts (SAMOL *et al.*, 2011a). Is the protein functional in terms of catalytic activity? Aberrantly folded or inactive protein molecules might be recognized and degraded.

- Is Pchlide synthesis disturbed in etiolated *Atoep16-1;7* seedlings? Why does no photobleaching occur in the absence of PORA? Either chlorophyll biosynthesis or singlet oxygen-dependent signalling might be disturbed in this mutant.

2.8.1 Characterization of the Mutants *Atoep16-1;6* and *Atoep16-1;7*

First, the level of free (photoinactive) and protein-bound (photoactive) Pchlide was determined and compared to the wild type. As described in chapter 1.2, these spectral pigment forms reflect the functional state of the PORA and PORB and their bound pigments. As summarized by SAMOL *et al.* (2011b), in mutant *Atoep16-1;6*, only low levels of photoactive Pchlide-F_{655} (as compared to the wild-type) were measurable. At the same time, elevated amounts of Pchlide-F_{631} were present. Because a PORA protein band could be detected on Western blot separating etioplast proteins we concluded that PORA is not assembled into larger LHPP complexes permitting greening. Indeed, tetrazolium staining confirmed the photodestructive effect of free Pchlide molecules in the dark, leading to photobleaching and cell death upon illumination of etiolated seedlings (Figure 42 A and SAMOL *et al.*, 2011a). By contrast, in etiolated seedlings of mutant *Atoep16-1;7* no elevated amounts of free Pchlide-F_{631} were detected (SAMOL *et al.*, 2011a).

Obviously, cell death induction by singlet oxygen requires free Pchlide molecules in mutant *Atoep16-1;6* and is therefore age-dependent (Figure 42 B). When etiolated seedlings of the wild-type, and *Atoep16-1;6* and *Atoep16-1;7* mutants were grown in the dark for 3 days and then further cultivated in strong white light (125 µE m^{-2} s^{-1}) for 3 weeks, they all greened and developed. When 4 days-old etiolated seedlings were illuminated, however, their subsequent greening and development was different. Etiolated seedlings of the *Atoep16-1;6* mutant were susceptible to strong white light and died. By contrast, wild-type and *Atoep16-1;7* seedlings of the same age greened and developed into juvenile plants.
Astonishingly, seedlings from all three genotypes died when their growth in the dark was extended to 5 or more days. This experiment demonstrated that (i) Pchlide accumulation and sequestration (binding to the PORA and PORB) is developmentally controlled, that (ii) perturbations in pigment and POR homoeostasis cause cell death by free pigment molecules

operating as photosensitizers, and that (iii) greening can occur in the absence of PORA if no excess pigments are present. All these results are in line with previous observations made on the *det340* mutant of *A. thaliana* that does not express functional PORA protein due to a mutation in phytochrome A signalling but nevertheless develops normally (LEBEDEV *et al.*, 1995 and S. REINBOTHE, personal information).

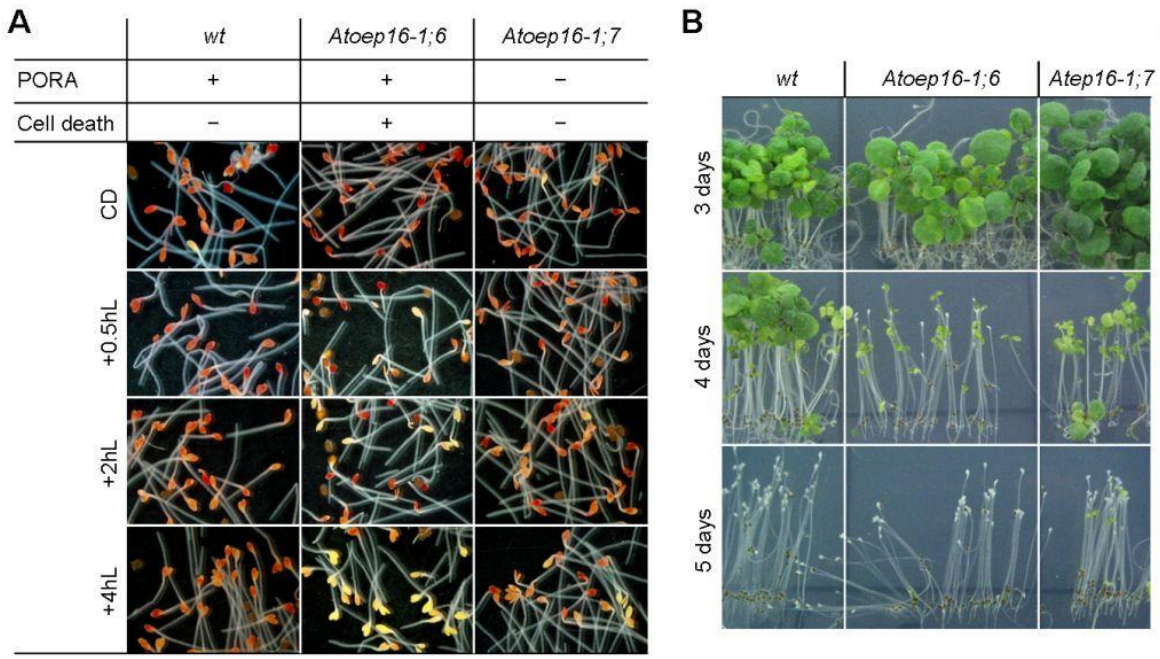

Figure 42. Comparison of the features "cell death" and "presence of PORA" protein in *A. thaliana* wild-type and mutants *Atoep16-1;6* and *Atoep16-1;7*. A, The seedlings were grown for 4.5 days in darkness (CD) and then exposed to white light (125 µE m^{-2} s^{-1}) for the indicated time (+xhL) and the upper third subjected to TTC staining for determination of their viability. Red and orange cotyledons represent viable seedlings whereas dead seedlings have a yellow to pale colour. B, Cell death in the *A. thaliana* wild-type and the mutants *Atoep16-1;6* and *Atoep16-1;7* in correlation to seedling age. The seedlings were grown for the indicated time in the dark and then further cultivated in strong white light (125 µE m^{-2} s^{-1}) for 3 weeks. White and closed cotyledons indicate that cell death had occurred.

Next, the transcript levels of *PORA/PORB* and *FLU* were analysed in mutants *Atoep16-1;6* and *Atoep16-1;7* by Northern blot (Figure 43 A) and RT-PCR analyses (Figure 43 B). In order to prove the identity and correct reading frame of the RT-PCR-amplified transcripts, the cDNAs obtained from the mutants *Atoep16-1;6* and *Atoep16-1;7* were cloned into the vector pDONR221 and the inserts sequenced with the primers M13-fwd and M13-rev (GATC, Konstanz). The obtained sequences were compared with information from public data bases (BLAST).

Since the *A. thaliana flu* mutant was shown earlier to react to non-permissive dark-to-light shifts with a cell death program (MESKAUSKIENE *et al.*, 2001) that is very similar to that found for the *Atoep16-1* (POLLMANN *et al.*, 2007) and *Atoep16-1;6* mutant (SAMOL *et al.*, 2011a), *FLU* transcript levels were determined in parallel to those for the PORA and PORB. To this end, a corresponding *flu* mutant (SALK_002383) was employed.

Sequencing of the RT-PCR products in pDONR221 revealed that one of the cDNA bands obtained with the *FLU* specific primers (Figure 43 B) corresponded to *FLU* transcripts. The cDNAs amplified with primers that are specific for *pPORA* and *pPORB* represented a mixture of both, *pPORA* and *pPORB* transcripts. The analysed transcripts were identical to the wild-type sequences in case of all three genes.

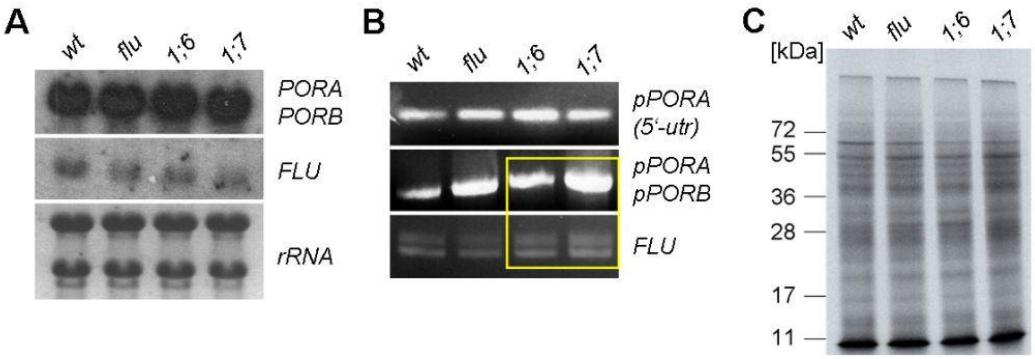

Figure 43. Transcript analysis of etiolated 5 days-old seedlings of mutants *Atoep16-1;6*, *Atoep16-1;7* and *flu* in comparison with the wild-type. A, Northern blot analysis of *PORA/PORB* and *FLU* transcripts in the indicated *A. thaliana* genotypes. 10 µg RNA/lane was loaded. The ^{32}P-labelled probes corresponded to the complete coding sequence of the two POR proteins and of the FLU protein. B, as A, but showing a semi-quantitative RT-PCR analysis. The identity of the amplicons was proven by cloning the red framed bands into pDONR221 and sequencing of the inserts with the primers M13-fwd and M13-rev. 3 µg total RNA was used for RT-PCR. The used primers are listed in Table 8. The sizes of the products are 100 bp (*pPORA-5'-utr*), 1279 bp (*pPORA*), 1267 bp (*pPORB*) and 760 bp (*FLU*). C, *In vitro* translation of total RNA extracted from 5 days-old etiolated seedlings of the indicated plant lines in a wheat germ lysate with ^{35}S-methionine. 3 µg of total RNA were used for translation. Analysis of the synthesized proteins was carried out by SDS-PAGE and autoradiography.

Northern blot analyses revealed that wild-type amounts of all three transcripts were present in mutants *Atoep16-1;6* and *Atoep16-1;7* (Figure 43 A). Since the PORA and pPORB mRNAs are closely related in their mature parts and share an identity of 83 %, the probe used in the Northern experiments detected both *POR* transcripts. This limitation did not impede the conclusion that no change was detectable in *POR* transcript abundance that would be expected if PORA or PORB were absent in mutant *Atoep16-1;7*. For FLU, no

changes in expression were seen on the Northern blots for mutants *Atoep16-1;6* and *Atoep16-1;7.* Two bands were seen whose abundance was similar for wild-type as well as *Atoep16-1;6* and *Atoep16-1;7* mutant plants. Reduced but present levels of *FLU* transcripts detected on Northern blots and after RT-PCR in the *flu* mutant SALK_002383 indicated that it seemed to be leaky and expressed both *FLU* transcript bands (Figure 43 A and B).

Since the transcripts of *PORA* and *PORB* can be distinguished by their 5'-untranslated regions specific primers were used to amplify only the 5'-untranslated region of *pPORA* transcripts. Again, no depression in expression was seen in *Atoep16-1;6*, *Atoep16-1;7* and *flu* as compared with wild-type plants.

Based on the results of the Northern and RT-PCR analyses no indication was obtained for the synthesis of aberrant or unfunctional FLU, PORA or PORB protein molecules in *Atoep16-1;6* and *Atoep16-1;7.* To gain a deeper insight into the changes that may occur in the different mutants, *in vitro* translations were carried out in a cell free protein-synthesizing system. Isolated total RNA was subjected to translation in a wheat germ extract in the presence of ^{35}S-methionine (Figure 43 C). This allowed to reveal whether changes in the relative proportions of individual messengers in the analyzed messenger population was expected to provide information about the changes in gene expression in wild-type, *flu, Atoep16-1;6* and *Atoep16-1;7* plants. Surprisingly, no gross alterations were detectable (Figure 43 C), suggesting that the physiologically different responses of *flu, Atoep16-1;6, Atoep16-1;7* and wild-type seedlings in response to light were, to a large extent, controlled post-transcriptionally. This may include changes in translation and the post-translational uptake of the cyptolasmic precursor proteins.

If the latter hypothesis occurred, changes at the protein level should lead to the accumulation of unimported precursors and their degradation in the cytosol. As a consequence a depletion of photosynthetic proteins of cytoplasmic origin should be detectable in etioplasts during their differentiation into chloroplasts. To test this hypothesis, the protein patterns of *Atoep16-1;6* and *Atoep16-1;7* seedlings that were grown in the dark for 4.5 days and subsequently exposed to white light of low intensity were compared. Low light intensities were used to perhaps allow the identification of unimported precursors in total leaf extracts. Then, the patterns of proteins synthesized *in vivo* in the presence of ^{35}S-methionine (Figure 44 A, etiolated seedlings), the pattern of proteins accumulating at defined time points of the greening process (Figure 44 C) and the amount of individual plastid proteins (Figure 44 C, lower part) were investigated in parallel.

Protein gel blot analyses carried out to follow the expression of nucleus-encoded proteins such as POR and LHCII and plastid-encoded proteins such as LSU in etiolated as well as light-exposed seedlings proved that no gross alterations occurred (Figure 44 B and C). All investigated proteins were present in wild-type amounts in etiolated as well as light grown mutant seedlings. The constant expression of LSU (plastid-encoded) indicated that the mutants did not exhibit major defects in amino acid import and that plastid-protein biosynthesis proceeded normal. In all types of etiolated seedlings, a slight light-dependent reduction of LSU amount was noticed (Figure 44 B). Because LHCII and PORB are imported by the common TIC/TOC translocon, their equal levels in wild-type and mutant seedlings indicate that this import pathway was functional.

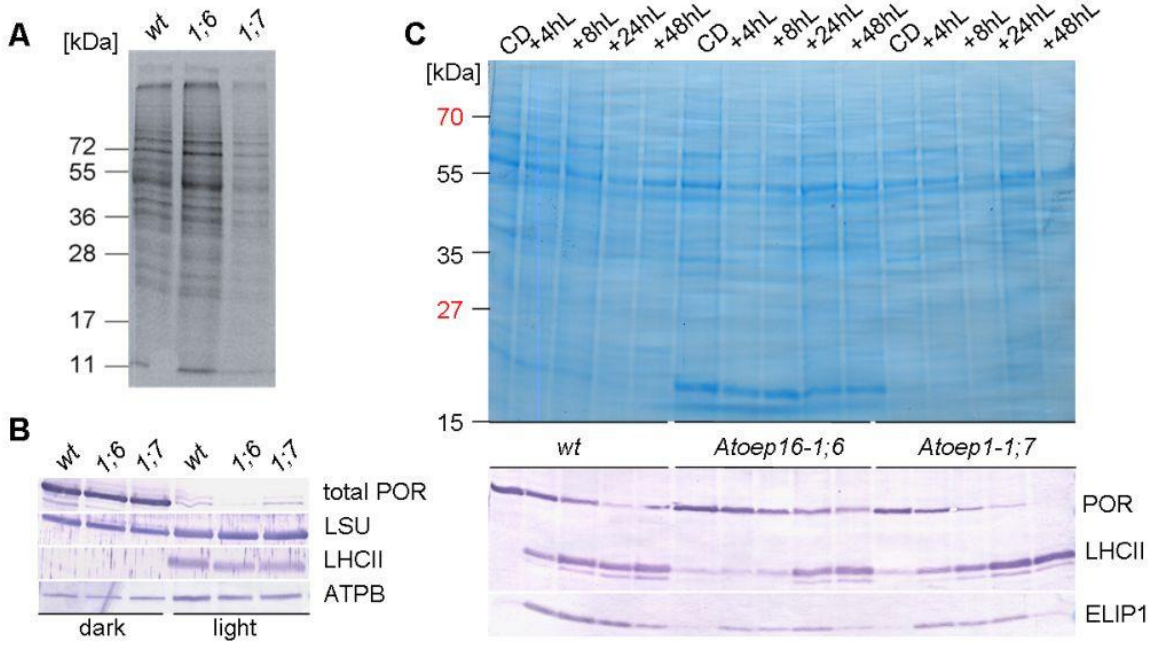

Figure 44. Protein synthesis and accumulation in the mutants *Atoep16-1;6* and *Atoep16-1;7*. Total leaf protein extracts were prepared and 20 µg of protein was loaded per lane. A, Pattern of *in vivo* ^{35}S-labelled proteins in 4.5 days-old etiolated seedlings. Labelling was carried out for 2 h in darkness. B, Western Blot analysis of POR (PORA and PORB), LSU, LHCII and ATPB in 4.5 days-old etiolated and 4.5 days-old light-grown seedlings. ATPB served as loading control. C, Protein pattern in the course of illumination of etiolated seedlings. The seedlings were grown for 4.5 days in darkness and then exposed to standard white light (70 µE m^{-2} s^{-1}) and the upper third harvested for protein analysis. Total protein extracts were prepared and 20 µg proteins/lane subjected to SDS-PAGE and Western blot analysis using the corresponding antisera (total POR, LHCII and ELIP1). Protein detection was carried out by either Coomassie staining and NBT-BCIP in the case of Western blotting.

Since PORA rapidly declines from etiolated seedlings upon light exposure (ARMSTRONG *et al.*, 1995; HOLTORF *et al.*, 1995), the results in Figure 44 B point to a normal expression, uptake and light-induced degradation of mature PORA in mutants *Atoep16-1;6* and *Atoep16-1;7.* This result is at first glance astonishing for mutant *Atoep16-1;7* that does not accumulate mature PORA protein in etioplasts (SAMOL *et al.*, 2011a). Given that total protein extracts were analysed in the current experiments we conclude that the detected band may represent PORB that is unstable in the absence of PORA. As shown in Figure 32 for *Athp20* and wild-type seedlings also the amounts of PORB protein decreased upon light exposure of dark-grown seedlings. An alternative explanation could be that unimported PORA precursor molecules accumulate in the cytosol and are artificially processed into mature enzyme by proteases.

Interestingly, a ~17 kDa protein was stronger expressed in mutant *Atoep16-1;6* (Figure 44 B, Coomassie staining). The identity of this protein needs to be determined in future experiments. In additional Western blot studies reduced amounts of the ELIP1 protein were found during the early stages of greening both in mutant *Atoep16-1;6* and *Atoep16-1;7*. Moreover, the accumulation of LHCII was significantly delayed in mutant *Atoep16-1;6*.

2.8.2 Analysis of a Complemented *Atoep16-1;6* Line

Mutants *Atoep16-1;6* and *Atoep16-1;7* contain and lack PORA, respectively, but their physiological behaviour in response to a dark-to-light shift is somehow unexpected. *Atoep16-1;6* shows a cell death phenotype despite the presence of PORA, whereas *Atoep16-1;7* has no cell death phenotype even while lacking PORA in etioplasts. Because pPORA of barley has previously been demonstrated to escape from the PTC complex in light-adapted plants (KIM & APEL, 2004) and because a default import pathway was discovered that relies on pPORA's interaction with TOC75 and other TOC and TIC components (SCHEMENEWITZ *et al.*, 2007) we hypothesized that the accumulation of mature PORA in mutant *Atoep16-1;6* may be accounted for the operation an OEP16-1-independent, but TOC75-requiring protein import pathway (also chapter 3.2.2.1). The operation of this pathway might have been the result of an additional mutation besides the one in the *AtOEP16-1* gene that triggered default import (SAMOL *et al.*, 2011b).

In order to test this hypothesis, Iga SAMOL generated transgenic lines expressing OEP16-1 protein and respective GFP fusion proteins under the control of the strong constitutive 35S

cauliflower mosaic virus promoter in the *Atoep16-1;6* mutant background. One of the generated lines termed *E_6* was made available for my experiments that aimed at testing the role of OEP16-1 in pPORA import and the establishment of functional LHPP complexes.

Homozygous plants from the T_3 generation were used in all subsequent experiments. In a first set of experiments Iga SAMOL and I asked whether the Pchlide-dependency of pPORA import would be restored and if so it would allow normal greening. To tackle this question, *in vitro* import experiments were carried out in combination with cross-linking using DTNB (TOKATLIDIS *et al.*, 1996; REINBOTHE *et al.*, 2004a; POLLMANN *et al.*, 2007). We expected that if the Pchlide-dependent import of pPORA would be restored by the introduced OEP16-1 protein, the amount of free Pchlide should be reduced as compared to the untransformed *Atoep16-1;6* mutant. Consequently, etiolated seedlings of line *E_6* should green normally upon light exposure. To test this, greening *versus* photobleaching was assessed in parallel and compared with that in wild-type and *Atoep16-1;6* seedlings (SAMOL *et al.*, 2011b).

For the actual *in vitro* import experiments, precursor proteins consisting of the transit peptides of PORA and PORB referred to as transA and transB and the dihydrofolate reductase (DHFR) reporter protein of mouse were synthesized in a wheat germ lysate in the presence of ^{35}S-methionine and activated with DTNB (HABEEB, 1972) for cross-linking. Then, the precursors were incubated for 15 min with etioplasts and chloroplasts that had been isolated from 5 days-old dark-grown and light-grown seedlings, respectively. The import reactions were conducted with *Atoep16-1;6* and *Atoep16-1;6+35S-OEP16-1 E_6* plastids under conditions that promote the complete translocation into the plastids (2.5 mM Mg-ATP and 0.1 mM Mg-GTP; Figure 45 A) or permitted only the binding of the precursor to the plastid envelope protein import machinery (TOC *versus* OEP16-1; 0.1 mM Mg-ATP; Figure 45 B).

Figure 45 summarizes the results and shows cross-link products formed between transA-DHFR and plastid envelope proteins in lines *Atoep16-1;6* and *Atoep16-1;6+35S-OEP16-1 E_6* after their separation by non-reducing SDS-PAGE and autoradiography. In addition to the analysis of the total crosslink products, a fraction of detergent-solubilised envelope membranes was subjected to co-immunoprecipitation using TOC75 and OEP16-1 antisera (Figure 45 B, lane 4 and 8).

Etioplasts and chloroplasts of mutant *Atoep16-1;6* and the complemented line *E_6* were both able to import a fraction of ^{35}S-mathionine-labelled transA-DHFR (Figure 45 A, PORA). For plastids from mutant *Atoep16-1;6*, a cross-link product of ~106 kDa was formed which

consisted of the precursor (31 kDa) and TOC75, as evidenced from respective co-immunoprecipitations (Figure 45 B, lane 8). By contrast, import into etioplasts and chloroplasts of line *E_6* led to the formation of a different cross-link product of ~46 kDa that contained OEP16-1, as proven by the respective co-immunoprecipitation (Figure 45 B, lane 4). At the chosen conditions where plastids are offered in excess, no free, unlinked precursors were seen, pointing to the high specificity of binding of the ^{35}S-labelled precursors to the plastid envelope import machineries (Figure 45 B, lane 1 and 5).

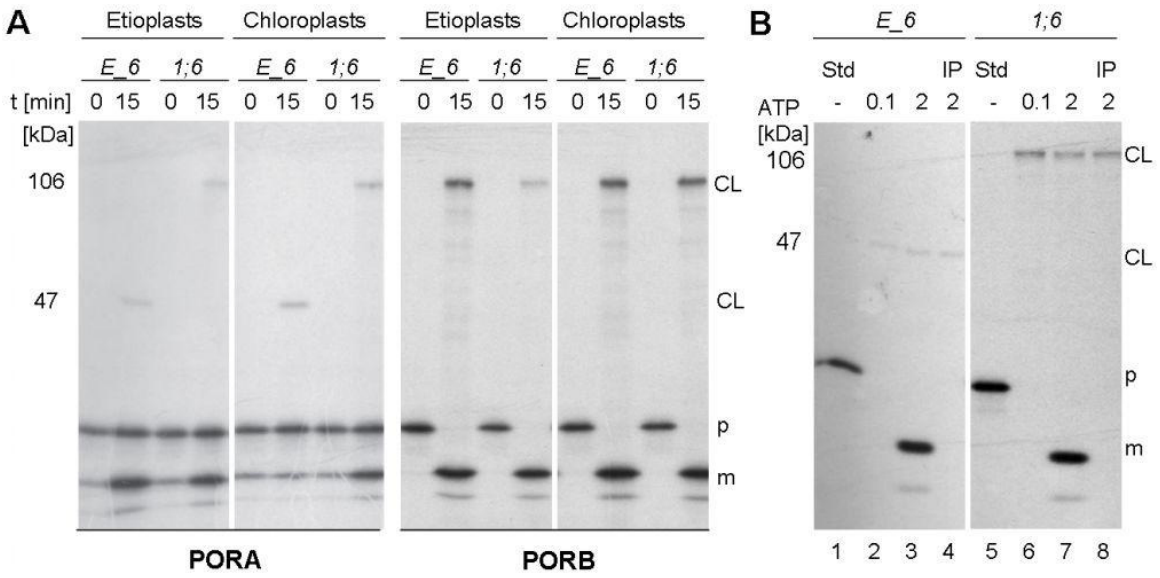

Figure 45. The complementation of the mutant *Atoep16-1;6* with functional OEP16-1 protein restores the OEP16-1-dependent import of pPORA into etioplasts and chloroplasts. A, Cross-linking of DTNB-activated ^{35}S-transA-DHFR and ^{35}S-transB-DHFR in etioplasts and chloroplasts isolated from mutant *Atoep16-1;6* (*1;6*) and the T_3 generation of *Atoep16-1;6+35S-OEP16-1 E_6* (*E_6*). The autoradiographs show levels of precursor (p), mature (m) proteins and cross-link products (CL) of a size of ~47 kDa and ~106 kDa at time point zero and after 15 min of import. The ~47 kDa cross-linked product is caused by the formation of a disulfide bond between transA-DHFR and OEP16-1. The ~106 kDa cross-link product is formed between transA-DHFR or transB-DHFR and TOC75. B, Identification of cross-link products formed with DTNB-activated ^{35}S-transA-DHFR in chloroplasts isolated from mutant *Atoep16-1;6* and *Atoep16-1;6+35S-OEP16-1 E_6*. Import reactions were carried out at the indicated Mg-ATP concentrations and 0.1 mM Mg-GTP for 15 min in the dark. An aliquot of the high Mg-ATP containing assays (lanes 3 and 7) was subjected to co-immunoprecipitation with either OEP16-1 or TOC75 antibodies (IP, lanes 4 and 8). The autoradiogram shows precursor (p) and mature (m) proteins as well as crosslink products (CL) of 47 ~kDa and ~106 kDa at time zero (lanes 1 and 5) and after 15 min of import (lanes 2-4 and 6-8). Std stands for standard and indicates the quantity of used precursor protein.

Interestingly and in line with previous observations (REINBOTHE *et al.*, 1995, 1997, 2000), etioplasts imported a greater proportion of transA-DHFR than the corresponding chloroplasts

(Figure 45 A, PORA, line *E_6*). Since Pchlide is only present in etioplasts but not in chloroplasts to allow for the substrate dependency of import of pPORA, these findings underscore that the Pchlide dependency of import of pPORA was restored in the complemented line *E_6*.

When the import reactions were carried out with transB-DHFR, the precursor was readily imported and no differences between lines *Atoep16-1;6* and *E_6* could be observed (Figure 45 A, PORB). Import of DTNB-activated transB-DHFR led in either case to the formation of a cross-link product of ~106 kDa that contained TOC75, as demonstrated by co-immunoprecpitation (data not shown). This demonstrates that the protein import via the TIC/TOC complex was similar in *Atoep16-1;6* and complemented *E_6* seedlings and that the difference between both seedling types was confined to the pPORA import.

The restoration of the Pchlide dependency of import of pPORA could be confirmed by *in planta* translocation studies (Figure 46). Transgenic plants expressing pPORA-GFP (consisting of the full-length PORA precursor fused to GFP) were generated with the wild-type and the mutants *Atoep16-1;6* and *Atoep16-1;6+35S-OEP16-1 E_6* as genetic background. Selection of transformed plants was performed by the addition of kanamycin into the growth medium and subsequent PCR analysis. The import of pPORA-GFP *in planta* then was followed by confocal laser scanning microscopy.

Etioplasts of both the wild-type and the complemented mutant line *E_6* were able to import pPORA-GFP (Figure 46 A). The GFP fluorescence was sharply focussed in etioplasts. pPORA-GFP could also be imported into etioplasts of mutant *Atoep16-1;6*. However, the amount of fluorescent signal per plastid was drastically reduced and some discontinuous distribution of fluorescence occurred. This observation could be explained by the accumulation of unimported precursor protein. Indeed, analysis of pPORA-GFP protein accumulation in Percoll/sucrose-purified etioplasts unveiled the presence of unimported pPORA-GFP precursor molecules (Figure 46 B). Obviously, pPORA-GFP bound to but was not imported into etioplasts and processed. In line *E_6* most of the pPORA-GFP precursor was imported and processed to mature size in etioplasts, such that similar levels of PORA-GFP accumulated as those found in the wild-type.

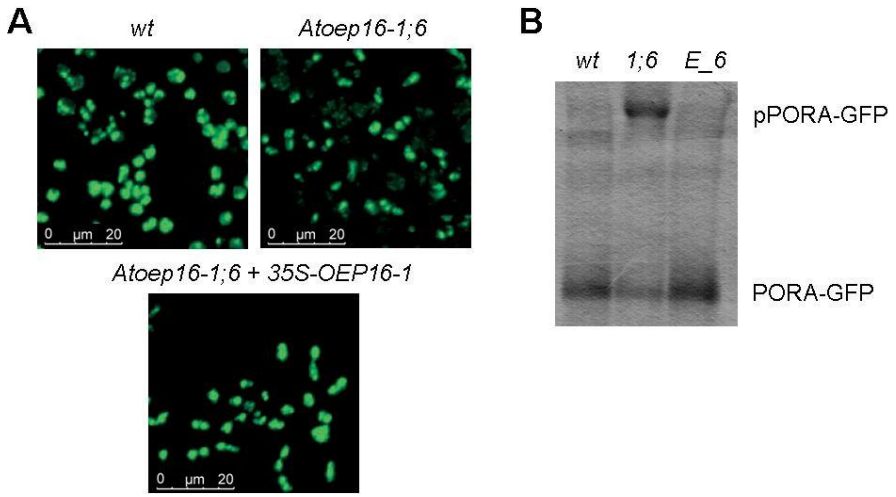

Figure 46. *In planta* import of pPORA-GFP into plastids of 5 days-old etiolated seedlings of the T_2 generation of stably transformed *A. thaliana* wild-type (*wt*) and the mutants *Atoep16-1;6* (*1;6*) and *Atoep16-1;6+35S-OEP16-1 E_6* (*E_6*). A, Fluorescence signals of GFP were collected by confocal laser scanning microscopy. B, Expression analysis of pPORA-GFP protein isolated from Percoll/sucrose-purified etioplasts after blocking the degradation of pPORA-GFP with protease inhibitor cocktail (REINBOTHE *et al.*, 1995b). pPORA-GFP was detected by Western blotting using an antiserum against GFP. Each lane contained 25 µg of etioplast proteins.

Since the reintroduction of functional OEP16-1 efficiently rescued the Pchlide-dependency of pPORA import, it was interesting to see whether the PORA protein was functional and re-established photoactive Pchlide (Pchlide-F_{655}). Low temperature fluorescence spectroscopy was used to assess the functional state of the PORA and bound pigments in mutant *Atoep16-1;6* and its complemented line *E_6.* For comparison, etiolated wild-type seedlings were included in the low temperature pigment analysis (Figure 47 A). Whereas Pchlide-F_{655} corresponds to photoactive PORB-bound Pchlide *a* and indicates the formation of functional LHPP complexes, Pchlide-F_{631} is photoinactive and represents a mixture of free and PORA-bound Pchlide *b*. Free Pchlide molecules operate as photosensitizers and trigger cell death upon light exposure (see chapter 1.2).

As mentioned before, etiolated seedlings of mutant *Atoep16-1;6* contained elevated amounts of Pchlide-F_{631} but low, in most cases, undetectable levels of photoactive Pchlide-F_{655}. The reintroduction of *OEP16-1* in line *E_6* changed this pigment distribution and promoted the establishment of Pchlide-F_{655}, while decreasing the level Pchlide-F_{631} (Figure 47 A). Thus, functional PORA:PORB-Pchlide-NADPH complexes were likely to be formed in line *E_6*. This conclusion was confirmed by the detection of LHPP complexes in etioplasts by native PAGE and Western blotting, using an antiserum against total POR (Figure 47 B). In both,

the wild-type and line *E_6* LHPP complexes were present, whereas PORB and minor amounts of PORA were detectable but not able to assemble into LHPP complexes in mutant *Atoep16-1;6*.

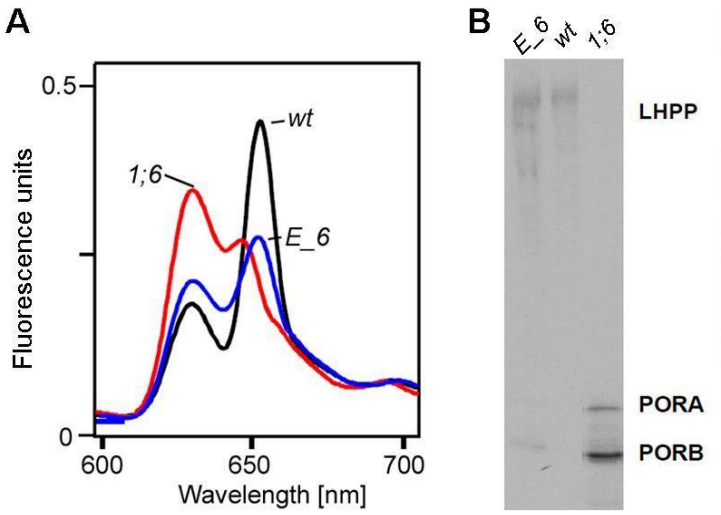

Figure 47. The reintroduction of function OEP16-1 leads to the formation of PORA:PORB-Pchlide-NADPH supracomplexes indicative of the presence of LHPP in etioplasts. A, Low temperature fluorescence analysis at 77 K of pigments of 5 days-old etiolated seedlings of mutant *Atoep16-1;6*, (*1;6*) line *Atoep16-1;6+35S-OEP16-1 E_6* (*E_6*) and the wild-type (*wt*). The two peaks correspond to photoinactive Pchlide-F_{631} and photoactive Pchlide-F_{655}. Spectral intensities refer to an equal cotyledon surface area. B, Non-denaturing PAGE to detect PORA:PORB supracomplexes in purified etioplasts by Western blotting and antiserum against POR.

Finally, seedlings of the line *Atoep16-1;6+35S-OEP16-1 E_6* were analysed with regard to their ability to green or to undergo cell death upon exposure to strong white light (see also SAMOL *et al.*, 2011b). The measurement of singlet oxygen as the cell death-inducing agent was determined based on the quenching of DanePy fluorescence emission due to its reaction with singlet oxygen (HIDEG *et al.*, 1998). Whereas a quenching of the DanePy emission and thus singlet oxygen production was detectable in the seedlings of the mutant *Atoep16-1;6*, the complemented line *E_6* behaved like the wild-type (Figure 48 A).

Since singlet oxygen is cytotoxic and causes the reprogramming of gene expression, leading to the activation of stress-induced genes, pulse labelling was performed with ^{35}S-methionine. As shown for the *flu* mutant, singlet oxygen is a powerful signalling compound that activates genes for enzyme of ethylene and jasmonic acid biosynthesis and signalling. Both plant hormones have documented key roles in stress responses and plant defence against biotic

and abiotic cues (MESKASKIENE *et al.*, 2001, OP DEN CAMP *et al.*, 2003, summarized in REINBOTHE *et al.*, 2009 and REINBOTHE *et al.*, 2010).

Etiolated seedlings that had been germinated for 5 days in the dark were exposed to white light for 24 h. Two hours prior to leaf harvest, the upper thirds of the seedlings were cut and incubated with a solution of ^{35}S-methionine. Protein extracts were prepared and analysed by SDS-PAGE and autoradiography (Figure 48 B).

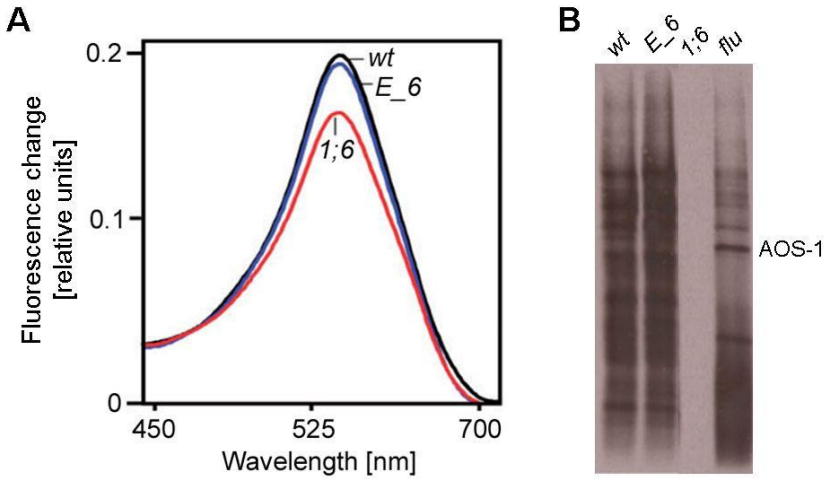

Figure 48. Cell death rescue in the mutant line *Atoep16-1;6+35S-OEP16-1 E_6* in comparison to the wild-type and the mutant *Atoep16-1;6*. A, Singlet oxygen measurements in 5 days-old etiolated seedlings that were exposed to strong white light for 30 min. DanePy fluorescence emission spectra were collected after excitation at 331 nm. B, Synthesis of proteins in etiolated seedlings after their illumination with non-permissive white light for 24 h. For comparison, the mutant *flu* was included to demonstrate the induction of stress-related proteins. Protein labelling with ^{35}S-methionine was performed 2 h before end of illumination. Each line contained 20 µg of total protein extracts separated by SDS-PAGE and detected by autoradiography.

Etiolated seedlings of mutant *Atoep16-1;6* responded to illumination with a complete arrest of protein synthesis. By contrast, seedlings of the complemented line *E_6* were able to pursue protein synthesis upon a dark-to-light shift and the protein pattern seemed indistinguishable from that of wild-type seedlings. In the *flu* mutant used as reference, light exposure led to the production of stress-related proteins such as AOS-1, confirming that the chosen cultivation regime and light conditions permitted the activation of the singlet oxygen-dependent signalling cascade identified by K. APEL and co-workers.

DISCUSSION

The import of the majority of nucleus-encoded plastid proteins is ensured by the common TIC/TOC pathway (LI & CHIU, 2010). These proteins share the feature of possessing N-terminal extensions collectively referred to as plastid transit peptides that mediate their transport to the chloroplast surface and their subsequent translocation across the envelope membranes. Upon their arrival in the stroma, the plastid transit peptides are cleaved off. It was initially thought that all of the different cytosolic precursors enter the chloroplast through the TIC/TOC machineries. However, recent evidence supports the existence of multiple, differentially regulated import pathways that exhibit substrate- and tissue-specificity in order to adjust protein import to the actual developmental and environmental conditions (JARVIS *et al.*, 1998; BAUER *et al.*, 2000; IVANOVA *et al.*, 2004; KUBIS *et al.*, 2004). Moreover, an increasing number of non-canonical import pathways such as the plastid import via the endomembrane system was discovered that complement the general plastid import pathway (e.g. VILLAREJO *et al.*, 2005). Also the import of proteins located in the outer envelope membranes, except of TOC75, seems not to involve the common TOC translocon (JARVIS, 2008). Whether the import of these proteins really does not involve the common TOC translocon is controversially discussed (TU *et al.*, 2004).

Proteomics analyses of chloroplasts by KLEFFMANN *et al.* (2004) revealed a large number of proteins lacking cleavable transit peptides. Two such proteins are ceQORH (MIRAS *et al.*, 2002) and TIC32 (NADA & SOLL, 2004). Both proteins are located in the inner envelope membrane of chloroplasts. Their import did not involve the standard protein import machinery (NADA & SOLL, 2004; MIRAS *et al.*, 2007) but was dependent on translocation machineries that have thus far not been characterized.

Proteomics analyses of the chloroplast envelope membranes revealed the existence of two protein pairs, termed HP20/HP22 and HP30/HP30-2 (FERRO *et al.*, 2002; FERRO *et al.*, 2003) that could play a role in the import of transit peptide-less plastid precursors. These proteins are related to the components of the mitochondrial import machinery TIM17 and TIM22, two members of the family of preproteins and amino acid transporters (PRAT) (RASSOW *et al.*, 1999). Despite their common structural features including the presence of 4 transmembrane helices, PRAT proteins have distinct expression patterns, suggesting a large functional diversity beyond their role in protein translocation (MURCHA *et al.*, 2007). Because of their relationship to the PRAT family one could speculate that these 4 proteins represent members of yet uncharacterized import pathways of plastidic proteins. Other

members of the PRAT family comprise the OEP16 subfamily. OEP16-1 of *A. thaliana* was described to play a role as voltage-gated amino acid-selective channel and/or as the import pore for the precursor of PORA (POHLMEYER *et al.*, 1998; REINBOTHE *et al.*, 2004a). Its actual role will be discussed in chapter 3.2.

3.1 The Physiological Role of HP20/HP22 and HP30/HP30-2 in the Chloroplast Envelopes

3.1.1 HP20/QTC24 mediates the Import of the Transit Peptide-less Precursor Protein ceQORH

The fact that the import of the chloroplast envelope quinone oxidoreductase homolog, ceQORH, does not require TOC159- and TOC75 (MIRAS *et al.*, 2007) suggests the operation of a novel import pathway. Multiple, regulated versions of the TIC and TOC machinery were described previously (JARVIS *et al.*, 1998; BAUER *et al.*, 2000; IVANOVA *et al.*, 2004; KUBIS *et al.*, 2004) of which some could be involved in ceQORH import. For example, one might imagine that ceQORH is imported by a TOC subcomplex containing TOC132, TOC120 or TOC90 instead of TOC159 (INABA & SCHNELL, 2008). Since ceQORH does not play a role in photosynthesis, this proposal would correspond to the fact that TOC complexes involving TOC132/TOC120 preferentially import non-photosynthetic housekeeping proteins (BAUER *et al.*, 2000; KUBIS *et al.*, 2004).

However, when only the so-called soluble domain of ceQORH, the part of the amino acids 60-100, was used for *in vitro* import, TOC159 could be cross-linked. This underscored the necessity of the C- and N-terminus for the direction of ceQORH to its specific translocon complex (MIRAS *et al.*, 2007). The observation of TOC159-dependent import of (60-100)-ceQORH could be confirmed in this work by (i) *in vitro* import experiments in which (60-100)-ceQORH was simultaneously imported with the complete ceQORH and both precursor proteins did not compete with each other (Figure 7) and (ii) co-purification of (60-100)-ceQORH together with TOC75 (Figure 8 A).

MIRAS *et al.* (2007) described that a ~30 kDa protein seems to be involved in ceQORH's translocation across the chloroplast envelope membranes. This result could be confirmed and extended in the present work and ceQORH was shown to interact with at least five plastid envelope proteins during import (Figure 9). The corresponding complex was designated

ceQORH translocon complex (QTC). One of the five co-purified proteins, QTC24, corresponds to HP20/HP22, as demonstrated by amino acid sequence alignments. Thus, its proposed function in protein translocation, that was based on the relationship of HP20/HP22 to other PRAT family members, such as TIM17 and TIM22 operating as components of the mitochondrial import machinery, could be confirmed experimentally. It is conceivable that QTC24/HP20 interacts with other known TOC components such as TOC132/TOC120 and TOC33/TOC34 during ceQORH import. However, sequencing of the other four proteins that co-purified with ceQORH during import thus far did not reveal clear results. We thus can only speculate about their implication in ceQORH import since at least QTC120 and QTC33 had a size that is similar to that of TOC120 and TOC33, respectively. Further experiments are needed to verify this hypothesis. For example, blocking of TOC120 and TOC33 by respective antibodies and Fab fragments should drop import of ceQORH if these proteins were part of the QTC complex. In addition, chloroplasts of mutants deficient in these TOC components could be tested for their ability to import ceQORH.

The blocking of the QTC translocation channel with QTC24 antibodies resulted in the complete inhibition of ceQORH translocation and also reduced the ability of ceQORH to bind at this translocon complex. Together with the proof that HP20/QTC24 is an intrinsic membrane protein in the outer chloroplast envelope membrane (Figure 22 A), these results indicated that QTC24 establishes a hydrophilic translocation pore. The fact that the binding of ceQORH was reduced suggested that one part of QTC24 must be exposed at the chloroplast envelope into the cytosol and function in ceQORH binding. This could be confirmed by the partial sensitivity of HP20/QTC24 to thermolysin (Figure 22 A). The low detectable quantity of HP20/QTC24 in conjunction with the low ceQORH expression indicates that the QTC translocon is of low abundance in chloroplasts of green leaves. Previous quantitative receptor binding studies have shown that chloroplasts contain approximately 4-5-fold less import sites for ceQORH than for the small subunit of RubisCO and (60-100)-ceQORH-GFP that both use TOC75 for import (MIRAS *et al.*, 2007).

Further proof for a role of HP20 in ceQORH import was obtained from the observation that, the corresponding *Athp20* mutant was defective in ceQORH import in the *in vitro* uptake assays with chloroplasts and etioplasts. HP20 and its most closely related counterpart in the PRAT family, HP22, thus do not seem to act redundantly. Otherwise, chloroplasts obtained from the *Athp20* mutant plants should have been able to import ceQORH *in vitro* which was

obviously not the case (Figure 26). The *in planta* analyses (Figure 27) showing an association of ceQORH with mesophyll cell and, to a weaker extent, also guard cell chloroplasts of the *Athp20* mutant at first glance seem to weaken this conclusion. However, the biochemical experiments show that plastids that were depleted of QTC24 still bound significant amounts of ceQORH. Thus, the detection of GFP florescence at the outer edges of chloroplasts *in planta* (Figure 27) is likely due to the presence of other QTCs that mediate this binding step.

MIRAS *et al.* (2007) have shown that the full-length ceQORH protein was not imported into guard cell chloroplasts of the wild-type, whereas truncated versions of ceQORH could be imported most likely through a TOC75-mediated pathway. Therefore, the authors concluded that the pathway required for ceQORH import is not present or unfunctional in this cell type. The partial association of full-length ceQORH-GFP with plastids in guard cells of the *Athp20* mutants and of wild-type (Figure 27) at first glance seems to be in contradiction to the observation by MIRAS *et al*. (2007) that the QTC translocon is not present or active in guard cells. However, it cannot be excluded that other QTCs are artificially up-regulated, such as QTC130 to seemingly compensate for the absence of QTC24/HP20. On the other hand, care must be taken with the interpretation of the *in planta* import studies since mistargeting of fluorescence-labelled proteins due to a too high expression level of a protein (HAWES *et al.*, 2001) with normally low expression can be observed (see also chapter 3.1.2). Additional experimental tools to resolve this question could be monoclonal antibodies that could be used in electron microscopic immunolocalization studies.

3.1.2 Localization of HP20 and HP30 and their Topology in Envelope Membranes

An attempt was made to confirm the plastid envelope localization of HP20 and HP30 obtained from proteomics analyses (FERRO *et al.*, 2002; FERRO *et al.*, 2003).

The *in vivo* localization studies carried out with HP20-GFP and HP30-GFP indeed showed an association with chloroplast envelopes because the GFP fluorescence was concentrated at the periphery of the plastids. However, a more precise interpretation whether the chimeric proteins are only bound to the outer surface or integrated into the envelope membranes appears to be difficult.

On the other hand, localization studies of fluorescence-labelled proteins by confocal laser scanning microscopy were performed by others and interpreted as localization in the

chloroplast envelope membranes (LEE *et al.*, 2001; ASEEVA *et al.*, 2004; DUY *et al.*, 2007). In these and other cases (FERRO *et al.*, 2002; LEE *et al.*, 2003b; REIDEL *et al.*, 2008), the results were affirmed by biochemical localization studies that revealed the presence of these proteins in the inner or outer envelope membrane. A common feature in these studies was the sharp focus of the GFP signal in the periphery of chloroplasts, forming halo-like structures, that was interpreted as localization in the envelope membranes. A quite similar distribution of GFP fluorescence was obtained in our analysis for HP20-GFP and HP30-GFP. The fact that both proteins were partially found in the cytosol after their expression in tobacco protoplasts as well as in guard cells of *A. thaliana* might be due the artificially high expression level (Figure 20, Figure 21).

The cytosolic localization of HP20-GFP in guard cells shown in the current study corroborates the proposal of MIRAS *et al.* (2007) that the ceQORH-specific translocon is not present or not operative in guard cells since full length ceQORH could not be imported in chloroplasts of this cell type *in planta*. However, at least in some guard cells an association of HP20-GFP with chloroplasts was found which might be interpreted as the result of an abnormal high expression level of the transgene and missorting of the encoded product (Figure 20 B).

The expression level and functionality were shown before to be important factors that influence proper targeting of fluorescence-labelled proteins. According to HAWES *et al.* (2001), too strong expression of fluorescent protein chimeras can lead to mistargeting. Such strong expressions can be due to the use of the 35S cauliflower mosaic virus promotor which is highly active and results in a strong expression of transgenes in most plants cells (KARIMI *et al.*, 2002). This high expression (possibly also due to the presence of multiple insertions of the created constructs in the genome) can cause the formation of large fluorescent "aggregates" that accumulate in the cell. Since HP20, HP30 and ceQORH are proteins with normally very low expression levels in green leaves (according to the BAR website), an artificially caused strong expression might cause missorting into the cytosol that results in the formation of these "aggregates". Furthermore, the strength of fluorescence signals can also vary in the different cell compartments due to protein folding, pH and proteolytic effects (HAWES *et al.*, 2001). Also the structure and the correct folding of the introduced proteins are important for their interaction with other cellular components at the chloroplast surface or in the cytosol.

The localization of HP20/QTC24 in the chloroplast envelopes could be confirmed biochemically. It is an intrinsic protein in the outer envelope membrane that is partially sensitive to thermolysin indicating that hydrophilic domains are exposed into the cytosol. However, PUDELSKI *et al.* (2010) propose a localization of HP20 and HP22, termed PRAT1.1 and PRAT1.2, in the inner envelope membrane. In addition, the authors suggest in their article that both, HP30 and HP30-2 (termed PRAT2.1 and PRAT2.2 respectively), are dually located in the inner chloroplast envelope membrane and in the inner mitochondrial membrane (PUDELSKI *et al.*, 2010). However, as found for HP20 and HP22 (chapter 3.1.1), this proposal was based on only preliminary results.

Computer-assisted topology predictions performed for HP20 and HP30 in this work suggest that both may contain four transmembrane helices. Indeed, all PRAT proteins share this property. Pure structure predictions in principal confirm the topology analyses presented by PUDELSKI *et al.* (2010). The exact position of the transmembrane domains differs by a few amino acids. Moreover, the determination of the N- and C-terminal orientation of PRAT2 (HP30/HP30-2) identified the N-terminus to reside in the inter membrane space of mitochondria and chloroplasts, respectively (PUDELSKI *et al.*, 2010). This result is at variance with the topology prediction of HP30 performed in this work (Figure 23). In addition, PUDELSKI *et al*. (2010) found that PRAT2.1 (HP30) and PRAT2.2 (HP30-2) have a somehow peculiar role in the PRAT family because of their dual localization and the presence of a unique sterile alpha motif (SAM) domain in their C-termini. Since the SAM domain was described to play a role in signal transduction, protein and nucleotide binding, the authors suggest that the SAM domain in PRAT2.1 (HP30) and PRAT2.2 (HP30-2) may function in homo- or heterooligomerization (PUDELSKI *et al.*, 2010).

3.1.3 *Athp20* and *Athp30* Plants are Not Defective in the Plastid Import of Standard Precursor Proteins and Amino Acids

The analysis of chloroplasts of the *Athp20;2* mutant with regard to the presence of components of previously characterized import pathways, such as TOC75 and TIC110 as well as OEP16-1, indicated that these pathways are intact since wild-type amounts of these proteins were present in the mutant (Figure 25). This was underscored by *in vitro* import experiments. Precursor proteins that are imported via the common TIC/TOC pathway, such as pSSU, pFD, pLHCII and pPORB, were taken up into isolated chloroplasts of *Athp20* with

the same efficiency as that measured for wild-type chloroplasts (Figure 26). The same observation was made for the import of pPORA whose import required Pchlide produced by 5-ALA feeding. Additionally, the overall analysis of import of nucleus-encoded plastid precursor proteins that had been synthesized *in vitro* from total RNA revealed that the *Athp20* as well as the *Athp30* were also not defective in general protein import (data not shown), although two-dimensional separation of the proteins is needed to back up this point. Nevertheless, these results indicate that *Athp20* and *Athp30* chloroplasts did not exhibit major defects in general protein import. Furthermore, no role of HP20 and HP30 in the import of TIC32 could be observed in *in vitro* (data not shown) or *in planta* approaches. Whether the QTC translocon is involved in import of other plastid precursor proteins beside ceQORH is unknown and shall be characterized in future work, using proteomics approaches of isolated chloroplasts and etioplasts from mesophyll and guard cells of the *Athp20* mutants. *In organello* protein biosynthesis with isolated chloroplasts and ^{35}S-methionine was used to assess a potential lack in uptake of amino acids into the plastid compartment in the *Athp20* and *Athp30* mutants. This approach did not reveal detectable differences between plastids isolated from mutant *Athp20* and mutant *Athp30*, as compared to wild-type plants (Figure 30). Uptake experiments with other radiolabelled amino acids are needed to proof the results obtained from the *in organello* labelling.

3.1.4 Analysis of the Phenotype of *Athp20* and *Athp30* Plants cultivated under Standard Growth Conditions

Under standard laboratory growth conditions the *Athp20* and *Athp30* plants had no phenotype and looked like wild-type (Figure 29). Moreover, *Athp20* and *Athp30* had no visible drop in total and *in organello* protein biosynthesis and accumulation (Figure 30). Along with the lack of a detectable growth defect these data suggest that HP20 and HP30 do not accomplish essential roles *in planta*. One could argue that their close relatives, HP22 and HP30-2, respectively, could have at least in part complementary functions that would permit normal growth. Similar to *Athp20* and *Athp30,* also a respective ceQORH knock-out mutant had no visible phenotype under standard growth conditions (S. REINBOTHE, personal information), suggesting that this protein and its respective import pore for faithful translocation from the cytosol across the outer envelope into the inner envelope membrane may be operative only under very restricted conditions and/or windows of plant development.

In order to find out whether HP20 and HP30 (and their close relatives) might have a function under specific developmental conditions, the phenotype and the pattern of total and plastid-specific proteins of the corresponding knock-out plants were investigated during the early stages of greening when etiolated seedlings are exposed to light and are especially prone to photooxidative damage, and under conditions that artificially induce leaf senescence.

3.1.5 The Accumulation of Plastid-encoded Proteins is delayed during the De-etiolation of *Athp20* Seedlings

The de-etiolation/photomorphogenesis response is very complex and involves the light-dependent inhibition of hypocotyl growth, apical hook straightening, opening of cotyledons, and the development of etioplasts to chloroplasts (WATERS & LANGDALE, 2009). Mostly phytochromes perceive light of different wavelength and initiate a signalling cascade that results in the switch from heterotrophic to photoautotrophic growth. The latter requires chlorophyll biosynthesis that is strictly light-dependent in angiosperms and accompanied by the expression of plastid and nuclear genes for photosynthetic proteins. Given that chlorophyll and its precursors such as Pchlide are powerful photosensitizers that can trigger photooxidative stress, we analysed the greening of the *Athp20* and *Athp30* mutants under different light conditions.

Illumination experiments were conducted with dark-grown *Athp20* and *Athp30* mutant seedlings at low and high light intensities. No differences in the greening and accumulation of plastidic proteins were observed in etiolated *Athp30* seedlings compared to the wild-type.

By contrast, *Athp20* seedlings were slightly impaired in greening and accumulated less chlorophyll per time unit analysed. The cotyledons of *Athp20* seedlings were less green as those of wild-type seedlings after 6-8 h of irradiation, although no drastic differences of the chlorophyll contents could be measured experimentally. More strikingly, the accumulation of the plastid-encoded photosynthetic proteins, such as the D1 protein of photosystem II and the α–subunit of cytochrome *b*-559 (αCytb_{559}), was delayed in mutant *Athp20* relative to the wild-type. Moreover, the nucleus-encoded ELIP1 protein, which is an indicator for photooxidative stress, was affected in mutant *Athp20*. ELIPs are related to the LHCII proteins and located in the thylakoid membranes but may be rather involved in energy dissipation than in light harvesting. Furthermore, ELIPs are only induced in adult plants upon light stress or in the first hours of greening when the seedlings develop the photosynthetic apparatus and are prone to photooxidation (MONTANÉ & KLOPPSTECH, 2000).

In mutant *Athp20* we assume that enhanced ELIP expression may be due to the delayed assembly of the D1-containing reaction centres of photosystem II.

It is tempting to hypothesize that the delayed biosynthesis of the plastid-encoded D1, αCytb_{559}, and LSU proteins in mutant *Athp20* might be caused by a reduced uptake of cytoplasmic amino acid into the developing chloroplast. However, this effect seems to be restricted to the early stages of the development of etioplasts to chloroplasts since no differences in the contents of D1, αCytb_{559} and LSU were detected for chloroplasts from 2.5 weeks-old light-grown *Athp20 versus* wild-type plants (chapter 2.6.1). Work is needed to proof whether the amino acid import is indeed impaired in *Athp20* etioplasts during the initial stages of greening. To this end, amino acid uptake experiments will be conducted with isolated etioplasts.

3.1.6 HP20 and HP30 play no Role during Senescence

Leaf senescence represents the final stage of leaf development and is an active and highly regulated degeneration and cell death process basically ruled by the developmental age (THOMAS *et al.*, 2003). It is a type of programmed cell death that can be triggered by internal and external factors, such as age, environmental stresses, plant hormones and other growth regulators, and it is mediated by an active genetic program (GUO & GAN, 2005, LIM *et al.*, 2007). By virtue of its action, the remobilization of nutrients from the leaf as source tissue to sinks such as roots and seeds is ensured. Since leaves are the major photosynthetic organs, an optimal utilization of nutrients is critical for plant viability (LIM *et al.*, 2007). Once senescence-inducing signals are set, expression of a large number of senescence-associated genes (*SAG*s) occurs (LIM *et al.*, 2007). *SAGs* encode proteins that mediate processes like active degeneration of cellular structures and macromolecules, nutrient recycling, and programmed cell death. The earliest and most significant changes during leaf senescence occur in chloroplasts and involve the disassembly of the grana and stroma thylakoids, the breakdown of chlorophyll, and the formation of plastoglobules (LIM *et al.*, 2007). These processes must be tightly coordinated in time and space to avoid harmful secondary effects. For this reason it was interesting to analyse whether HP20 and HP30 might play a role in recruiting senescence-induced proteins for export or help transferring amino acids from the plastid compartment to the cytosol.

Under the conditions of induced leaf senescence tested in this work, i.e., incubation of the leaves in solutions of ABA or MeJa, two senescence-inducing hormones, and dark-treatments, no differences in the chlorophyll loss could be observed between wild-type, *Athp20* and *Athp30* mutant plants. Neither the visual phenotype nor the pattern of analysed total leaf proteins was influenced in mutant *Athp20* and mutant *Athp30*, disproving that HP20 and HP30 play essential roles in the senescence process.

3.1.7 *Athp30/Athp30-2*-RNAi Plants exhibit a Chlorotic Phenotype during Early Plant Development

Athp20- and *Athp30*-RNAi plants were created in order co-suppress the expression of HP20 and its closest relative HP22 and of HP30 and HP30-2, respectively.

The established *Athp30-RNAi* plants had an interesting phenotype and displayed an impairment in greening when they were grown in continuous white light. The plants were smaller and the leaves were pale green and contained less chlorophyll. These effects were reduced when the plants were kept under dark-light cycles and seemed to depend on the light intensity and on plant age (Figure 41). Although the extent of silencing and consequently the reduction in transcript level of *HP30* and *HP30-2* and perhaps other PRAT family members was not determined, one might hypothesize that HP30 and HP30-2 act synergistically. Otherwise, similar defects should have been observed in the *Athp30* single knock-out mutants which was not the case. This point of view is supported by results obtained for *Athp30/Athp30-2* double-knock-out mutants that exhibited a severe chlorotic phenotype and a disturbed cell structure including aberrant chloroplasts (KRAUS *et al.,* 2009). Thus, the presence and function of either HP30 or HP30-2 is essential for chloroplast development and plant viability in *A. thaliana*. In line with this view, the re-introduction of functional HP30 led to a restoration of the wild-type phenotype (KRAUS *et al.*, 2009).

Interestingly, the observed phenotype resembles that of mutants called *snowy cotyledon 1* and *2* (initially *cyo1*) (ALBRECHT *et al.*, 2006; ALBRECHT *et al.*, 2008; SHIMADA *et al.*, 2007). *SCO1* and *SCO2* encode a chloroplast elongation factor G and a novel plastidic protein possessing a DnaJ-like zink finger domain, respectively, that were proposed to be involved in the folding of thylakoid-located proteins. These mutants were also impaired during early developmental stages since their cotyledons were pale green and had reduced levels of chlorophylls, whereas mature plants showed a wild-type phenotype. Although wild-type levels of mRNAs of plastid- and nucleus-encoded proteins were detected, the amounts of the

corresponding proteins were drastically reduced. Moreover, etiolated *sco2* seedlings were not able to green after an extended growth in darkness although their etioplasts did not exhibit any defects. The phenotypic similarities between the *Athp30-RNAi* plants and the *sco1* and *sco2* mutants indicate that *Athp30-RNAi* plants might be impaired in plastidic protein biosynthesis and that HP30 and HP30-2 could play a role in the import of amino acids.

3.1.8 The Role of HP20 and HP30 – Conclusions

The protein pairs HP20/HP22 and HP30/HP30-2 were first identified by proteomics of the chloroplast envelope membranes (FERRO *et al.*, 2002; FERRO *et al.*, 2003). Due to their structural characteristics, they belong to the family of preprotein and amino acid transporters. On the other hand, a plastid-located quinone oxidoreductase homologous to that of prokaryotes was described to be imported into plastids independently of a transit peptide and without using TOC159 and TOC75 as translocon components. In this thesis, at least 5 proteins could be purified as interaction partners of ceQORH during import. One of the isolated proteins, termed QTC24, turned out to be identical to HP20. Further analysis revealed that HP20 establishes a hydrophilic translocation pore in the outer envelope membrane. *In vitro* import experiments with *in vitro* synthesized ceQORH and chloroplasts isolated from a *Athp20* mutant revealed that these plastids were unable to import ceQORH and that HP22 could not functionally replace HP20 in ceQORH import. Moreover, the *Athp20* mutant seemed to be impaired in the expression of plastid-encoded proteins during the differentiation of etioplasts into chloroplasts that could be due to an impairment of amino acid transport across the outer envelope membrane.

The role of HP30 is less clear at the moment. No defects in the import of nucleus-encoded precursor proteins were detectable for plastids isolated from *Athp30* mutant plants. The observed phenotype of *Athp30-RNAi* plants, however, and the findings obtained for *Athp30/Athp30-2* double-knock-out mutant plants by KRAUS *et al.* (2009) suggest that HP30 and HP30-2 act synergistically and thereby are essential for plant viability and chloroplast biogenesis in the early stages of seedling development and greening.

3.2 The Physiological Function of *A. thaliana* OEP16-1: Translocation Channel for the Plastid Import of pPORA and/or Amino Acid Transporter

3.2.1 Two Functions proposed for OEP16-1

Based on its sequence relationship to proteins of the PRAT family, a function of OEP16-1 in the transport of amino acids, peptides and/or proteins can be hypothesized. The role as voltage-gated, amino acid-selective channel was proven by POHLMEYER *et al.* (1997) and PHILIPPAR *et al.* (2007), whereas a role as the import channel for pPORA was demonstrated by REINBOTHE *et al.* (2004a and 2004b), POLLMANN *et al.* (2007) and SCHEMENEWITZ *et al.* (2007). Both functions are not mutually exclusive and were re-evaluated in the present work. Interestingly, the characterization of a corresponding *A. thaliana* knock-out mutant (*Atoep16-1*) provided contradictory results (see chapter 1.5.1 and Table 2).

PHILIPPAR *et al.* (2007) argued that the Pchlide-dependent pPORA import represents an artefact resulting from the use of idiosyncratic methods. This conclusion is in obvious contrast to *in planta* and *in vitro* import studies performed by other groups that confirmed the Pchlide-dependent import of pPORA (KIM & APEL, 2004; YUAN *et al.*, 2010). In a recent review PUDELSKI *et al.* (2010) propose that OEP16-1 might be involved in the cold acclimation since the corresponding transcripts were strongly induced by cold stress whereas osmotic stress, salicylic and ABA stress did not significantly change the OEP16-1 expression pattern. BALDI *et al.* (1999) reported that the barley *OEP16-1* gene has a particularly high expression level during cold acclimation in cereals. PUDELSKI *et al.* (2010) further speculated about an interaction of OEP16-1 with PRAT2 (= HP30/HP30-2) during amino acid transfer since equal quantities of both proteins are present in the plastid envelope membranes.

In the work of POLLMANN *et al.* (2007) OEP16-1 was demonstrated to function as the import pore for pPORA. Consequently, the lack of OEP16-1 in the *Atoep16-1* mutant led to a block of pPORA import, lack of the PLB and LHPP complexes in etioplasts, accumulation of free porphyrin pigments, photobleaching and cell death after light exposure of dark-grown seedlings. In order to explain the *Atoep16-1* mutant phenotype, POLLMANN *et al.* (2007) presented the following model: In wild-type seedlings PORA:Pchlide*b*-NADPH and PORB:Pchlide*a*-NADPH ternary complexes form supramolecular LHPP complexes in the PLB (chapter 1.2). Once enough LHPP has been produced, excess PORA:Pchlide*b*-NADPH

complexes would function as Pchlide sensor and interact with the FLU protein that blocks the C5-pathway and Pchlide production. This negative feedback control seems not to be operational in the *Atoep16-1* mutant since no PORA is imported. Thus, no PORA:Pchlide*b*-NADPH ternary complexes can be formed to bind overproduced free Pchlide, which then acts as photosensitizer during illumination.

Table 2. Controversial roles of OEP16-1 in pPORA import inferred from studies on the *Atoep16-1* mutant (SALK_024018) performed by POLLMANN *et al.* (2007) and PHILIPPAR *et al*. (2007). + / – stands for present / absent; n.d. stands for not determined/documented.

		POLLMANN *et al.* (2007)	PHILIPPAR *et al.* (2007)
Pchlide-dependence of pPORA import (*in vitro*) in general		yes	no
***Atoep16-1* mutant**			
Number of T-DNA insertions		1	n.d.
Number of back-crosses with wild-type		2	n.d.
Presence of OEP16-1		–	–
Presence of PORA / PORB		– / +	+ / +
Amino acid / precursor uptake			
Amino acid uptake (import of ^{14}C-labelled amino acids)		normal	n.d.
Import of standard precursors (*in vitro*)		normal	n.d.
Import of pPORA	*in vitro*	– (only binding at the chloroplast envelope)	+
	in vivo	–	+
Used import pathway of pPORA		via OEP16-1 (cross-linking)	via TIC/TOC (competitive inhibition)
Seedling development			
Normal growth conditions		normal (continuous light)	normal (day-night-rhythm)
Photobleaching inducing conditions		cell death phenotype	n.d.
Accumulation of free porphyrin pigments		yes (Pchlide *a*)	n.d.
Etioplast ultrastructure			
Presence of PLB		–	+ (~wt)
Presence of LHPP		–	n.d.

How could the contradictory results obtained for the phenotype of the *Atoep16-1* mutant be explained? We hypothesized that additional mutations are present in the genome of the *Atoep16-1* mutant and that these exogenic mutations affect the establishment of the

phenotype during greening. Since POLLMANN *et al.* (2007) presented Southern blots which revealed the presence of only one single T-DNA insertion these additional mutations might be point or footprint mutations or may be caused by pretty small T-DNA fragments not detectable with kanamycin resistance gene probe (POLLMANN *et al.*, 2007). To trace the presence of such mutations the original *Atoep16-1* (SALK_024018) seed stock was rescreened and four different mutant classes were identified by Iga SAMOL.

3.2.2 Re-screen of the SALK_024018 Seed-stock and Characterization of its Genetic Background

3.2.2.1 The *Atoep16-1* Mutant comprises at least Four Subtypes with different Phenotypes

Independent homozygous plants of the original *Atoep16-1* seed-stock were back-crossed once with the wild-type and plants that were homozygous for the *Atoep16-1*mutation were used to establish seed stocks (SAMOL *et al.*, 2011a). Seedlings obtained from these seed stocks were analysed further with regard to the presence of PORA and capability to green. Four subclasses of *Atoep16-1*mutants were obtained, designated *Atoep16-1;5-1;8*. These subclasses were different in their PORA content and their capability to green after irradiation of etiolated seedlings (Table 3). Due to their characteristics, line *Atoep16-1;5* was concluded to correspond to the line described by POLLMANN *et al.* (2007), whereas line *Atoep16-1;8* was hypothesized to correspond to the line identified by PHILIPPAR *et al.* (2007). Line *Atoep16-1;6* is identical to line F6-4a that was used by PUDELSKI *et al.* (2009). In both laboratories, this line reproducibly contained PORA but nevertheless died because of accumulation of free Pchlide molecules operating as photosensitizers and giving rise to singlet oxygen. However, differences were observed with regard to the Pchlide accumulation kinetics. In our experiments line *Atoep16-1;6* accumulated notable amounts of Pchlide only after at least 4.5 days of growth in darkness (SAMOL *et al.*, 2011b), whereas PUDELSKI *et al.* (2009) argued that Pchlide fluorescence indicative of the presence of free pigment is seen as early as 2 d after the onset of germination.

Despite the presence of PORA, etiolated seedlings of mutant *Atoep16-1;6* (F6-4) suffered from photooxidative damage when illuminated (PUDELSKI *et al.,* 2009; SAMOL *et al.*, 2011a). These results at first glance suggest an uncoupling between PORA accumulation and photoprotection anticipated for this enzyme (BUHR *et al.*, 2008). Similarly, an uncoupling

between PORA accumulation and Pchlide sequestration was observed for mutant *Atoep16-1;7* that greened normally even in the absence of PORA. However, mutant *Atoep16-1;7* contained drastically reduced Pchlide levels in the dark that could be photoconverted by PORB. LEBEDEV *et al.* (1995) provided evidence that greening can proceed via a non-canonical pathway not requiring PORA.

Table 3. Phenotypic properties of the four *Atoep16-1* subclasses of mutants isolated from SALK_024018 (Summarized from SAMOL *et al.*, 2011a). Pchlide-F_{655}, the so-termed photoactive Pchlide, is an indicator for functional PORA:PORB:pigment complexes whereas Pchlide-F_{631} represents a mixture of PORA-bound Pchlide *b* and free, non-protein-bound Pchlide molecules (chapter 1.2). Abbreviations/Symbols: + / −, present / absent; t_{50}, half life; n.d., not detectable; ↑/↓, accumulation / reduction, number indicates the degree of accumulation / reduction.

		Atoep16-1;5	***Atoep16-1;6***	***Atoep16-1;7***	***Atoep16-1;8***
Number of T-DNA insertions		1	1	1	1
Presence of OEP16-1		−	−	−	−
Presence of PORA / PORB		− / +	+ / +	− / +	+ / +
pPORA import	*in vitro*	−	+	−	+
	via	−	TOC75	−	TOC75
	in vivo	−	+	−	+
Cell death phenotype / t_{50}		+ / 4 h	+ / 8 h	− / n.d.	− / n.d.
Accumulation of Pchlide		+	+	−	−
Pchlide-F_{631} / Pchlide-F_{655} (in comparison to the wild-type)		↑↑ / −	↑ / ↓	↓ / −	wt / ↓
Accumulation of $^1O_2$ (in comparison to the wild-type)		↑↑↑	↑↑	~wt	~wt
Corresponds to line		*Atoep16-1* POLLMANN *et al.* (2007)	*F6-4a* PUDELSKI *et al.* (2009)	−	*oep16.1-1* PHILIPPAR *et al.* (2007)

3.2.2.2 Is there a Correlation between the OEP16-1-Deficiency, the Defect of pPORA Import and the Cell Death Phenotype of the *Atoep16-1* Mutant?

A causal relationship between the reduction in the overall POR content and impairment of greening was originally made for *A. thaliana* wild-type seedlings that were grown in non-photooxidative far-red (cFR-) light (RUNGE *et al.*, 1996; SPERLING *et al.*, 1997). Such plants had yellow leaves and did not green normally in white light. The absence of PORA and substantially reduced levels of PORB resulted in a reduced size of the prolamellar bodies.

Upon transfer to standard white light, the seedlings suffered from photooxidative damage and were devoid of thylakoid membranes.

LEBEDEV *et al.* (1995) and SPERLING *et al.* (1998) have provided direct evidence for the implication of PORA in the greening of etiolated seedlings. In these previous studies a *photomorphogenic deetiolated* (*det340)* mutant of *A. thaliana* was used which showed morphological features such as short hypocotyls, open apical hooks, and open cotyledons in the dark. This mutant was devoid of PORA and photoactive Pchlide-F_{655}, had reduced amounts of PORB and contained aberrant PLBs. Only when grown under low light intensities *det340* seedlings were able to green. Growth under standard and high light intensities, however, was accompanied by a disturbed chlorophyll accumulation and *det340* seedlings were highly susceptible to photooxidative damage due to high levels of photoinactive Pchlide-F_{631}. SPERLING *et al.* (1998) overexpressed PORA or PORB cDNAs in this mutant and reported that this would restore normally sized PLBs as well as photoactive Pchlide-F_{655}. However, no clear POR protein data were shown to confirm the specific expression of the PORA and PORB proteins and their activity (SPERLING *et al.*, 1998). The evidence for redundant roles of the PORA and PORB, as claimed by SPERLING *et al.* (1998) is thus weak and indeed an independent study using the same transgenic lines as those used by SPERLING *et al.* (1998) detected photooxidative damage during a dark-to-light shift (MCCORMAC & TERRY, 2002 and 2004).

Together, the experiments by LEBEDEV *et al.* (1995), SPERLING *et al.* (1997 and 1998) and RUNGE *et al.* (1996) provide direct evidence that PORA is important for conferring photoprotection to new-born, etiolated seedlings. This hypothesis was confirmed by BUHR *et al.* (2008) using *in vitro*-mutagenesis studies on PORA of barley.

No differences in the PORA transcript levels were found in seedlings of mutants *Atoep16-1;6* and *Atoep16-1;7* as compared to the wild-type (Figure 43). Furthermore, sequencing of the *PORA* transcripts after RT-PCR did not reveal differences in *Atoep16-1;6* and *Atoep16-1;7*. This excludes the possibility that either unfunctional, inactive PORA was synthesized in mutant *Atoep16-1;6* or that the enzyme possessed an aberrant structure and was therefore protease-hypersensitive in mutant *Atoep16-1;7*. The explanation left over is that the differences in PORA accumulation are caused by the operation of different import pathways. *In vitro* import studies of a transA-DHFR derivative consisting of the transit peptide of PORA and the dihydrofolate reductase (DHFR) reporter protein of mouse coupled with cross-linking studies via DTNB (SAMOL *et al.*, 2011a, Table 3) showed that plastids

from mutant *Atoep16-1;6* import transA-DHFR via a TOC75-dependent pathway, whereas plastids of mutant *Atoep16-1;7* are unable to import transA-DHFR because of the lack of OEP16-1. No cross-link products and no import was observed with plastids of mutant *Atoep16-1;7*. It is tempting to hypothesize that two independent exogenic mutations are present in mutants *Atoep16-1;6* and *Atoep16-1;7* that differentially affect the establishment of the phenotype. While the first mutation is present in mutant *Atoep16-1;6* and leads to a default import of pPORA, the second mutation affects Pchlide synthesis and drastically reduces pigment accumulation. This second mutation may be in components of the feedback loop that limit excess Pchlide accumulation in the dark. Precedents of this type of mutations exist in the literature. GOSLINGS *et al.* (2004) isolated a suppressor mutant of *flu* that contains drastically reduced pigment levels. Default import of pPORA through the TOC75 channel does not allow the interaction of PORA with its substrate Pchlide *b*. As a consequence, no ternary PORA-Pchlide *b*-NADPH complexes are formed that could assemble into LHPP. This can be deduced from the low temperature measurements that revealed an almost complete absence of Pchlide-F_{655}.

The point or footprint mutation present in mutant *Atoep16-1;6* seems to hit a regulatory component of the PTC and TOC machineries. As convincingly shown by KIM & APEL (2004), the substrate-dependent import was confined to the cotyledon stage, whereas pPORA import was not dependent on Pchlide in leaves of mature green plants. Obviously, cytosolic targeting factors, such as 14-3-3 proteins or HSP70, are responsible for directing the PORA precursor protein to the TIC/TOC machinery in mature plants (SCHEMENEWITZ *et al.*, 2007). A 14-3-3 protein binding site was identified in the mature region of the PORA that governed substrate-independent, TOC75-mediated import. Since the transA-DHFR precursor employed in this analysis does not contain this identified binding site for 14-3-3 proteins, (SCHEMENEWITZ *et al.*, 2007), we conclude that pPORA import in *Atoep16-1;6* plastids is not likely to be due to 14-3-3 and HSP70 protein. Instead, another, yet to be identified pathway must be operational in mutant *Atoep16-1;6* that gave rise to TIC/TOC-dependent import.

Further proof for the causal relationship between the cell death phenotype and the lack of OEP16-1 protein comes from the segregation analysis on backcrossed *Atoep16-1;6* mutant plants. In the T_2 generation of such a backcross, the plants segregated in 40 wild-type seedlings, 89 seedlings with a weak bleaching phenotype and 41 with a strong cell death phenotype. This corresponds to a monohybrid, semi-dominant expected ratio of 42.5 to 85.0 to 42.5 ($\chi^2 = 0.21$; $P = 0.975$) (SAMOL *et al.*, 2011b). In fact no seedlings were obtained that

were homozygous for the *Atoep16-1* mutation and lacked the cell death phenotype. On the other hand, no seedlings were rescued that were wild-type for the *AtOEP16-1* gene but displayed the cell death phenotype. Hence, not any additional mutation but the *Atoep16-1* insertion is responsible for this phenotype comprising the defect of pPORA import, lack of Pchlide sequestration and the singlet oxygen production.

The most compelling evidence for a correlation between the presence of OEP16-1 and accumulation of functional, pigment-complexed and LHPP-assembled PORA was provided from the genetic transformation experiments. Importantly, genetic transformation of the *Atoep16-1;6* mutant with functional OEP16-1 protein restored the wild-type phenotype. Three different cDNA constructs were generated by Iga SAMOL, 35S-OEP16-1; GFP-OEP16-1; OEP16-1-YFP, and tested for their capability to suppress the cell death phenotype in mutant *Atoep16-1;6*. The obtained homozygous plants of the T_3 generation were analysed with regard to the expression of OEP16-1 and PORA and the establishment of the cell death phenotype (SAMOL *et al.*, 2011b and chapter 2.8.2). Moreover, the cytolocalization of the produced fluorescence-tagged proteins was determined (SAMOL *et al.*, 2011b and chapter 2.8.2). Nine transgenic T_3 lines were obtained that expressed 35S-*OEP16-1* and five of these showed rescue from photobleaching. Six transgenic lines expressed 35S-*GFP-OEP16-1* and one of these provided rescue from photobleaching. Four transgenic lines were obtained expressing 35S-*OEP16-1-YFP*, but none rescued from photobleaching (SAMOL *et al.*, 2011b). The latter may express an incorrectly folded or improperly targeted fusion protein not permitting to establish an active PORA import pore (SAMOL *et al.*, 2011b). The former two lines obviously contained functional and properly targeted OEP16-1 protein. *In vitro* protein import and crosslinking studies showed that the reintroduced OEP16-1 interacts with transA-DHFR and restores the Pchlide dependency of import. In a generated stable transgenic line expressing a pPORA-GFP reporter, higher rates of import of the fusion protein were seen, as compared to line *Atoep16-1;6.* In the respective backcross of mutant *Atoep16-1;6* expressing pPORA-GFP, however, no import of the reporter protein was possible and the chimeric precursor was therefore degraded in the cytosol.

As a consequence of OEP16-1 expression and restoration of Pchlide-dependent pPORA import normal greening was seen in line *E_6*. Low temperature pigment measurements demonstrated that a significant fraction of photoinactive Pchlide-F_{631} was shifted into

photoactive Pchlide-F_{655} (Figure 47, SAMOL *et al.*, 2011b), thus ultimately confirming that OEP16-1 is required for pPORA import and greening.

Moreover, no singlet oxygen could be measured with DanePy in the complemented *Atoep16-1;6* line, i.e., line *E_6*, and no DNA fragmentation indicative of cellular damage was detectable anymore. Final pulse-labelling studies showed a restoration of protein synthesis that was drastically reduced in mutant *Atoep16-1;6* as a result of Pchlide-sensitized singlet oxygen evolution (Figure 48 and SAMOL *et al.*, 2011b).

Table 4. Phenotypic analysis of the complementation of line *Atoep16-1;6* with 35S-OEP16-1 (Summarized from SAMOL *et al.* (2011b)). Although the level of photoactive Pchlide-F_{655} in line *E_6* was slightly lower in than in the wild-type a remarkable shift of Pchlide-F_{631} to Pchlide-F_{655} occurred that was caused by the reintegration of functional OEP16-1 protein and subsequent PORA import. Abbreviations/Symbols: + / −, present / absent; ↑/↓, accumulation / reduction, number indicates the degree of accumulation / reduction, HMW/LMW, high/low molecular weight DNA.

		Atoep16-1;6	*Atoep16-1;6+ 35S-OEP16-1*
in vitro import of transA-DHFR into	etioplasts	+	+
	chloroplasts	+	+
	via	TOC75	OEP16-1
in vivo import of pPORA-GFP		+	+
Greening of etiolated seedlings under photobleaching conditions		cell death	normal
Pchlide accumulation		↑↑	wt
Pchlide-F_{631} / Pchlide-F_{655} (in comparison to the wild-type)		↑ / ↓	~wt / ↓
Presence of LHPP		−	+
Accumulation of $^1O_2$ (in comparison to the wild-type)		↑↑	~wt
DNA degradation	HMW-DNA	↓	wt
	LMW-DNA	↑	wt
Synthesis of stress induced proteins		−	+

3.2.3 Existence of additional Mutations in the Genome of the *Atoep16-1* Mutant and their putative Impact on Cell Death

Contradictory results were obtained by PUDELSKI *et al.* (2009) and our group (POLLMANN *et al.*, 2007, SAMOL *et al.* 2011a) with regard to the number of T-DNA insertions detected in the seed stock of SALK_024018. At least in part, these differences may reflect the different

numbers of backcrosses carried out prior to further analysis. Recombination is a random process and it is therefore conceivable that even repeated backcrosses may not provide the same genetic background as single or double crosses (POLLMANN *et al.*, 2007 and SAMOL *et al.* 2011a, respectively).

PUDELSKI *et al.* (2009) described *Atoep16-1* mutant lines that contained wild-type alleles of the *OEP16-1* gene but expressed a cell death phenotype. Thus, the presence of additional T-DNA insertions that cause cell death was hypothesized. PUDELSKI *et al.* (2009) found two additional T-DNA insertions besides the one in the *AtOEP16-1* gene. The first insertion was found 4 bp upstream of the coding region of At1g70370 encoding a homolog of AroGP1, a noncatalytic β-subunit of the polygalacturonase isoenzymes (PG1) from potato. This enzyme is involved in the regulation of pectin solubilisation and depolymerisation in the apoplast. The other T-DNA insertion was identified with a truncated right border in the putative promotor region of At3g29200, encoding for a plastid-localized chorismate mutase 1 (CM1), which is part of the shikimate pathway (biosynthesis of aromatic amino acids). However, the genotype of both additional T-DNA insertions did not co-segregate with the cell death phenotype, too. Consequently, PUDELSKI *et al.* (2009) excluded direct involvements of these genes in etioplast-to-chloroplast transition, greening and cell death regulation and proposed indirect effects. Since CM1 is localized in the plastid, its lack could pleiotropically affect other plastid processes. The most obvious interpretation that CM1 may enter the plastids via an OEP16-mediated import pathway was disregarded by PUDELSKI *et al.* (2009).

PUDELSKI *et al.* (2009) proposed in their study that point or footprint mutations not detectable by Southern blotting may be the cause of the cell death phenotype. Line F6-4 which corresponds to mutant *Atoep16-1;6* contains a single T-DNA fragment but may possess such mutations. As one candidate gene that might be affected in mutant *Atoep16-1;6* we tested the presence and functionality of *FLU* (Figure 43) that plays an important role in the feedback loop preventing excess Pchlide accumulation in the dark (MESKAUSKIENE *et al.*, 2001). Based on the analysis of transcript level by Northern blotting and sequencing of RT-PCR-amplified RNA we conclude that neither is affected in *Atoep16-1;6* plants. Both *FLU* levels and *FLU* sequence were the same as those in wild-type. A similar conclusion was drawn by (PUDELSKI *et al.*, 2009).

Direct hits in the *PORA* and *PORB* gene could additionally account for the cell death phenotype seen in mutant *Atoep16-1;6.* However, Northern blotting and DNA sequencing

did not reveal possible differences in expression or functionality of the PORA and PORB proteins (Figure 43). This result disproved a direct implication of the *PORA* and *PORB* as direct sites of secondary mutation(s) obviously present in mutant *Atoep16-1;6.*

On the basis of these results and in line with previous considerations, the presence of additional mutations must be anticipitated. The possible nature of such mutations is unknown and shall be determined in future work using mapping and whole genome sequencing approaches.

Yet to be identified mutations besides the one in the *AtOEP16-1* gene must be present. *Atoep16-1;7* expressed no cell death phenotype despite the absence of PORA and the lack of photoactive Pchlide-F_{655}. It is attractive to hypothesize that the "hidden" mutation present in mutant *Atoep16-1;7* suppressed the cell death phenotype. Most likely DNA rearrangements provoked by the insertion and loss of T-DNAs gave rise to this type of suppressor mutation (LATHAM *et al.*, 2006).

3.2.4 Characterization of the Cell Death Phenotype in the OEP16-1 Mutants

3.2.4.1 The Expression of the Phenotype is strictly Age-dependent

The cell death phenotype described by PUDELSKI *et al.* (2009) was not as strong as in our studies. Important factors that might have influenced this result are the seedling age and the growth conditions, especially light quality and quantity. HUQ *et al.* (2004) showed that the hypocotyl length of etiolated seedlings which is an indicator of plant development in darkness is tightly connected to the progression of the cell death phenotype as seen in *pif1* plants lacking PHYTOCHROME-INTERACTING FACTOR 1, a crucial transcription factor for greening. PIF1 normally prevents the accumulation of excess Pchlide in the dark. In etiolated *pif1* seedlings, excess amounts of Pchlide accumulate along over time in darkness and cause photooxidative damage when the seedlings are subsequently illuminated. Similar to these results, the *Atoep16-1;6* mutant showed exaggerated cell death when kept longer in the dark and survived and greened normally when transferred to light at an early seedling stage (SAMOL *et al.*, 2011a; SAMOL *et al.*, 2011b & Figure 42).

Moreover, the photon fluence rate (often equated with the light intensity) plays an important role for the extent of photobleaching *versus* greening in mutant *Atoep16-1;6*. Whereas low photon fluence rates of 25 µE m^{-2} s^{-1} allowed almost normal greening and prevented cellular damage, the extent of cell death increased when high fluence rates of 210 µE m^{-2} sec^{-1} were

applied (SAMOL *et al.*, 2011a). In the case of the *pif1* mutant, fluence rates (light intensities) of 50 µE m^{-2} s^{-1} were sufficient to cause photodamage. Another factor that influences the establishment of the cell death phenotype in our experiments was the sugar content of the growth medium. Sucrose at a concentration of 1-3 % (w/v) was able to partially prevent photobleaching (not shown). Sucrose provides a carbon source and operates at the same time as an intracellular signal that exerts effects at the levels of transcription and translation (NICOLAI *et al.*, 2006).

Although PUDELSKI *et al.* (2009) used photon fluence rates of 350 µE m^{-2} s^{-1} only a weak photobleaching phenotype was expressed in 2.5 days-old F6-4 (*Atoep16-1;6)* mutant seedlings. Whether these experiments were carried out with media containing or lacking sucrose could not be deduced from the published experimental details. Nevertheless, the results of PUDELSKI *et al.* (2009) confirm that the most important factor defining the extent of photobleaching *versus* greening is the age of etiolated seedlings and amount of Pchlide accumulated.

3.2.4.2 The physiological Response of Etiolated *Atoep16-1;5* Seedlings to Photooxidative Stress Differs from that of the *flu* Mutant

Another OEP16-1-deficient mutant contained in the SALK_024018 seed stock is represented by *Atoep16-1;5* that corresponds to the *Atoep16-1* described by POLLMANN *et al.* (2007). The cell death phenotype of mutant *Atoep16-1;5* was very similar to that of the *flu* mutant described by MESKAUSKIENE *et al.* (2001). However, time course experiments revealed some important differences in cell death execution that reflected differences in Pchlide level and composition that may also apply to mutant *Atoep16-1;6.* While the total level of Pchlide in etiolated seedlings was 8.5-fold elevated in *flu* as compared to the wild-type, only 4.5-fold higher pigment levels were seen in *Atoep16-1* seedlings. Interestingly, also the actual pigment composition differed. While *flu* seedlings accumulated Pchlide *b*, *Atoep16-1* seedlings accumulated Pchlide *a* (POLLMANN *et al.*, 2007).

Another, quite interesting observation that may directly apply to our current study on *Atoep16-1;6* concerns the mechanism by which singlet oxygen operated in cell death execution. While *flu* seedlings responded to a non-permissive dark-to-light shift with a rapid induction and polysomal binding of messengers for stress proteins and enzymes involved in ethylene and jasmonic acid biosynthesis and signalling (OP DEN CAMP *et al.*, 2003), *Atoep16-1;6* seedlings were unable to do so (SAMOL et al., 2011a). Taken together, these

results highlight the existence of more than one cell death pathway that is triggered by singlet oxygen in *A. thaliana*.

3.2.5 The Role of OEP16-1 - Conclusions

Two non-exclusive functions currently being considered for the OEP16-1 protein in the outer envelope of chloroplasts are (i) a voltage-gated, amino acid-selective channel (POHLMEYER *et al.*, 1997; PHILIPPAR *et al.*, 2007) and (ii) an import channel of pPORA (REINBOTHE *et al.*, 2004a, POLLMANN *et al.*, 2007). In the present study, further evidence is provided for the second role. Accordingly, pPORA is imported via OEP16-1 in a Pchlide-dependent manner; this pathway is operative only in young, etiolated seedlings. During import, PORA interacts with Pchlide *b* and forms ternary complexes with its substrate Pchlide *b* and NADPH that in turn assemble with PORB-Pchlide*a*-NADPH ternary complexes to establish large light-harvesting POR-Pchlide (LHPP) complexes in the PLB of etioplasts. The function of these complexes is to harness low amounts of photons for immediate Chlide *a* production and to dissipate excess light energy in a nonhazardous manner. These light-harvesting and photoprotective functions enable dark-grown seedlings germinating underneath the soil or under fallen leaves to switch from heterotrophic to photoautotrophic growth once light becomes available.

Once enough LHPP has been made, an as yet unknown feedback mechanism switches in the early steps of tetrapyrrole synthesis. Maybe non-assembled PORA-Pchlide*b*-NADPH ternary complexes, together with the FLU protein may be part of this feedback loop. On the other hand heme has been reported to inhibit the formation of 5-ALA, the first committed precursor of all tetrapyrroles in plants, by acting at the level of glutamate-tRNA reductase (MESKAUSKIENE *et al.*, 2001).

In order to permit greening without provoking oxidative damages, POR needs to be imported post-translationally from the cytosol. The following results strongly support a role of OEP16-1 in pPORA import: (i) the expression pattern of OEP16-1 and PORA overlap during plant development; (ii) the induced singlet oxygen-mediated cell death phenotype co-segregates with the T-DNA insertion in the *OEP16-1* gene after back-cross with the wild-type and (iii) the complementation with functional OEP16-1 protein could restore the wild-type phenotype.

However, the genetic characterization of the SALK_024018 seed stock revealed other factors that may be involved in controlling etioplast-to-chloroplast differentiation. Since there are still some open points, such as the absence of a photobleaching phenotype in line *Atoep16-1;7* which was PORA-deficient, the following points might help to finally proof the relationship between the OEP16-1 knock-out, pPORA import defect, and the progression of the singlet oxygen-mediated cell death. It will in fact be important to obtain *Atoep16-1*-RNAi mutants to vindicate our previous observations. On the other hand, the nature of the exogenic mutations in some of the identified *Atoep16-1* mutant lines needs to be unravelled by mapping and whole genome sequencing approaches. Last but not least, the characterization of the components of the singlet oxygen-triggered but jasmonic acid-dependent cell death pathway and the role of translation need to be explored. Answering these questions will provide new insights into the miracle of greening and mystery of death in higher plants.

MATERIALS & METHODS

4.1 Material

4.1.1 Plant Material

Because of its completely sequenced genome the model plant *Arabidopsis thaliana* is a useful instrument to study the role of genes by reverse genetic approaches. Experimental work was performed with the variety Columbia (Col-0). T-DNA insertion lines were identified in the Salk Institute Genomic Analysis Laboratory collection (SIGnAL, ALONSO *et al.*, 2003) and on the website of The *A. thaliana* Information Resource (Tair) and ordered from the Nottingham *A. thaliana* Stock Centre (NASC) (Table 5). Tobacco (*Nicotiana benthamiana*) was used for transient transformation in order to analyse the subcellular localization of proteins coupled with fluorescence tags.

Table 5. List of *A. thaliana* T-DNA insertion lines used in this work.

Protein	Gene	Line	New Name/Subtype	Reference
HP20	At4g26670	SALK_020671	*Athp20;1*	this work
		SALK_125640	*Athp20;2*	
		SALK_074935C	*Athp20;3*	
		SALK_125736	*Athp20;4*	
HP30	At3g49560	SALK_031707	*Athp30;1*	this work
		SALK_112126	*Athp30;2*	
		SALK_046194	*Athp30;3*	
OEP16-1	At2g28900	SALK_024018	*Atoep16-1*	POLLMANN *et al*., 2007
			Atoep16-1;6	SAMOL *et al.*, 2011a
			Atoep16-1;7	SAMOL *et al.*, 2011a
FLU	At3g14110	SALK_002383	*flu*	SAMOL *et al.*, 2011a
Other lines				
Atoep16-1;6 + 35S-OEP16-1 E_6				SAMOL *et al.*, 2011b
wt + 35S-GFP				E. Boex-Fontvieille[a]

[a] Laboratoire Plastes et Différenciation Cellulaire (UJF/CNRS/FRE3017), Université Joseph Fourier 1, Grenoble, France

4.1.2 Bacteria

Table 6. Genotypes and brief description of the used bacterial strains.

Species	Genotype	Application	Reference
E. coli DB3.1	F⁻ *gyr* A462 *end* A1 Δ(*sr*1-*rec*A) *mcr*B *mrr hsd*S20($r_B^-m_B^-$) *sup*E44 *ara*14 *gal*K2 *lac*Y1 *pro*A2 *rps*L20(Sm^r) *xyl*5 Δ*leu mtl*1	Propagation of empty Gateway donor and destination vectors.	Invitrogen
E. coli DH5α	F⁻ *rec*A1 *end*A1 *hsd*R17(r_k^-, m_k^-) *sup*E44 λ*thi*-1 *gyr*A96 *rel*A1	Cloning and propagation of created plasmids. Its sensitivity to CcdB protein allows a negative selection of after Gateway cloning reactions.	Invitrogen
E. coli BL21-AI	F⁻ *ompT hsdS*$_B$($r_B^-m_B^-$) *gal dcm araB*::*T7RNAP-tetA*	Heterologous expression of proteins with N-terminal $(His)_6$-tags.	Invitrogen
A. tumefaciens AGL1	AGL0 *rec*A::*bla* pTiBo542ΔT Mop^+, Cb^R	Stable transformation of *A. thaliana* and tobacco.	LAZO *et al.*, 1991

4.1.3 Nucleic Acids

4.1.3.1 cDNA Clones

Table 7. List of used cDNA clones.

Protein	Gene	Clone	Reference
HP20	At4g26670	RAFL06-13-H13	Riken BioResouce Center (Japan)
HP30	At3g49560	RAFL-09-15-P16	
HP22	At5g55510	S63288	Arabidopsis Biological Resource Center (ABRC) of the Ohio State University (USA)
HP30-2	At5g24650	U21408	
ceQORH	At3g13010		Gift of N. ROLLAND[a]
TIC32	At4g23430		

[a] Laboratoire Physiologie Cellulaire Végétale, UMR5168/CNRS/CEA/INRA/Université Joseph Fourier, Grenoble, France

cDNA clones that were used as templates for the synthesis of precursor proteins for *in vitro* import experiments, were ferredoxin (pFD), the light harvesting chlorophyll *a/b*-binding protein of photosystem II (pLHCII), the small subunit of ribulose-1,5-bisphosphate carboxylase/oxygenase (pSSU), the NADPH:Pchlide oxidoreductase A (pPORA) and B (pPORB), ceQORH-GFP, (60-100)-ceQORH-GFP, ceQORH-$(His)_6$ and TIC32-$(His)_6$ and were described in MIRAS *et al.* (2007) and POLLMANN *et al.* (2007).

4.1.3.2 Oligonucleotides

Table 8. List of oligonucleotides and their application. Restriction sites are highlighted in the corresponding colour. Start and stop codons are underlined. Synthesis was carried out by Sigma-Genosys (La Verpillière, France), MWG Biotech AG (Ebersberg) and Invitrogen (Karlsruhe).

Notation	Sequence (5' - 3')	Application
Prot HP20F1	attB1[a] + GCGGCGAACGATTCTTCA	Cloning (without start codon) into pDEST17 for heterologous expression of N-terminally His-tagged proteins.
Prot HP20R1	attB2[b] + TTAGAACTTCCTTGGTTTAGC	
Prot HP30F1	attB1 + GTGGTAGGCGGCGGAGGAGAA	
Prot HP30R1	attB2 + CTACTTTCGTTTGCCCTTTATCTC	
At5g5551-FW1	attB1 + GCGGCCGAGAATTCTTCAAAC	
At5g5551-RW1	attB2 + TCAACGAGCATGAGGAAATTT	
At5g24650-FW1	attB1 + GGGAAAGACGGAGAAGGAGAC	
At5g24650-RW1	attB2 + TCAACCACGACTTCCCCGCTT	
Hp20GFPF1	attB1 + ATGGCGGCGAACGATTCTTCA	Cloning (without stop codon) into pK7FWG2 or pB7RWG2 for *in vivo* localization via C-terminally tagged GFP/RFP.
Hp20GFPR1	attB2 + AAGCTTCCTTGGTTTAGCTAA	
Hp30GFPF1	attB1 + ATGGTGGTAGGCGGCGGAGGAGAA	
Hp30GFPR1	attB2 + CTTTCGTTTGCCCTTTATCTC	
Tic32RFPF1	attB1 + ATGTGGTTTTTTGGATCG	
Tic32RFPR1	attB2 + AGAACTGCTTTCTCCTGA	
ceqorhFWatt	attB1 + ATGGCTGGAAAACTCATGCACGCTC	
ceqorhRWatt	attB2 + TGGCTCGACAATGATCTTCCCAGTA	
FdGFP	attB1 + ATGGCTTCTACACTCTCTACC	
FdGFPR1	attB2 + AGCAGTAAGTTCCTCCTCCTT	
LBa1	TGGTTCACGTAGTGGGCCATCG	Genotyping of *A. thaliana* T-DNA insertion lines.
HP20PF	CTATTGACATCGACGGGAAT	
HP20PR	TGCAAATGATCCTTTGAAGC	
HP30GT1	AAGCGGATTAGAGGCAAAGAG	
HP30GT2	GATTGGCCAATTGTATGAACC	
KanF2	CTATGACTGGGCACAACAGAC	Production of Digoxigenin-labelled probes for specific DNA or RNA detection on southern and northern blots.
KanR2	GAAGGCGATAGAAGGCGATG	
LB GT1	ACTTAATAACACATTGCGGACG	
LB GT2	CTTAATCGCCTTGCAGCACATC	
hp20-F1	GTGACGAAGCGACCGATAATG	
hp20-R1	ATTTCTTCAGGGATCGGGAGAG	
hp30-F1	GCGATGGCGAGTTTATTCAACG	
hp30-R1	CCTTTATCTCCGGGTCCCTCT	

POR-fwd	attB1 + ATGGCCCTTCAAGCTGCTTCT	Detection of transcripts by RT-PCR and subsequent cloning.
POR-rev	attB2 + TTTAGGCCAAGCCTACGAGC	
PORA-utr-fwd	attB1 + TAACATTCACATTACACTCT	
PORA-utr-rev	attB2 + TGTTTCGTTTAAGACTTAAA	
FLU-fwd	attB1 + ATGTGGCAGGGAATTGGGAGG	
FLU-rev	attB2 + TCAGTCAGTCTCTAACCGAGC	
HP20RNAiF3	GACGGATCCCTCGAGTAATGATTCCTCGAAGGCATT	Production of RNAi constructs in pHannibal (forward primers with *Bam*HI and *Xho*I; reverse primers with *Kpn*I and *Hind*III restriction sites).
HP20RNAiF4	GACGGATCCCTCGAGTGCCTTCTGAAGCAAATCCGA	
HP20RNAiR3	CTGAAGCTTGGTACCAAACGTGAGACAACTCTGTAG	
HP20RNAiR4	CTGAAGCTTGGTACCTTTGATTTCTTCAGGGATCGG	
HP30RNAiF3	GACGGATCCCTCGAGGTTTCAGGTTAAATTCAAAGA	
HP30RNAiF4	GACGGATCCCTCGAGTCTGCAGTGGTGGCAGCGTTA	
HP30RNAiR3	CTGAAGCTTGGTACCAGCAGTAGTGATTGCATTCAT	
HP30RNAiR4	CTGAAGCTTGGTACCATCATAAGTCTTGGCCCTGGT	
RNAiPDKF1	TGACAAGTGATGTGTAAGACG	Identification of transformed *A. thaliana* plants by amplification of the PDK intron in RNAi lines, the *gfp/rfp* sequences and the connection between cDNA and fluorescence tag.
RNAiPDKR1	AATGATAGATCTTGCGCTTTG	
FdGFPF2	TCTCGTGGCAGAGTGACTGC	
HP20GFPF2	CTCAGGCTCTTGTGGGTGGT	
HP30GFPF2	AGATGCAGGGCAGTCTGCTAA	
Tic32RFPF2	CGGTTCTCGTATCCAGAAGGAGT	
QORGFPF2	AACCGCTCTCCAAGCTCTTAC	
egfp1	ATGGTGAGCAAGGGCGAG	
egfp2	GGTGCGCTCCTGGACGTA	
rfp1	CGACTACTTGAAGCTGTCCT	
rfp2	CTCGTACTGTTCCACGATG	
rfp3	AAGTTCATCACGCGCTCCCACT	
[a] attB1	GGGGACAAGTTTGTACAAAAAAGCAGGCTCC	
[b] attB2	GGGGACCACTTTGTACAAGAAAGCTGGGTC	

4.1.3.3 Plasmids

Table 9. Brief description of applied plasmids.

Notation	Description	Reference
pDONR221	Gateway donor vector for the creation of entry clones with the gene of interest by Gateway BP reaction.	Invitrogen
pDEST17	Gateway expression vector for heterologous expression of N-terminally $(His)_6$-tagged proteins.	Invitrogen
pK7FWG2	Binary Gateway destination vector for C-terminal fusion of GFP to the cDNA of interest and a kanamycin gene as plant selection marker.	KARIMI *et al.*, 2005
pB7RWG2	Binary Gateway destination vector for C-terminal fusion of RFP to the cDNA of interest and a Basta gene as plant selection marker.	KARIMI *et al.*, 2005
pB7WG2	Binary Gateway destination vector for constitutive expression of the cDNA of interest and a Basta gene as plant selection marker.	KARIMI *et al.*, 2005
pB7WG2-GFP	Binary Gateway vector with integrated GFP without a plastidic signal sequence, as control for cytosolic localization in transformed plants.	Boex-Fontvieille, E.[a]
pHannibal	Cloning vector for the creation of intron-containing RNAi constructs.	WESLEY *et al.*, 2001
pArt27	Binary vector for the transfer of RNAi constructs into plants with a kanamycin gene as plant selection marker.	GLEAVE, 1992
pSP73	Cloning vector with a multiple cloning site and SP6 and T7 RNA polymerase promotors for *in vitro* transcription/translation.	Promega

[a] Laboratoire Plastes et Différenciation Cellulaire (UJF/CNRS/FRE3017), Université Joseph Fourier 1, Grenoble, France

4.1.4 Antibodies

Table 10. List of applied antibodies.

Antibody directed against	Reference
HP20 from *A. thaliana* HP30 from *A. thaliana*	this work
tetra-His, BSA-free	Qiagen
Enhanced GFP	Euromedex
Total outer chloroplast envelope proteins	Gift of S. MIRAS[a]
OEP37 of *Pisum sativum*	SCHNELL *et al.*, 1994
TOC75 of *Pisum sativum*	MA *et al.*, 1996
PTC52, synthetic peptide of the *Hordeum vulgare* cDNA clone	REINBOTHE *et al.*, 2004a

OEP16-1 of *A. thaliana*	SAMOL *et al.*, 2011b
TIC110 of *A. thaliana*	LÜBECK *et al.*, 1996
TIC32 of *A. thaliana*	HÖRMANN *et al.*, 2004
IEP36 of *Pisum sativum*	SCHNELL *et al.*, 1990
LSU of *Pisum sativum* RubisCO	Gift of J. ELLIS[b]
SSU of *Pisum sativum* RubisCO	Gift of J. ELLIS[b]
Ferredoxin of spinach	SMEEKENS *et al.*, 1985
LLS1 (lethal leaf spot protein) of maize, monoclonal	YANG *et al.*, 2004
LOX2 from etiolated cucumber cotyledons	Gift of C. WASTERNACK[c]
AOS from *A. thaliana*	Gift of S. POLLMANN[d]
Succinate dehydrogenase	S. MIRAS[a], G. SCHATZ[e]
Fumarase	S. MIRAS[a], G. SCHATZ[e]
TIM23	S. MIRAS[a], G. SCHATZ[e]
LHCII of *A. thaliana*	
ELIP1 of *A. thaliana*	
POR of *Triticum aestivum*	
PsbA/D1, core component of photosystem II, global antibody	Agrisera, Vännäs, Sweden
PsbE, Cytochrome b_{559} of *A. thaliana*	
PsbO, 33kDa subunit of OEC of spinach	
F-type ATP Synthase subunit B (AtpB)	
Anti-Rabbit IgG –Alkaline Phosphatase	
Anti-Rabbit IgG – Horseradish Peroxidase	
Anti-Mouse IgG – Alkaline Phosphatase	Sigma-Aldrich
Anti-Goat IgG – Alkaline Phosphatase	
Anti-Chicken IgY – Alkaline Phosphatase	
Anti-Digoxigenin-Alkaline Phosphatase, Fab fragments	Roche

[a] Laboratoire Physiologie Cellulaire Végétale, UMR5168/CNRS/CEA/INRA/UJF, Grenoble, France

[b] Department of Biological Sciences, University of Warwick, Coventry, CV4 7AL, England

[c] Institute of Plant Biochemistry, Halle/Saale

[d] Lehrstuhl für Pflanzenphysiologie, Ruhr-Universität Bochum

[e] Biozentrum, University of Basel, Switzerland

4.1.5 Chemicals and Instruments

Chemicals and consumables were purchased in analysis quality from Roth (Karlsruhe or Lauterbourg, France), Dominique Dutscher (Brumath, France), Merck (Darmstadt), Sigma-Aldrich (Steinheim or La Verpillière, France), VWR (Strasbourg, France). All molecular

biological chemicals and common enzymes were ordered from MBI Fermentas (St. Leon-Rot), Euromedex (Souffelweyersheim, France), Roche (Mannheim), Invitrogen (Karlsruhe), GE Healthcare (München) or Qiagen (Hilden). Common instruments were purchased from Eppendorf (Hamburg) and Bio-Rad (München). Instruments that are not mentioned in the text conformed to the common lab standard.

4.1.6 Software and Internet Databases

SimVector 3.0 (Premier Biosoft International) was used to plan cloning steps, restriction analyses and the construction of plasmid maps.

W^2H (Version 4, 2001) contains the software package of the University of Wisconsin Genetics Computer Group (GCG) Version 9.1 (DEVEREUX *et al.*, 1984) that was used for multiple sequence alignments.

Prediction of subcellular localization
ChloroP (EMANUELSSON *et al.*, 1999)
TargetP (EMANUELSSON *et al.*, 2000)
WoLF PSORT (HORTON *et al.*, 2007)
Predotar (SMALL *et al.*, 2004)
MultiLoc (HOEGLUND *et al.*, 2006)

Topology-prediction of membrane proteins
TMpred (HOFMANN & STOFFEL, 1993)
TopPred (VON HEIJNE, 1992)
HMMTOP (TUSNÁDY & SIMON, 2001)

Other used databases
http://blast.ncbi.nlm.nih.gov/Blast.cgi (Analysis of sequence similarities)
http://signal.salk.edu/cgi-bin/tdnaexpress (T-DNA Express: *A. thaliana* Gene Mapping Tool)
http://www.arabidopsis.org (The *Arabidopsis* Information Resource/Tair)
http://bar.utoronto.ca/ (Gene Expression Data)
http://www.rnaiweb.com (RNAi guidelines)
http://aramemnon.botanik.uni-koeln.de (Plant Membrane Protein Database)

4.2 Cultivation of Plants

4.2.1 *In vitro* Cultivation of *A. thaliana*

For surface-sterilization the needed amount of seeds was incubated for 10 min in 500 µl of sterilization solution with agitation at room temperature (1300 rpm; Thermomixer comfort,

Eppendorf). After centrifugation (14000 rpm, 1 min, room temperature, centrifuge 5415D, Eppendorf), the sterilization solution was decanted and the seeds were incubated for 2 min in 70% ethyl alcohol with agitation. Then, the seeds were washed 5-times with sterile distilled water, taken up in liquid 0.1% (w/v) agarose and spread on MS agar plates (containing the appropriate antibiotics, if necessary; MURASHIGE & SKOOG, 1962). Alternatively, drops of ~25 seeds in water were sown on the MS agar plates. To overcome the dormancy (stratification), the plates were placed for 48 h into the dark at 4 °C before light exposure. The plants were grown in climate chambers with 16/8 h day/night periods and a light intensity of 70 µE m^{-2} s^{-1} at 23 °C (provided by Mazda Fluor 58 W and Osram Fluora 58 W lamps).

Sterilization Solution	MS Agar
1.56 % (w/v) Sodium hypochlorite	4.36 g/l MS Salts (Sigma-Aldrich)
0.1 % (v/v) Tween-20	optional + 10 g/l Sucrose
	optional + 0.5 g/l MES
	pH 5.8
	1.0 % (w/v) Agar

4.2.2 Culture Conditions of Etiolated *A. thaliana* Seedlings and Light Exposure

Drops of ~25 seeds were sown on MS agar plates (+/− sugar and MES) and, after stratification and irradiation for 1-2 h at 125 µE m^{-2} s^{-1} (provided Mazda Fluor 58 W lamps) and at 25 °C, cultivated in the dark at 25 °C. 4.5 days-old etiolated seedlings were exposed to continuous white light of different intensities: 30-40 µE m^{-2} s^{-1} (low light), 70 µE m^{-2} s^{-1} (standard light) or 125 µE m^{-2} s^{-1} (strong light; provided Mazda Fluor 58 W lamps) as indicated in the text. Mostly, the upper third of the seedlings was taken for analysis.

4.2.3 Cultivation of *A. thaliana* and Tobacco on Soil

A. thaliana and tobacco seeds were spread on sterilized and insecticide-treated soil and covered with a plastic hood. After stratification, the plants were grown in continuous light (70 µE m^{-2} s^{-1} by Mazda Fluor 58 W lamps) at 23 °C and the plastic hood was removed after approximately 10 days. Alternatively, *in vitro* grown *A. thaliana* plants that were further cultured soil.

4.3 Cultivation of Bacteria

4.3.1 General Cultivation of *Escherichia coli* and *Agrobacterium tumefaciens*

Depending on the purpose *E. coli* bacteria were grown on LB agar plates or in liquid culture with agitation (220 rpm) over-night at 37 °C and in the presence of antibiotics (Table 11).
The growth of agrobacteria was performed on YEP agar plates for up to 2 days, in liquid culture for ~20 h with agitation (220 rpm) at 28 °C.
Stock cultures were produced by mixing 850 µl of a well-grown over-night culture with 150 µl of 99% (v/v) glycerol and freezing in liquid nitrogen. Long term storage was carried out at -80 °C.

Table 11. List of used antibiotics and their application.

Bacteria	Antibiotics	Final concentration
E. coli	Kanamycin	50 µg/ml
	Ampicillin	100 µg/ml
	Chloramphenicol	50 µg/ml
	Spectinomycin	25 µg/ml
Agrobacteria	Spectinomycin	100 µg/ml

LB Medium	YEP Medium
10 g/l NaCl	5 g/l NaCl
10 g/l Tryptone	10 g/l Tryptone
5 g/l Yeast extract	10 g/l Yeast extract
(+1.5 % (w/v) Agar)	(+ 1.5 % (w/v) Agar)

4.3.2 Cultivation of *E. coli* for heterologous Protein Expression

The expression of recombinant $(His)_6$-tagged proteins in *E. coli* BL21-AI was performed according to the instructions of the Manual of the *E. coli* Expression System with Gateway Technology (Version G, Invitrogen).

4.4 Molecular Biological Methods

4.4.1 Determination of Nucleic Acid Concentration

The nucleic acid concentration was measured with a spectrophotometer (BioPhotometer, Eppendorf). The optical density at 260 nm of 1 corresponds to 50 µg DNA or to 40 µg RNA. An indication of purity with regard to interfering proteins was provided by the ratio of the optical densities at 260 nm and 280 nm that should be at 1.8-2.0.

4.4.2 Amplification of DNA Fragments by Polymerase-Chain-Reaction (PCR)

Defined DNA sequences were amplified by PCR and specific primers. For PCR products that should be cloned, the Expand High Fidelity PCR System (Roche) containing a *Taq*-polymerase with proofreading activity was used. Otherwise, the *Taq* Polymerase and buffers by MBI Fermentas (*Taq* DNA-Polymerase LC recombinant, 1 U/µl) were taken. Table 12 shows the components of typical PCR reactions.

Table 12. Components of a standard PCR reaction.

	Final concentration
10x PCR buffer (+KCl)	1x (10 mM Tris-HCl, 50 mM KCl)
25 mM $MgCl_2$	1.5 mM
50x dNTPs (10 mM of each)	1x (0.2 mM of each)
Taq-DNA polymerase (1 U/µl)	1 U
Forward primer (10 µM)	0.2 µM
Reverse primer (10 µM)	0.2 µM
DNA template	10 ng plasmid DNA or 200 ng genomic DNA

Reactions were performed in the thermocycler (Mastercycler personal, Eppendorf) as followed and analysed by agarose gel electrophoresis (chapter 4.4.6):

1. Start DNA denaturation	95 °C	2 min
2. DNA denaturation	95 °C	1 min
3. Annealing of primers	50-63 °C	2 min
4. Extension with *Taq* polymerase	72 °C	1 min/kb
5. Repeat step 2-4	29-39 times	
6. Final extension	72 °C	5 min

4.4.3 Enzymatic Digestion of DNA and Dephosphorylation of 5'-Ends

The specific digestion of DNA was used for cloning and as control of individual cloning steps. Double-stranded DNA was incubated with an appropriate amount of restriction enzymes type II in a buffer recommended by MBI Fermentas at the optimum temperature (typically at 37 °C). Routinely, 1 µg of plasmid DNA was incubated with 1 U of a restriction enzyme in a total volume of 20 µl (Table 13). To ensure complete digestion, the reactions were incubated for 2-3 h. If genomic DNA was digested for southern blotting, RNaseA (MBI Fermentas) was added and the reactions were incubated over-night. The enzymes were

inactivated as recommended by the supplier and the products analysed by agarose gel electrophoresis (chapter 4.4.6).

Table 13. Components in a typical digestion reaction.

	Plasmid DNA	Genomic DNA
DNA	0.5 - 2 µg	10 µg
Enzyme (10 U/µl)	0.5 - 2 U	10 U
RNaseA A (10 mg/ml)	--	0.2 µg
10x Reaction Buffer	1x	1x

If necessary, 5'-ends of vector DNA were dephosphorylated after digestion by adding 2-times 10 U of a calf intestine alkaline phosphatase (MBI Fermentas) per 1 µg of vector DNA into the same tube and subsequent incubation for 30 min at 37°C each time. The dephosphorylation was stopped by incubation for 15 min at 85°C. For ligation, the restriction fragments were separated by agarose gel electrophoresis and extracted from the gel (chapter 4.4.6).

4.4.4 Ligation of DNA Fragments

Ligation of DNA fragments into adequate linearized cloning vectors was performed with the T4-DNA ligase by MBI Fermentas. The used insert to vector ratio was 3:1. The reactions were supplemented with 1 U of T4-DNA-ligase per 150 ng insert per 50 ng vector and incubated over-night at 22°C. The reactions were stopped by an incubation of the mixture for 10 min at 65°C and then transformed into *E. coli* DH5α (chapter 4.4.8).

4.4.5 Cloning with Gateway Technology

The Gateway Technology by Invitrogen (Manual Version E) was used to create various fusion genes (with N-terminal $(His)_6$-tags or different C-terminal reporter tags in appropriate destination vectors).

4.4.6 Agarose Gel Electrophoresis and DNA Extraction

Depending on the size of the DNA fragments and the required degree of band separation a gel concentration of 0.8-1.5 % agarose (in 1x TAE buffer) was chosen and the gel was run at 4-10 V/cm (in Sub-Cell GT or Mini Sub-Cell GT, power supply PowerPac3000, Bio-Rad).

Visualization of DNA was achieved by mixing the liquid agarose with ethidium bromide to a final concentration of 0.5 µg/ml and illumination of the gel by UV light (366 nm) after migration.

1x TAE Buffer	6x Gel Loading Dye
40 mM Tris-acetate	0.25 % (w/v) Bromophenolblue
1 mM EDTA, pH 8.0	0.25 % (w/v) Xylenecyanol
	15 % (w/v) Ficoll 400

If the separated products needed be used for downstream applications like cloning, the bands were cut out of the gel under UV light and DNA was eluted with the NucleoSpin Extract II kit of Macherey-Nagel (Hoerdt, France) according to the supplier's recommendations.

4.4.7 Sequencing of double-stranded DNA

Sequencing was carried out by GATC Biotech (Konstanz). Analysis of the obtained DNA sequences was performed by a nucleotide BLAST search (http://www.ncbi.nlm.nih.gov/).

4.4.8 Preparation and Transformation of Competent *E. coli* Cells

A culture of 250 ml of LB medium was inoculated with an over-night culture and grown to an optical density at 600 nm of 0.5. The chilled bacteria were harvested by centrifugation (4000 rpm, 10 min, 4 °C, centrifuge J-6M/E, rotor JA-14, Beckman) and washed in 125 ml of a cold 0.1 M $MgCl_2$ solution. Then, the bacteria were resuspended in 70 ml of a cold 0.1 M $CaCl_2$ solution and incubated for 20 min on ice. After a final centrifugation the competent bacteria were resuspended in 12.5 ml of a freezing solution. Aliquots were frozen in liquid nitrogen and stored at -80 °C.

Freezing Solution
86 mM $CaCl_2$
14% (w/v) Glycerol

If *E. coli* cells should be transformed with products of Gateway recombination reactions, the instructions described in the Gateway Technology Manual (Version E, Invitrogen) were used.

In all other cases the following steps were carried out: Competent bacteria were mixed with a complete ligation reaction or up to 25 ng of plasmid DNA per 50 µl of competent cells and incubated for 30 min on ice. The DNA was taken up into the bacteria by a heat shock of 90 s

at 42 °C. The re-chilled bacteria were incubated in 800 µl of LB medium for 1 h with agitation at 37 °C (Thermomixer comfort, Eppendorf) and spread on selective LB agar plates. For further analysis of the plasmids, over-night cultures of 3 ml LB medium were inoculated with a single colony.

4.4.9 Plasmid DNA Preparation from *E. coli*

Plasmid DNA was isolated from 3 ml cultures by alkaline lysis. The bacteria were harvested by centrifugation (3500 rpm, 10 min, 4 °C, centrifuge 5804R, rotor F-45-30-11, Eppendorf), resuspended in 300 µl of resuspendation buffer, mixed with 300 µl of lysis buffer and incubated for 5 min on ice. Then, 300 µl of neutralization buffer were added, the samples mixed and centrifuged immediately (14000 rpm, 20 min, 4 °C). The supernatant was centrifuged again for 10 min and the obtained second supernatant filled into a new tube. The DNA was precipitated by the addition of 450 µl of isopropyl alcohol and centrifugation (14000 rpm, 20 min, 15 °C). The DNA pellet was washed with ice-cold 70 % ethyl alcohol, dried for 15 min under vacuum and finally dissolved in 30 µl of sterile distilled water.

Resuspendation Buffer	Lysis Buffer	Neutralization Buffer
50 mM Tris-HCl, pH 8.0	200 mM NaOH	3 M Potassium acetate
10 mM EDTA, pH 8.0	1% (w/v) SDS	pH 4.8
100 µg/ml RNaseA		

High quality/quantities of plasmid DNA was isolated with the GeneJet Plasmid Miniprep Kit (MBI Fermentas) and the Plasmid Maxiprep Kit (Qiagen).

4.4.10 Preparation and Transformation of Competent Agrobacteria

The production and transformation of competent agrobacteria (*A. tumefaciens* AGL1) was exactly performed as described in the protocol of HÖFGEN *et al.* (1988). Generated clones were selected on YEP agar plates containing the corresponding antibiotics (Table 11). For analysis of produced clones, 3 ml over-night cultures were inoculated with a colony.

4.4.11 Plasmid DNA Preparation from Agrobacteria

Plasmid DNA was isolated from 3 ml cultures. The bacteria were harvested by centrifugation (6000 rpm, 10 min, 4 °C, centrifuge 5804R, rotor F-45-30-11, Eppendorf) and resuspended in 100 µl of resuspendation buffer. After adding 400 µg of lysozyme (Sigma-Aldrich) the

samples were incubated for 30 min at 37 °C. Then, 200 µl of lysis buffer were added and the DNA extracted by adding 50 µl of a phenol: chloroform:isoamyl alcohol solution (25:24:1) and strong mixing of the samples. After that, 200 µl of neutralization buffer were added and the samples centrifuged (13000 rpm, 5 min, room temperature, centrifuge 5415D, Eppendorf). The supernatant was filled into a new tube, mixed with 500 µl of chloroform and centrifuged again. The upper phase was extracted a second time with chloroform and the plasmid DNA precipitated by incubation with 0.7 volumes of isopropyl alcohol for 15 min at room temperature and centrifugation (14000 rpm, 40 min, 18 °C, centrifuge 5804R, rotor F-45-30-11, Eppendorf). Finally, the DNA was washed with 70 % ethyl alcohol; dried under vacuum and dissolved in 30 µl of sterile distilled water.

Resuspendation Buffer	Lysis Buffer	Neutralization Buffer
50 mM Glucose	200 mM NaOH	3 M Potassium acetate
25 mM Tris-HCl, pH 8.0	1% (w/v) SDS	pH 4.8
10 mM EDTA, pH 8.0		
100 µg/ml RNaseA		

4.4.12 Isolation of Genomic DNA from Plant Tissues

For the isolation of small quantities of genomic DNA, a leaf of 3 weeks-old plants was ground thoroughly in 500 µl of Edward's buffer. After centrifugation (13200 rpm, 1 min, room temperature, centrifuge 5415D, Eppendorf), 300 µl of the supernatant was taken and mixed with the equivalent volume of isopropyl alcohol and incubated for 5 min at room temperature to precipitate DNA. After centrifugation for 5 min, the DNA was dried and dissolved in 20 µl of sterile distilled water for at least 2 h at 4 °C.

Edward's Buffer
200 mM Tris-HCl, pH 8.0
250 mM NaCl
25 mM EDTA, pH 8.0
0.5 % SDS

Larger quantities of high quality genomic DNA were purified with the Nucleon PhytoPure Genomic DNA Extraction Kit by GE Healthcare.

4.4.13 Southern Transfer

For specific detection of DNA sequences (chapter 4.4.18) the genomic DNA was digested and separated by agarose gel electrophoresis (chapter 4.4.3 and 4.4.6). DNA visualization

was carried out by adding ethidium bromide to a 1 % agarose gel to a final concentration of 0.08 µg/ml and illumination of the gel with UV after the migration at 1 V/cm for approximately 8 h. Prior to transfer, the gel was cut and incubated 2-times for 20 min in denaturation-/transfer buffer. The capillary transfer of the separated genomic DNA onto an uncharged nylon membrane (Amersham Hybond-N membrane, GE Healthcare) was carried out over-night as described in SAMBROOK *et al.* (1989) using the denaturation-/transfer buffer. At the next morning, the membrane was incubated for 15 min in neutralization buffer and dried for ~1 h at room temperature. The DNA was cross-linked by a treatment of the membrane for 2 h at 80 °C.

Denaturation-/Transfer Buffer	Neutralization Buffer
1 M NaCl	1 M NaCl
400 mM NaOH	500 mM Tris, pH 7.2

4.4.14 Isolation of mRNA and total RNA from Plant Tissues

mRNA was extracted using the Dynabeads mRNA DIRECT™ Kit (Invitrogen). This extraction method is based on the A-T base pairing between the poly A tail of mRNA and oligo(dT) sequences that are bound to the surface of the Dynabeads. DNA, proteins and other RNAs do not bind and are eliminated by washing steps.

Total RNA destined for RT-PCR was extracted with the RNeasy Plant Mini Kit (Qiagen). Otherwise, the following protocol was applied: Approximately 100-200 mg plant tissue was reduced in liquid nitrogen to a fine powder and vigorously mixed for 3 min with 500 µl of a phenol:chloroform:isoamyl alcohol solution (25:24:1), 500 µl of extraction buffer and glass pearls (amount of ~300 µl). After centrifugation (13200 rpm, 5 min, room temperature, centrifuge 5415D, Eppendorf), the upper phase was filled into a new tube and extracted 2-times with 500 µl of chloroform. The RNA was precipitated over-night at 4 °C with LiCl (2 M final concentration) and subsequent centrifugation (14000 rpm, 1 h, 4 °C, centrifuge 5804R, rotor F-45-30-11, Eppendorf). Then, the RNA was washed with 80 % ethyl alcohol, dried and dissolved in 400 µl of a 0.3 M Na-acetate (pH 4.8-5.2) solution. After extraction with chloroform the upper phase was mixed with 1 ml of 100 % ethyl alcohol and the RNA precipitated for 3 h at -20 °C and centrifuged (14000 rpm, 45 min, 4 °C). Finally, the RNA was washed with 1 ml of 80 % ethyl alcohol and the dried pellet dissolved in 50 µl of DEPC-treated distilled water.

Extraction Buffer
2% Triton-X 100
1% SDS
100 mM NaCl
10 mM Tris-HCl, pH 8.0
1 mM EDTA, pH 8.0

DEPC-H_2O
0.001 % (v/v) DEPC
mix over-night and autoclave

4.4.15 Reverse Transcription of RNA

Complementary DNA was generated by reverse transcription of 3.0 µg of total RNA with the RevertAid™ H Minus M-MuLV Reverse Transcriptase (MBI Fermentas) following the protocol provided by Fermentas.

4.4.16 RNA Gel Electrophoresis through Agarose Gels containing Formaldehyde

Electrophoretic RNA separation was performed under denaturing conditions in 1.2 % (w/v) agarose gels (in MOPS buffer with 0.37 M formaldehyde and 0.25 µ/ml ethidium bromide) and MOPS buffer as running buffer at ~1.3 V/cm for approximately 5 h (in Sub-Cell GT system, power supply PowerPac3000, Bio-Rad).
Prior to migration, the RNA was denatured by adding 1x MOPS buffer, 2.2 M formaldehyde and 50 % formamide (final concentrations) and subsequent incubation for 15 min at 65 °C. Gel loading dye was added and the samples loaded after a pre-run of the gel for 10 min to eliminate contaminations from the gel slots. After migration, the RNA was visualized with UV light (366 nm). Mostly, these gels were used for northern blot analyses.

10x MOPS Buffer
200 mM MOPS
50 mM Sodium acetate
10 mM EDTA
pH 7.0

10x Gel Loading Dye
50 % Glycerol
1 mM EDTA, pH 8.0
0.25 % Bromophenol blue
0.25 % Xylene cyanol

4.4.17 Northern Transfer

After electrophoresis the RNA gel was trimmed and directly used for alkaline capillary transfer. The transfer onto an uncharged nylon membrane was performed as described in chapter 4.4.13. At the next morning, the membrane was neutralized for 15 min, dried for ~1 h at room temperature and the RNA cross-linked for 2 h at 80 °C.

Transfer Buffer	Neutralization Buffer
3 M NaCl	200 mM Na_3PO_4/Na_2HPO_4
8 mM NaOH	pH 6.8

4.4.18 Specific Detection of RNA and DNA on Nylon Membranes

4.4.18.1 Synthesis of Digoxigenin-labelled Probes

Digoxigenin-labelled probes were produced by PCR reactions (chapter 4.4.2) with 40 cycles using a 10x mix of dNTPs containing DIG-11-dUTPs (Roche). The products were subjected to agarose gel electrophoresis and extracted from the gel (chapter 4.4.6) and stored at -20 °C. The concentration was estimated after migration of a small aliquot of the purified probe through a second agarose gel. For hybridization, the probes were denatured for 5 min at 98 °C and directly added to the preheated hybridization buffer.

10x dNTP + DIG-11-dUTP

0.7 mM DIG-11-dUTP
1.3 mM dTTP
2 mM dGTP, dCTP, dATP (each)

4.4.18.2 Synthesis of ^{32}P-labelled Probes

For synthesis of ^{32}P-labelled probes the RadPrime DNA Labelling System by Invitrogen was applied. The probes contained [α-^{32}P]dATP and [α-^{32}P]dCTP (HARTMANN ANALYTIC GmbH, Braunschweig). After synthesis, the probes were purified with MicroSpin S-400 HR Columns (Amersham Biosciences, GE Healthcare). Detection of these probes was directly performed after the washing steps of the membrane by autoradiography (chapter 4.7.7).

4.4.18.3 Hybridization and Detection of DIG-labelled Probes

The membranes with the cross-linked RNA or DNA were first prehybridized with hybridization buffer for at least 4 h at 62 °C in glass tubes in a hybridization oven (Hybrigene, Techne, Cambridge). After this time, the buffer was replaced by fresh preheated hybridization buffer containing the denatured probe for hybridization over-night at 62 °C. Unspecifically bound probes were removed by washing the membrane twice for 30 min in 2x SSC/0.1% (w/v) SDS at room temperature and twice for 30 min in 0.1x SSC/0.1 % (w/v) SDS at 68-70 °C. Next, the membrane was equilibrated in 1x maleic acid buffer and blocked for 60 min in blocking buffer. After that, the membrane was incubated in a fresh dilution

(1:10000) of anti-DIG Fab fragments (Roche) in blocking buffer for 45 min and washed twice in 1x maleic acid buffer. For chemiluminescence reaction the membrane was equilibrated in detection buffer that was completely drained off after 5 min. The substrate CSPD (Roche) was dropped onto the membrane and incubated for 5 min in darkness. The membrane was covered with plastic film and ECL Hyperfilms (Amersham, GE Healthcare) were exposed at room temperature for 15 min up to several hours corresponding to the signal intensity of the probe. Revelation of the Hyperfilms was performed as described in chapter 4.7.7.

20x SSC	Hybridization Buffer (DNA)	Hybridization Buffer (RNA)
3 M NaCl	5x SSC	50 % Formamide
300 mM Sodium citrate	0.1 % (w/v) N-Lauroylsarcosine	5x SSC
pH 7.0	0.02 % (w/v) SDS	0.1 % (w/v) N-Lauroylsarcosine
	1 % (w/v) Blocking reagent (Roche)	0.02 % (w/v) SDS
		2 % (w/v) Blocking reagent

5x Maleic acid Buffer	Blocking Buffer	Detection Buffer
500 mM Maleic acid	1x Maleic acid buffer	100 mM Tris
750 mM NaCl	1 % (w/v) Blocking reagent	100 mM NaCl
pH 7.5		pH 9.5

4.5 RNA Silencing

For the construction of inverted repeats that give rise to double stranded RNA and induce the directed degradation of mRNA (RUIZ-FERRER & VOINNET, 2009), the instructions described in Current Protocols in Molecular Biology (Unit 26.6 by YIN *et al.*, 2005) and on the website of the RNAi WEB were applied.

Adequate constructs with a hairpin-loop forming intron (PDK, pyruvate orthophosphate dikinase) between sense and antisense gene fragments were created with the help of the vector pHannibal (WESLEY *et al.*, 2001). The gene fragments were synthesized by PCR and appropriate primers (Table 8) with added restriction sites defining the final orientation (sense/antisense) after cloning. The generated constructs were transferred into the binary vector pArt27 (GLEAVE, 1992) and *A. thaliana* wild-type plants were transformed by floral dipping.

4.6 Genetic Manipulation of Plants

4.6.1 Transient Transformation of Tobacco Leaves

Tobacco leaves were transiently transformed by infiltration with agrobacteria. A 50 ml culture of agrobacteria in YEP-RAK medium with freshly added 10 mM MES and 100 µM acetosyringone was grown over-night (at 28 °C; 220 rpm) and the agrobacteria harvested by centrifugation (4000 rpm, 20 min, 4 °C, centrifuge 5804R, rotor A-4-44, Eppendorf). The pellet was washed with double-distilled sterile water, resuspended in infiltration buffer to an optical density at 600 nm of 1.0 and incubated for ~2 h at room temperature. For transformation the agrobacteria were infiltrated at the lower side of the leaves (cell interspaces) with a 1 ml blunt end tip syringe. Two days later, protoplasts were prepared and analysed.

YEP-RAK Medium
5 g/l Beef extract
5 g/l Peptone
5 g/l Sucrose
1 g/l Yeast extract
pH 7,2

Infiltration Buffer
10 mM $MgCl_2$
10 mM MES, pH 5,6
100 µM Acetosyringone

4.6.2 Stable Transformation of *A. thaliana*

For stable transformation of *A. thaliana* the floral dip method of CLOUGH & BENT (1998) was adapted. Healthy looking plants with many buds as possible were transformed. First, a 250 ml culture of agrobacteria was grown for 18-20 h at 28 °C under agitation (220 rpm). The bacteria were harvested by centrifugation (5000 rpm, 15 min, room temperature, centrifuge J-6M/E, rotor JA-14, Beckman) and resuspended in infiltration medium to an optical density at 600 nm of 0.8-1.0. Next, the stems and buds of 4-5 weeks old *A. thaliana* plants were dipped for 4 min into the agrobacteria suspension. Alternatively, the plants were infiltrated in vacuum for 7-10 min and subsequent fast aeration. After that, the excess of the infiltration suspension was drained off and the plants were placed horizontally into a plant growing dish and covered with a plastic hood. At the next day, the plastic hood was removed and the plants were further cultivated until seeds could be harvested.

Depending on the binary vector used for plant transformation, transformed plants were identified on MS agar plates containing 50 µg/ml kanamycin or by spraying the leaves of

10 days-old soil-grown plants with a Basta solution (0.25 mg/ml in tap water). Selected transgenic lines were further analysed by extraction of genomic DNA and PCR.

Infiltration Medium
2.18 g/l MS salts
1x B5-Vitamins
50 g/l Sucrose
0.5 g/l MES
pH 5.7
0.044 µM BAP
50 µl/l Silwet L-77 (Lehle Seeds, Round Rock, Texas, USA)

1000x B5-Vitamins Solution
100 mg/ml *myo*-Inositol
10 mg/ml Thiamin hydrochloride
1 mg/ml Nicotinic acid
1 mg/ml Pyridoxine hydrochloride

4.6.3 Controlled Crossing of *A. thaliana*

Plant crossing was carried out according to the *A. thaliana* Laboratory Manual (WEIGEL & GLAZEBROOK, 2002). In order to reduce self-fertilization, plants must be used before anthers begin to shed pollen onto the stigma. Flowers were taken in which the tips of petals were just visible. All other flowers were removed without damaging the stem. Using a dissection microscope and forceps the anthers, sepals and petals were removed from the female parent flower leaving the carpels intact. Then, the flowers were pollinated by brushing the convex surface of the anthers of the male parent flower against the stigmatic surface of the exposed carpels. The success of crossing was detected by measuring the elongation of the siliques. After 2-3 weeks the T_2 seeds were harvested.

4.7 General Protein Biochemical Methods

4.7.1 Protein Extraction from Plants

Plant material was reduced in liquid nitrogen to a fine powder and mixed with the equivalent volume of 2x SDS sample buffer. The samples were denatured by boiling for 10 min at 95 °C, chilled and centrifuged (13200 rpm, 5 min, room temperature, centrifuge 5415D, Eppendorf). The supernatant was filled into a new tube and the extracts stored at -20 °C.

2x SDS Sample Buffer
125 mM Tris-HCl, pH 6.8
10 % (v/v) Glycerol
10 % (v/v) β-Mercaptoethanol
4 % (w/v) SDS

4.7.2 TCA Precipitation

The proteins were mixed with TCA to a final concentration of 5 % (w/v), precipitated overnight at 4 °C and centrifuged (14000 rpm, 10 min, 4°C, centrifuge 5804R, rotor F-45-30-11, Eppendorf). The protein pellets were washed twice with 1 ml of absolute acetone and twice with 1 ml of absolute ethyl alcohol. Finally, the proteins were dried at room temperature, dissolved in an appropriate volume of 1x SDS sample buffer and stored at -20°C.

4.7.3 Quantification of Proteins

The determination of protein concentration was carried out using the protocol by ESEN *et al.* (1978). Reference values were 1x SDS sample buffer and denatured BSA (5 mg/ml) in 1x SDS sample buffer. Every sample was measured twice. Aliquots of 2 µl were dropped onto a square of 1 cm^2 of Whatman 3MM paper (Schleicher & Schuell) and dried. Then, the entire filter was subsequently incubated for 5 min in a fixation solution and for 15 min in a coloration solution. For elimination of the background colour the filter was briefly rinsed with double distilled water and incubated twice for 1 min in boiling water. Dried filter pieces were incubated in 1 ml of a 0.5 % (w/v) SDS solution for minimal 30 min at 55 °C or overnight at room temperature to elute the blue stain. Finally, the absorbance was measured at 578 nm and the protein concentrations calculated using the standards described above.

Fixation Solution	Coloration Solution
25 % (v/v) Isopropyl alcohol	25 % (v/v) Isopropyl alcohol
10 % (v/v) Acetic acid	10 % (v/v) Acetic acid
	0.1 % (w/v) Coomassie brilliant blue G250

4.7.4 One-Dimensional SDS Polyacrylamide Gel Electrophoresis (SDS-PAGE)

The separation of proteins under denaturing conditions was performed via SDS polyacrylamide gel electrophoresis with a discontinuous system according to LAEMMLI (1970) using 12.5 % (w/v) polyacrylamide separation gels or exponential gradient gels (11-20 % (w/v) polyacrylamide) according to SCHARF & NOVER (1982), respectively, by using the Minigel-Twin System (Biometra) or the Protean II xi Cell System (Bio-Rad) and the PowerPac3000 power supply (Bio-Rad).

Simple gels were composed of a normal 12.5 % (w/v) polyacrylamide separation gel and a 3.6 % (w/v) polyacrylamide stacking gel (Table 14). Polyacrylamide gradient gels were prepared by mixing “heavy” and “light” solution with a gradient former (Model 385, Bio-

Rad) and a peristaltic pump (Minipuls 3, ABiMED Gilson). If the gels exceeded the size of 15 x 15 cm, bottom gels were made.

For electrophoresis the protein samples (10-40 µg protein) were mixed with 1x SDS sample buffer (blue), boiled for 10 min at 95 °C for denaturation, centrifuged and loaded into the rinsed gel slots. Migration was performed at 4 °C with SDS running buffer at 10 mA in the stacking gel and then according to the desired separation and sharpness of protein bands at 10-30 mA/gel. After separation the gels were either used for the transfer of proteins onto a nitrocellulose membrane (chapter 4.7.8) or staining with Coomassie blue or silver nitrate (chapter 4.7.5 and 4.7.6).

Table 14. Composition of gel solutions.

	Stacking Gel	**Separation Gel**	**Light Solution**	**Heavy Solution**	**Bottom Gel**
Sucrose	--	--	--	1 g	2-3 ml of Separation Gel or Light Solution
Acrylamide/Bisacryl-amide (30%, 37.5:1)	3.6 % (w/v)	12.5 % (w/v)	10 % (w/v)	20 % (w/v)	
Tris-HCl	125 mM pH 6.8	420 mM pH 8.8	400 mM pH 8.8	400 mM pH 8.8	
SDS	0.1 % (w/v)	0.1 % (w/v)	0.1 % (w/v)	0.1 % (w/v)	
APS	0.25 % (w/v)	0.06 % (w/v)	0.048 (w/v)	0.1 % (w/v)	0.15 % (w/v)
TEMED	0.1 % (v/v)	0.1 % (v/v)	0.02 % (w/v)	0.04 % (w/v)	0.5 % (v/v)

SDS Running Buffer
192 mM Glycine
25 mM Tris-HCl
0.1 % (w/v) SDS

2x SDS Sample Buffer (blue)
125 mM Tris-HCl, pH 6.8
10 % (v/v) Glycerol
10 % (v/v) β-Mercaptoethanol
4 % (w/v) SDS
0.001 % (w/v) Bromophenol blue

4.7.5 Staining of SDS-Polyacrylamide Gels with Coomassie Brilliant Blue

Coomassie staining was used for detection of proteins on gels with minimal 10 µg proteins/lane. The gels were incubated for at least 30 min each time in fixation solution and staining solution with mild agitation at room temperature. To remove the background colour, the gels were incubated again in fixation solution. This step was repeated several times until protein bands became visible.

Fixation solution
30 % (v/v) Methyl alcohol
7 % (v/v) Acetic acid

Staining solution
50 % (v/v) Methyl alcohol
10 % (v/v) Acetic acid
0.3 % (w/v) Coomassie brilliant blue G250

4.7.6 Silver Nitrate Staining of Polyacrylamid Gels

To detect small protein amounts SDS gels (<10 µg protein/sample) were stained with silver nitrate according to SHEVCHENKO *et al.* (1996). First, the proteins were fixed by incubation of the gel for at least 20 min with mild agitation at room temperature in solution I. After that, the gels were successively incubated for 10 min in solution II and in double distilled water. To keep the background transparent, the gel was shaken for 1 min in a freshly prepared 0.02 % (w/v) sodium thiosulfate solution and immediately rinsed in water. Afterwards, the gels were incubated for 20 min in solution IV and washed twice for 1 min in water. Depending on the coloration the gels were developed in solution V for 1-5 min and the staining stopped in solution III.

Solution I	Solution II	Solution III
50 % (v/v) Methyl alcohol 5 % (v/v) Acetic acid	50 % (v/v) Methyl alcohol	5 % (v/v) Acetic acid

Solution IV	Solution V
0.1 % (w/v) Silver nitrate	2 % (w/v) Sodium carbonate 0.04 % (v/v) Formaldehyde

4.7.7 Conservation of SDS Gels and Autoradiography

For conservation, the gels were incubated for 10 min in a 5 % (v/v) glycerol solution, placed between a sheet of Whatman 3MM paper (Schleicher & Schuell) and a cellophane membrane (Bio-RAD) and dried under vacuum for 2 h at 80 °C (Gel Dryer Model 583, Bio-Rad).

Radioactively labelled proteins were detected by autoradiography. The Hyperfilms MS (Amersham, GE Healthcare) were exposed at -80 °C. If necessary, the gels were soaked in amplify fluorographic reagent (Amersham, GE Healthcare) before drying to enhance the signal intensity of ^{35}S-labelled proteins. After exposition, the films were developed for up to 2 min in 5-fold diluted GBX Developer and Fixer (Kodak), washed briefly in water and fixed for 2 min in 5-fold diluted GBX Fixer and Replenisher (Kodak). Finally, the films were rinsed with water and dried.

4.7.8 Western Blotting

4.7.8.1 Electrophoretic Transfer of Proteins onto Nitrocellulose Membranes

The transfer of electrophoretically separated proteins (chapter 4.7.4) onto a nitrocellulose membrane (reinforced NC, Optitran BA-85, 0.45 µm, Schleicher & Schuell) was carried out according to TOWBIN *et al.* (1979) in a blotting tank (Trans Blot Cell, Bio-Rad) over-night at 4 °C and 250 mA (Power supply PowerPac3000, Bio-Rad).

Reversible staining of the immobilized proteins was achieved by immersing the membrane in a Ponceau S staining solution for 2 min with mild agitation and subsequent washing in double distilled water until the background was eliminated and the protein bands became visible. The coloration was completely removed by incubating the membrane for approximately 15 min in 1x TBS-Tween-20.

Transfer Buffer
192 mM Glycine
25 mM Tris
20 % (v/v) Methyl alcohol

Ponceau S Staining Solution
0.5 % (w/v) Ponceau S
1 % (v/v) Acetic acid

10x TBS Buffer
5 M NaCl
200 mM Tris-HCl
pH 7.5

TBS-Tween-20
1x TBS buffer
0.05 % (v/v) Tween-20

4.7.8.2 Immunological Detection of Immobilized Proteins

For specific detection of proteins on nitrocellulose membranes, unspecific binding sites were saturated during incubation of the membrane for 1 h in blocking solution at room temperature and mild agitation. Incubation of the nitrocellulose membranes in the presence of primary antibodies was carried out for 1 h. Unspecifically bound antibodies were eliminated by washing the membrane 3-times for 15 min in fresh blocking buffer. Afterwards, the membrane was incubated for 1 h with a secondary antibody (diluted blocking buffer) and washed 3-times for 15 min in TBS-Tween-20 (chapter 4.7.8.1).

For detection of the bands based on the alkaline phosphatase activity, the membrane was first equilibrated in 1x colour buffer for 5 min and then incubated with NBT-BCIP-colour buffer until protein bands became visible. The alkaline phosphatase reaction was stopped by adding some drops of concentrated hydrochloric acid and rinsing of the membrane with double distilled water.

Alternatively, the secondary antibody was coupled with a horseradish peroxidase. In this case, the detection occurred with the Amersham ECL Western blotting detection reagents and analysis system (GE Healthcare) according to the supplier's recommendations.

Blocking Buffer	10x Colour Buffer	NBT-BCIP-Colour Buffer
1x TBS buffer	1 M NaCl	1x Colour buffer
0.05 % (v/v) Tween-20	1 M Tris-HCl	330 µg/ml NBT
5 % (w/v) Non-fat milk powder	pH 9.0	165 µg/ml BCIP

4.7.9 Preparation of Soluble and Insoluble Protein Extracts from Bacteria

Mostly, the heterologous expression of recombinant proteins in *E. coli* results in their accumulation referred to as inclusion bodies. In order to know whether the expressed protein is soluble or insoluble and what kind of lysis and purification instructions had to be applied, these two fractions needed to be separated. This was realised according to the protocol supplied in the *E. coli* Expression System with Gateway Technology Manual (Version G).

4.7.10 Protein Purification and Antibody Production

4.7.10.1 Purification of HP20-$(His)_6$

For purification of HP20 the protocols described in The QIAexpressionist (Qiagen, June 2003) were adapted. Approximately 2-3 g of centrifuged bacteria were suspended in 5 ml of buffer B containing additionally 1.25 mM PMSF and incubated for 30 min with agitation (240 rpm) at 4 °C. Subsequent sonication was used 6-times for 30 s with meantime chilling on ice to facilitate cell lysis. The resulting suspension was further shaken for 30 min at 4 °C and then centrifuged to sediment cell debris (14000 rpm, 30 min, 4 °C, centrifuge 5804R, rotor F-45-30-11, Eppendorf). The supernatant (cleared lysate) was recovered and, after taking a sample for SDS-PAGE analysis, mixed for 1 h with 500 µl of 3-times in buffer B washed Ni-NTA-agarose (Qiagen) at 4 °C. Then, the lysate-matrix-solution was poured into an empty column and the flow-through collected. Unspecifically bound proteins were eliminated by washing the column twice with 4 ml of buffer C. Elution of the purified protein occurred 4-times with 500 µl of buffer E and 5-times with 500 µl of an elution buffer that was initially used for protein purification with FPLC (see below). All purification steps were analysed by SDS-PAGE and silver staining. Finally, the collected eluates were

subjected to SDS-PAGE and bands corresponding to HP20-$(His)_6$ were excised after Coomassie staining and sent for antibody production.

Buffer B	Buffer C	Buffer E
8 M Urea	8 M Urea	8 M Urea
500 mM NaCl	500 mM NaCl	500 mM NaCl
100 mM Disodium phosphate	100 mM Disodium phosphate	100 mM Disodium phosphate
10 mM Tris	10 mM Tris	10 mM Tris
20 mM Imidazole	20 mM Imidazole	pH 4.5
pH 8.0	pH 6.3	

4.7.10.2 Purification of HP30-$(His)_6$

HP30 was purified using a Ni-NTA matrix in a 1 ml HisTrap HP column (Amersham, GE Healthcare) and fast protein liquid chromatography (FPLC, ÄKTApurifier by GE Healthcare) measuring the absorbance at 280 nm for protein detection.

Bacterial pellets (approximately 13 g) were thawed on ice and resuspended in 20 ml of lysis buffer containing 1.25 mM PMSF and lysed 2-times by a French press (Thermo Scientific). The resulting solution was incubated for 1 h at room temperature with strong agitation (220 rpm) and then centrifuged (14000 rpm, 25 min, 4 °C, centrifuge J-6M/E, rotor JA-20, Beckman). The cleared lysate (supernatant) was mixed with additional 20 ml of lysis buffer, filtered through a membrane (pore size of 0,45 µm) and subjected to FPLC after equilibration of the HisTrap column with lysis buffer. The lysate circulated over-night at 4 °C and 0.5 ml/min to bind the recombinant protein at the Ni-NTA matrix. Thereafter, the column was washed with 25 ml of wash buffer and samples were taken at the beginning and the end of the washing procedure. The purified protein was eluted by elution buffer and aliquots of 500 µl were collected. All purification steps were analysed by SDS-PAGE and silver staining. For antibody production preparative SDS gels were run and the corresponding protein band excised after Coomassie staining.

Lysis Buffer	Wash Buffer	Elution Buffer
6 M Urea	6 M Urea	6 M Urea
500 mM NaCl	500 mM NaCl	500 mM NaCl
20 mM Disodium phosphate	20 mM Disodium phosphate	20 mM Disodium phosphate
20 mM Imidazole	40 mM Imidazole	500 mM Imidazole
pH 8.0	pH 8.0	pH 8.0

4.7.10.3 Antibody Production

The antibodies were synthesized in rabbits during 82 days by the enterprise Interchim (Montlucon Cedex, France). 2.5 mg of the purified proteins were used for primary immunization and two boosts in regular intervals that were carried out for two rabbits per antigen. The antibody production was checked after 39 and 67 days by testing the antisera by western blotting.

4.7.10.4 Antibody Purification

Antibody purification was carried out by affinity purification using a protocol described by HÖHFELD *et al*. (1991). The crude antiserum of the HP20 antibody was purified against the purified HP20-$(His)_6$ protein that was blotted onto nitrocellulose membrane and the corresponding band cut out of the membrane prior to antibody purification.

4.8 Preparation of Protoplasts

Small pieces of the corresponding leaves were incubated in K3AS medium for 4 h in the dark and the released protoplasts collected and centrifuged without break (20 min, 200*g*, 4 °C, centrifuge 5804R, rotor A-4-44, Eppendorf). Intact protoplasts floating on the surface were collected, gently diluted in a fresh tube with the 4-fold volume of W5 medium and centrifuged again but with break (20 min, 200*g*, at 4 °C). The supernatant was removed and the sedimented protoplasts analysed.

K3AS Medium	W5 Medium
1x MS Salts, pH 5.8	150 mM NaCl
3 mM $CaCl_2$	130 $CaCl_2$
400 mM Sucrose	5 mM KCl
1 % Cellulose	5 mM Sucrose
0.5 % Driselase	pH 5.8
0.2 % Macroenzyme	

4.9 Preparation of intact Plastids

For the isolation of chloroplasts leaves of 2-3 weeks old green plants were used. Etioplasts were prepared from 4-5 days-old dark-grown seedlings under green save light. The leaves (~10 g) were mortared gently in 75-100 ml of lysis buffer and the resulting suspension was filtered by gentle pressing through a gauze membrane with a pore size of 30 µm. The crude

plastids were sedimented by centrifugation (5 min, 1500*g*, 4 °C, centrifuge J-6M/E, rotor JA-20, Beckman) and resuspended in 1 ml of wash buffer. Then, the plastids were subjected to differential centrifugation (45 min, 8000*g*, 4 °C, slow start, slow break, centrifuge Avanti-J30, rotor JA-24.15 or JS-24.38) through Percoll (GE Healthcare) density gradients composed of 6 ml of a 40 % Percoll solution, 6 ml of a 60 % Percoll solution and 7 ml of a 80 % Percoll solution. After centrifugation, intact chloroplasts were visible at the 60-80 % interphase and recovered. In the case of co-purification of chloroplasts and mitochondria, the Percoll gradients were composed of five Percoll solutions: 3 ml of a 5 % Percoll solution, 3 ml of a 10 % Percoll solution, 3.5 ml of a 20 % Percoll solution, 3.5 ml of a 30 % Percoll solution and 3 ml of a 60 % Percoll solution. Intact chloroplasts were concentrated at the 30-60 % interphase, mitochondria at the 20-30% interphase and broken organelles at the 5-10 % interphase. For elimination of the Percoll solution the plastids were washed by adding wash buffer and centrifugation (15 min, 1500*g*, 4 °C). The resulting plastids were resuspended in a small volume of wash buffer and the amount of purified chloroplasts measured by dilution of a small aliquot in acetone and determination of absorbance at 665 nm. A value of 0.005 corresponded to 5 x 10^7 plastids. Subfractionation into envelopes, stroma and thylakoids was carried out as described by Li *et al.* (1991).

Lysis Buffer	Wash Buffer	Percoll Solution
330 mM Sucrose	300 mM Sucrose	5-80 % (v/v) Percoll
50 mM Hepes	50 mM Hepes	330 mM Sucrose
3 mM $MgCl_2$	3 mM $MgCl_2$	50 mM Hepes
0.1 % (w/v) BSA	pH 7.6	pH 7.6
pH 7.6		

4.10 *In vivo* and *in vitro* Synthesis of ^{35}S-labelled Proteins

4.10.1 Analysis of Cytosolic Protein Biosynthesis

In vivo labelling of proteins was carried out with etiolated *A. thaliana* seedlings that were irradiated for different time periods or light grown plants. Labelling was performed during the last 2 h of treatment. The upper third of the seedlings was cut and incubated in 1-2 ml of labelling solution. Green leaves of mature *A. thaliana* plants were cut into small pieces (1-2 mm^2), put into an appropriate volume of labelling solution and infiltrated under vacuum for 5 min and then incubated with gentle agitation for 2 h in the light. The labelled plant

material was dried on cellulose and frozen in liquid nitrogen. Protein extracts were prepared and labelled proteins were analysed by SDS-PAGE and autoradiography.

Labelling Solution
0.425 nM L-Methionine (Roth)
0.55 µCi L-[^{35}S]-Methionine (10 mCi, > 1000 Ci/mmol, Perkin Elmer)
0.1 % (v/v) Tween-20
In tap water

4.10.2 Analysis of Plastidic Protein Biosynthesis

In organello protein synthesis was carried out as a control for intactness and functionality of purified chloroplasts. Radiolabelled methionine that is present in an *in organello* labelling mix (KLEIN & MULLET, 1987) is incorporated into the newly synthesized proteins.
Labelling assays (50 µl) were composed of 1x *in organello* labelling mix and 5 x 10^7 purified chloroplasts and incubated for 2.5 h at 23 °C under gentle agitation. The reactions were stopped by the addition of the equivalent volume of 2x SDS sample buffer and subsequent boiling for 10 min at 95 °C and analysed by SDS-PAGE and autoradiography (chapter 4.7.4 and 4.7.7).

2x *In organello* Labelling Mix
700 mM Sucrose
100 mM Hepes, pH 8.0
80 µM Amino acid mixture without methionine (Promega)
20 mM DTT (Dithiothreitol)
50 µCi L-[^{35}S]-Methionine
10 mM Mg-ATP, pH 7.0
10 mM $MgCl_2$

4.10.3 *In vitro* Synthesis of ^{35}S-labelled Proteins

Synthesis of radioactively labelled precursor proteins for import studies and *in vitro* translation of total RNA was performed with the TNT Coupled Wheat Germ Extract System (Promega) according to the supplier's recommendations in the presence of L-[^{35}S]-methionine (10 mCi, > 1000 Ci/mmol, Perkin Elmer). The concentration of ^{35}S-methionine-radiolabelled protein that had to be used for import experiments was estimated based on the signal on the autoradiogram.

4.11 *In vitro* Protein Import Studies

4.11.1 *In vitro* Import into Plastids

Protein import into isolated *A. thaliana* chloroplasts and etioplasts was performed as described by REINBOTHE *et al.* (2005) using cDNA-encoded, wheat germ-translated ^{35}S-precursors. Different conditions were chosen:

1. If necessary the purified chloroplasts were energy-depleted according to THEG *et al.* (1989) by incubating them for 1 h in the dark (on ice).
2. The import experiments occurred in the dark or light in the presence of either 2-5 mM Mg-ATP and 0.1 Mg-GTP for complete plastid import or 0.1 mM Mg-ATP and 0.1 mM Mg-GTP for binding and insertion of the precursor across the outer and inner plastid envelope membranes.
3. In the case of the import of pPORA, energy-depleted chloroplasts were supplemented with phosphate-buffered 5-ALA (0.5 mM final concentration) for 15 min at 25 °C in the dark giving rise to Pchlide to induce its substrate-dependent import (REINBOTHE *et al.*, 1995a). These reactions occurred always in the dark.
4. In order to analyse whether a certain protein acts as receptor protein during import or as a hydrophilic translocation channel, the import reactions were carried out after pre-incubation of the chloroplasts with the corresponding antibodies. For this, intact chloroplasts were incubated with a small aliquot of an antiserum over-night at 4 °C or for 2 h at 23 °C.
5. In some cases, urea-denatured precursor proteins were used for import. The denaturation occurred in the presence of 8 M urea. For import the precursors were diluted that the final urea concentration did not exceed 0.2 M urea (REINBOTHE *et al.*, 2000).
6. Thermolysin treatment of plastids after the import reactions was performed in order to degrade non-imported proteins (CLINE *et al.*, 1984). After incubation for 30 min on ice, the reaction was stopped by the addition of 2x SDS sample buffer.

Import assays (final volume of 50 µl) contained 1x *in vitro* import buffer (modified from DELLA CIOPPA *et al.,* 1986), a defined amount of precursor proteins or total RNA translation products and 5 x 10^7 intact plastids. Uptake of radiolabelled proteins into plastids occurred at 23 °C with gentle agitation and was stopped either directly after addition of the plastids (time point zero) or after 15 min by 2x SDS sample buffer. Import assays were analysed by

SDS-PAGE and autoradiography or the radioactivity of the imported precursor protein was counted using a scintillation counter.

2x *in vitro* Import Buffer
660 mM Sucrose
100 mM Hepes
20 mM Potassium gluconate
10 mM Methionine
10 mM Sodium bicarbonate
3 mM Magnesium sulfate
3 mM ATP
2 % (w/v) BSA
pH 7.6

4.11.2 Purification and Identification of Envelope Proteins involved in the Import of ceQORH

The purification and identification of components of the ceQORH translocon was performed as described by SCHNELL *et al.* (1994), TOKATLIDIS *et al.* (1996) and REINBOTHE *et al.* (2004a).

The urea-denatured ^{35}S-labelled ceQORH proteins were incubated with energy-depleted chloroplasts for 15 min in the presence of 0.1 mM Mg-ATP and 0.1 mM Mg-GTP. The reactions were stopped by dilution of the plastids with ice-cold import buffer lacking ATP and GTP. Intact chloroplasts were re-isolated on Percoll and disrupted by incubation in a hypotonic medium to yield crude envelope fractions after centrifugation. These crude envelopes were subfractionated into light outer membrane fractions, intermediate density fractions and slightly denser inner membrane fractions by flotation into linear 10-40 % sucrose gradients (centrifugation at 70000*g*, 60 min at 4 °C; slow start, slow break, centrifuge Avanti-J30, rotor JA-24.15 or JS-24.38) and collected. Each fraction was analysed after protein precipitation with 5 % (w/v) TCA by SDS-PAGE and Western blotting or autoradiography.

The intermediate density fractions, which should represent the highest amounts of radiolabelled ceQORH proteins (radioactivity measured with a scintillation counter) because of its insertion across the chloroplast envelopes, were used to purify proteins that were involved in ceQORH import. For this, protein import complexes were solubilised from these fractions for 15 min on ice in a solubilisation buffer and centrifuged at 100000*g* for 15 min at 4 °C. Fractions of 10 ml of the resulting supernatant were incubated for 1 h at 4 °C with

0.25 ml of Ni-NTA-agarose beads in solubilisation buffer for purification by the $(His)_6$-tag fused to the ceQORH. The beads were then washed twice with a wash buffer, and the bound protein eluted with elution buffer, precipitated by methanol/chloroform and suspended in 1x SDS sample buffer. The proteins were subjected to SDS/10-20 % polyacrylamide gel electrophoresis, Coomassie staining or autoradiography. The resulting protein bands on Coomassie gels were excised and subjected to micro-sequence analysis as described by CHANG (1983). Analysis of the received protein sequences was carried out by protein BLAST search.

Solubilisation Buffer	Wash Buffer	Elution Buffer
2 % (v/v) Triton X-100	50 mM Tris-HCl	2 % (v/v) SDS
50 mM Tris-HCl	300 mM NaCl	100 mM EDTA
300 mM NaCl	20 mM Imidazole-HCl	50 mM Pipes-NaOH
20 mM Imidazole-HCl	pH 8.0	pH 7.4
pH 8.0	1 mM PMSF	
1 mM PMSF		

Hypotonic Medium	Buffers for Sucrose-Gradients
10 mM MOPS	10/40 % (w/v) Sucrose
4 mM $MgCl_2$	10 mM MOPS
1 mM PMSF	4 mM $MgCl_2$
pH 7.8	pH 7.8

4.11.3 Chemical Cross-Linking during Protein Import into Chloroplasts

Chemical cross-linking was based on a publication by TOKATLIDIS *et al.* (1996) where the identification of a translocation component of the inner envelope of mitochondria via chemical cross-linking with Ellman's reagent (DTNB; 5,5'-Dithiobis-2-nitrobenzoic acid; Pierce Biotechnology, Rockford, Illinois, USA) was described. The chemical background is the formation of stable disulfide bonds between a thiol group of a DTNB activated precursor and a second thiol group of a component of the protein import machinery when they are in close proximity to each other (TOKATLIDIS *et al.*, 1996; HABEEB, 1972).

The ^{35}S-labelled precursor proteins were activated with DTNB for 30 min at 10 °C. The cross-linker was quenched with 100 mM glycine. Import reactions were carried out as described above. The proteins were recovered from the different samples by precipitation with TCA (5 % (w/v) final concentration), taken up in SDS sample buffer without β-mercaptoethanol, resolved by PAGE on 11-20 % (w/v) polyacrylamid gradients under non-reducing conditions (TOKATLIDIS *et al.*, 1996), and detected by autoradiography. To

determine the amount of imported protein, the radioactivity of imported precursor was measured with a scintillation counter after thermolysin treatment of the chloroplasts.
In order to demonstrate the identity of the cross-linked chloroplast envelope protein co-immunoprecipitations were carried out as described by WIEDMANN *et al.* (1987).

4.12 Biochemical Localization and Topology Investigations of Chloroplast Membrane Proteins

4.12.1 Protease Treatment of Chloroplasts

Thermolysin is useful to probe polypeptides that are located at the membrane surface of the outer envelopes of intact chloroplasts whereas the inner envelope and envelope permeability as well as chloroplast activities are not affected (CLINE *et al.*, 1984). For this treatment, the intact plastids were treated with 50 µg/ml thermolysin (Sigma-Aldrich) for 30 min on ice in the presence of 0.1 mM $CaCl_2$.
In contrast to thermolysin, trypsin is a protease that is able to access the intermembrane space via penetration of the outer envelope and leads to the breakdown of the inner plastid envelope proteins up to their membrane parts. The treatment was performed as described by REINBOTHE *et al.* (2004a) and CLINE *et al.* (1984).
Both treatments were stopped by the addition of SDS sample buffer and plastid proteins were analysed by SDS-PAGE and Western blotting.

4.12.2 Protein Extraction from Chloroplast Envelopes with NaCl/$NaCO_3$

In order to demonstrate that a protein is an integral membrane protein, the isolated outer envelopes were extracted with high salt concentrations or by alkaline treatment. If the proteins of interest were still insoluble, they were judged as integral membrane proteins. Intact chloroplasts were incubated in 1 N NaCl or 0.1 M Na_2CO_3, pH 11 for 30 min on ice followed by the separation into supernatant and pellet (centrifugation at for 20 min at 72000*g* and 4 °C). The reactions were analysed by SDS-PAGE and Western blotting.

4.13 Pigment Analyses

4.13.1 Chlorophyll Quantification

For determination of chlorophyll contents in *A. thaliana* cotyledons the pigments were extracted with DMF (N,N´-Dimethylformamide) according to PORRA *et al.* (1989).
The cotyledons were cut, the fresh weight measured and incubated over-night at -20 °C in 990 µl of N,N'-dimethylformamide. Leaf peaces and insoluble parts were sedimented by centrifugation (14000 rpm, 5 min, room temperature, centrifuge 5415D, Eppendorf). Then, the absorption (A) was measured at the wavelengths of 646.8 nm, 663.8 nm and 750 nm. The calculation of the chlorophyll concentration in µg/ml occurred according to the following formulas:

Chlorophyll (Chl) content [µg/ml]:

$$\text{Chl a} = 12.00 \times (A_{663.8} - A_{750}) - 3.11 \times (A_{646.8} - A_{750})$$

$$\text{Chl b} = 20.78 \times (A_{646.8} - A_{750}) - 4.88 \times (A_{663.8} - A_{750})$$

$$\text{Chl a+b} = 17.67 \times (A_{646.8} - A_{750}) + 7.12 \times (A_{663.8} - A_{750})$$

4.13.2 Determination of Pchlide-F_{631} and Pchlide-F_{655}

Photoactive Pchlide-F_{655} and photoinactive Pchlide-F_{631} was determined according to LEBEDEV *et al.* (1995) by low temperature spectroscopy at 77 K. A determined quantity of cotyledons was cut from the plants and the pigments extracted under green safe light with 80 % acetone at 4 °C. The emission spectra were collected between 575–725 nm after excitation at 440 nm using the spectrometer model LS50B (Perkin Elmer Corp.).

4.14 Determination of Cell Death

4.14.1 Tetrazolium Staining of Plant Tissues

Tetrazolium staining was used to measure the vitality of plant tissues. In healthy tissue the colourless TTC is reduced to bright red TPF (1,3,5-Triphenylformazan) by the activity of dehydrogenases that are mostly associated with mitochondria (COMAS *et al.*, 2000). Instead, in necrotic tissue the TTC remains colourless because the dehydrogenases are inactivated and/or degraded during cell death.

For staining, the upper third of the seedlings was cut and the cotyledons were incubated in a 1% (w/v) TTC solution over-night at room temperature in the dark. On the next day, the cotyledons were photographed. Only cotyledons that were illuminated for up to 4 h were used for staining. Thereafter, the vitality of seedlings could be judged by the photobleaching *versus* greening of cotyledons.

4.14.2 Singlet Oxygen Measurements

The evolution of singlet oxygen was determined with DanePy (3-(*N*-diethylaminoethyl)-*N*-dansyl) aminomethyl-2,5-dihydro-2,2,5,5-tetramethyl-1*H*-pyrrole; HIDEG *et al.*, 1998). These measurements are based on the reaction of DanePy with singlet oxygen that leads to quenching of the fluorescence intensity the dansyl moiety. Cotyledons of irradiated *A. thaliana* seedlings were detached and shortly infiltrated in DanePy. The fluorescence emission spectra were collected between 425-625 nm after excitation at 330 nm (spectrometer model LS50, Perkin Elmer, Corp.).

4.15 Detection of Fluorescent Proteins by Confocal Microscopy

Detection of fluorescent fusion proteins in plant cells was performed using the confocal laser scanning microscope Leica TCS SP5 and documented with the Leica confocal software LAS AF. GFP signals were collected by excitation with an argon laser (488 nm) in combination with a 510-525 nm emission filter. RFP signals were detected by excitation at 561 nm and an emission filter of 575-605 nm. Simultaneously, chlorophyll fluorescence signals were collected by excitation at 488 nm and an emission filter at 650-750 nm. For adequate magnification a 63x objective was used.

REFERENCES

ALBRECHT V, INGENFELD A & APEL K (2006) Characterization of the *snowy cotyledon 1* mutant of *Arabidopsis thaliana*: the impact of chloroplast elongation factor G on chloroplast development and plant viability. *Plant Mol Biol* **60**, 507-518.

ALBRECHT V, INGENFELD A & APEL K (2008) *Snowy cotyledon 2*: the identification of a zink finger domain protein essential for chloroplast development in cotyledons but not in true leaves. *Plant Mol Biol* **66**, 599-608.

ALONSO JM, STEPANOVA AN, LEISSE TJ, KIM CJ, CHEN H, SHINN P, STEVENSON DK, ZIMMERMANN J, BARAJAS P, CHEUK R, GADRINAB C, HELLER C, JESKE A, KOESEMA E, MEYERS CC, PARKER H, PREDNIS L, ANSARI Y, CHOY N, DEEN H, GERALT M, HAZARI N, HOM E, KARNES M, MULHOLLAND C, NDUBAKU R, SCHMIDT I, GUZMAN P, AGUILAR-HENONIN L, SCHMID M, WEIGEL D, CARTER DE, MARCHAND T, RISSEEUW E, BRODGEN D, ZEKO A, CROSBY WL, BERRY CC & ECKER JR (2003) Genome-wide insertional mutagenesis of *Arabidopsis thaliana*. *Science* **301**, 653-657.

ARMSTRONG GA, RUNGE S, FRICK G, SPERLING U & APEL K (1995) Identification of NADPH: protochlorophyllide oxidoreductases A and B: a branched pathway for light-dependent chlorophyll biosynthesis in *Arabidopsis thaliana*. *Plant Physiol* **108**, 1505-1517.

ARMSTRONG GA, APEL K & RÜDIGER W (2000) Does a light-harvesting protochlorophyllide *a/b*-binding protein complex exist? *Trends Plant Sci* **5**, 40-44.

ARONSSON H, SOHRT K & SOLL J (2000) NADPH:protochlorophyllide oxidoreductase uses the general import route into chloroplasts. *Biol Chem* **381**, 1263-1267.

ASEEVA E, OSSENBÜHL F, EICHACKER LA, WANNER G, SOLL J & VOTHKNECHT UC (2004) Complex formation of Vipp1 depends on its alpha-helical PspA-like domain, *J Biol Chem* **279**, 35535-35541.

BAE W, LEE YJ, KIM DH, LEE J, KIM S, SOHN EJ & HWANG I (2008) AKR2A-mediated import of chloroplast outer membrane proteins is essential for chloroplast biogenesis. *Nat Cell Biol* **10**, 220-227.

BALDI P, GROSSI M, PECCHIONI N, VALÈ G & CATTIVELLI L (1999) High expression level of a gene coding for a chloroplastic amino acid selective channel protein is correlated to cold acclimation in cereals. *Plant Mol Biol* **41**, 233-243.

BARTSCH S, MONNET J, SELBACH K, QUIGLEY F, GRAY J, VON WETTSTEIN D, REINBOTHE S & REINBOTHE C (2008) Three thioredoxin targets in the inner envelope membrane of chloroplasts function in protein import and chlorophyll metabolism. *Proc Natl Acad Sci USA* **105**, 4933-4938.

BAUER J, CHEN K, HILTBRUNNER A, WEHRLI E, EUGSTER M, SCHNELL D & KESSLER F (2000) The major protein import receptor of plastids is essential for chloroplast biogenesis. *Nature* **403**, 203-207.

BECKER T, HRITZ J, VOGEL M, CALIEBE A, BUKAU B, SOLL J & SCHLEIFF E (2004) Toc12, a novel subunit of the intermembrane space preprotein translocon of chloroplasts. *Mol Biol Cell* **15**, 5130-5144.

BLOCK MA, DOUCE R, JOYARD J & ROLLAND N (2007) Chloroplast envelope membranes: a dynamic interface between plastids and the cytosol. *Photosynth Res* **92**, 225-244.

BOARDMAN NK (1962) Studies on a protochlorophyllide-protein complex I. Purification and molecular-weight determination. *Biochim Biophys Acta* **62**, 63-79.

BÖLTER B, MAY T & SOLL J (1998) A protein import receptor in pea chloroplasts, Toc86, is only a proteolytic fragment of a larger polypeptide. *FEBS Lett* **441**, 59-62.

BRUCE BD (2001) The paradox of plastid transit peptides: conservation of function despite divergence in primary structure. *Biochim Biophys Acta* **1541**, 2-21.

BUHR F, EL BAKKOURI M, VALDEZ O, POLLMANN S, LEBEDEV N, REINBOTHE S & REINBOTHE C (2008) Photoprotective role of NADPH:protochlorophyllide oxidoreductase A. *Proc Natl Acad Sci USA* **105**, 12629-12634.

CALIEBE A, GRIMM R, KAISER G, LÜBECK J, SOLL J & HEINS L (1997) The chloroplastic protein import machinery contains a Rieske-type iron-sulfur cluster and a mononuclear iron-binding protein. *EMBO J* **16**, 7342-7350.

CARRIE C, GIRAUD E & WHELAN J (2009) Protein transport in organelles: dual targeting of proteins to mitochondria and chloroplasts. *FEBS J* **276**, 1187-1195.

CHANG JY (1983) Manual micro-sequence analysis of polypeptides using dimethylaminobenzene isothiocyanate. *Methods Enzymol* **91**, 455-466.

CHEN MH, HUANG LF, LI HM, CHEN YR & YU SM (2004) Signal peptide-dependent targeting of a rice α-amylase and cargo proteins to plastids and extracellular compartments of plant cells. *Plant Physiol* **135**, 1367-1377.

CHEN X, SMITH MD, FITZPATRICK L & SCHNELL DJ (2002) *In vivo* analysis of the role of atTic20 in protein import into chloroplasts. *Plant Cell* **14**, 641-654.

CHOU ML, CHU CC, CHEN LJ, AKITA M & LI HM (2006) Stimulation of transit-peptide release and ATP hydrolysis by a cochaperone during protein import into chloroplasts. *J Cell Biol* **175**, 893-900.

CHIGRI F, HÖRMANN F, STAMP A, STAMMERS DK, BÖLTER B, SOLL J & VOTHKNECHT UC (2006) Calcium regulation of chloroplast protein translocation is mediated by calmodulin binding to Tic32. *Proc Natl Acad Sci USA* **103**, 16051-16056.

CLINE K, WERNER-WASHBURNE M, ANDREWS J & KEEGSTRA K (1984) Thermolysin is a suitable protease for probing the surface of intact pea chloroplasts. *Plant Physiol* **75**, 675-678.

CLOUGH SJ & BENT AF (1998) Floral dip: a simplified method for *Agrobacterium*-mediated transformation of *Arabidopsis thaliana*. *Plant J* **16**, 735-743.

COMAS LH, EISSENSTAT DM & LAKSO AN (2000) Assessing root death and root system dynamics in a study of grape canopy pruning. *New Phytol* **147**, 171-178.

DAHLIN C & CLINE K (1991) Developmental regulation of the plastid protein import apparatus. *Plant Cell* **3**, 1131-1140.

DAHLIN C, ARONSSON H, ALMQVIST J & SUNDQVIST C (2000) Protochlorophyllide-independent import of two NADPH:Pchlide oxidoreductase proteins (PORA and PORB) from barley into isolated plastids. *Physiol Plant* **109**, 298-303.

DELLA-CIOPPA G, BAUER SC, KLEIN BK, SHAH DM, FRALEY RT & KISHMORE GM (1986) Translocation of the precursor of 5-enolpyruvylshikimate-3-phosphate synthase into chloroplasts of higher plants *in vitro*. *Proc Natl Acad Sci USA* **83**, 6873-6877.

DEVEREUX J, HAEBERLI P & SMITHIES O (1984) A comprehensive set of sequence analysis programs for the VAX. *Nucl Acids Res* **12**, 387-395.

DOUCE R & JOYARD J (1990) Biochemistry and function of the plastid envelope. *Annu Rev Cell Biol* **6**, 173-216.

DOUZERY EJP, SNELL EA, BAPTESTE E, DELSUC F & HERVÉ P (2004) The timing of eukaryotic evolution: does a relaxed molecular clock reconcile proteins and fossils? *Proc Natl Acad Sci USA* **101**, 15386-15391.

DREA S, LAO N, WOLFE K & KAVANGH T (2006) Gene duplication, exon gain and neofunctionalization of OEP16-related genes in land plants. *Plant J* **46**, 723-735.

DUY D, WANNER G, MEDA AR, VON WIRÉN N, SOLL J & PHILIPPAR K (2007) PIC1, an ancient permease in *Arabidopsis* chloroplasts, mediates iron transport. *Plant Cell* **19**, 986-1006.

EMANUELSSON O, NIELSEN H & VON HEIJNE G (1999) ChloroP, a neural network-based method for predicting chloroplast transit peptides and their cleavage sites. *Protein Sci* **8**, 978-984.

EMANUELSSON O, NIELSEN H, BRUNAK S & VON HEIJNE G (2000) Predicting subcellular localization of proteins based on their N-terminal amino acid sequence. *J Mol Biol* **300**, 1005-1016.

ESEN A (1978) A simple method for quantitative, semiquantitative, and qualitative assay of protein. *Analytical Biochemistry* **89**, 264-273.

FERRO M, SALVI D, RIVIÈRE-ROLLAND H, VERMAT T, SEIGNEURIN-BERNY D, GRUNWALD D, GARIN J, JOYARD J & ROLLAND N (2002) Integral membrane proteins of the chloroplast envelope: identification and subcellular localization of new transporters. *Proc Natl Acad Sci USA* **99**, 11487-11492.

FERRO M, SALVI D, BRUGIÈRE S, MIRAS S, KOWALSKI S, LOUWAGIE M, GARIN J, JOYARD J & ROLLAND N (2003) Proteomics of the chloroplast envelope membranes from *Arabidopsis thaliana*. *Mol Cell Proteomics* **2.5**, 325-345.

GLEAVE AP (1992) A versatile binary vector system with a T-DNA organisational structure conducive to efficient integration of cloned DNA into the plant genome. *Plant Mol Biol* **20**, 1203-1207.

GOSLINGS D, MESKAUSKIENE R, KIM C, LEE KP, NATER M & APEL K (2004) Concurrent interactions of heme and FLU with Glu tRNA reductase (HEMA1), the target of metabolic feedback inhibition of tetrapyrrole biosynthesis, in dark- and light-grown Arabidopsis plants. *Plant J* **40**, 957-967.

GOULD SB, WALLER RF & MCFADDEN GI (2008) Plastid evolution. *Annu Rev Plant Biol* **59**, 491-517.

GUO Y & GAN S (2005) Leaf senescence: signals, execution, and regulation. *Curr Topics Developmental Biol* **71**, 83-112.

GUTENSOHN M, SCHULZ B, NICOLAY P & FLÜGGE UI (2000) Functional analysis of the two *Arabidopsis* homologues of Toc34, a component of the chloroplast protein import apparatus. *Plant J* **23**, 771-783.

HABEEB AFSA (1972) Reaction of protein sulfhydryl groups with Ellman's reagent. *Methods Enzymol* **25**, 457-464.

HAWES C, SAINT-JORE CM, BRANDIZZI F, ZHENG H, ANDREEVA AV & BOEVINK P (2001) Cytoplasmic illuminations: *in planta* targeting of fluorescent proteins to cellular organelles. *Protoplasma* **215**, 77-88.

HE Y, FUKUSHIGE H, HILDEBRAND DF & GAN S (2002) Evidence supporting a role of jasmonic acid in *Arabidopsis* leaf senescence. *Plant Physiol* **128**, 876-884.

HEINS L, MEHRLE A, HEMMLER R, WAGNER R, KÜCHLER M, HÖRMANN F, SVESHNIKOV D & SOLL J (2002) The preprotein conducting channel at the inner envelope membrane of plastids. *EMBO J* **21**, 2616-2625.

HIDEG E, KÁLAI T, HIDEG K & VASS I (1998) Photoinhibition of photosynthesis *in vivo* results in singlet oxygen production detection via nitroxide-induced fluorescence quenching in broad bean leaves. *Biochemistry* **37**, 11405-11411.

HILTBRUNNER A, GRUNIG K, ALVAREZ-HUERTA M, INFANGER S, BAUER J & KESSLER F (2004) AtToc90, a new GTP-binding component of the *Arabidopsis* chloroplast protein import machinery. *Plant Mol Biol* **54**, 427-440.

HINNAH SC, WAGNER R, SVESHNIKOVA N, HARRER R & SOLL J (2002) The chloroplast protein import channel Toc75: pore properties and interaction with transit peptides. *Biophys J* **83**, 899-911.

HÖFGEN R & WILLMITZER L (1988) Storage of competent cells for *Agrobacterium* transformation. *Nucl Acids Res* **16**, 9877.

HÖGLUND A, DÖNNES P, BLUM T, ADOLPH HW & KOHLBACHER O (2006) MultiLoc: prediction of protein subcellular localization using N-terminal targeting sequences, sequence motifs, and amino acid composition. *Bioinformatics* **22**, 1158-1165.

HOFMANN K & STOFFEL W (1993) TMbase – A database of membrane spanning protein segments. *Biol Chem Hoppe-Seyler* **374**, 166-170.

HÖHFELD J, VEENHUIS M & KUNAU WH (1991) PAS3, a *Saccharomyces cerevisiae* gene encoding a peroxisomal integral membrane protein essential for peroxisome biogenesis. *J Cell Biol* **114**, 1167-1178.

HOLTORF H, REINBOTHE S, REINBOTHE C, BEREZA B & APEL K (1995) Two routes of chlorophyllide synthesis that are differentially regulated by light in barley (*Hordeum vulgare* L.). *Proc Natl Acad Sci USA* **92**, 3254-3258.

HÖRMANN F, KÜCHLER M, SVESHNIKOV D, OPPERMANN U, LI Y & SOLL J (2004) Tic32, an essential component in chloroplast biogenesis. *J Biol Chem* **279**, 34756-34762.

HORTON P, PARK KJ, OBAYASHI T, FUJITA N, HARADA H, ADAMS-COLLIER CJ & NAKAI K (2007) WoLF PSORT: protein localization predictor. *Nucleic Acids Res* **35** (Web Server issue):W585-7.

HUANG CY, AYLIFFE MA, TIMMIS JM (2003) Direct measurement of the transfer rate of chloroplast DNA to the nucleus. *Nature* **422**, 72-76.

HUQ E, AL-SADY B, HUDSON M, KIM C, APEL K & QUAIL PH (2004) Phytochrome-interacting factor 1 is a critical bHLH regulator of chlorophyll biosynthesis. *Science* **305**, 1937-1941.

INABA T, LI M, AVAREZ-HUERTA M, KESSLER F & SCHNELL DJ (2003) atTic110 functions as a scaffold for coordinating the stromal events of protein import into chloroplasts. *J Biol Chem* **278**, 38617-38627.

INABA T & SCHNELL DJ (2008) Protein trafficking to plastids: one theme, many variations. *Biochem J* **413**, 15-28.

INABA T (2010) Bilateral communication between plastid and the nucleus: plastid protein import and plastid-to-nucleus retrograde signaling. *Biosci Biotechnol Biochem* **74**, 471-476.

IVANOVA Y, SMITH MD, CHEN K & SCHNELL DJ (2004) Members of the Toc159 import receptor family represent distinct pathways for protein targeting to plastids. *Mol Biol Cell* **15**, 3379-3392.

JACKSON DT, FRÖHLICH JE & KEEGSTRA K (1998) The hydrophilic domain of Tic110, an inner envelope membrane component of the chloroplastic protein translocation apparatus, faces the stromal compartment. *J Biol Chem* **273**, 16583-16588.

JACKSON-CONSTAN D, AKITA M & KEEGSTRA K (2001) Molecular chaperones involved in chloroplast protein import. *Biochim Biophys Acta* **1541**, 102-113.

JÄGER-VOTTERO P, DORNE AJ, JORDANOV J, DOUCE R & JOYARD J (1997) Redox chains in chloroplast envelope membranes: spectroscopic evidence for the presence of electron carriers, including iron-sulfur centers. *Proc Natl Acad Sci USA* **94**, 1597-1602.

JARVIS P, CHEN LJ, LI H, PETO CA, FRANKHAUSER C & CHORY J (1998) An *Arabidopsis* mutant defective in the plastid general import apparatus. *Science* **282**, 100-103.

JARVIS P (2008) Targeting of nucleus-encoded proteins to chloroplasts in plants. *New Phytol* **179**, 257-285.

JOYARD J, BLOCK M, PINEAU B, ALBRIEUX C & DOUCE R (1990) Envelope membranes from mature spinach chloroplasts contain a NADPH:protochlorophyllide reductase on the cytosolic side of the outer membrane. *J Biol Chem* **265**, 21820-21827.

KARIMI M, DE MEYER B & HILSON P (2005) Modular cloning in plant cells. *Trends Plant Sci* **10**, 103-105.

KESSLER F, BLOBEL G, PATEL HA & SCHNELL DJ (1994) Identification of two GTP-binding proteins in the chloroplast protein import machinery. *Science* **266**, 1035-1039.

KESSLER F & BLOBEL G (1996) Interaction of the protein import and folding machineries in the chloroplast. *Proc Natl Acad Sci USA* **93**, 7684-7689.

KIM C & APEL K (2004) Substrate-dependent and organ-specific chloroplast protein import *in planta*. *Plant Cell* **16**, 88-98.

KIM C, HAM H & APEL K (2005) Multiplicity of different cell- and organ-specific import routes for the NADPH-protochlorophyllide oxidoreductase A and B in plastids of *Arabidopsis* seedlings. *Plant J* **42**, 329-340.

KIM C, MESKAUSKIENE R, APEL K & LALOI C (2008) No single way to understand singlet oxygen signalling in plants. *EMBO reports* **9**, 435-439.

KLEFFMANN T, RUSSENBERGER D, VON ZYCHLINSKI A, CHRISTOPHER W, SJOLANDER K, GRUISSEM W & BAGINSKY S (2004) The *Arabidopsis thaliana* chloroplast proteome reveals pathway abundance and novel protein functions. *Curr Biol* **14**, 354-362.

KLEIN RR & MULLET JE (1987) Control of gene expression during higher plant chloroplast biogenesis. *J Biol Chem* **262**, 4341-4348.

KLEINE T, VOIGT C & LEISTER D (2009) Plastid signalling to the nucleus: messengers still lost in the mists? *Trends Genet* **25**, 185-192.

KOLOSSOV VL & REBEIZ CA (2003) Chloroplast Biogenesis 88. Protochlorophyllide *b* occurs in green but not in etiolated plants. *J Biol Chem* **278**, 49675-49678.

KOURANOV A & SCHNELL DJ (1997) Analysis of the interactions of preproteins with the import machinery over the course of protein import into chloroplasts. *J Cell Biol* **139**, 1677-1685.

KOURANOV A, CHEN X, FUKS B & SCHNELL DJ (1998) Tic20 and Tic22 are new components of the protein import apparatus at the chloroplast inner envelope membrane. *J Cell Biol* **143**, 991-1002.

KRAUS S, BAUMGARTNER M, GÜGEL I, SOLL J & PHILIPPAR K (2009) Novel membrane transporter in the chloroplast envelope are essential for plant development. Abstract of poster presentation at the Leopoldina-Symposium *Molecular Genetics of Chloroplasts & Mitochondria*, Berlin.

KUBIS S, BALDWIN A, PATEL R, RAZZAQ A, DUPREE P, LILLEY K, KURTH J, LEISTER D & JARVIS P (2003) The *Arabidopsis ppi1* mutant is specifically defective in the expression, chloroplast import, and accumulation of photosynthetic proteins. *Plant Cell* **15**, 1859-1871.

KUBIS S, PATEL R, COMBE J, BÉDARD J, KOVACHEVA S, LILLEY K, BIEHL A, LEISTER D, RIOS G, KONCZ C & JARVIS P (2004) Functional specialization amongst the *Arabidopsis* Toc159 family of chloroplast protein import receptors. *Plant Cell* **16**, 2059-2077.

LAEMMLI UK (1970) Cleavage of structural proteins during the assembly of the head of bacteriophage T4. *Nature* **227**, 680-685.

LATHAM, J, WILSON AK & STEINBRECHER R (2006) The mutational consequences of plant transformation. *J Biomed Biotech* **2006** (25376), 1-7.

LAUDERT D & WEILER EW (1998) Allene oxide synthase: a major control point in *Arabidopsis thaliana* octadecanoid signalling. *Plant J* **15**, 675–684.

LAZO GR, STEIN PA & LUDWIG RA (1991) A DNA transformation-competent *Arabidopsis* genomic library in *Agrobacterium*. *Biotechnology* **9**, 963-967.

LEBEDEV N, VAN CLEVE B, ARMSTRONG GA & APEL K (1995) Chlorophyll synthesis in a deetiolated (det340) mutant of *Arabidopsis* without NADPH-protochlorophyllide (Pchlide) oxidoreductase (POR) A and photoactive Pchlide-F655. *Plant Cell* **7**, 2081-2090.

LEE YJ, KIM DH, KIM YW & HWANG I (2001) Identification of a signal that distinguishes between the chloroplast outer envelope membrane and the endomembrane system *in vivo*. *Plant Cell* **13**, 2175-2190.

LEE KP, KIM C, LEE DW & APEL K (2003a) *TIRGINA d*, required for regulating the biosynthesis of tetrapyrroles in barley, is an ortholog of the *FLU* gene of *Arabidopsis thaliana*. *FEBS Lett* **553**, 119-124.

LEE KH, KIM SJ, LEE YJ, JIN JB & HWANG I (2003b) The M domain of atToc159 plays an essential role in the import of proteins into chloroplasts and chloroplast biogenesis. *J Biol Chem* **278**, 36794-36805..

LI HM, MOORE T & KEEGSTRA K (1991) Targeting of proteins to the outer envelope membrane uses a different pathway than transport into chloroplasts. *Plant Cell* **3**, 709-717.

LI HM & CHIU CC (2010) Protein transport into chloroplasts. *Annu Rev Plant Biol* **61**, 157-180.

LIM PO, KIM HJ & NAM HG (2007) Leaf senescence. *Annu Rev Plant Biol* **58**, 115-36.

LIN JF & WU SH (2004) Molecular events in senescing *Arabidopsis* leaves. *Plant J* **39**, 612-628.

LOPEZ-JUEZ E & PYKE KA (2005) Plastids unleashed: their development and their integration in plant development. *Int J Dev Biol* **49**, 557-577.

LÜBECK J, SOLL J, AKITA M, NIELSEN E & KEEGSTRA K (1996) Topology of IEP110, a component of the chloroplastic protein import machinery present in the inner envelope membrane. *EMBO J* **15**, 4230-4238.

MA Y, KOURANOV A, LASALA SE & SCHNELL DJ (1996) Two components of the chloroplast protein import apparatus, IAP86 and IAP75, interact with the transit sequence during the recognition and translocation of precursor proteins at the outer envelope. *J Cell Biol*, **134**, 315-327.

MACKENZIE SA (2005) Plant organellar protein targeting: a traffic plan still under construction. *Trends Cell Biol* **15**, 548-554.

MAY T & SOLL J (2000) 14-3-3 proteins form a guidance complex with chloroplast precursor proteins in plants. *Plant Cell* **12**, 53-64.

MCCORMAC AC & TERRY MJ (2002) Light-signalling pathways leading to the co-ordinated expression of *HEMA1* and *Lhcb* during chloroplast development in *Arabidopsis thaliana*. *Plant J* **32**, 549-559.

MCCORMAC AC & TERRY MJ (2004) The nuclear genes *Lhcb* and *HEMA1* are differentially sensitive to plastid signals and suggest distinct roles for the GUN1 and GUN5 plastid-signalling pathways during de-etiolation. *Plant J* **40**, 672-685.

MESKAUSKIENE R, NATER M, GOSLING D, KESSLER F, OP DEN CAMP R & APEL K (2001) FLU: a negative regulator of chlorophyll biosynthesis in *Arabidopsis thaliana*. *Proc Natl Acad Sci USA* **98**, 12826-12831.

MIRAS S, SALVI D, FERRO M, GRUNWALD D, GARIN J, JOYARD J & ROLLAND N (2002) Non-canonical transit peptide for import into the chloroplast. *J Biol Chem* **277**, 47770-47778.

MIRAS S, SALVI D, PIETTE L, SEIGNEURIN-BERNY D, GRUNWALD D, REINBOTHE C, JOYARD J, REINBOTHE S & ROLLAND N (2007) Toc159- and Toc75-independent import of a transit sequence-less precursor into the inner envelope of chloroplasts. *J Biol Chem* **282**, 29482–29492.

MONTANÉ MH & KLOPPSTECH K (2000) The family of light-harvesting-related proteins (LHCs, ELIPs, HLIPs): was the harvesting of light their primary function? *Gene* **258**, 1-8.

MURASHIGE T & SKOOG F (1962) A revised medium for rapid growth and bioassays with tobacco tissue cultures. *Physiologia Plantarum* **15**, 473-497.

MURCHA MW, ELHAFEZ D, LISTER R, TONTI-FILIPPINI J, BAUMGARTNER M, PHILIPPAR K, CARRIE C, MOKRANJAC D, SOLL J & WHELAN J (2007) Characterization of the *preprotein and amino acid transporter* gene family in *Arabidopsis*. *Plant Physiol* **143**, 199-212.

NADA A & SOLL J (2004) Inner envelope protein 32 is imported into chloroplasts by a novel pathway. *J Cell Sci* **117**, 3975-3982.

NANJO Y, OKA H, IKARASHI N, KANEKO K, KITAJIMA A, MITSUI T, MUNOZ FJ, RODRIGUEZ-LOPEZ M, BAROJA-FERNANDEZ E & POZUETA-ROMERO J (2006) Rice plastidial N-glycosylated nucleotide pyrophosphatase/phosphodiesterase is transported from the ER-Golgi to the chloroplast through the secretory pathway. *Plant Cell* **18**, 2582-2592.

NICOLAI M, RONCATO MA, CANOY AS, ROUQUIÉ D, SARDA X, FREYSSINET G & ROBAGLIA C (2006) Large-scale analysis of mRNA translation states during sucrose starvation in Arabidopsis cells identifies cell proliferation and chromatin structure as targets of translational control. *Plant Physiol* **141**, 663-673.

OP DEN CAMP RGL, PRZYBYLA D, OCHSENBEIN C, LALOI C, KIM C, DANON A, WAGNER D, HIDEG E, GÖBEL C, FEUSSNER I, NATER M & APEL K (2003) Rapid induction of distinct stress responses after the release of singlet oxygen in *Arabidopsis*. *Plant Cell* **15**, 2320-2332.

PERRY SE, BUVINGER WE, BENNET J & KEEGSTRA K (1991) Synthetic analogues of a transit peptide inhibit binding or translocation of chloroplastic precursor proteins. *J Biol Chem* **266**, 1182-1189.

PERRY SE & KEEGSTRA K (1994) Envelope membrane proteins that interact with chloroplastic precursor proteins. *Plant Cell* **6**, 93-105.

PHILIPPAR K, GEIS T, ILKAVETS I, OSTER U, SCHWENKERT S, MEURER J & SOLL J (2007) Chloroplast biogenesis: the use of mutants to study the etioplast-chloroplast transition. *Proc Natl Acad Sci USA* **104,** 678-683.

PINEAU B, GÉRARD-HIRNE C, DOUCE R & JOYARD J (1993) Identification of the main species of tetrapyrrolic pigments in envelope membranes from spinach chloroplasts. *Plant Physiol* **102**, 821-828.

POHLMEYER K, SOLL J, STEINKAMP T, HINNAH S & WAGNER R (1997) Isolation and characterization of an amino-selective channel protein present in the chloroplastic outer envelope membrane. *Proc Natl Acad Sci USA* **94**, 9504-9509.

POLLMANN S, SPRINGER A, BUHR F, LAHROUSSI A, SAMOL I, BONNEVILLE JM, TICHTINSKY G, VON WETTSTEIN D, REINBOTHE C & REINBOTHE S (2007) A plant porphyria related to defects in plastid import of protochlorophyllide oxidoreductase A. *Proc Natl Acad Sci USA* **104**, 2019-2023.

PORRA RJ, THOMPSON WA & KRIEDEMANN PE (1989) Determination of accurate extinction coefficients and simultaneous equations for essaying chlorophylls *a* and *b* extracted with four different solvents: verification of the concentration of chlorophyll standards by atomic absorption spectroscopy. *Biochim Biophys Acta* **975**, 384-394.

PRUZINSKÁ A, TANNER G, ANDERS I, ROCA M & HÖRTENSTEINER S (2003) Chlorophyll breakdown: pheophorbide *a* oxygenase is a Rieske-type iron-sulfur protein, encoded by the *accelerated cell death 1* gene. *Proc Natl Acad Sci USA* **100**, 15259-15264.

PUDELSKI B, SOLL J & PHILIPPAR K (2009) A search for factors influencing etioplast-chloroplast translation. *Proc Natl Acad Sci USA* **106**, 12201-12206.

PUDELSKI B, KRAUS S, SOLL J & PHILIPPAR K (2010) The plant PRAT proteins – preprotein and amino acid transport in mitochondria and chloroplasts. *Plant Biol* **12** (Suppl 1) 42-55.

QBADOU S, BECKER T, MIRUS O, TEWS I, SOLL J & SCHLEIFF E (2006) The molecular chaperone Hsp90 delivers precursor proteins to the chloroplast import receptor Toc64. *EMBO J* **25**, 1836-1847.

RASSOW J, DEKKER PJT, VAN WILPE S, MEIJER M & SOLL J (1999) The preprotein translocase of the mitochondrial inner membrane: function and evolution. *J Mol Biol* **286**, 105-120.

REIDEL EJ, TURGEON R & CHENG L (2008) A maltose transporter from apple is expressed in source and sink tissues and complements the *Arabidopsis* maltose export-defective mutant. *Plant Cell Physiol* **49**, 1607-1613.

REINBOTHE S, RUNGE S, REINBOTHE C, VAN CLEVE B & APEL K (1995a) Substrate-dependent transport of the NADPH:protochlorophyllide oxidoreductase into isolated plastids. *Plant Cell* **7**, 161–172.

REINBOTHE C, APEL K & REINBOTHE S (1995b) A light-induced protease from barley plastids degrades NADPH:protochlorophyllide oxidoreductase complexed with chlorophyllide. *Mol Cell Biol* **15**, 6206-6212.

REINBOTHE S, REINBOTHE C, HOLTORF H & APEL K (1995c) Two NADPH:protochlorophyllide oxidoreductases in barley: evidence for the selective disappearance of PORA during the light-induced greening of etiolated seedlings. *Plant Cell* **7**, 1933-1940.

REINBOTHE C, LEBEDEV N, APEL K & REINBOTHE S (1997) Regulation of chloroplast protein import through a protochlorophyllide-responsive transit peptide. *Proc Natl Acad Sci USA* **94**, 8890-8894.

REINBOTHE C, LEBEDEV N & REINBOTHE S (1999) A protochlorophyllide light-harvesting complex involved in the de-etiolation of higher plants. *Nature* **397**, 80-84.

REINBOTHE S, MACHE R & REINBOTHE C (2000) A second, substrate-dependent site of protein import into chloroplasts. *Proc Natl Acad Sci USA* **97**, 9795–9800.

REINBOTHE C, BUHR F, POLLMANN S & REINBOTHE S (2003) *In vitro* reconstitution of light-harvesting POR-protochlorophyllide complex with protochlorophyllides *a* and *b*. *J Biol Chem* **278**, 807-815.

REINBOTHE S, QUIGLEY F, GRAY J, SCHEMENEWITZ A & REINBOTHE C (2004a) Identification of plastid envelope proteins required for import of protochlorophyllide oxidoreductase A into the chloroplast of barley. *Proc Natl Acad Sci USA* **101**, 2197-2202.

REINBOTHE S, QUIGLEY F, SPRINGER A, SCHEMENEWITZ A & REINBOTHE C (2004b) The outer plastid envelope protein Oep16: role as precursor translocase in import of protochlorophyllide oxidoreductase A. *Proc Natl Acad Sci USA* **101**, 2203-2208.

REINBOTHE S, POLLMANN S, SPRINGER A, JAMES RJ, TICHTINSKY G & REINBOTHE C (2005) A role of Toc33 in the protochlorophyllide-dependent plastid import pathway of NADPH: protochlorophyllide oxidoreductase (POR) A. *Plant J* **42**, 1-12.

REINBOTHE C, SPRINGER A, SAMOL I & REINBOTHE S (2009) Plant oxylipins: role of jasmonic acid during programmed cell death, defence and leaf senescence. *FEBS J* **276**, 4666-4681.

REINBOTHE C, EL BAKKOURI M, BUHR F, MURAKI N, NOMATA J, KURISU G, FUJITA Y & REINBOTHE S (2010) Chlorophyll biosynthesis: spotlight on protochlorophyllide reduction. *Trends Plant Sci* **15**, 614-624.

REYES-PRIETO A, WEBER APM & BHATTACHARYA D (2007) The origin and establishment of the plastidic algae and plants. *Annu Rev Genet* **41**, 147-168.

RICHTER S & LAMPPA GK (1998) A chloroplast processing enzyme functions as the general stromal processing peptidase. *Proc Natl Acad Sci USA* **95**, 7463-7468.

RUIZ-FERRER V & VOINNET O (2009) Roles of plant small RNAs in biotic stress responses. *Annu Rev Plant Biol* **60**, 485-510.

RUNGE S, SPERLING U, FRICK G, APEL K & ARMSTRONG GA (1996) Distinct roles for light-dependent NADPH:protochlorophyllide oxidoreductase (POR) A and B during greening in higher plants. *Plant J* **9**, 513-523.

SAMBROOK J, FRITSCH EF & MANIATIS T (1989) Molecular cloning. A laboratory manual. Second Edition. *Cold Spring Harbor Laboratory Press.*

SAMOL I, BUHR F, SPRINGER A, POLLMANN S, LAHROUSSI A, ROSSIG C, VON WETTSTEIN D, REINBOTHE C & REINBOTHE S (2011a) Implication of the *oep16-1* mutation in a *flu*-independent, singlet oxygen-regulated cell death pathway in *Arabidopsis thaliana*. *Plant Cell Physiol* **52**, 84-95.

SAMOL I, ROSSIG C, BUHR F, SPRINGER A, POLLMANN S, LAHROUSSI A, VON WETTSTEIN D, REINBOTHE C & REINBOTHE S (2011b) The outer chloroplast envelope protein OEP16-1 for plastid import of NADPH:protochlorophyllide oxidoreductase A in *Arabidopsis thaliana*. *Plant Cell Physiol* **52**, 96-111.

SCHALLER F, ZERBE P, REINBOTHE S, REINBOTHE C, HOFMANN E & POLLMANN S (2008) The allene oxide cyclase family of *Arabidopsis thaliana* – localization and cyclization. *FEBS J* **275**, 2428-2441.

SCHARF KD & NOVER L (1982) Heat-shock-induced alterations of ribosomal protein phosphorylation in plant cell cultures. *Cell* **30**, 427-437.

SCHEMENEWITZ A, POLLMANN S, REINBOTHE C & REINBOTHE S (2007) A substrate-independent, 14:3:3 protein-mediated plastid import pathway of NADPH:protochlorophyllide oxidoreductase A. *Proc Natl Acad Sci USA* **104**, 8538-8543.

SCHLEIFF E, SOLL J, KÜCHLER M, KÜHLBRANDT W & HARRER R (2003) Characterization of the translocon of the outer envelope of chloroplasts. *J Cell Biol* **160**, 541-551.

SCHLEYER M, SCHMIDT B & NEUPERT W (1982) Requirement of a membrane potential for the posttranslational transfer of proteins into mitochondria. *Eur J Biochem* **125**, 109-116.

SCHNELL DJ, BLOBEL G & PAIN D (1990) The chloroplast import receptor is an integral membrane protein of chloroplast envelope contact sites. *J Cell Biol* **111**, 1825-1838.

SCHNELL DJ, BLOBEL G & PAIN D (1991) Signal peptide analogs derived from two chloroplast precursors interact with the signal recognition system of the chloroplast envelope. *J Biol Chem* **266**, 3335-3342.

SCHNELL DJ & BLOBEL G (1993) Identification of intermediates in the pathway of protein import into chloroplasts and their localization to envelope contact sites. *J Cell Biol* **120**, 103-115.

SCHNELL DJ, KESSLER F & BLOBEL G (1994) Isolation of components of the chloroplast protein import machinery. *Science* **266**, 1007-1020.

SCHNELL DJ, BLOBEL G, KEEGSTRA K, KESSLER F, KO K & SOLL J (1997) A consensus nomenclature for the protein-import components of the chloroplast envelope. *Trends Cell Biol* **266**, 1007-1012.

SHEVCHENKO A, WILM M, VORM O, MANN M (1996). Mass spectrometric sequencing of proteins from silver-stained polyacrylamid gels. *Anal Chem* **68**, 850-858.

SHIMADA H, MOCHIZUKI M, OGURA K, FRÖHLICH JE, OSTERYOUNG KW, SHIRANO Y, SHIBATA D, MASUDA S, MORI, K & TAKAMIYA KI (2007) *Arabidopsis* cotyledon-specific chloroplast biogenesis factor CYO1 is a protein disulfide isomerase. *Plant Cell* **19**, 3157-3169.

SMALL I, PEETERS N, LEGEAI F & LURIN C (2004) Predotar: a tool for rapidly screening proteomics for N-terminal targeting sequences. *Proteomics* **4**, 1581-1590.

SMEEKENS S, VAN BINSBERGEN J & WEISBEEK P (1985) The plant ferredoxin precursor: nucleotide sequence of a full length cDNA clone. *Nucleic Acids Res* **13**, 3179-3194.

SMITH MD, ROUNDS CM, WANG F, CHEN K, AFITLHILE M & SCHNELL DJ (2004) atTOC159 is a selective peptide receptor for the import of nucleus-encoded chloroplast proteins. *J Cell Biol* **165**, 323-334.

SPERLING U, VAN CLEVE B, FRICK G, APEL K & ARMSTRONG GA (1997) Overexpression of light-dependent PORA or PORB in plants depleted of endogenous POR by far-red light enhances seedling survival in white light and protects against photooxidative damage. *Plant J* **12**, 649-658.

SPERLING U, FRANCK F, VAN CLEVE B, FRICK G, APEL K & ARMSTRONG GA (1998) Etioplast differentiation in *Arabidopsis*: both PORA and PORB restore the prolamellar body and photoactive protochlorophyllide-F655 to the *cop1* photomorphogenic mutant. *Plant Cell* **10**, 283-296.

STEGEMANN S, HARTMANN S, RUF S & BOCK R (2003) High-frequency gene transfer from the chloroplast genome to the nucleus. *Proc Natl Acad Sci USA* **100**, 8828-8833.

STENGEL A, BENZ JP, SOLL J & BÖLTER B (2010) Redox-regulation of protein import into chloroplasts and mitochondria. *Plant Signal Behav* **5**, 105-109.

SUNDQVIST C & DAHLIN C (1997) With chlorophyll pigments from prolamellar bodies to light-harvesting complexes. *Physiol Plant* **100**, 748-759.

SVESHNIKOVA N, SOLL J, SCHLEIFF E (2000a) Toc34 is a preprotein receptor regulated by GTP and phosphorylation. *Proc Natl Acad Sci USA* **97**, 4973-4978.

SVESHNIKOVA N, GRIMM R, SOLL J & SCHLEIFF E (2000b) Topology studies of the chloroplast protein import channel Toc75. *Biol Chem* **381**, 687-693.

THEG SM, BAUERLE C, OLSEN LJ, SELMAN BR & KEEGSTRA K (1989) Internal ATP is the only energy requirement for the translocation of precursor proteins across chloroplastic membranes. *J Biol Chem* **264**, 6730-6736.

THOMAS H, OUGHAM HJ, WAGSTAFF C & STEAD AD (2003) Defining senescence and death. *J Exp Bot* **54**, 1127-1132.

TIMMIS JN, AYLIFFE MA, HUANG CY & MARTIN W (2004) Endosymbiotic gene transfer: organelle genomes forge eukaryotic chromosomes. *Nature Reviews Genetics* **5**, 123-135.

TOKATLIDIS K, JUNNE T, MOES S, SCHATZ G, GLICK BS & KRONIDOU N (1996) Translocation arrest of an intramitochondrial sorting signal next to Tim11 at the inner-membrane import site. *Nature* **384**, 585-588.

TOWBIN H, STAEHELIN T & GORDON J (1979) Electrophoretic transfer of proteins from polyacrylamide gels to nitrocellulose sheets: procedure and some applications. *Proc Natl Acad Sci USA* **76**, 4350-4364.

TRANEL PJ & KEEGSTRA K (1996) A novel, bipartite transit peptide targets OEP75 to the outer membrane of the chloroplastic envelope. *Plant Cell* **8**, 2093-2104.

TU SL, CHEN LJ, SMITH MD, SU YS, SCHNELL DJ & LI HM (2004) Import pathways of chloroplast interior proteins and the outer-membrane protein OEP14 converge at TOC75. *Plant Cell* **16**, 2078-2088.

TUSNÁDY GE & SIMON I (2001) The HMMTOP transmembrane topology prediction server. *Bioinformatics* **17**, 849-850.

VILLAREJO A, BURÉN S, LARSSON S, DÉJARDIN S, MONNÉ M, RUDHE C, KARLSSON J, JANSSON S, LEROUGE P, ROLLAND N, VON HEIJNE G, GREBE M, BAKO L & SAMUELSSON G (2005) Evidence for a protein transported through the secretory pathway en route to the higher plant chloroplast. *Nat Cell Biol* **7**, 1224-1231.

VOJTA A, ALAVI M, BECKER T, HÖRMANN F, KÜCHLER M, SOLL J, THOMSEN R & SCHLEIFF E (2004) The protein translocon of the plastid envelopes. *J Biol Chem* **279**, 21401-21405.

VON HEIJNE G (1992) Membrane protein structure prediction: hydrophobicity analysis and the 'Positive Inside' Rule. *J Mol Biol* **225**, 487-494.

VON WETTSTEIN D, GOUGH S & KANNANGARA CG (1995) Chlorophyll biosynthesis. *Plant Cell* **7**, 1039-1057.

VÖRÖS K, FEUSSNER I, KÜHN H, LEE J, GRANER A, LÖBLER M, PARTHIER B & WASTERNACK C (1998) Characterization of a methyljasmonate-inducible lipoxygenase from barley (*Hordeum vulgare* cv. Salome) leaves. *Eur J Biochem* **251**, 36-44.

WATERS MT & LANGDALE JA (2009) The making of a chloroplast. *EMBO J* **28**, 2861-2873.

WEAVER LM, GAN SS, QUIRINO B & AMASINO RM (1998) A comparison of the expression patterns of several senescence-associated genes in response to stress and hormone treatment. *Plant Mol Biol* **37**, 455-469.

WEIGEL D & GLAZEBROOK J (2002) *Arabidopsis:* A laboratory manual. *Cold Spring Harbor Laboratory Press,* Cold Spring Harbour, New York.

WESLEY VS, HELLIWELL C, SMITH NA, WANG MB, ROUSE D, LIU Q, GOODING PS, SINGH SR, ABBOTT D, STOUTJESIJK A, ROBINSON SP, GLEAVE AG & WATERHOUSE PM (2001) Construct design for efficient, effective and high-throughput gene silencing in plants. *Plant J* **27**, 581-590.

WIEDMANN M, KURZCHALIA TV, BIELKA H & RAPOPORT TA (1987) Direct probing of the interaction between the signal sequence of nascent preprolactin and the signal recognition particle by specific cross-linking. *J Cell Biol* **104**, 201-208.

WINTER D, VINEGAR B, NAHAL H, AMMAR R, WILSON GV & PROVART NJ (2007) An „Electronic Fluorescent Pictograph" browser for exploring and analyzing large-scale biological data sets. *PLoS one* **8**, e718.

YANG M, WARDZALA E, JOHAL GS & GRAY J (2004) The wound-inducible *Lls1* gene from maize is an orthologue of the *Arabidopsis Acd1* gene, and the LLS1 protein is present in non-photosynthetic tissues. *Plant Mol Biol* **54**, 175-191.

YIN Y, CHORY Y & BAULCOMBE D (2005) RNAi in transgenic plants. *Current Protocols in Molecular Biology* 26.6.1-26.6.19. Wiley & Sons, Inc.

YOON HS, HACKETT JD, CINIGLIA C, PINTO G & BHATTACHARYA D (2004) A molecular timeline for the origin of photosynthetic eukaryotes. *Mol Biol Evol* **21**, 809-818.

YOUNG ME, KEEGSTRA K & FRÖHLICH JE (1999) GTP promotes the formation of early-import intermediates but is not required during the translocation step of protein import into chloroplasts. *Plant Physiol* **121**, 237-244.

YUAN M, YUAN S, ZHANG ZW, XU F, CHEN YE, DU YB & LIN HH (2010) Putative mutation mechanism and light responses of a protochlorophyllide oxidoreductase-less barley mutant *NYB*. *Plant Cell Physiol* **51**, 1361-1371.

APPENDIX I

Expression Data of *HP20* and *HP30* in *A. thaliana*

provided by the Bio-Array Resource (BAR)

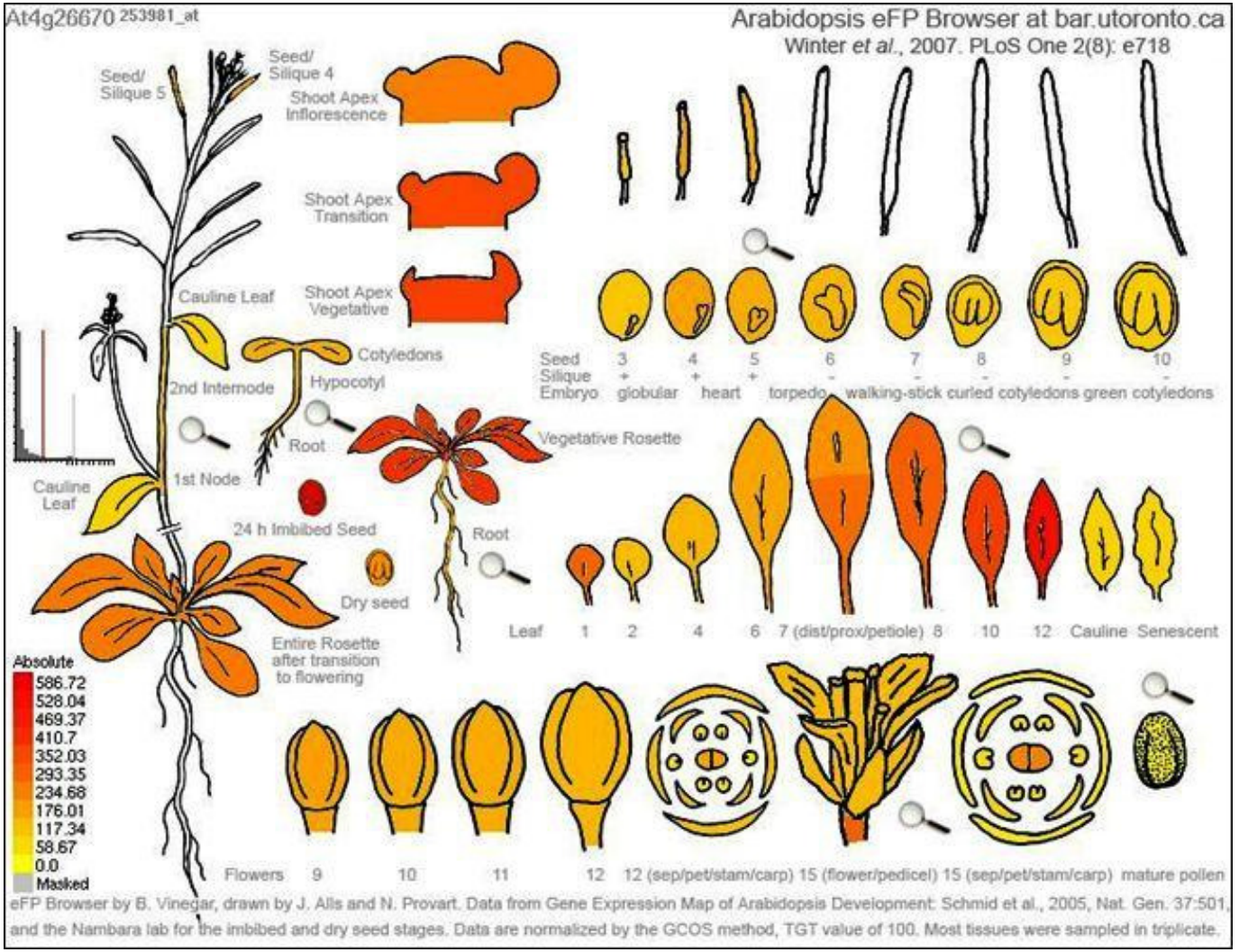

Figure 49. Overview about the Expression pattern of *HP20* (At4g26670) at the total plant level (*A. thaliana* eFP Browser) from the website bar.utoronto.com. Maximum expression values (red) correspond to 586.72. The lower the expression values, the more yellow are the corresponding plant tissues. No colour indicates no expression.

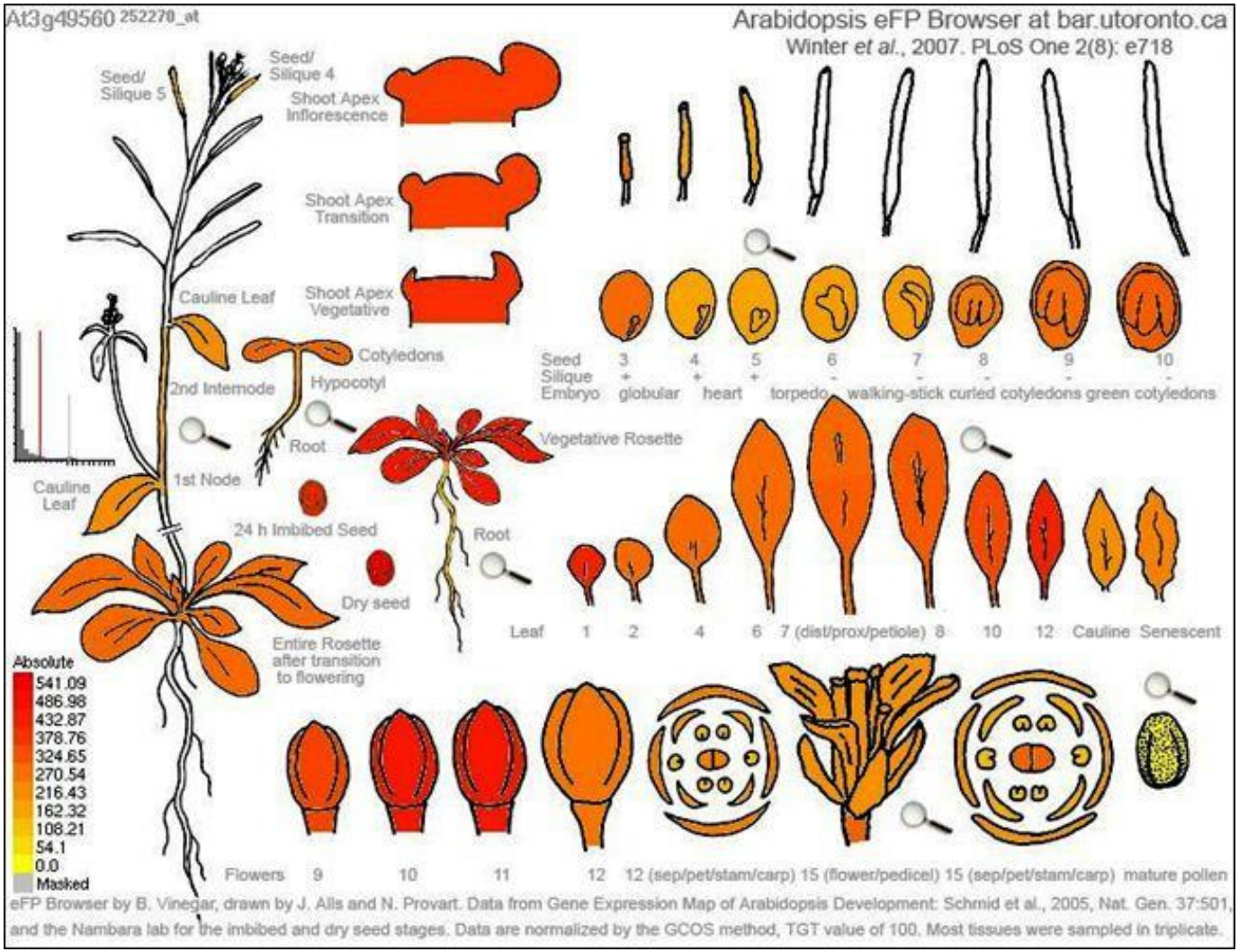

Figure 50. Overview about the Expression pattern of *HP30* (At3g49560) at the total plant level (*A. thaliana* eFP Browser) from the website bar.utoronto.com. Maximum expression values (red) correspond to 541.09. The lower the expression values, the more yellow are the corresponding plant tissues. No colour indicates no expression.

APPENDIX II

Multiple cDNA Sequence Alignment of the Members of the PRAT Family

cDNA Sequence Alignment of the PRAT family using the program GCG

```
At4g26670 HP20        DQ405270        Len: 1175  Check: 8558  Weight: 1.00
At5g55510 HP22        DQ405271        Len: 1175  Check: 9317  Weight: 1.00
At3g49560 HP30        DQ405266        Len: 1175  Check: 9376  Weight: 1.00
At5g24650 HP30-2      DQ405267        Len: 1175  Check: 3850  Weight: 1.00
At2g28900 ATOEP16-1   DQ386642        Len: 1175  Check: 3982  Weight: 1.00
At4g16160 ATOEP16-2   NM_179063       Len: 1175  Check: 6897  Weight: 1.00
At2g42210 ATOEP16-3   DQ386643        Len: 1175  Check: 5881  Weight: 1.00
At3g26880 ATOEP16-4   NM_001035842    Len: 1175  Check: 5077  Weight: 1.00
At1g20350 ATTIM17-1   BT005239        Len: 1175  Check: 1335  Weight: 1.00
At2g37410 A2TTIM17-2  NM_201892       Len: 1175  Check: 1746  Weight: 1.00
At5g11690 ATTIM17-3   NM_121207       Len: 1175  Check: 6577  Weight: 1.00
At1g18320 ATTIM22-1   DQ405269        Len: 1175  Check: 2750  Weight: 1.00
At3g10110 ATTIM22-2   DQ405268        Len: 1175  Check: 2750  Weight: 1.00
At1g72750 ATTIM23-2   NM_105934       Len: 1175  Check: 2348  Weight: 1.00
At3g04800 ATTIM23-3   BT025747        Len: 1175  Check: 6132  Weight: 1.00
At3g25120             DQ405272        Len: 1175  Check: 1522  Weight: 1.00

                      1                                                  50
At4g26670 HP20        ~~~~~~~~~~ ~~~~~~~~~~ ~~~~~~~~~~ ~~~~~~~~~~ ~~~~~~~~~~
At5g55510 HP22        ~~~~~~~~~~ ~~~~~~~~~~ ~~~~~~~~~~ ~~~~~~~~~~ ~~~~~~~~~~
At3g49560 HP30        ~~~~~~~~~~ ~~~~~~~~~~ ~~~~~~~~~~ ~~~~~~~~~~ ~~~~~~~~~~
At5g24650 HP30-2      ~~~~~~~~~~ ~~~~~~~~~~ ~~~~~~~~~~ ~~~~~~~~~~ ~~~~~~~~~~
At2g28900 ATOEP16-1   ~~~~~~~~~~ ~~~~~~~~~~ ~~~~~~~~~~ ~~~~~~~~~~ ~~~~~~~~~~
At4g16160 ATOEP16-2   ~~~~~~~~~~ ~~~~~~~~~~ ~~~~~~~~~~ ~~~~~~~~~~ ~~~~~~~~~~
At2g42210 ATOEP16-3   ~~~~~~~~~~ ~~~~~~~~~~ ~~~~~~~~~~ ~~~~~~~~~~ ~~~~~~~~~~
At3g26880 ATOEP16-4   ~~~~~~~~~~ ~~~~~~~~~~ ~~~~~~~~~~ ~~~~~~~~~~ ~~~~~~~~~~
At1g20350 ATTIM17-1   ~~~~~~~~~~ ~~~~~~~~~~ ~~~~~~~~~~ ~~~~~~~~~~ ~~~~~~~~~~
At2g37410 ATTIM17-2   ~~~~~~~~~~ ~~~~~~~~~~ ~~~~~~~~~~ ~~~~~~~~~~ ~~~~~~~~~~
At5g11690 ATTIM17-3   ~~~~AAAGAC CAGGGTGTTT TTTTTCTGAC AAAACAAATT GTAACACTCA
At1g18320 ATTIM22-1   ~~~~~~~~~~ ~~~~~~~~~~ ~~~~~~~~~~ ~~~~~~~~~~ ~~~~~~~~~~
At3g10110 ATTIM22-2   ~~~~~~~~~~ ~~~~~~~~~~ ~~~~~~~~~~ ~~~~~~~~~~ ~~~~~~~~~~
At1g72750 ATTIM23-2   ACAACTGGAC TGAGTCTTTC CCTAAAAACC CTAAACATAG ATTTTTAGTT
At3g04800 ATTIM23-3   ~~~~~~~~~~ ~~~~~~~~~~ ~~~~~~~~~~ ~~~~~~~~~~ ~~~~~~~~~~
At3g25120             ~~~~~~~~~~ ~~~~~~~~~~ ~~~~~~~~~~ ~~~~~~~~~~ ~~~~~~~~~~

                      51                                                 100
At4g26670 HP20        ~~~~~~~~~~ ~~~~~~~~~~ ~~~~~~~~~~ ~~~~~~~~~~ ~~~~~~~~~~
At5g55510 HP22        ~~~~~~~~~~ ~~~~~~~~~~ ~~~~~~~~~~ ~~~~~~~~~~ ~~~~~~~~~~
At3g49560 HP30        ~~~~~~~~~~ ~~~~~~~~~~ ~~~~~~~~~~ ~~~~~~~~~~ ~~~~~~~~~~
At5g24650 HP30-2      ~~~~~~~~~~ ~~~~~~~~~~ ~~~~~~~~~~ ~~~~~~~~~~ ~~~~~~~~~~
At2g28900 ATOEP16-1   ~~~~~~~~~~ ~~~~~~~~~~ ~~~~~~~~~~ ~~~~~~~~~~ ~~~~~~~~~~
At4g16160 ATOEP16-2   ~~~~~~~~~~ ~~~~~~~~~~ ~~~~~~~~~~ ~~~~~~~~~~ ~~~~~~~~~~
At2g42210 ATOEP16-3   ~~~~~~~~~~ ~~~~~~~~~~ ~~~~~~~~~~ ~~~~~~~~~~ ~~~~~~~~~~
At3g26880 ATOEP16-4   ~~~~~~~~~~ ~~~~~~~~~~ ~~~~~~~~~~ ~~~~~~~~~~ ~~~~~~~~~~
At1g20350 ATTIM17-1   ~~~~~~~~~~ ~~~~~~~~~~ ~~~~~~~~~~ ~~~~~~~~~~ ~~~~~~~~~~
At2g37410 ATTIM17-2   ~~~~~~~~~~ ~~~~~~~~~~ ~~~~~~~~~~ ~~~~~~~~~~ ~~~~~~~~~~
At5g11690 ATTIM17-3   CTAGGCATAG CATTCTAGTT AGTTCTGCAG AAATTTATAG CGACACTGGT
At1g18320 ATTIM22-1   ~~~~~~~~~~ ~~~~~~~~~~ ~~~~~~~~~~ ~~~~~~~~~~ ~~~~~~~~~~
At3g10110 ATTIM22-2   ~~~~~~~~~~ ~~~~~~~~~~ ~~~~~~~~~~ ~~~~~~~~~~ ~~~~~~~~~~
At1g72750 ATTIM23-2   TAGTTTGGTT TCATTTCTCA TTTCGGCAAC CAAACCAAAC ATTCAGAGAG
At3g04800 ATTIM23-3   ~~~~~~~~~~ ~~~~~~~~~~ ~~~~~~~~~~ ~~~~~~~~~~ ~~~~~~~~~~
At3g25120             ~~~~~~~~~~ ~~~~~~~~~~ ~~~~~~~~~~ ~~~~~~~~~~ ~~~~~~~~~~
```

```
                    101                                                 150
At4g26670 HP20      ~~~~~~~~~~ ~~~~~~~~~~ ~~~~~~~~~~ ~~~~~~~~~~ ~~~~~~~~~~
At5g55510 HP22      ~~~~~~~~~~ ~~~~~~~~~~ ~~~~~~~~~~ ~~~~~~~~~~ ~~~~~~~~~~
At3g49560 HP30      ~~~~~~~~~~ ~~~~~~~~~~ ~~~~~~~~~~ ~~~~~~~~~A TGGTGGTAGG
At5g24650 HP30-2    ~~~~~~~~~~ ~~~~~~~~~~ ~~~~~~~~~~ ~~~~~~~~~~ ~~~~~~~~~~
At2g28900 ATOEP16-1 ~~~~~~~~~~ ~~~~~~~~~~ ~~~~~~~~~~ ~~~~~~~~~~ ~~~~~~~~~~
At4g16160 ATOEP16-2 ~~~~~~~~~~ ~~~~~~~~~~ ~~~~~~~~~~ ~~~~~~~~~~ ~~~~~~~~~~
At2g42210 ATOEP16-3 ~~~~~~~~~~ ~~~~~~~~~~ ~~~~~~~~~~ ~~~~~~~~~~ ~~~~~~~~~~
At3g26880 ATOEP16-4 ~~~~~~~~~~ ~~~~~~~~~~ ~~~~~~~~~~ ~~~~~~~~~~ ~~~~~~~~~~
At1g20350 ATTIM17-1 ~~~~~~~~~~ ~~~~~~~~~~ ~~~~~~~~~~ ~~~~~~~~~~ ~~~~~~~~~~
At2g37410 ATTIM17-2 ~~~~~~~~~~ ~~~~~~~~~~ ~~~~~~~~~~ ~~~~~~~~~~ ~~~~~~~~~~
At5g11690 ATTIM17-3 CCAAATTAGG AGGAGCGAGA GCGAAGGTAC GAGTGAGGAT TTACAATTGT
At1g18320 ATTIM22-1 ~~~~~~~~~~ ~~~~~~~~~~ ~~~~~~~~~~ ~~~~~~~~~~ ~~~~~~~~~~
At3g10110 ATTIM22-2 ~~~~~~~~~~ ~~~~~~~~~~ ~~~~~~~~~~ ~~~~~~~~~~ ~~~~~~~~~~
At1g72750 ATTIM23-2 ACACAACACA ACCACATCAT CACACGTTTC TCTCTCTCTC TTTCCTCTCC
At3g04800 ATTIM23-3 ~~~~~~~~~~ ~~~~~~~~~~ ~~~~~~~~~~ ~~~~~~~~~~ ~~~~~~~~~~
At3g25120           ~~~~~~~~~~ ~~~~~~~~~~ ~~~~~~~~~~ ~~~~~~~~~~ ~~~~~~~~~~

                    151                                                 200
At4g26670 HP20      ~~~~~~~~~~ ~~~~~~~~~~ ~~~~~~~~~~ ~~~~~~~~~~ ~~~~~~~~~~
At5g55510 HP22      ~~~~~~~~~~ ~~~~~~~~~~ ~~~~~~~~~~ ~~~~~~~~~~ ~~~~~~~~~~
At3g49560 HP30      CGGCGGAGGA GAAGGAGATC AGAAGAGAAG CAGCGGAGAA ATGATGGCGA
At5g24650 HP30-2    ~~~ATGGGGA AAGACGGAGA AGGAGACAAG AAGC.GAGAA ACAATGGCGG
At2g28900 ATOEP16-1 ~~~~~~~~~~ ~~~~~~~~~~ ~~~~~~~~~~ ~~~~~~~~~~ ~~~~~~~~~~
At4g16160 ATOEP16-2 ~~~~~~~~~~ ~~~~~~~~~~ ~~~~~~~~~~ ~~~~~~~~~~ ~~~~~~~~~~
At2g42210 ATOEP16-3 ~~~~~~~~~~ ~~~~~~~~~~ ~~~~~~~~~~ ~~~~~~~~~~ ~~~~~~~~~~
At3g26880 ATOEP16-4 ~~~~~~~~~~ ~~~~~~~~~~ ~~~~~~~~~~ ~~~~~~~~~~ ~~~~~~~~~~
At1g20350 ATTIM17-1 ~~~~~~~~~~ ~~~~~~~~~~ ~~~~~~~~~~ ~~~~~~~~~~ ~~~~~~~~~~
At2g37410 ATTIM17-2 ~~~~~~~~~~ ~~~~CCTCCT TCATTTTTTC TCTCTCTCTC AAACTCGTCT
At5g11690 ATTIM17-3 CGATCGTTTT CACCTAGAAA CCCTAATTTC GGGGGCTCGC ACGCCCTCTC
At1g18320 ATTIM22-1 ~~~~~~~~~~ ~~~~~~~~~~ ~~~~~~~~~~ ~~~~~~~~~~ ~~~~~~~~~~
At3g10110 ATTIM22-2 ~~~~~~~~~~ ~~~~~~~~~~ ~~~~~~~~~~ ~~~~~~~~~~ ~~~~~~~~~~
At1g72750 ATTIM23-2 GTCGTCTCTC TCTCTCTAGC CACCACCAAA ATCCTTAAAA CCTAGACTTT
At3g04800 ATTIM23-3 ~~~~~~~~~~ ~~~~~~~~~~ ~~~~~~~~~~ ~~~~~~~~~~ ~~~~~~~~~~
At3g25120           ~~~~~~~~~~ ~~~~~~~~~~ ~~~~~~~~~~ ~~~~~~~~~~ ~~~~~~~~~~

                    201                                                 250
At4g26670 HP20      ~~~~~~~ATG GCGGCGAACG ATTCTTCAAA TGCTATTGAC ATCGACGGGA
At5g55510 HP22      ~~~~~~~ATG GCGGCCGAGA ATTCTTCAAA CGCTATTAAC GTCGATACGA
At3g49560 HP30      TGGCGAGTTT ATTCAACGAT CAGCAGAATC CAATTCAACA GTTTCAGGTT
At5g24650 HP30-2    TGATGAGCTT AATGAAGGAT CAACAGAATC CAATTCAACA GTTTCAAGTC
At2g28900 ATOEP16-1 ~~~~~~~~~~ ~~~~~~~~~~ ~~~~~~~~~~ ~~~~~~~~~~ ~~~~~~~ATG
At4g16160 ATOEP16-2 ~~~~~~~~GA AGCAACAAGT GAAGAAAGAA AGAAAAAAAT GGAGAAGAGT
At2g42210 ATOEP16-3 ~~~~~~~~~~ ~~~~~~~~~~ ~~~~~~~~~~ ~~~~~~~~~~ ~~~~~~~~~~
At3g26880 ATOEP16-4 ~~~~~~~~~~ ~~~~~~~~~~ ~~~~~~~~~~ ~~~~~~GGAC GGAGAGGTAA
At1g20350 ATTIM17-1 ~~~~~~~~~~ ~~~~~~~~~~ ~~~~~~~~~~ ~~~~~~~~~~ ~~~~~~~~~~
At2g37410 ATTIM17-2 CTAAAACTCG TCCGTCGATT AATTCCTCGT TAGTCTCAGG TTTGATAGAA
At5g11690 ATTIM17-3 TGATTAGAAG CGACTTCATT ATCGGTCACT AGAATCTGCT GCTTCTTTTC
At1g18320 ATTIM22-1 ~~~~~~~~~~ ~~~~~~~~~~ ~~~~~~~~~~ ~~~~~~~~~~ ~~~~~~~~~~
At3g10110 ATTIM22-2 ~~~~~~~~~~ ~~~~~~~~~~ ~~~~~~~~~~ ~~~~~~~~~~ ~~~~~~~~~~
At1g72750 ATTIM23-2 TCTCTTCCAT CGATGGCGGC TAATAACAGA TCCGATCATG GGTCAGACGA
At3g04800 ATTIM23-3 ~~~~~~ATGG CGGATCCGAT GAACCATAGC ACCGGGCATC AACAACAGCA
At3g25120           ~~~~~~~~~~ ~~~~~~~~~~ ~~~~~~~~~~ ~~~~~~~~~~ ~~~~~~~~~~

                    251                                                 300
At4g26670 HP20      ATCTCGACTC CGATTCGAAT CTTAACACTG ACGGTGACGA AGCGACCGAT
At5g55510 HP22      GTCTCGATTC CGATTCAAAA CCTAACCGTG ACGCTAATGA TATGACTGAT
At3g49560 HP30      AAATTCAAAG AAGTAGAAAC TAATTTCAAG ACATGGTTGT CGAAACAGTC
At5g24650 HP30-2    AAATTCAAGG AGATTGAGAC TGGTTTCAAG TCGTGGTTAT CAAAACAGAA
At2g28900 ATOEP16-1 CCTTCAAGCA CATTCTCCGG GACTGTTAGC ACGCCGAAGC TGTCGGTGGC
```

```
At4g16160 ATOEP16-2  GGAGGAAGAA TTGTAATGGA TGAGATAAGA AGCTTTGAGA AGGCACACTT
At2g42210 ATOEP16-3  ~~~~~~~~~~ ~~~~~~~~~~ ~~~~ATGGAT CCAGCTGAAA TGAGATATTT
At3g26880 ATOEP16-4  CAAAACAAAA GGGTTTTGTC CTAATTCAAT TTTGCAGAGA TGGAGGAAGA
At1g20350 ATTIM17-1  ~~~~~~~~~~ ~~~~~~~~~~ ~~ATGGGAAC TCCAGAATCA TCGAGAGAGC
At2g37410 ATTIM17-2  TCATTGCCTG AGGCATCTAA TAATGGGAAC ACCAGAGACA TCTCGGGAGC
At5g11690 ATTIM17-3  TGAAACTAGC ATTGTCAGGA ACATGGACAC TAAGAAGAAA TCTAAGGAAC
At1g18320 ATTIM22-1  ATGGCAGATT CGAGTGCTGC TGAAACAACA ACCGGTGCTT CTTCTCCCCC
At3g10110 ATTIM22-2  ATGGCAGATT CGAGTGCTGC TGAAACAACA ACCGGTGCTT CTTCTCCCCC
At1g72750 ATTIM23-2  AAACACAAGA CTTTACAATC CTTACCAAAA CTACGAAGTC CCAATCAACA
At3g04800 ATTIM23-3  GAAGTACCGT CAGTACAATC CTTACCAACA AGTCAATCTT CC........
At3g25120            ~~~~~~~~~~ ~~~~~~~~~~ ~~~~~~~ATG GCGTTGGGTG ATCGGAAATC

                     301                                                350
At4g26670 HP20       AATGATTCCT CGAAGGCATT GGTTACTATC CCTGCTCCAG CCGTTTGTCT
At5g55510 HP22       CATGACTCTT CTTCTAAAGC ATTGGTAATC CCTGCTCCCG CCGTTTGTCT
At3g49560 HP30       GATTCCGGTG GAAGCCGCCG TCGTATCCAC CATGAGCGGT GTACAAGGAG
At5g24650 HP30-2     GTTACCGGTG GAAGCCGCCG TTGTCACGGC CATGGGTGGT GTTCAGGGAG
At2g28900 ATOEP16-1  AGTGGACATG GGAAACCCTT TTCTCAATCT CACCGTTGAT GCCTTCCTCA
At4g16160 ATOEP16-2  GTTCGATCTT GGTCATCCTC TTCTTAACCG TATCGCAGAT TCCTTCGTTA
At2g42210 ATOEP16-3  GGAAGAAGAG GATGGTCCGT TGATGAAGAC AATCAAAGGT AGTATCACTG
At3g26880 ATOEP16-4  ATTGCTCTCC GCCGTGCCGT GCTCTTCCCT AACCGTCGAG TCAGTTCTCC
At1g20350 ATTIM17-1  CATGTCCGGA TCGGATCCTA GATGATGTCG GAGGTGCGTT TGCGATGGGT
At2g37410 ATTIM17-2  CTTGCCCTGA TCGTATACTC GATGATATCG GTGGTGCTTT TGGTATGGGA
At5g11690 ATTIM17-3  ATGGCCTATA CCGTATAGTC AATGCTATCG GTTATGCATT TGGAGCGGGA
At1g18320 ATTIM22-1  CGTGGCTTCT GATGAGAACT CTACCCAGAT TCAACCGATC CGGATGCCAA
At3g10110 ATTIM22-2  CGTGGCTTCT GATGAGAACT CTACCCAGAT TCAACCGATC CGGATGCCAA
At1g72750 ATTIM23-2  AATCTCAGTA CCTTTACAAG CTTCCTACCT CCCCTGAGTT TCTCTTCACG
At3g04800 ATTIM23-3  .GTACCGTAA GCTCTACGAA CTCCCAACTT CTCCTGAGTT TCTCTTCGAA
At3g25120            CCCAGAACAA ACAAATCAGG CGTTATCTCC TCCGACGCCT ATTGTGCAGG

                     351                                                400
At4g26670 HP20       TTTCCGGTTC GCCGGAGATG CTGCTGGTGG CGCCGTTATG GGCTCTATCT
At5g55510 HP22       TGTACGTTTC GCCGGAGATG CTGCTAGTGG CGCATTCATG GGCTCTGTAT
At3g49560 HP30       CTTTCATTGG TGGTCTCATG GGAACACTCT CTCCTGAAAT GCCTCAAGCC
At5g24650 HP30-2     CTTTTATCGG TGGTTTAATG GGAACTTTAT CTCCTGAAAT GCCTCAGGCT
At2g28900 ATOEP16-1  AGATCGGAGC TGTTGGAGTC ACTAAATCTC TTGCAGAAGA CACTTACAAG
At4g16160 ATOEP16-2  AAGCCGCCGG AGTGGGAGCT TTACAAGCCG TGTCAAGGGA AGCTTACTTT
At2g42210 ATOEP16-3  GTTTTGGTGC TGGGACTATT TACGGAACCA TTTTAGCCAC ATGGAAAGAT
At3g26880 ATOEP16-4  GTGTCGCGAC GGCCGGTGGA TTATATGGGT TATGCGCCGG ACCTCGTGAC
At1g20350 ATTIM17-1  GCTGTTGGTG GATCAGCGTA TCACCTCATA AGAGGAATCT ACAACTCTCC
At2g37410 ATTIM17-2  GCTGTTGGAG GATCTGCCTT TCATTTCATT AAAGGGACTT ACAATTCTCC
At5g11690 ATTIM17-3  GCTGTTGGAG GTTCTGTATA TCATTTCGTG AGAGGGGCAT ACAATTCCCC
At1g18320 ATTIM22-1  CCATCGAGGA GATCCGAGCT CAAGAGGTTT GGA.ACAACT GCGCCGTTCG
At3g10110 ATTIM22-2  CCATCGAGGA GATCCGAGCT CAAGAGGTTT GGA.ACAACT GCGCCGTTCG
At1g72750 ATTIM23-2  GAGGAGGCTT TAAGGCAACG TAGATCTTGG GGTGAGAATC TCACTTTCTA
At3g04800 ATTIM23-3  GAAGAAGCTA CGAAAAAACG CTTAACATGG GGAGAGAACC TCACCTTCTT
At3g25120            AAAATGGAAC TCCGACGAAG CGTGTGTTGA TCACTTCCCT TTTAGCAGGA

                     401                                                450
At4g26670 HP20       TCGGATATGG TTCAGGATTG TTCAAGAAGA AAGGCTTCAA AGGATCATTT
At5g55510 HP22       TTGGCTATGG CTCTGGATTG TTTAAGAAGA AAGGGTTTAA AGGATCATTT
At3g49560 HP30       GGCGTTGACC CTCAAGCCAT AGCTTCGATG AAACAAGCTC AGGCTCTTGT
At5g24650 HP30-2     GGTATTGACC CTCAAGCTAT GGCTTCGCTA AAGCAAACTC AGGCTCTTGT
At2g28900 ATOEP16-1  GCCATCGACA AAGGGAGTCT CTCCAAGAGC ACTTTGGAGC ATGCGCTTAA
At4g16160 ATOEP16-2  ACCGTGGTTG ACGGGGCAGG TTTTGACTCG AACAACGTGG GTCCACCGTC
At2g42210 ATOEP16-3  GTTCCAAGAG TGGAGAGAAA TGTGGCTCTT CCAGGACTTA TTAGAACACT
At3g26880 ATOEP16-4  GCTCGTAAAA TAGGTTTAAG CGGCGTTTCT CAGGCTTCCT TTGTGGCGAA
At1g20350 ATTIM17-1  CGGCGGAGCT CGTCTCTCCG GCGGCGTTCA AGCTTTGAGA ATGAGCGGGC
At2g37410 ATTIM17-2  TAAAGGTAGT CGCTTTGTTG GAGGAACACA ATCGGTGAGC ATGAACGCAC
At5g11690 ATTIM17-3  AATAGGTGCT CGATATGTTG GAGGAACACA AGCGGCTAGC ATGAATGCTC
```

```
At1g18320 ATTIM22-1  CGCTGTTACT AGTGGAGTCA TGGGAGGAGG ACTCGGGTTG ATGATGGGTT
At3g10110 ATTIM22-2  CGCTGTTACT AGTGGAGTCA TGGGAGGAGG ACTCGGGTTG ATGATGGGTT
At1g72750 ATTIM23-2  CACCGGAACA GCTTACCTCG GTGGCTCCGT TGCCGGAGCT TCTGTTGGAG
At3g04800 ATTIM23-3  CACCGGTTGG GGTTATTGCA CTGGATCTGT TCTCGGAGCC TTCAAGGGTA
At3g25120            GTAATTGGTG GAGGAGCTGG TTTAGTGTCT AAACACCGGA TAGCTCATCC

                     451                                                500
At4g26670 HP20       GCAGATGCAG GGCAGTC.TG CTAAGACTTT TGCTGTTTTA TCTGGAGTCC
At5g55510 HP22       GTGGATGCGG GTCAGTC.TG CAAAGACTTT TGCGGTTTTA TCTGGAGTAC
At3g49560 HP30       GGGTGGTCCT TGGGTCCAAG CTCGGAATTT TGCTGCAATT ACTGGTGTGA
At5g24650 HP30-2     TGGTGGGCCT TTGGTTCAAG CTCGGAACTT TGCTGCTATA ACTGGTGTTA
At2g28900 ATOEP16-1  GAAGTTGTGT AAAGAAGGTG TTTACTGGGG AGCTGCTGGT GGAGTGTACA
At4g16160 ATOEP16-2  GGAGATTACA GGGAACAAGA AACATAGGTT CCCTAATCTC AGAGGGGAAA
At2g42210 ATOEP16-3  GAAGATGATG GGAACCCATG GGCTGACTTT TGCTGCTATA GGAGGTGTTT
At3g26880 ATOEP16-4  ATCCATTGGC AGATTCGGAT TTCAATGCGG TCTTGTAAGT GGTGTGTTTA
At1g20350 ATTIM17-1  CGAGAAGCGG AGGAAGCTTC TCCGTGTGGG GTGGTCTTTA CTCAACCTTC
At2g37410 ATTIM17-2  CTCGTACTGG AGGCAGTTTT GCTGTTTGGG GAGGTTTATT CTCGACATTT
At5g11690 ATTIM17-3  CTCGCTTGGG AGGCACTTTT GCTGTATTTG GAGGATTGCT CTCAACATTT
At1g18320 ATTIM22-1  TGTTCTTGGG GGCATTAGAT AATCCTATTA CGCATGATAC TATGACGGCT
At3g10110 ATTIM22-2  TGTTCTTGGG GGCATTAGAT AATCCTATTA CGCATGATAC TATGACGGCT
At1g72750 ATTIM23-2  TCATCACTGG AGTCAAAAGC TTCGAATCTG GCGACACTAC TAAGCTCAAA
At3g04800 ATTIM23-3  CAATTGCGGG GATGCGAGCC GCCGAACGAG GCGAATCCCT AAAGATCCGA
At3g25120            CAATATTCCT ACTGTTTACG CTGCTAATTT TGCTATTGTC GCCGGTTGCT

                     501                                                550
At4g26670 HP20       ACAGTTTGGT TGTTTGCCTT CTGAAGCAAA TCCGAGGCAA AGATGACGCC
At5g55510 HP22       ACAGTTTAGT TGTTTGCCTT CTAAAACAAA TACGAGGCAA AGATGACGCC
At3g49560 HP30       ATGCTGGAAT TGCTTCTGTT ATGAAGCGGA TTAGAGGCAA AGAGGATATT
At5g24650 HP30-2     ATGCTGGTAT TGCTTGTGTT ATGAAACGGA TTAGAGGCAA GGAGGATTTA
At2g28900 ATOEP16-1  TTGGAACAGA ATACGGAATC GAACGTATCC GTGGCAGCAG AGATTGGAAA
At4g16160 ATOEP16-2  GCAGCAAATC TCTTGATGCA TTGGTGAAGA ACACAGGAAA AGAATCTCTC
At2g42210 ATOEP16-3  ACATCGGTGT TGAACAGCTG GTTCAGAATT TTAGATCCAA GAGAGATTTT
At3g26880 ATOEP16-4  CTATGACACA TTGTGGGCTT CAACGATATC GAGGCAAGAA TGATTGGGTG
At1g20350 ATTIM17-1  GATTGTGCGT TGGTGTACGC AAGACAAAAG GAAGATCCAT GGAACTCGAT
At2g37410 ATTIM17-2  GACTGTACCA TGGTGTACCT AAGGCAAAAG GAGGATCCTT GGAACTCTAT
At5g11690 ATTIM17-3  GACTATGCAT TGGTGCGCAT CAGGAAGAAG GAAGATCCAT GGAACTCCAT
At1g18320 ATTIM22-1  AGGCAGCAGT TTGTGTTCAC GGCAAAACAA ATGGGGCAAA GGAGTTGGA.
At3g10110 ATTIM22-2  AGGCAGCAGT TTGTGTTCAC GGCAAAACAA ATGGGGCAAA GGAGTTGGA.
At1g72750 ATTIM23-2  ATCAACAGGA TCTTGAACTC TTCTGGTCAA ACTGGTCGAA CTTGGGGGTA.
At3g04800 ATTIM23-3  ACTAATCGGA TTTTGAACTC CGGTGGACTC GTTGCAAGAC GCGGCGGGA.
At3g25120            ATTGCGGAGC TCGTGAATCT GTGAGAATAA CTCGAAGATC AGAACACGAT

                     551                                                600
At4g26670 HP20       ATTAATGTTG GAGTAGCAGG GTGTTGCACT GGTCTTGCTC TTAGTTTCCC
At5g55510 HP22       ATTAATGTTG GAGTTGCTGG GTGTTGTACT GGCCTTGCTC TTAGTTTCCC
At3g49560 HP30       GAATCTGCAG TGGTGGCAGC GTTAGGATCT GGATTTGCAT ACTCATTGGT
At5g24650 HP30-2     GAATCTGCTG TGGTCGCAGC ATTCGGATCT GGAGTTGCAT ATTCTCTTGT
At2g28900 ATOEP16-1  AACGCAATGT TAGCAGGCGC GGCGACAGGA GCAGTGCTCT CAGCGGTTGG
At4g16160 ATOEP16-2  CAATGGGGGC TAGCGGCAGG GTTATACTCA GGTATCACTT ACGGTATGAC
At2g42210 ATOEP16-3  TACAATGGTG CTATTGGTGG TTTTGTCGCT GGAGCTTCTG TGCTTGGCTA
At3g26880 ATOEP16-4  AATGCTTTGG TAGGAGGAGC TGTGGCGGGA GCAGCTGTTG CCATTAGCAC
At1g20350 ATTIM17-1  CTTATCTGGT GCAGCCACTG GAGGATTCCT CTCGTTGCGT CAAGGCTTAG
At2g37410 ATTIM17-2  CATTGCTGGT GCTGCAACTG GAGGGTTTCT GTCTATGCGG CAAGGGGCTG
At5g11690 ATTIM17-3  CGTAGCGGGT GCTGCTACAG GTGGAGTTCT GTCTATCCGA AAAGGGGTTG
At1g18320 ATTIM22-1  .ATTCCTGTA AGACATTTGC AGTTATGGGT TTGGTTTTCT CTGCTGCAGA
At3g10110 ATTIM22-2  .ATTCCTGTA AGACATTTGC AGTTATGGGT TTGGTTTTCT CTGCTGCAGA
At1g72750 ATTIM23-2  .ATCGGATTG GTATCATTGG ATTGGTTTAC GCAGGGATCG AGAGTGGTAT
At3g04800 ATTIM23-3  .ATTGCTTAG GATCCGTAGG GTTGATGTTT GCTGCTATGG AGAGCGGTGT
At3g25120            GATTTAATGA ACTCAGCTAT TGGAGGACTT TTTAGTGGTG CTTTGCTTGG
```

```
                        601                                                 650
At4g26670 HP20          TGCTGCTCCA CAGGCTCTTC TACAGAGTTG TCTCACGTTT GGGGCATTCT
At5g55510 HP22          CGGTGCACCG CAAGCAATGC TACAGAGTTG TCTCACTTTT GGTGCCTTCT
At3g49560 HP30          GAGCCAAGGA TTGCAAGGAC AACCTATGAA TGCAATCACT ACTGCTGCTG
At5g24650 HP30-2        GAGCGCAGGA TTACAAGGAC AGCCTATGAA TGCAATCACC ACTGCTGCTG
At2g28900 ATOEP16-1     TAAGAAAGGC AAAGACACTA TTGTGATCGA TGCCATTCTT GGTGGCGCGC
At4g16160 ATOEP16-2     AGAGGTTCGT GGAGGAGCTC ATGATTGGCG GAACAGCGCG GTAGCTGGAG
At2g42210 ATOEP16-3     TAGAGCAAGG AGCATCCCGA CAGCGATAGC TGCAGGTGCA ACACTAGCTG
At3g26880 ATOEP16-4     AAGAAACTGG ACACAGGTTG TTGGCATGGC TGGCCTCGTC TCTGCTTTTA
At1g20350 ATTIM17-1     GCGCGTCTGC TAGATCGGCT TTAGTCGGAG GTGTGTTGTT GGCTATGATA
At2g37410 ATTIM17-2     GTGCTGCTTC GAGATCAGCT ATTTTTGGAG GGGTTTTGCT TGCTTTGATT
At5g11690 ATTIM17-3     TTGCAGCTTC AACATCAGCG GTTATGTTTG GTTTTTTTTT GGCTGTACTC
At1g18320 ATTIM22-1     ATGCATTGTC GAAAAGGCAA GAGCTAAGCA TGACACTGTA AACACCGCTA
At3g10110 ATTIM22-2     ATGCATTGTC GAAAAGGCAA GAGCTAAGCA TGACACTGTA AACACCGCTA
At1g72750 ATTIM23-2     TGTGGCTGCC ACGGATAGAG ATGATGTT.. .TGGACCAGT GTGGTGGCTG
At3g04800 ATTIM23-3     TACGTATATG AGAGACGGAG ACGACGGTTC GTTGACAACT GTGATCGCTG
At3g25120               AAGACTTCAA GGAGGTCCTA AGGGTGCGAT TCGCTACTCT CTAGTTTTTG

                        651                                                 700
At4g26670 HP20          CTTTTATTCT TGAGGGACTC AACAAAAGAC AAACAGCTTT GGCACACTCG
At5g55510 HP22          CCTTCATCCT TGAAGGACTC AACAAAAGAC AAACGGCTTT GGCTCACTCT
At3g49560 HP30          GTTTTGCTGT TTTTCAAGGA GTGTTTTTTA AATTGGGAGA AAGATTCTCT
At5g24650 HP30-2        GTTTCGCTGT TTTTCAAGGA GTGTTTTTCA AGTTGGGTGA AAGGTTCTCT
At2g28900 ATOEP16-1     TTGCAACCGC TTCTCAGTTC GTTAACAATC ATTATTTCTA CTGA~~~~~~
At4g16160 ATOEP16-2     CATTGACAGG AGCGGCAATG GCTATGACGA CGTCTGAGAG GACAAGCCAT
At2g42210 ATOEP16-3     TTACCTCTGC TTT.....GA TTGATTCTGG AGGTCAGACC ACAAGAGTAG
At3g26880 ATOEP16-4     GTGTTTTGGC TAATTGCACC AGGACAGAAA ACCCAAACAA CACTAATTAA
At1g20350 ATTIM17-1     GAAGGAGTTG GTATCATGTT AAACAAAGTT CAGAGTACTG CGCATAACGA
At2g37410 ATTIM17-2     GAAGGAGCTG GGATCATGTT GAACAAGGTA CTGGCTCAGC CTCAGAATAT
At5g11690 ATTIM17-3     AA...CCCTC CGTTCGGGAG CAAGTAAGCT TTTTGGGTTG TCTTTGATGA
At1g18320 ATTIM22-1     TAGCTGGATG TGTTACCGGT GGTTCAATGT CCGCCCGAGG TGGGCCAAAA
At3g10110 ATTIM22-2     TAGCTGGATG TGTTACCGGT GGTTCAATGT CCGCCCGAGG TGGGCCAAAA
At1g72750 ATTIM23-2     GTCTTGGAAC CGGAGCTGTT TGTAGAGCGG CGAGAGGAGT GAGATCTGCA
At3g04800 ATTIM23-3     GTTTAGCCAC TGGTGTGCTT TACAGAGCTG CTTCTGGACC TAGATCCGCT
At3g25120               CTGCTGTAGG CACAGCATTT GATTATGCTA CCCTTAAAGG AAAACCAATG

                        701                                                 750
At4g26670 HP20          GTCTCGTTGA GACACCAAAC CGGACTGTTC CAAGATCATC ATCGTGCTTT
At5g55510 HP22          GTCTCGTTTA GACAACAAAC CAGAAGTCCC CAACATGATT TAC......C
At3g49560 HP30          AAACCGAGTA CTGAAGATCC ATTTTTCACA AGAGGAAGGA CAATGCTAGT
At5g24650 HP30-2        AAACCAAGTG TTGAAGATCC ATATTACACC CGGGGAAGAT CTATGTTGTT
At2g28900 ATOEP16-1     ~~~~~~~~~~ ~~~~~~~~~~ ~~~~~~~~~~ ~~~~~~~~~~ ~~~~~~~~~~
At4g16160 ATOEP16-2     GAGCAAGTGG TTCAGTCTGC TCTCACTGGA GCAGCTATTT CCACCGCTGC
At2g42210 ATOEP16-3     ACAATGGCAG AGAATACTAT CCTTACACCG TCGAGAAAAG AGCTGAAGCT
At3g26880 ATOEP16-4     GCTTGCAGGT CTTTGACAAG TCCATTCAAG AAACTGTATG GAATTGGAAC
At1g20350 ATTIM17-1     GCAGTTCATG GAGGAT..CA TGCAGCTACT TCTTTACCAT ATGGTATGGG
At2g37410 ATTIM17-2     GATGATGGAG GACCCTGGAA TGCAAGGAAT GCCTGGGATG CAGGGAATGC
At5g11690 ATTIM17-3     GAATGTCATT TAGACTTTCA TG..ATAATT GCCTTTTCGT TATCAATTCT
At1g18320 ATTIM22-1     GCTGCGTGTA TAGGTTGCGC TGGATTTGCA ACTTTCTCTG TACTCATAGA
At3g10110 ATTIM22-2     GCTGCGTGTA TAGGTTGCGC TGGATTTGCA ACTTTCTCTG TACTCATAGA
At1g72750 ATTIM23-2     GCTGTAGCTG GTGCTCTTGG TGGACTTGCG GCTGGAGCTG TTGTAGCTGG
At3g04800 ATTIM23-3     GTGGTTGCCG GAGCTGTCGG AGGAGTTGCG GCTTTGGCTG CAGTTGCTGG
At3g25120               TTAGAGAGCT ACCGTAACAT GGAGTCATTC AAGTTACCTG AATGGTCTCC

                        751                                                 800
At4g26670 HP20          ACCACTCTCT CTTGCTCTCC CGATCCCTGA AGAAATCAAA GGAGCCTTTT
At5g55510 HP22          GCTGCTCTCG TTGGCTATCC CAATCCATGA TGAAATCAAA GGAGCTTTCT
At3g49560 HP30          GAAGCTAGGT TTGGAGAAAT ACGAGAAGAA CTTCAAGAAA GGACTTTTAA
At5g24650 HP30-2        GAAACTGGGT CTAGAGAAGT ATGAGAAGAA CTTCAAGAAA GGTTTATTAG
At2g28900 ATOEP16-1     ~~~~~~~~~~ ~~~~~~~~~~ ~~~~~~~~~~ ~~~~~~~~~~ ~~~~~~~~~~
```

```
At4g16160 ATOEP16-2  TAATCTCCTT TCTAGCGTTT TCTAGATGAT TTGTATTAGA AGCTTTAATG
At2g42210 ATOEP16-3  GATTCCTGA~ ~~~~~~~~~~ ~~~~~~~~~~ ~~~~~~~~~~ ~~~~~~~~~~
At3g26880 ATOEP16-4  TTGAAGATCA ATACACTGAC TCTCCGGTTC GATCCTATTT AGTTGGCTGA
At1g20350 ATTIM17-1  TCAGATATCT GGTCAGTCCG TACCGGTACC GGAGACTTCT TCTTCTTCTT
At2g37410 ATTIM17-2  AGGGAATGCC TGGGATGCCC GGAATGCAAG GAATGCCTGG GATGCAAGGA
At5g11690 ATTIM17-3  TCAAAATTAC TGTTTCATGG AAAGTTTAAC AGATTTCGTG GTTGAGAATT
At1g18320 ATTIM22-1  GAAGTTCTTT GATAGGCATA CATAA~~~~~ ~~~~~~~~~~ ~~~~~~~~~~
At3g10110 ATTIM22-2  GAAGTTCTTT GATAGGCATA CATAA~~~~~ ~~~~~~~~~~ ~~~~~~~~~~
At1g72750 ATTIM23-2  GAAGCAAATT GTGAAGCGGT ATGTGCCCAT TTGAAGACTG CAAGAGTCTA
At3g04800 ATTIM23-3  AAGACGCATC GTCAAGCGAT TCGTTCCAAT CTAA~~~~~~ ~~~~~~~~~~
At3g25120            TATTAAAGTC CTCGACGAAG AAGCCTTAGC AAAGAAGAAA GCTCATGAAG

                     801                                                850
At4g26670 HP20       CTTCTTTCTG CAAGTCCTTA GCTAAACCAA GGAAGTTCTA A~~~~~~~~~
At5g55510 HP22       CTTCTTTCTG CAACTCCTTA ACGAAACCCA AGAAGCTCAA ATTTCCTCAT
At3g49560 HP30       CTGATCCCAC ATTGCCATTG CTCACTGATA GCGCGCTGAA AGATGCGAAC
At5g24650 HP30-2     CTGACCCAAC TCTGCCATTG CTCACTGATA GCGCGCTAAG AGACGTGAGC
At2g28900 ATOEP16-1  ~~~~~~~~~~ ~~~~~~~~~~ ~~~~~~~~~~ ~~~~~~~~~~ ~~~~~~~~~~
At4g16160 ATOEP16-2  CATAAGGGTT GTTTCATGTA TCAGTTATGT TTCTTTTTGT GAAAACGAAT
At2g42210 ATOEP16-3  ~~~~~~~~~~ ~~~~~~~~~~ ~~~~~~~~~~ ~~~~~~~~~~ ~~~~~~~~~~
At3g26880 ATOEP16-4  ACCCGTGGAT GGTTCTTCTT TTCTATAGAC CACACTTTTG GTCTTGTCTC
At1g20350 ATTIM17-1  CTGGTTCGGT ATCTTGGTTT GGGAGTTTGT TTAAGAAGAA GAAAGAAACA
At2g37410 ATTIM17-2  ATG..CAGAT GGGGCAGATG CAGAGTCAAG CACAGATAAG GTCAGAGAGT
At5g11690 ATTIM17-3  TCTGATCATT TTTGTATAAA CGTCATCAAG AACTAATTAT TGCTATTCAA
At1g18320 ATTIM22-1  ~~~~~~~~~~ ~~~~~~~~~~ ~~~~~~~~~~ ~~~~~~~~~~ ~~~~~~~~~~
At3g10110 ATTIM22-2  ~~~~~~~~~~ ~~~~~~~~~~ ~~~~~~~~~~ ~~~~~~~~~~ ~~~~~~~~~~
At1g72750 ATTIM23-2  ATTGGCAGAC TCTTTTTCGG GTCGTTGTTG AAATTTTTGA TAGGGGAAAT
At3g04800 ATTIM23-3  ~~~~~~~~~~ ~~~~~~~~~~ ~~~~~~~~~~ ~~~~~~~~~~ ~~~~~~~~~~
At3g25120            AGAAGATATT CCCTGAAAGA GTCCTCGGCA AATTGAACAA AGAATAG~~~

                     851                                                900
At4g26670 HP20       ~~~~~~~~~~ ~~~~~~~~~~ ~~~~~~~~~~ ~~~~~~~~~~ ~~~~~~~~~~
At5g55510 HP22       GCTCGTTGA~ ~~~~~~~~~~ ~~~~~~~~~~ ~~~~~~~~~~ ~~~~~~~~~~
At3g49560 HP30       ATCCCACCAG GGCCAAGACT TATGATACTA GATCATATCC AGAGGGACCC
At5g24650 HP30-2     ATCCCGCCTG GACCAAGGCT ACTGATACTT GATCACATCC AAAGGGACCC
At2g28900 ATOEP16-1  ~~~~~~~~~~ ~~~~~~~~~~ ~~~~~~~~~~ ~~~~~~~~~~ ~~~~~~~~~~
At4g16160 ATOEP16-2  TCGCTAAAGG TCTACTAAGA TCTTTTCCTG AAACTCTCGA AGCTGGAGAG
At2g42210 ATOEP16-3  ~~~~~~~~~~ ~~~~~~~~~~ ~~~~~~~~~~ ~~~~~~~~~~ ~~~~~~~~~~
At3g26880 ATOEP16-4  TCTGTAGTCA TCATGTACAC ACAAAGTCCC TCGAACCCGA AACCGTATTT
At1g20350 ATTIM17-1  GAGGATCATC ATTCAGAGAG CAGAACTCAC ATTTTGGAGA GCTTTGATGC
At2g37410 ATTIM17-2  CAAAACCAGA ATACAGCTTC ATCATCATCA TCATCATCAT GGTTTGGAGG
At5g11690 ATTIM17-3  GTGTTCCTTT TTGAA~~~~~ ~~~~~~~~~~ ~~~~~~~~~~ ~~~~~~~~~~
At1g18320 ATTIM22-1  ~~~~~~~~~~ ~~~~~~~~~~ ~~~~~~~~~~ ~~~~~~~~~~ ~~~~~~~~~~
At3g10110 ATTIM22-2  ~~~~~~~~~~ ~~~~~~~~~~ ~~~~~~~~~~ ~~~~~~~~~~ ~~~~~~~~~~
At1g72750 ATTIM23-2  GGTGAGAATT TGATAGGTTT GGTATGTCTT GGAATCATAA AAATGAAAAC
At3g04800 ATTIM23-3  ~~~~~~~~~~ ~~~~~~~~~~ ~~~~~~~~~~ ~~~~~~~~~~ ~~~~~~~~~~
At3g25120            ~~~~~~~~~~ ~~~~~~~~~~ ~~~~~~~~~~ ~~~~~~~~~~ ~~~~~~~~~~

                     901                                                950
At4g26670 HP20       ~~~~~~~~~~ ~~~~~~~~~~ ~~~~~~~~~~ ~~~~~~~~~~ ~~~~~~~~~~
At5g55510 HP22       ~~~~~~~~~~ ~~~~~~~~~~ ~~~~~~~~~~ ~~~~~~~~~~ ~~~~~~~~~~
At3g49560 HP30       GGAGATAAAG GGCAAACGAA AGTAG~~~~~ ~~~~~~~~~~ ~~~~~~~~~~
At5g24650 HP30-2     TGAGCTAAAG GGCAAGCGGG GAAGTCGTGG TTGA~~~~~~ ~~~~~~~~~~
At2g28900 ATOEP16-1  ~~~~~~~~~~ ~~~~~~~~~~ ~~~~~~~~~~ ~~~~~~~~~~ ~~~~~~~~~~
At4g16160 ATOEP16-2  AGATCGTTTT GTTATCTGTT TGGAAAATAT TTGCACTATA TATATCTTGA
At2g42210 ATOEP16-3  ~~~~~~~~~~ ~~~~~~~~~~ ~~~~~~~~~~ ~~~~~~~~~~ ~~~~~~~~~~
At3g26880 ATOEP16-4  GCATCAATGC TTATTACTGT ATAATGTTAT TTACAAGATA GAGATAGTCA
At1g20350 ATTIM17-1  TCCTCCTGTG CCTACTTATG AGTTTAAGTG A~~~~~~~~~ ~~~~~~~~~~
At2g37410 ATTIM17-2  GCTTTTTGAT AAGAAAAAGG AGGAGGTGCA ACCAGGCAGT GAAAGTAAAA
At5g11690 ATTIM17-3  ~~~~~~~~~~ ~~~~~~~~~~ ~~~~~~~~~~ ~~~~~~~~~~ ~~~~~~~~~~
```

```
At1g18320 ATTIM22-1  ~~~~~~~~~~ ~~~~~~~~~~ ~~~~~~~~~~ ~~~~~~~~~~ ~~~~~~~~~~
At3g10110 ATTIM22-2  ~~~~~~~~~~ ~~~~~~~~~~ ~~~~~~~~~~ ~~~~~~~~~~ ~~~~~~~~~~
At1g72750 ATTIM23-2  TTTATTTGGT TTCTAGAGGT ACAACAAGTC TGTATGTCAA GTCATAATGC
At3g04800 ATTIM23-3  ~~~~~~~~~~ ~~~~~~~~~~ ~~~~~~~~~~ ~~~~~~~~~~ ~~~~~~~~~~
At3g25120            ~~~~~~~~~~ ~~~~~~~~~~ ~~~~~~~~~~ ~~~~~~~~~~ ~~~~~~~~~~

                     951                                                1000
At4g26670 HP20       ~~~~~~~~~~ ~~~~~~~~~~ ~~~~~~~~~~ ~~~~~~~~~~ ~~~~~~~~~~
At5g55510 HP22       ~~~~~~~~~~ ~~~~~~~~~~ ~~~~~~~~~~ ~~~~~~~~~~ ~~~~~~~~~~
At3g49560 HP30       ~~~~~~~~~~ ~~~~~~~~~~ ~~~~~~~~~~ ~~~~~~~~~~ ~~~~~~~~~~
At5g24650 HP30-2     ~~~~~~~~~~ ~~~~~~~~~~ ~~~~~~~~~~ ~~~~~~~~~~ ~~~~~~~~~~
At2g28900 ATOEP16-1  ~~~~~~~~~~ ~~~~~~~~~~ ~~~~~~~~~~ ~~~~~~~~~~ ~~~~~~~~~~
At4g16160 ATOEP16-2  GTAGTACCTA TTACGTAACC ~~~~~~~~~~ ~~~~~~~~~~ ~~~~~~~~~~
At2g42210 ATOEP16-3  ~~~~~~~~~~ ~~~~~~~~~~ ~~~~~~~~~~ ~~~~~~~~~~ ~~~~~~~~~~
At3g26880 ATOEP16-4  TAGAAAAATT AAAACATCAA AACTGATTTT TAATAAAGTG TATGTTAATA
At1g20350 ATTIM17-1  ~~~~~~~~~~ ~~~~~~~~~~ ~~~~~~~~~~ ~~~~~~~~~~ ~~~~~~~~~~
At2g37410 ATTIM17-2  CAGAGGTGTT GGAGAGTTTT GATGCTCCTC CGGTGCCATC ATTTGAGTTC
At5g11690 ATTIM17-3  ~~~~~~~~~~ ~~~~~~~~~~ ~~~~~~~~~~ ~~~~~~~~~~ ~~~~~~~~~~
At1g18320 ATTIM22-1  ~~~~~~~~~~ ~~~~~~~~~~ ~~~~~~~~~~ ~~~~~~~~~~ ~~~~~~~~~~
At3g10110 ATTIM22-2  ~~~~~~~~~~ ~~~~~~~~~~ ~~~~~~~~~~ ~~~~~~~~~~ ~~~~~~~~~~
At1g72750 ATTIM23-2  AGTTTCACTT TGAAGAATAA CCTGCAAACC TTTTTCTTAT ATTCATACTG
At3g04800 ATTIM23-3  ~~~~~~~~~~ ~~~~~~~~~~ ~~~~~~~~~~ ~~~~~~~~~~ ~~~~~~~~~~
At3g25120            ~~~~~~~~~~ ~~~~~~~~~~ ~~~~~~~~~~ ~~~~~~~~~~ ~~~~~~~~~~

                     1001                                               1050
At4g26670 HP20       ~~~~~~~~~~ ~~~~~~~~~~ ~~~~~~~~~~ ~~~~~~~~~~ ~~~~~~~~~~
At5g55510 HP22       ~~~~~~~~~~ ~~~~~~~~~~ ~~~~~~~~~~ ~~~~~~~~~~ ~~~~~~~~~~
At3g49560 HP30       ~~~~~~~~~~ ~~~~~~~~~~ ~~~~~~~~~~ ~~~~~~~~~~ ~~~~~~~~~~
At5g24650 HP30-2     ~~~~~~~~~~ ~~~~~~~~~~ ~~~~~~~~~~ ~~~~~~~~~~ ~~~~~~~~~~
At2g28900 ATOEP16-1  ~~~~~~~~~~ ~~~~~~~~~~ ~~~~~~~~~~ ~~~~~~~~~~ ~~~~~~~~~~
At4g16160 ATOEP16-2  ~~~~~~~~~~ ~~~~~~~~~~ ~~~~~~~~~~ ~~~~~~~~~~ ~~~~~~~~~~
At2g42210 ATOEP16-3  ~~~~~~~~~~ ~~~~~~~~~~ ~~~~~~~~~~ ~~~~~~~~~~ ~~~~~~~~~~
At3g26880 ATOEP16-4  GCCATGCTGT TTCTTAGGAA AGCCAGTTTA TTCACGAATC CACCATTTTT
At1g20350 ATTIM17-1  ~~~~~~~~~~ ~~~~~~~~~~ ~~~~~~~~~~ ~~~~~~~~~~ ~~~~~~~~~~
At2g37410 ATTIM17-2  AAGTAAGCTT TGTGGACATC TATTTCTCTG TCATCCAATG GTTTACCTAC
At5g11690 ATTIM17-3  ~~~~~~~~~~ ~~~~~~~~~~ ~~~~~~~~~~ ~~~~~~~~~~ ~~~~~~~~~~
At1g18320 ATTIM22-1  ~~~~~~~~~~ ~~~~~~~~~~ ~~~~~~~~~~ ~~~~~~~~~~ ~~~~~~~~~~
At3g10110 ATTIM22-2  ~~~~~~~~~~ ~~~~~~~~~~ ~~~~~~~~~~ ~~~~~~~~~~ ~~~~~~~~~~
At1g72750 ATTIM23-2  ATTAAATGTT TTGCCGATTG GTAATTTAAT TTGTCATGAG TGTGTTTGTT
At3g04800 ATTIM23-3  ~~~~~~~~~~ ~~~~~~~~~~ ~~~~~~~~~~ ~~~~~~~~~~ ~~~~~~~~~~
At3g25120            ~~~~~~~~~~ ~~~~~~~~~~ ~~~~~~~~~~ ~~~~~~~~~~ ~~~~~~~~~~

                     1051                                               1100
At4g26670 HP20       ~~~~~~~~~~ ~~~~~~~~~~ ~~~~~~~~~~ ~~~~~~~~~~ ~~~~~~~~~~
At5g55510 HP22       ~~~~~~~~~~ ~~~~~~~~~~ ~~~~~~~~~~ ~~~~~~~~~~ ~~~~~~~~~~
At3g49560 HP30       ~~~~~~~~~~ ~~~~~~~~~~ ~~~~~~~~~~ ~~~~~~~~~~ ~~~~~~~~~~
At5g24650 HP30-2     ~~~~~~~~~~ ~~~~~~~~~~ ~~~~~~~~~~ ~~~~~~~~~~ ~~~~~~~~~~
At2g28900 ATOEP16-1  ~~~~~~~~~~ ~~~~~~~~~~ ~~~~~~~~~~ ~~~~~~~~~~ ~~~~~~~~~~
At4g16160 ATOEP16-2  ~~~~~~~~~~ ~~~~~~~~~~ ~~~~~~~~~~ ~~~~~~~~~~ ~~~~~~~~~~
At2g42210 ATOEP16-3  ~~~~~~~~~~ ~~~~~~~~~~ ~~~~~~~~~~ ~~~~~~~~~~ ~~~~~~~~~~
At3g26880 ATOEP16-4  CTACTTC~~~ ~~~~~~~~~~ ~~~~~~~~~~ ~~~~~~~~~~ ~~~~~~~~~~
At1g20350 ATTIM17-1  ~~~~~~~~~~ ~~~~~~~~~~ ~~~~~~~~~~ ~~~~~~~~~~ ~~~~~~~~~~
At2g37410 ATTIM17-2  TGCCTCAACT ATCAATTCCA TTTCGTCGTC TTTTTGTCTA TCCTAAGTTC
At5g11690 ATTIM17-3  ~~~~~~~~~~ ~~~~~~~~~~ ~~~~~~~~~~ ~~~~~~~~~~ ~~~~~~~~~~
At1g18320 ATTIM22-1  ~~~~~~~~~~ ~~~~~~~~~~ ~~~~~~~~~~ ~~~~~~~~~~ ~~~~~~~~~~
At3g10110 ATTIM22-2  ~~~~~~~~~~ ~~~~~~~~~~ ~~~~~~~~~~ ~~~~~~~~~~ ~~~~~~~~~~
At1g72750 ATTIM23-2  CTAGTTAGTG TTTTATGTTT CTGTTTTTGA TCAATGTTAA CTCTTTCTTG
At3g04800 ATTIM23-3  ~~~~~~~~~~ ~~~~~~~~~~ ~~~~~~~~~~ ~~~~~~~~~~ ~~~~~~~~~~
At3g25120            ~~~~~~~~~~ ~~~~~~~~~~ ~~~~~~~~~~ ~~~~~~~~~~ ~~~~~~~~~~
```

```
                    1101                                                1150
At4g26670 HP20      ~~~~~~~~~~ ~~~~~~~~~~ ~~~~~~~~~~ ~~~~~~~~~~ ~~~~~~~~~~
At5g55510 HP22      ~~~~~~~~~~ ~~~~~~~~~~ ~~~~~~~~~~ ~~~~~~~~~~ ~~~~~~~~~~
At3g49560 HP30      ~~~~~~~~~~ ~~~~~~~~~~ ~~~~~~~~~~ ~~~~~~~~~~ ~~~~~~~~~~
At5g24650 HP30-2    ~~~~~~~~~~ ~~~~~~~~~~ ~~~~~~~~~~ ~~~~~~~~~~ ~~~~~~~~~~
At2g28900 ATOEP16-1 ~~~~~~~~~~ ~~~~~~~~~~ ~~~~~~~~~~ ~~~~~~~~~~ ~~~~~~~~~~
At4g16160 ATOEP16-2 ~~~~~~~~~~ ~~~~~~~~~~ ~~~~~~~~~~ ~~~~~~~~~~ ~~~~~~~~~~
At2g42210 ATOEP16-3 ~~~~~~~~~~ ~~~~~~~~~~ ~~~~~~~~~~ ~~~~~~~~~~ ~~~~~~~~~~
At3g26880 ATOEP16-4 ~~~~~~~~~~ ~~~~~~~~~~ ~~~~~~~~~~ ~~~~~~~~~~ ~~~~~~~~~~
At1g20350 ATTIM17-1 ~~~~~~~~~~ ~~~~~~~~~~ ~~~~~~~~~~ ~~~~~~~~~~ ~~~~~~~~~~
At2g37410 ATTIM17-2 TCAGCTGAAT TCTTCTTGTT CATGGAAGAA TCAGCATGCT ATGTTCTCTC
At5g11690 ATTIM17-3 ~~~~~~~~~~ ~~~~~~~~~~ ~~~~~~~~~~ ~~~~~~~~~~ ~~~~~~~~~~
At1g18320 ATTIM22-1 ~~~~~~~~~~ ~~~~~~~~~~ ~~~~~~~~~~ ~~~~~~~~~~ ~~~~~~~~~~
At3g10110 ATTIM22-2 ~~~~~~~~~~ ~~~~~~~~~~ ~~~~~~~~~~ ~~~~~~~~~~ ~~~~~~~~~~
At1g72750 ATTIM23-2 ATTCGTTGAG AAACTGATGT GTTGTATTAC ATTTGAAAAT GAAGCTCTTC
At3g04800 ATTIM23-3 ~~~~~~~~~~ ~~~~~~~~~~ ~~~~~~~~~~ ~~~~~~~~~~ ~~~~~~~~~~
At3g25120           ~~~~~~~~~~ ~~~~~~~~~~ ~~~~~~~~~~ ~~~~~~~~~~ ~~~~~~~~~~

                    1151                 1175
At4g26670 HP20      ~~~~~~~~~~ ~~~~~~~~~~ ~~~~~
At5g55510 HP22      ~~~~~~~~~~ ~~~~~~~~~~ ~~~~~
At3g49560 HP30      ~~~~~~~~~~ ~~~~~~~~~~ ~~~~~
At5g24650 HP30-2    ~~~~~~~~~~ ~~~~~~~~~~ ~~~~~
At2g28900 ATOEP16-1 ~~~~~~~~~~ ~~~~~~~~~~ ~~~~~
At4g16160 ATOEP16-2 ~~~~~~~~~~ ~~~~~~~~~~ ~~~~~
At2g42210 ATOEP16-3 ~~~~~~~~~~ ~~~~~~~~~~ ~~~~~
At3g26880 ATOEP16-4 ~~~~~~~~~~ ~~~~~~~~~~ ~~~~~
At1g20350 ATTIM17-1 ~~~~~~~~~~ ~~~~~~~~~~ ~~~~~
At2g37410 ATTIM17-2 TCTTTTCACT TATGTGGAAA ATGTT
At5g11690 ATTIM17-3 ~~~~~~~~~~ ~~~~~~~~~~ ~~~~~
At1g18320 ATTIM22-1 ~~~~~~~~~~ ~~~~~~~~~~ ~~~~~
At3g10110 ATTIM22-2 ~~~~~~~~~~ ~~~~~~~~~~ ~~~~~
At1g72750 ATTIM23-2 TCTCAAGTTT TTTCT~~~~~ ~~~~~
At3g04800 ATTIM23-3 ~~~~~~~~~~ ~~~~~~~~~~ ~~~~~
At3g25120           ~~~~~~~~~~ ~~~~~~~~~~ ~~~~~
```

ACKNOWLEDGEMENTS

First and foremost, I want to express my sincere gratitude to PD Dr. Christiane Reinbothe and Prof. Dr. Steffen Reinbothe, my supervisors, for their continuous guidance and their confidence throughout this study. I am deeply grateful for their warm-hearted support during our time in France.

I am very thankful to em. Prof. Dr. Dr. h. c. Erwin Beck and Prof. Dr. Stephan Clemens who gave me the possibility to finish my thesis in Bayreuth. At this point I thank all the "new" and "old" members of the department of plant physiology, for their help, friendliness and tolerance.

I want to thank Prof. Dr. Stemmann for providing me the confocal laser scanning microscope that was essential for this work. I also acknowledge Markus Hermann for the detailed introduction into confocal microscopy and for his interest in my analyses.

I would like to thank my "grenoblois" co-workers Iga Samol, Hannane Ennajdaoui and Frank Buhr for their fruitful discussions and their considerable assistance.

I thank the French Ministry of Research and Education (Chair d'Excellence research project grant dedicated to Christiane Reinbothe) and the Deutsche Forschungs-gemeinschaft for financial support.

At last, am greatly indebted to my parents. Without them I would not have been able to go this way. They always supported me despite the temporarily large spatial distance and encouraged me very often to do the right thing and to finish this thesis. I hope I can give some of the time back that I had to spend for my PhD thesis.

ERKLÄRUNG

Hiermit erkläre ich, dass ich diese Arbeit selbstständig verfasst und keine anderen als die von mir angegebenen Quellen und Hilfsmittel genutzt habe.
Ferner erkläre ich, dass ich weder an der Universität Bayreuth noch anderweitig mit oder ohne Erfolg versucht habe, diese Dissertation einzureichen. Ich habe keine gleichartige Doktorprüfung an einer anderen Hochschule endgültig nicht bestanden.

Bayreuth, den 4. Mai 2011

Claudia Roßig